Polarized Plate Tectonics

Carlo Doglioni[*,1], **Giuliano Panza**[§,¶]
[*]Dipartimento di Scienze della Terra, Università Sapienza, Roma, Italy
[§]Dipartimento di Matematica e Geoscienze, Università di Trieste, ICTP-SAND group, Trieste, Italy
and Institute of Geophysics, China Earthquake Administration, Beijing, China
[¶]International Seismic Safety Organization (ISSO)
[1]Corresponding author: E-mail: carlo.doglioni@uniroma1.it

Contents

Abstract

The mechanisms driving plate motion and the Earth's geodynamics are still not entirely clarified. Lithospheric volumes recycled at subduction zones or emerging at rift zones testify mantle convection. The cooling of the planet and the related density gradients are invoked to explain mantle convection either driven from the hot interior or from the cooler outer boundary layer. In this paper we summarize a number of evidence supporting generalized asymmetries along the plate boundaries that point to a polarization of plate tectonics. W-directed slabs provide two to three times larger volumes to the mantle with respect to the opposite E- or NE-directed subduction zones. W-directed slabs are deeper and steeper, usually characterized by down-dip compression. Moreover, they show a shallow decollement and low elevated accretionary prism, a steep regional monocline with a deep trench or foredeep, a backarc basin with high heat flow and positive gravity anomaly. Conversely directed subduction zones show antithetic signatures and no similar backarc basin. Rift zones also show an asymmetry, e.g., faster Vs in the western lithosphere and a slightly deeper bathymetry with respect to the eastern flank. These evidences can be linked to the westward drift of the

Advances in Geophysics, Volume 56
ISSN 0065-2687
http://dx.doi.org/10.1016/bs.agph.2014.12.001

lithosphere relative to the underlying mantle and may explain the differences among subduction and rift zones as a function of their geographic polarity with respect to the "tectonic equator." Therefore also mantle convection and plate motion should be polarized. All this supports a general tuning of the Earth's geodynamics and mantle convection by astronomical forces.

1. INTRODUCTION

Plate tectonics provides the tectonic framework supporting Wegener's hypothesis of continental drift. Objections to the original formulation of continental drift and plate tectonics have been focused on the driving mechanism and on the evidence that light continental lithosphere is subducted in continent–continent collision areas (Anderson, 2007a; Mueller & Panza, 1986; Panza & Mueller, 1978; Panza, Calcagnile, Scandone, & Mueller, 1982; Panza & Suhadolc, 1990; Pfiffner, Lehner, Heitzmann, Müller, & Steck, 1997; Schubert et al., 2001; Suhadolc, Panza, & Mueller, 1988). Therefore, the origin of plate tectonics and the mechanisms governing the Earth's geodynamics are still under debate. The most accepted model for the dynamics of the planet is that tectonic plates are the surface expression of a convection system driven by the thermal gradient from the hot inner core (5500–6000 °C) and the surface of the Earth, being the shallowest about 100 km the upper thermal boundary layer, a <1300 °C internally not convecting layer called lithosphere. However, during the last decades it has been shown that:

1. mantle convection driven from below cannot explain the surface kinematics (Anderson, 2007);
2. plates do not move randomly as required by a simple Rayleigh–Bénard convective system, but rather follow a mainstream of motion (Crespi, Cuffaro, Doglioni, Giannone, & Riguzzi, 2007; Doglioni, 1990);
3. plate boundaries rather show asymmetric characters (Doglioni, Carminati, Cuffaro, & Scrocca, 2007; Panza, Doglioni, & Levshin, 2010).

Currently accepted engines for plate tectonics do not seem to supply sufficient energy for plate's motion and do not explain the globally observed asymmetries that from the Earth surface reach mantle depths. Moreover, convection models are generally computed as deforming a compositionally homogeneous mantle, whereas the Earth is chemically stratified and laterally highly heterogeneous (e.g., Anderson, 2006). Based on these assumptions, it is here reviewed an alternative model of plate tectonics, in which the internal

heat still maintains possible mantle convection, but mostly dominated from above (Anderson, 2001). The lithosphere is active in the process, likely sheared by astronomically forces. Moreover, in a not chemically homogeneous mantle, tomographic images are not indication of cold and hot volumes but also of chemical heterogeneity (Anderson, 2006; Foulger et al., 2013; Tackley, 2000; Thybo, 2006; Trampert, Deschamps, Resovsky, & Yuen, 2004). The Earth is subject to the secular cooling of a heterogeneous and stratified mantle, and to astronomical tuning. The combination of these two parameters is here inferred as the main controlling factor of plate tectonics. The planet is still hot enough to maintain at about 100 km depth the top of a layer where partial melting determines a low-velocity and low-viscosity layer at the top of the asthenosphere, allowing partial decoupling of the lithosphere with respect to the underlying mantle (Figure 1). The Earth's rotation and the tidal despinning generate a torque acting on the lithosphere, and producing a net westerly directed rotation of the lithosphere with respect to the underlying mantle, being this rotation decoupled in the low-velocity asthenospheric layer (LVZ) where some melting occurs (Figure 2).

Melting is testified by petrological models, slowing down seismic waves and magnetotelluric data both beneath oceans and continents (e.g., Crépisson et al., 2014; Naif, Key, Constable, & Evans, 2013; Panza, 1980 and references therein) favored by the presence of water (Figure 3), the superadiabatic condition of the LVZ (low-velocity zone) (Anderson, 2013) due to the thermal buffer of the overlying LID (lithospheric mantle) and shear heating. The overlying lithosphere acts as an insulator for the heat dissipated by the underlying mantle due to the pristine heat from the Earth's early stage of magma ocean, plus the heat delivered by radiogenic decay from the internal mantle itself (Hofmeister & Criss, 2005; Lay, Hernlund, & Buffet, 2008; Rybach, 1976). Moreover, in the LVZ has been inferred the presence of a large amount of H_2O delivered by the pargasite mineral when located at pressure >3 GPa, >100 km (Green, Hibberson, Kovacs, & Rosenthal, 2010) as in Figure 3. The asthenosphere is in superadiabatic condition, having a potential temperature (Tp) possibly higher than that of the underlying mantle, which has been inferred to be subadiabatic and less convecting (Anderson, 2013).

The viscosity of the asthenosphere is generally inferred by inverting uplift rates of postglacial rebound or glacial isostatic adjustment (GIA) e.g., Kornig & Muller (1989). However, the viscosity is the resistance to flow under a shear and postglacial rebound has two limitations: (1) it computes the vertical movements in the mantle and (2) thin layers such as the LVZ may be invisible by the GIA (for a discussion, see Doglioni, Ismail-Zadeh, Panza, & Riguzzi,

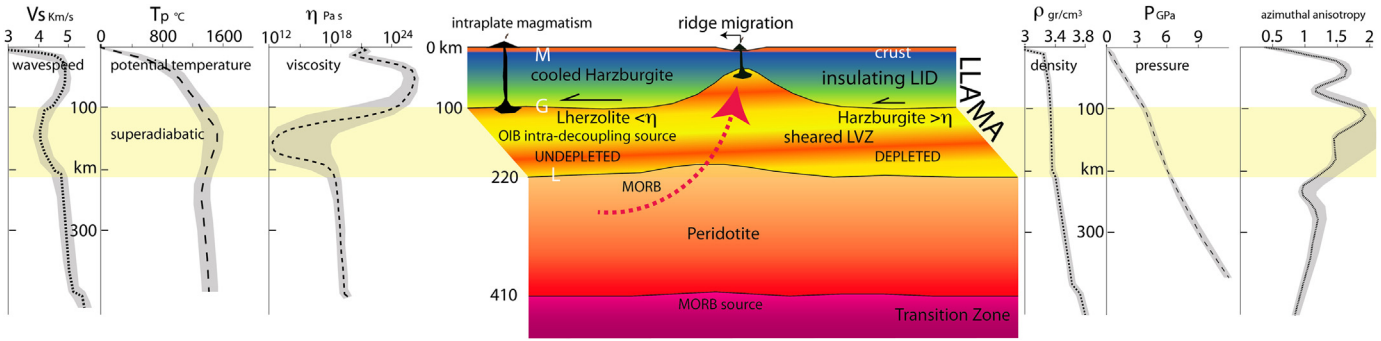

Figure 1 Main nomenclature and parameters used to describe the uppermost 450 km of the Earth, after Doglioni and Anderson (2015). *Data after Jin et al. (1994), Pollitz et al. (1998), Anderson (1989, 2007a, 2013), Doglioni et al. (2011), Tumanian et al. (2012) and references therein*. The gray bands are a gross representation of the uncertainties involved. M, Moho. The lithosphere and the seismic lid (LL) are underlain by aligned melt accumulations (AMA), a low-velocity anisotropic layer (LVZ) that extends from the Gutenberg (G) to the Lehmann (L) discontinuity. Their combination forms LLAMA. The amount of melt in the global LVZ is too small to explain seismic waves speeds and anisotropy unless the temperature is ~200 °C in excess of mid-ocean ridge basalt (MORB) temperatures, about the same excess required to explain Hawaiian tholeiites (Hirschmann, 2010) and oceanic heat flow. This suggests that within-plate volcanoes sample ambient (local) boundary layer mantle. The lowest wave speeds and the highest temperature magmas are associated with the well-known thermal overshoot. The most likely place to find magmas hotter than MORB is at this depth under mature plates, rather than in the subadiabatic interior. Most of the delay and lateral variability of teleseismic travel times occur in the upper 220 km.

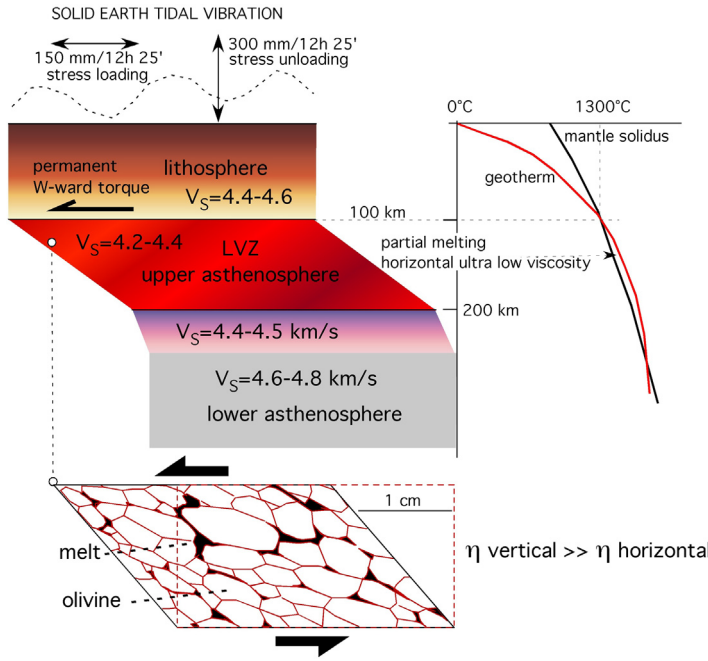

Figure 2 In the upper asthenosphere or lower lithosphere and the seismic lid with aligned melt accumulations, the geotherm is above the temperature of mantle solidus, and small pockets of melt can cause a strong decrease of the viscosity. In the low-velocity zone (LVZ) of the asthenosphere the viscosity can be much lower than the present-day estimates of the asthenosphere viscosity based on the postglacial rebound; in fact the viscosity under shear can be several orders of magnitude lower than the viscosity under vertical load, computed averaging the whole asthenosphere. The LVZ of the asthenosphere can be the basic decoupling zone for plate tectonics, where the lithosphere moves relative to the underlying mantle. Tidal waves are too small to generate plate tectonics. However, being swung horizontally by the solid tide of say 150 mm/semidiurnal, under a permanent torque the lithosphere may retain a small but permanent shift (e.g., 0.1 mm/semidiurnal). At the end of the year this slow restless motion amounts to a cumulative effect of several centimeters, which is consistent with the observed plate motion and thus could be what we consider the net rotation of the lithosphere. *After Riguzzi et al. (2010).*

2011; Scoppola, Boccaletti, Bevis, Carminati, & Doglioni, 2006). The LVZ is a layer in which the viscosity can be extremely lowered (Dingwell et al., 2004; Hirth & Kohlstedt, 1995; 2003; Mei, Bai, Hiraga, & Kohlstedt, 2002) and far lower than GIA estimates, when computed under horizontal shear (Hansen et al., 2012; Riguzzi et al., 2010; Scoppola et al., 2006). It could reach values as low as 10^{12} Pa s (Jin, Green, & Zhou, 1994). Therefore, the LVZ represents the basal fundamental decollement of plate tectonics and

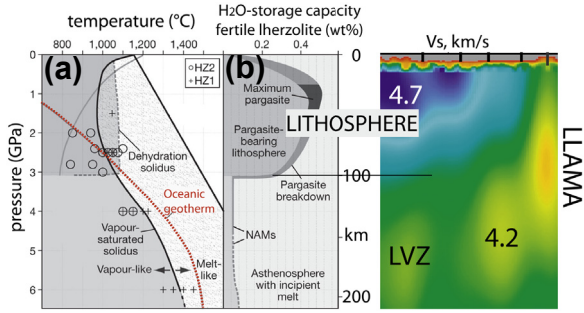

Figure 3 The two panels to the left (a,b), slightly modified after Green et al. (2010), show that, in a lherzolite, the pargasite releases water beneath the lithosphere due to the high-ambient pressure. This may contribute to the lowering of the viscosity in the low-velocity zone (LVZ) and to allow for decoupling between the lithosphere and the underlying mantle. The section to the right shows the shear waves velocity (Vs) in oceanic environment *(after Panza et al., 2010)* and it supports the mineralogical stratigraphy suggested in the panels (a,b). LLAMA, lithosphere and the seismic lid with aligned melt accumulations.

it is well expressed worldwide (Rychert & Shearer, 2009) by the slowdown of seismic waves (Figure 4). The westerly polarization of the lithosphere motion relative to the underlying mantle controls a diffuse asymmetry along plate boundaries, which are shaped by the "eastward" relative mantle flow with respect to the overlying lithosphere. Velocity gradients are the by-product of the lateral viscosity variations in the low-velocity layer, i.e., the decollement plane. The lower the viscosity, the faster westward motion of the overlying lithosphere (e.g., the Pacific plate). Low viscosity in the LVZ can be generated both by higher than standard ambient temperature (Figure 5) and the presence of fluids (Figure 3). Velocity gradients among plates determine tectonics at plate margins and related seismicity (Doglioni, 1993a). The horizontal component of the solid Earth's tide pushes plates to the "west." When faults reach the critical state, the vertical component of tides may trigger the earthquake due to variations of g. The same variation acts in opposite directions as a function of the fault type (Riguzzi, Panza, Varga, & Doglioni, 2010): it can determine the increase or decrease of $\sigma 1$ (maximum principal compressive stress) in extensional environments, or of $\sigma 3$ (minimum principal compressive stress) in compressional tectonic settings.

The origin and source depth of the so-called mantle plumes (Foulger & Jurdy, 2007; Foulger, Natland, Presnall, & Anderson, 2005; Green, 2003) is of paramount importance for the kinematics of the lithosphere relative to the mantle (Cuffaro & Doglioni, 2007; Shaw & Jackson, 1973). The intraplate

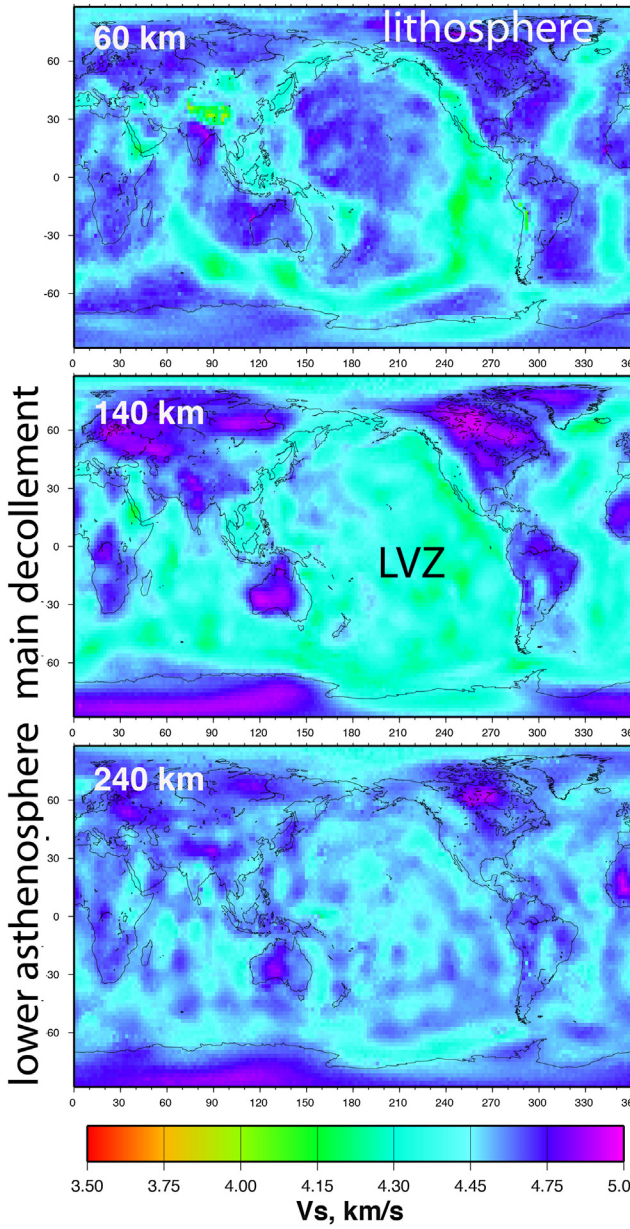

Figure 4 Earth slices at 60, 140, and 240 km depth of shear waves velocity (Vs). *(Data from CUB2, courtesy of Anatoli Levshin (pers. comm.).)* The 60 km depth evidences the distribution of the lithospheric high-velocity LID (blue (dark gray in print versions) areas); the 140 km depth shows the widespread distribution of the low-velocity zone (LVZ) that allows for the decoupling of the overlying lithosphere from the underlying mantle. The decoupling deepens beneath continental areas, locally persisting in the underlying 240 km depth slice, where Vs speed generally increases beneath the decoupling.

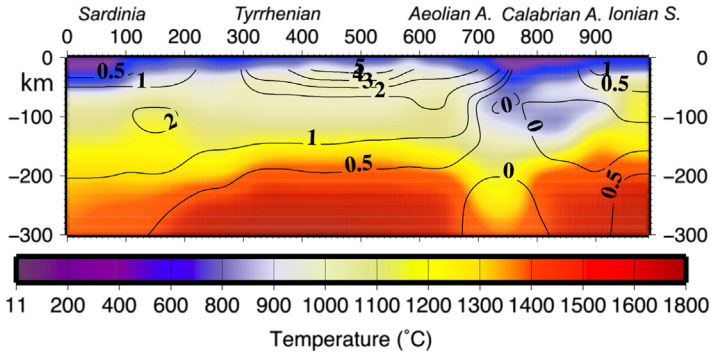

Figure 5 Thermal state of the lithosphere in a subduction–backarc system, across the Tyrrhenian Sea–Apennines. *(After Tumanian et al., 2012).* The extreme vertical and lateral variability of temperatures indicates the strong heterogeneity of the mantle in terms of composition and physical state. The high temperature (>1400–1500 °C) beneath 200 km of depth is consistent with a superadiabatic condition of the upper mantle. Isolines indicate the inferred melt fraction distribution based on chemical proxies of the backarc magmatism.

volcanic tracks such as the Hawaii best represent the motion of the lithosphere relative to the mantle (Figure 6). The source depth of the volcanism, within or below the decoupling surface, controls the kinematic models of fast or slow decoupling of the lithosphere. However, it has been shown that the Hawaii volcanic track is sourced from the shallow asthenosphere or LVZ (Anderson, 2000; 2011; Presnall & Gudfinnsson, 2011; Rychert, Laske, Harmon, & Shearer, 2013). In the following we synthetize the data and models pointing to a geodynamic polarized system, which can be the direct expression of the combination of the internal Earth's dynamics with the astronomical tuning.

1.1 Mantle Stratigraphy

Following Gutenberg (1959), the upper mantle region above ~220 km of depth is called "region B" or upper boundary layer (Anderson, 2013). At 220 km of depth, PREM model (Dziewonski & Anderson, 1981) defines a prominent discontinuity in seismic velocity. Region B contains the lithosphere (sensu lato) and the seismologically defined LID plus the LVZ. Although they are very different concepts, many authors (following McKenzie and Bickle, 1988) often equate LID, lithosphere, and thermal boundary layer (Anderson, 2007a). The lithosphere is the strong layer, for geological loads, and as measured from flexural studies is about half the thickness of the LID. Originally a rheological concept, the lithospheric mantle or LID assumed various connotations in petrology, including

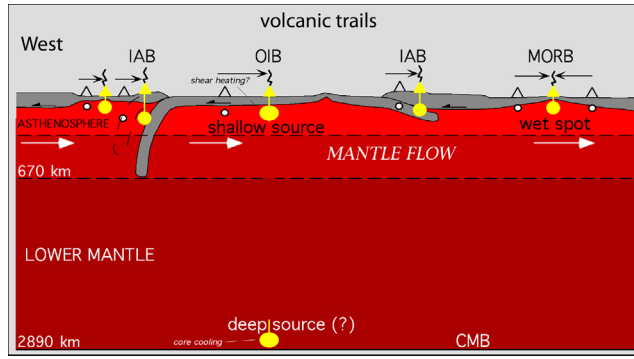

Figure 6 The main volcanic chains at the Earth's surface may have different origins and depths. The thin black arrows indicate the direction of migration of volcanism with time. Filled yellow triangles represent the youngest volcanic products. Yellow circles are the inferred magma sources. Volcanic trails originating on ridges may be wet spots (sensu Bonatti, 1990) fed from a fluid-rich asthenosphere. The hot spots located on plate boundaries are not fixed by definition, because both ridges and trenches move relative to each another and with respect to the mantle. Pacific hot spots, regardless of their source depth, are located within the plate and are virtually the only ones that can be considered reliable as a hot spot reference frame, although their source depth is still debated (asthenospheric or deeper mantle). Intraplate hot spots such as the Hawaii may be related to shear heating in the decoupling LVZ at the asthenosphere top (Doglioni et al., 2005). CMB, core–mantle boundary; IAB, island arc basalt; MORB; mid-ocean ridge basalt; OIB, ocean island basalt; open triangles, extinct volcanoes. *Modified after Cuffaro and Doglioni (2007).*

implications about isotope composition, temperature gradient, melting point, seismic velocity, and thermal conductivity (Anderson, 2011). According to Schuberth, Bunge, Steinle-Neumann, Moder, and Oeser (2009) modeling, the asthenosphere should be homogeneous and isothermal. As the lithosphere, the asthenosphere has been petrologically defined through major element, trace elements, and isotope composition. Seismology resolves reliably the velocity gradient between LID and LVZ. The LID and the LVZ are different from the lithosphere and asthenosphere concepts, respectively, although the LID-LVZ interface (i.e., the region of sharp drop of seismic velocity) is often called lithosphere–asthenosphere boundary (LAB), even if LVZ (V_P between 7.9 and 8.6 km/s; V_S between 4.0 and 4.4 km/s; density between 3.3 and 3.5 g/cm^3) may of course overlap with the top of the asthenosphere, but, in general, is neither homogeneous nor isothermal. Nevertheless the term lithosphere is sometimes used in literature referring to seismic LID, which is a layer with high seismic velocity (as a rule, $V_S \geq 4.35$ km/s, $V_P \geq 7.5$ km/s, density > 3.0 g/cm^3)

thermal boundary layer that comprises both crustal material and refractory peridotite.

The soft mantle LID is a portion of the lower lithospheric mantle material with anomalous behavior and low seismicity; this material is partially molten, with low V_S. The presence of this layer (V_P between 6.9 km/s and 8.2 km/s, $V_S < 4.35$ km/s; density between 3.0 g/cm^3 and 3.3 g/cm^3) is not limited nor directly bound to subduction areas. The mantle wedge (metasomatized LID) is the portion of mantle material found between a subducting slab and the overriding lithosphere where plastic deformation and magmatism occur (Abers, 2005; Abers et al., 2006; Koper, Wiens, Dorman, Hildebrand, & Webb, 1999; Syracuse & Abers, 2006); outside of this geodynamic setting, mantle material with similar physical behavior has been simply described as "soft mantle". In this region, according to Van Keken (2003), hydrothermal uprising flow causes partial melting of subducting slab material due to dehydration. The mantle wedges usually show a low-quality factor (Q) of seismic waves. The melts derived from the subducted crustal materials fertilize the overlying lithospheric mantle (i.e., metasomatized LID), as documented, for instance, by mantle xenoliths in the Mesozoic basalts of Himalaya (Chen et al., 2004; Ying, Zhang, Kita, Morishita, & Shimoda, 2006; Zhang & Sun, 2002). The term "lithospheric roots" is widely used in literature and should be intended as a structural term without specific implications on geochemical composition and thermal gradient.

2. TECTONIC EQUATOR AND WESTWARD DRIFT OF THE LITHOSPHERE

The analysis of past and present motion of plates points to a nonrandom distribution, but to their rather coherent flow (Figure 7). Wegener (1915) and Rittmann (1942) also noted a relevant westward component of plate motion. Past motion can be reconstructed based on magnetic anomalies in the oceanic crust and paleodirection of shortening in the orogens associated to subduction zones. Present motions can be described by the space geodesy data which are anchored to the International Terrestrial Reference Frame (e.g., Altamimi, Collilieux, Legrand, Garayt, & Boucher, 2007; Drewes & Meisel, 2003), i.e., the GPS, VLBI (very long baseline interferometry), and SLR (satellite laser ranging). Past movements coincide with present-day directions of motion (Argus, Gordon, & DeMets, 2011; DeMets, Gordon, & Argus, 2010; Liu, Yang, Stein, Zhu, & Engeln, 2000; Sella, Dixon, & Mao, 2002). The present-day movements are relative

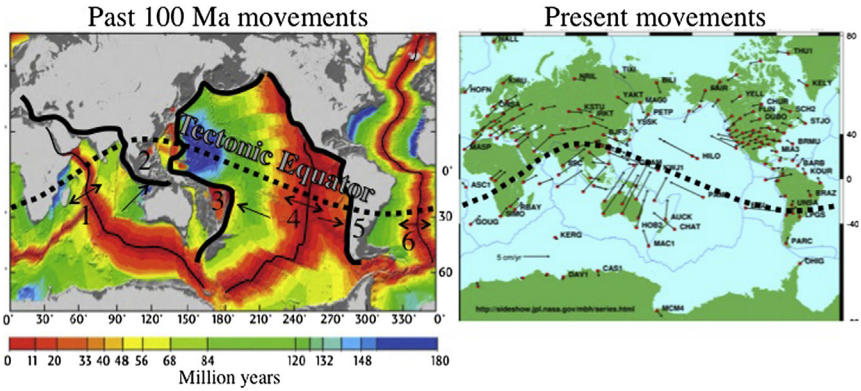

Figure 7 The direction of plate motions across the six major plate boundaries of the Earth (1, Indian ridge; 2, Alpine–Himalayan–Indonesia subduction zones; 3, Western Pacific subduction zone; 4, East Pacific Rise; 5, Andean subduction zone; 6, Mid-Atlantic ridge) show that lithospheric plates moved along a great-circle mainstream which can be schematically represented by the "tectonic equator." This flow appears persistent both in the geologic past (left) and in the present-day motion, as described by the GPS Nasa database (right, Heflin et al., 2007). The color scale in the left panel gives the ocean floor age.

to the hypothetic center of mass of the Earth, assuming that the sum of all vectors equals zero. This is the so-called no-net-rotation (NNR) reference frame. Starting from the Pacific motion direction and linking all the other relative motions in a global circuit using first-order tectonic features such as the (1) East Pacific Rise (EPR), (2) the Atlantic rift, (3) the Red Sea, the Indian Ocean ridge for the rift zones, and (4) the west Pacific subduction, (5) the Andean subduction (AS), and (6) the Zagros–Himalayas subduction for convergent margins (after Crespi et al., 2007) it results a coherent flow of plates. The mainstream of the lithosphere can be represented synthetically by the great circle defined as the "tectonic equator" (Doglioni, 1993a; Crespi et al., 2007). However, as indicated, for example, by the Hawaii volcanic track, plates move not only one relative to the other, but also relative to the mantle. Plates are decoupled at a depth that varies between 60 and 200 km (on average 100 km), in the LVZ, where seismic waves slow down because of the presence of some percentage of melt in the mantle peridotites (Anderson, 2011; Green et al., 2010; Hirschmann, 2010; Schmerr, 2012). This layer is at the base of the lithosphere and at the top of the asthenosphere. It is the basic decollement for plate tectonics. The shearing at the LVZ can explain the anisotropy of seismic waves (Marone & Romanowicz, 2007) that in general travel faster along the trend of motion of plates (Figure 8). This could be explained by the axis of crystals,

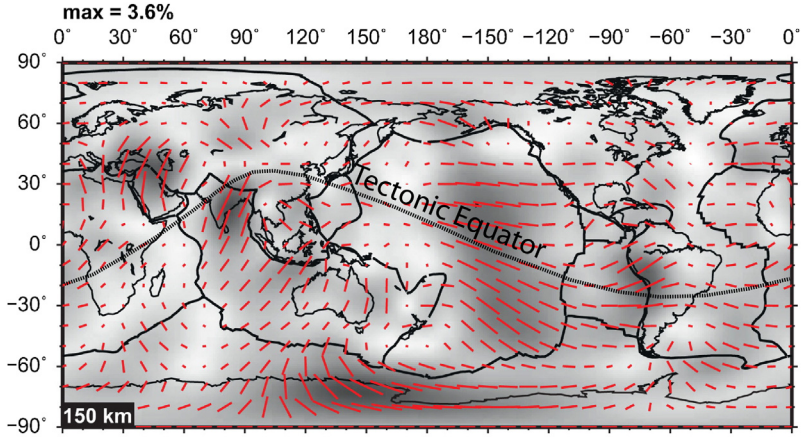

Figure 8 Gross representation of azimuthal anisotropy at 150 km depth according to Yuan and Beghei (2013). The red (gray in print versions) bars represent the fast direction of propagation for vertically polarized shear waves and their length is proportional to the amplitude of the anisotropy. On account of the large averaging volumes involved in anisotropy measurements, the gross agreement between the shape of the tectonic equator (TE) and the overall direction of azimuthal anisotropy can be interpreted as the result of the trend of lattice-preferred orientation of crystals within the decoupling layer (low-velocity zone, LVZ) plus the structural anisotropy due to the tilted, laminated structure of lithosphere and the seismic lid with aligned melt accumulations, generated by the shear of the plate that moves "westward," relative to the underlying mantle, along the TE. *After Doglioni and Anderson (2015).*

which are elongated along the direction of decoupling between lithosphere and underlying mantle.

The so-called hot spots are usually used as a reference frame for plate kinematics. However, they may generate a misleading reference to measure plate motion relative to the mantle because they are not fixed and they may partly originate in the lower lithosphere or the asthenosphere (Anderson, 1999; Anderson, 2011; Doglioni, Green, & Mongelli, 2005; Harpp, Wirth, & Korich, 2002; Panza, Raykova, Carminati, & Doglioni, 2007; Smith & Lewis, 1999). On the other hand, intraplate migrating hot spots, which are unrelated to rifts or plate margins in general, regardless of their origin in the mantle column, they do indicate relative motion between the lithosphere and the underlying mantle in which the hot spot source is located. Therefore, those independent volcanic trails may represent a reliable reference frame. The Pacific plate hot spots are sufficiently fixed relative to one another to represent an independent reference frame to compute plate motions. However, the interpretation of the LVZ (shallow hot spot reference frame) rather

than the deep lower mantle (deep hot spot reference frame) as the source for intraplate Pacific hot spots has several implications. If the source of the intraplate Pacific magmatism is in the LVZ (the decoupling layer), the decoupling between the lithosphere and the subasthenospheric mantle is greater than that recorded by hot spot volcanic tracks (>100 mm/year) due to undetectable shear (Anderson, 2007a,b; Boschi et al., 2007; Boyadzhiev, Brandmayr, Pinat, & Panza, 2008; Panza, Peccerillo, Aoudia, & Farina, 2007; Romanowicz, 2003; Waldhauser, Lippitsch, Kissling, & Ansorge, 2002) in the lower asthenosphere below the magmatic source. The shallower the source, the larger the décollement is. Usually, the computation of the westward drift is linked to the Pacific plate and assumes that the deep lower mantle, below the decoupling zone, is the source for the hot spots above (Gripp & Gordon, 2002; Jurdy, 1990; Ricard, Doglioni, & Sabadini, 1991). The Pacific plate is the fastest plate in all hot spot reference frames and it dominates the net rotation of the lithosphere. Therefore, as it seems quite natural, if the decoupling with respect to the subasthenospheric mantle is larger than usually assumed, the global westward drift of the lithosphere must be faster than the estimates made so far, and may vary between 50 and 90 mm/year. In this case, all plates, albeit moving at different velocities, move westward relative to the subasthenospheric mantle. Finally, a relatively faster decoupling can generate more shear heating in the asthenosphere (even >100 °C) and contribute to supply intraplate magmatism (Doglioni et al., 2005). If the viscosity of the asthenosphere is locally higher than normal, this amount of heating, in an undepleted mantle, could trigger the scattered observed intraplate Pacific volcanism. Variations in depth and geometry in the asthenosphere of these regions of higher viscosity could account for the irregular migration and velocities of surface volcanic tracks. This type of volcanic chain has different kinematic and magmatic origins with respect to the Atlantic hot spots or wet spots (Bonatti, 1990), which migrate with or close to the oceanic spreading center and are therefore related to the plate margin. Plume tracks at the Earth's surface probably have various origins (Foulger et al., 2005), such as wet spots, simple rifts, and shear heating (Doglioni et al., 2005).

Since plate boundaries move relative to each other and relative to the mantle, plumes located on or close to them cannot be considered useful for the definition of a reliable reference frame. The so-called hot spots located on or close to ridges have ages coincident or close to that of the oceanic crust on which they lay. Oceanic intraplate volcanic trails are rather independent and usually have a much younger age with respect to the underlying oceanic crust (e.g., Pacific ones). The preferred location of hot

spots in a shearing asthenosphere would seem to discount the existence of hot spot reference frames that include both intraplate and ridge-centered hot spots. A hot spot reference that considers only Pacific hot spots seems to be preferable due to their relative inertia and because those volcanic trails are independent from plate boundaries. In both hot spot reference frames (deep and shallow), the Pacific plate is the fastest moving plate on Earth, and it contains the most diffuse intraplate magmatism, regardless of its margins. Fastest velocity implies largest potential shear heating at its base. Considering the intraplate Pacific hot spots, the plate motions with respect to the mantle in two different reference frames, one fed from below the asthenosphere (deep reference), and one fed by the asthenosphere itself (shallow reference), provide different kinematics and stimulate opposite dynamic speculations. Plates move faster relative to the mantle if the source of hot spots is taken to be the middle-upper asthenosphere (shallow-fed hot spots), because the hot spot tracks would then not record the entire decoupling occurring in the LVZ. The shallow intra-asthenosphere origin for the hot spots would raise the Pacific velocity from a value of ~10 cm/year (estimated from deep reference) to a faster hypothetical velocity of ~20 cm/year. In this setting, the net rotation of the lithosphere relative to the mesosphere would increase from a value of about 0.4°/Ma (deep-fed hot spots, Gripp & Gordon, 2002) to about 1.5°/Ma (shallow-fed hot spots, Crespi et al., 2007; Cuffaro & Doglioni, 2007). In this framework, all plates move westward along a sinusoidal stream and plate rotation poles are mostly located in a restricted area at a mean latitude of 58°S. The shallow hot spot reference frame seems quite consistent with the persistent geological asymmetry (e.g., Panza et al., 2010) that suggests a global tuning of plate motions due to Earth's rotation.

Therefore, regardless the reference frame, when measuring plate motions relative to the mantle, or even relative to Antarctica, it always turns out that plates have a mean "westerly" directed component, that is also defined net rotation or westward drift of the lithosphere (Bostrom, 1971; Le Pichon, 1968); the resulting velocity of this rotation depends on the used reference. If the source of the magmatism describing linear features at the Earth's surface that allow to compute the relative motion of the lithosphere relative to the mantle are located below the decoupling layer, then the net rotation amounts to 0.2°−0.4°Ma (Conrad & Behn, 2010; Gripp & Gordon, 2002; Torsvik, Steinberger, Gurnis, & Gaina, 2010). In this reference frame the net rotation is only an average motion; since the Pacific plate is kinematically dominant and determines the residual western component

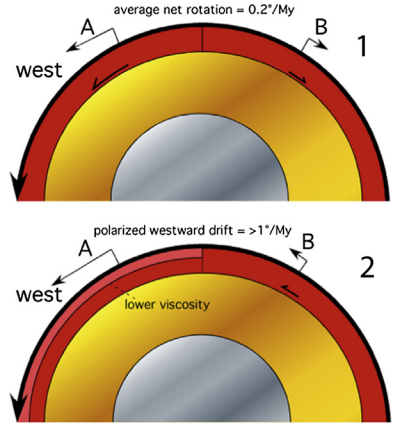

Figure 9 The sum of the plate vectors computed in the hot spots reference frames has a westerly directed component, i.e., the so-called net rotation. If the source of the hot spots is deep (e.g., at the core–mantle boundary), the net rotation amounts to only 0.2°–0.4°/Ma. In case the source of volcanic trails is rather sourced from within the low-velocity zone, the net rotation becomes a fully polarized westward drift of the lithosphere, summing to >1°/Ma. This second kinematic setting better fits the global tectonic asymmetric signatures.

(panel 1 in Figure 9), some plates (e.g., Nazca) still move E-ward relative to the mantle. However, volcanoes may be sourced from within the decoupling LVZ layer. Therefore, part of the decoupling recorded by the volcanic tracks may be lost. Since increasing petrologic and geophysical evidence support a shallow intra-asthenospheric origin of volcanic plumes (e.g., Anderson, 2011; Bonatti, 1990; Foulger et al., 2005; Presnall & Gudfinnsson, 2011), the net rotation of the lithosphere can be as fast as >1°Ma (Crespi et al., 2007; Cuffaro & Doglioni, 2007). In this plate motions reconstruction, all plates move "westerly" along an undulate flow (panel 2 in Figure 9) and the fastest plates are those having at their base an LVZ with lowest viscosity (e.g., the Pacific plate, Pollitz, Bürgmann, & Romanowicz, 1998). Regardless the lithosphere has a net rotation or a fully developed westward drift, plate motions are polarized toward the west, and the equator of this differential rotation closely overlaps the shape of the tectonic equator (TE) of Figure 7. The two extreme values of the rotation point to quite different plate motion relative to the mantle, i.e., a slow net rotation with some plates moving E-ward, or a complete W-ward drift in which all plates, albeit at different velocities, move W-ward (Figure 10). Since evidence in favor of shallow sources for the volcanic trails are growing, we favor the faster westerly oriented decoupling

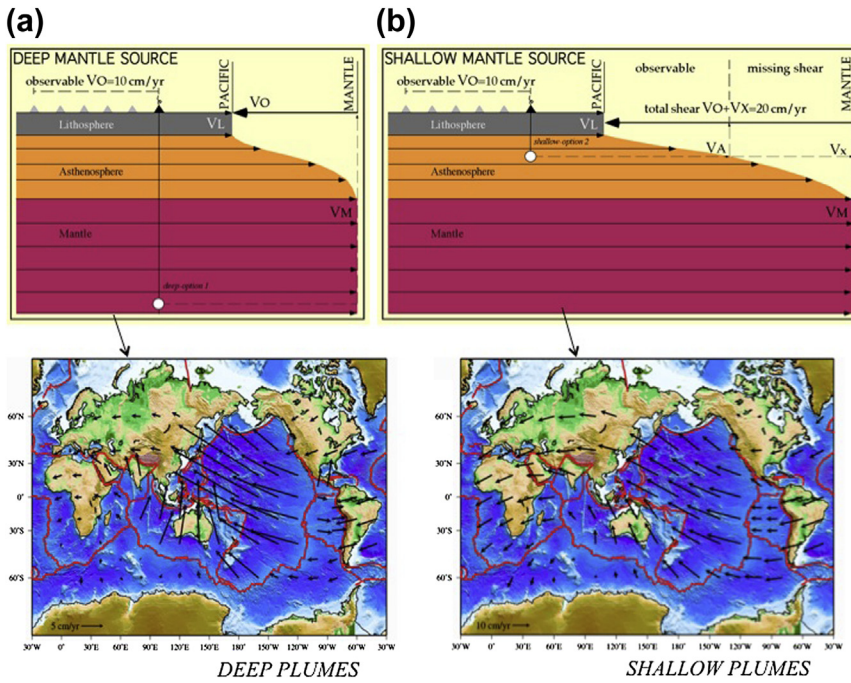

Figure 10 The Hawaiian volcanic track indicates that there is decoupling between the magma source and the lithosphere, which is moving relatively toward the WNW. (a) If the source is below the asthenosphere (e.g., in the subasthenospheric mantle), the track records the entire shear between lithosphere and mantle. (b) In the case of an asthenospheric source for the Hawaiian hot spot, the volcanic track does not record the entire shear between the lithosphere and subasthenospheric mantle, because part of it operates below the source (deep, missing shear). Moreover, the larger decoupling implies larger shear heating, which could be responsible for scattering the point like Pacific intraplate magmatism, *after Doglioni et al. (2005)*. Petrological and seismological data support a shallow source for the Hawaii volcanic trail (Anderson, 2011; Presnall & Gudfinnsson, 2011; Rychert et al., 2013). *After Cuffaro and Doglioni (2007). VO, velocity observed at the surface; VL, velocity of the lithosphere; VM, velocity of the subasthenospheric mantle; Vx, unrecorded velocity of the asthenosphere being below the magmatic source; VA, velocity of the asthenosphere.*

(Crespi et al., 2007). In case the depth is located at variable depths within the decoupling surface, plate motions relative to the mantle are characterized by different values and amount of westward drift. Therefore, plate kinematics is constrained by the different interpretation that is given to the origin and depth of the hot spots (Figure 11). The shallow hot spot reference frame gives a net rotation with an equator that closely overlaps the TE reinforcing its interpretation (Figure 12).

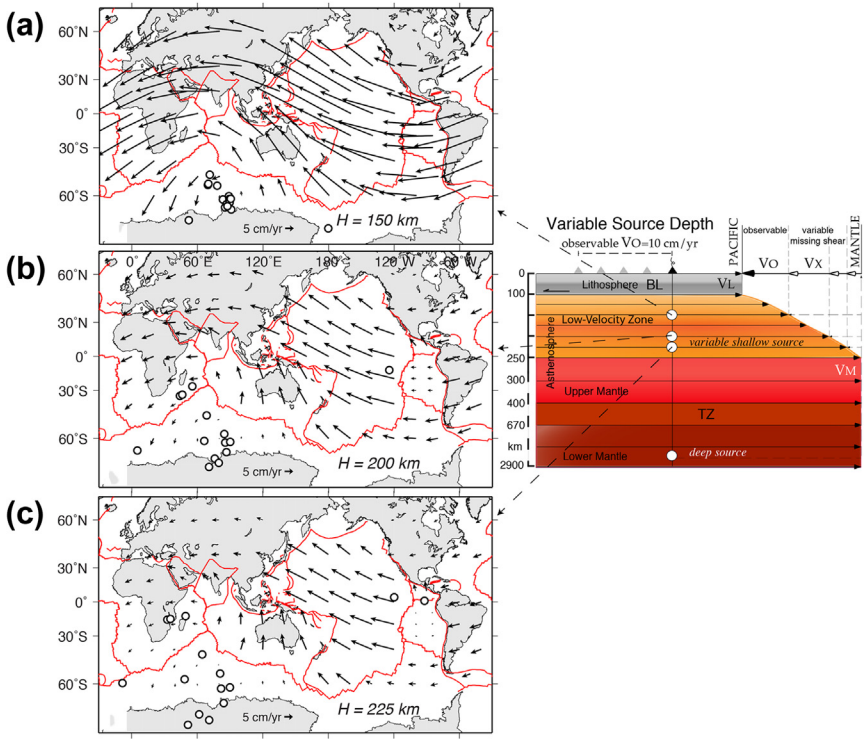

Figure 11 Plate kinematics computed assuming a hot spot reference frame "anchored" in the asthenosphere, i.e., within the decoupling zone. The faster decoupling and "westward" drift of the lithosphere (>1°Ma) occurs if the volcanic tracks are fed from a depth of about 150 km, (a), within the LVZ since the surficial age-progressive volcanic track does not record the entire decoupling between the lithosphere and the mantle beneath the LVZ. Computations made considering the two other deeper depths of magmatic sources at 200 and 225 km, (b) and (c), would provide a slower westward drift. An even deeper source (2800 km) would make the net rotation very slow, about 0.2–0.4°Ma. Note the clustering of the poles of rotation (open circles) in the southern Indian Ocean. The clustering increases as the source of the volcanic trails shallows. *Slightly modified after Doglioni et al. (2014).*

Moving along the flow lines of such polarized mainstream, plate velocity is inversely proportional to the viscosity of the LVZ. The lower the viscosity, the higher the velocity (e.g., the Pacific plate), or vice versa the higher the viscosity, the lower the velocity of the plate (Figure 13). The TE appears stable through time (at least 100 Ma) and makes an angle of about 30° relative to the geographic equator (Figure 14). The angle of the ecliptic plane plus the angle of the Moon's revolution sum to a very close value.

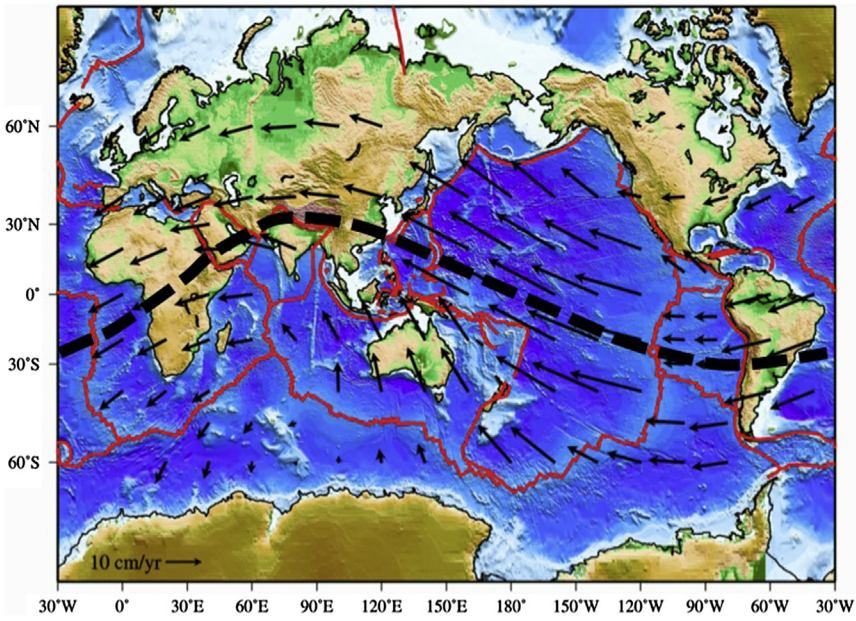

Figure 12 Model of plate motions relative to the mantle assuming an intra-asthenospheric source of volcanic trails. *(After Cuffaro & Doglioni, 2007)* The lithosphere has a net rotation toward the "west"; the equator of this rotation closely overlaps the tectonic equator.

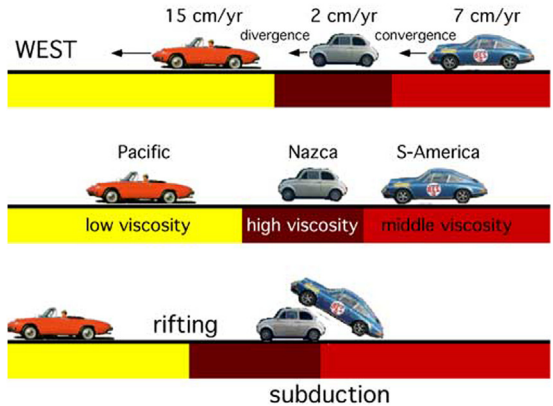

Figure 13 Plates move in a westerly direction at a speed controlled by the viscosity in the underlying LVZ. The westward velocity of the lithosphere increases with decreasing viscosity in the LVZ. Gradients in viscosity lead to the generation of the different plates and to their differential velocity, i.e., plate tectonics. When a lower viscosity LVZ is located beneath a plate to the west with respect to a plate to the east, the plate boundary experiences extension. Contraction occurs in the opposite setting. *(After Doglioni, 1993a)*.

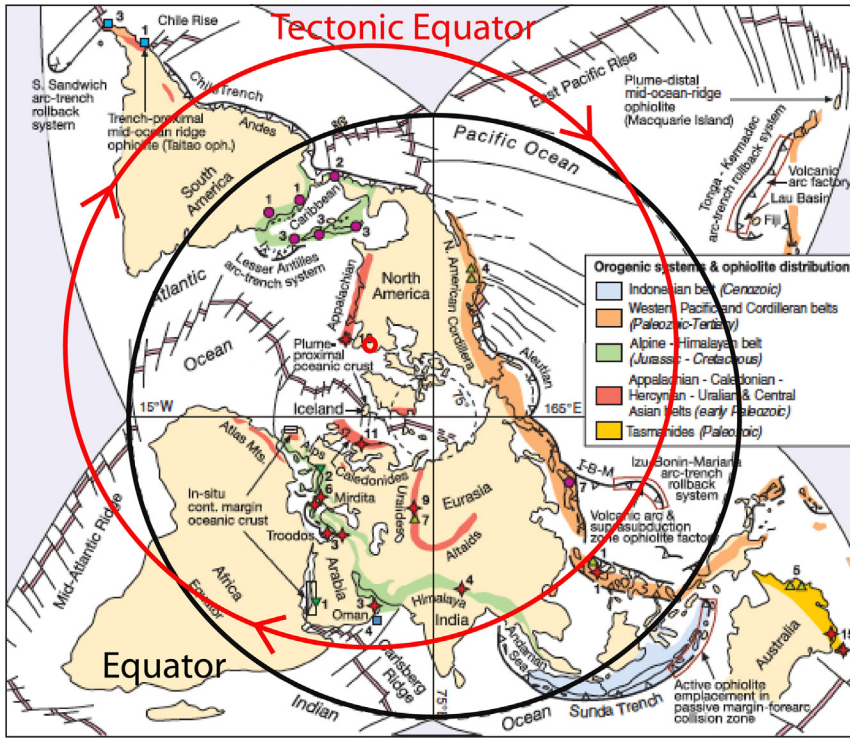

Figure 14 North pole view of the Earth illustrating the position of the tectonic equator relative to the geographic one. *Geological map after Dilek and Furnes (2011).*

Moreover, plates move faster at low latitudes, as recorded by kinematic data, and by seismicity, which decreases toward the polar areas (Riguzzi et al., 2010; Varga et al., 2012). Therefore, the shape of the TE (great circle) and angle relative to the geographic equator suggest an astronomical tuning of plate motions. The TE is a line that represents the circle of maximum average speed of plates. It may be interpreted as a circle contained in a plane perpendicular to the vertical axis of the cone described by the precession of the Earth's axis (Figure 15). In fact, the Maxwell time (the time requested for a solid material to flow) of the lithosphere has the same order of magnitude of the precession cycles (20–26 kyr), as illustrated in Figure 15. During their journey, some plates may experience a further internal rotation. Since any motion of a plate on a sphere is defined by a rotation, this extra movement has been defined as plate subrotation (Cuffaro, Caputo, & Doglioni, 2008), which may perturb the first mainstream of plates. Subrotations imply that plates have a first-order pole of rotation, plus a second pole of the

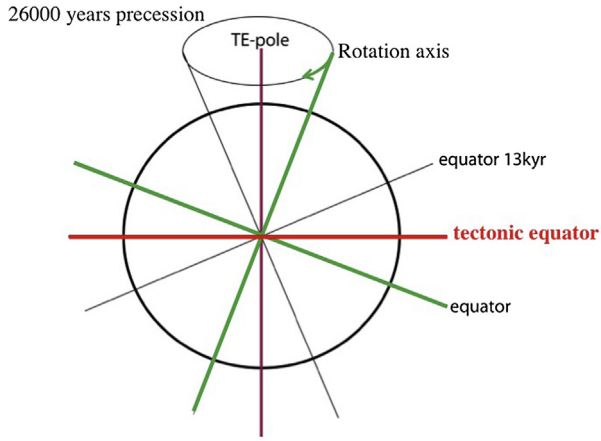

Figure 15 The tectonic equator describes the line along which the mean faster surface motion of the lithospheric plates takes place. The tectonic equator forms an angle of about 28°−30°, which is inferred as the sum of the angle of the ecliptic plane (23°) with the angle of the Moon's revolution plane (5°), with respect to the geographic equator. The location of the tectonic equator is inferred as the mean direction of the Earth's precession axis. The Maxwell relaxation time of the lithosphere (viscosity/rigidity ratio, $\sim 10^{23}$ Pa s/$\sim 10^{11}$Pa = $\sim 10^{12}$ s) is of the same order of magnitude of the 26 ka precession ($\sim 8.2 \times 10^{11}$ s). This could explain the stability of the tectonic equator during the geologic past. *After Doglioni, 2014*.

subrotation that is the only point of the plate maintaining the same distance with respect to the first pole (Figure 16).

As a consequence, global flow lines drawn along the axes of Cenozoic (65.5−0 Ma ago) stretching and shortening show a smooth and gradual variation. The flow lines may approximate the path of the eastward mainstream mantle flow relative to the overlying lithosphere, the long-wavelength undulation being possibly due to the inclination and instability of the Earth's rotation axis. The westward delay of the lithosphere with respect to the mantle (see also Panza et al., 2010) could be due to a minor angular velocity of the lithosphere relative to the underlying mantle, as a result of the deceleration of the Earth's rotation or, in a toroidal field, due to lateral heterogeneities within the lithosphere and the underlying upper mantle (Panza & Romanelli, 2014; Tumanian et al., 2012). Variations in the upper-mantle LVZ (e.g., Panza et al., 2010) allow for variable decoupling between lithosphere and asthenosphere and plate tectonic process may be driven by differential plate velocities. When there is compression or transpression, the eastern plate is moving faster westward, while if there is stretching or

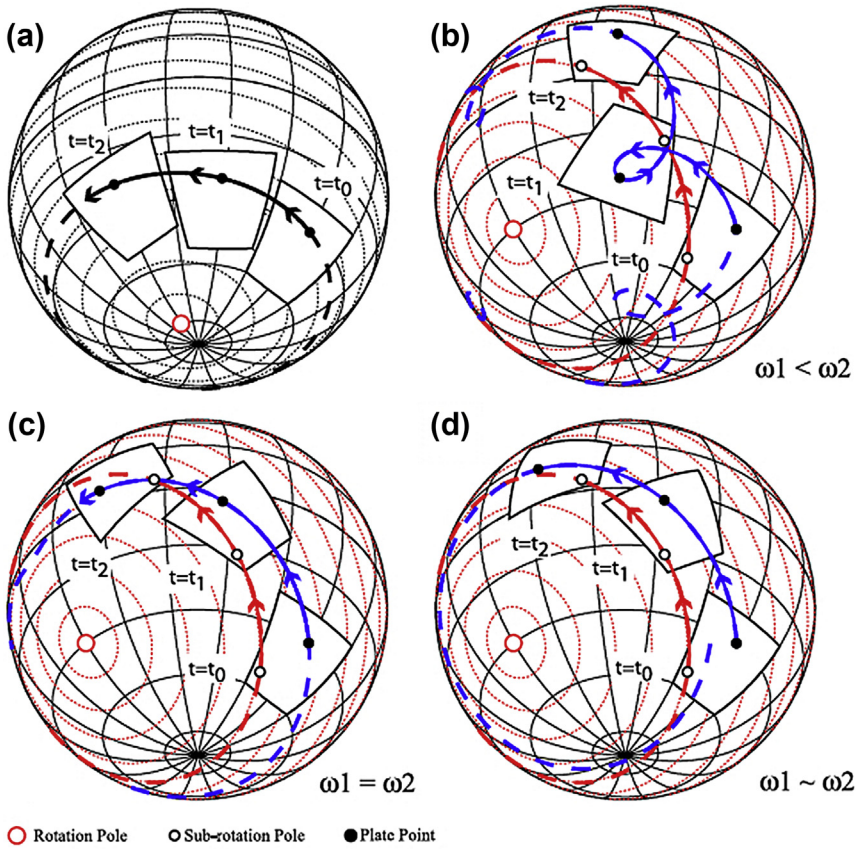

Figure 16 During their westerly directed journey, plates may experience some further rotation. This so-called subrotation deviates the mainstream of plate motion from the trend of the tectonic equator and may masque its presence. (a) One-rotation motion: at three different instants a plate rotates about the rotation pole, and one generic point follows a circular trace (black and red lines). (b) Two-rotation motion with $\omega 1 < \omega 2$: a generic point is constrained to move on a cycloid trajectory similar to the trace of the Moon around the Sun blue line. (c) Two-rotation motion with $\omega 1 = \omega 2$: a plate point moves on a circular trajectory, but it is not a small circle of the rotation pole. (d) When $\omega 1 \sim \omega 2$, a point of a plate follows a cycloid trajectory very similar to a circular one. In all cases, the subrotation pole is the only point that moves on a small circle centered on the main rotation pole of the plate. Several plates experienced subrotations with different angular velocity (e.g., counterclockwise (CCW): North America, Iberia, Arabia, India; clockwise (CW): South America, Antarctica. Apparently CCW subrotations occur in the northern hemisphere, and CW in the southern one). Subrotations may generate triple junctions. *After Cuffaro et al. (2008).*

transtension, the western plate moves faster westward. Relative plate motions are allowed by horizontal and vertical viscosity and density gradients both in the lithosphere and the underlying mantle (e.g., Forte & Peltier, 1987).

Tectonics and plate rotations of first order are localized along the global flow lines while those of second order are induced by localized body forces, therefore tectonic structures of the first order form perpendicular or with a great angle with respect to the mantle flow, while, for example, local rotations of plates may generate tectonic structures of the second order (e.g., the CCW rotation of Iberia generating both the Biscay Bay and the Pyrenees).

Lithospheric subduction into the mantle, particularly W-directed subduction, strongly enhances the coupling between the lithospheric plate and the underlying eastward mantle flow. Hence, subduction zones act as "nails" into the mantle and they strongly modify the relative plate velocities. The E- (or NE-) directed subduction zones have shallower dip than W- (or SW-) directed subductions and provide a much lower obstacle than the latter to the mantle flow, whose existence is naturally consistent with the ubiquitous asthenospheric LVZ (global circuit) detected below the TE-perturbed (TE-pert) (Panza et al., 2010), where no relevant obstacle is present against the global relative E-ward mantle flow. The concept of tectonic mainstream defined on the basis of geological evidence is consistent with space geodesy data, which supply a new unified way to describe plate motions with respect to the underlying mantle (Crespi et al., 2007). A parametric function in the form of a third-order Fourier series has been used to define the tectonic mainstream, based on the estimation of plate kinematics consistent both with velocities from space geodesy and geological evidence used as constraints. Three possible solutions under different hypotheses about the depth of the Pacific hot spot source, the velocity of the Pacific plate increasing with decreasing depth of the asthenospheric source, are confirming (1) the tectonic mainstream and (2) the net rotation of the lithosphere.

The shear-wave splitting technique (e.g., Savage, 1999) is an independent tool for detecting the asthenosphere seismic anisotropy, which is considered the result of the preferential orientation of olivine crystals in a sheared flowing mantle (Conder & Wiens, 2006; Silver & Holt, 2002). The direction of the anisotropy between lithosphere and underlying mantle (e.g., Barklage, Wiens, Nyblad, & Anandakrishnan, 2009; Debayle, Kennett, & Priestley, 2005; Fischer, Fouch, Wiens, & Boettcher, 1998; Montagner, 2002) aligns quite consistently with the absolute plate motions reconstructions, apart along subduction zones or other anomalous upper mantle portions. The level at which radial anisotropy is low, e.g., $<1\%$, due to the presence of

a relevant fraction of melt that inhibits the formation of preferential orientations in the texture of mantle rocks may be used to conventionally represent the decoupling level between the lithosphere and the underlying asthenospheric low-velocity layer (Panza et al., 2010).

A decoupling at the lithosphere base has been postulated in order to satisfy the geoid anomaly across transform zones by Craig and McKenzie (1986) who considered the existence of a thin low-viscosity layer beneath the lithosphere in their two-dimensional numerical models of convection in a fluid layer overlain by a solid conducting LID. Water content in the asthenosphere can drastically lower its viscosity to 10^{15} Pa•s (Asimow & Langmuir, 2003; Grove, Chatterjee, Parman, & Médard, 2006; Karato, Jung, Katayama, & Skemer, 2008; Korenaga & Karato, 2008). Moreover, the viscosity in the asthenospheric LVZ can be orders of magnitude lower when measured under horizontal shear with respect to the viscosity computed by vertical unloading due to postglacial rebound (Scoppola et al., 2006). Jin et al. (1994) have shown how the intracrystalline melt in the asthenospheric peridotites under shear can generate a viscosity of about 10^{12} Pa•s (Stevenson, 1994), a value compatible with the plate tectonics driven by the Earth's rotation (Scoppola et al., 2006). From literature (Jin et al., 1994; O'Driscoll et al., 2009; Pollitz et al. 1998) a contrast up to 10−15 orders of magnitude can be expected, which is well consistent with the decoupling, within the asthenosphere, between the lithosphere and the underlying mantle (Doglioni et al., 2011).

The presence of an ultralow-viscosity layer in the upper asthenosphere is thus a possibility consistent with the present-day available techniques of mantle sampling and laboratory experiment. Therefore, even if the occurrence of a westerly polarized lithosphere motion cannot be considered anymore a controversial phenomenon (Gripp & Gordon, 2002; Ricard et al., 1991, and reference therein), its origin may be due to different combined effects hard to single out. A mean lithospheric rotation (i.e., some plates like Nazca would still move eastward) could be preferred to a global phenomenon (e.g., Ricard et al. 1991) since the former preserves the angular momentum of the Earth without rapidly decelerating its rotation. However, Scoppola et al. (2006) have shown that a global lithospheric rotation is physically feasible, although with variable velocities of the different plates.

According to this model, plate tectonics would occur with the concurring contributions of the planet rotation under tidal torque, and lateral viscosity variations at the lithosphere-mantle interface, where, hosted in the LVZ asthenospheric layer, are supposed to occur thin hydrate layers with very-low

viscosity. These layers are beyond the reach of standard tomography due to the limitations of the theoretical tools employed: ray theory does not handle diffraction and frequency dependence, whereas normal mode perturbation theory requires weak and smooth lateral variations of structure (Anderson, 2007a,b; Boschi et al., 2007; Boyadzhiev et al., 2008; Foulger et al., 2013; Panza, Peccerillo, et al., 2007; Romanowicz, 2003; Vasco, Johnson, & Marques, 2003; Waldhauser et al., 2002). The viscosity of the upper asthenosphere is still unknown, but, as shown in Figures 1 and 2, the effective viscosity should be about 1000 times lower when measured for a horizontal shear with respect to vertical loading as simulated in classical postglacial rebound studies (Scoppola et al., 2006). This possibility is not contradicted by petrological and geophysical evidence about a very-low viscosity between 100 and 150 km of depth, within the LVZ of the upper asthenosphere (Hirth & Kohlstedt, 1996; Holtzman, Groebner, Zimmerman, Ginsberg, & Kohlstedt, 2003; Panza, 1980; Panza et al., 2010; Rychert, Fischer, & Rondenay, 2005). A 50–100 km thick layer with low viscosity remains invisible to postglacial rebound modeling (the channel flow model of Cathles, 1975). This layer, probably because well beyond the reach of standard tomography, is usually neglected and considered as a whole with the underlying higher viscosity lower asthenosphere and it is not included in current rheological models because of the real difficulty to handle numerically high-viscosity contrasts, as it is well described by Tackley (2008) and Ismail-Zadeh and Tackley (2010).

A global net rotation (Figures 2 and 9) is more coherent with the geological and geophysical asymmetries (Panza et al., 2010; Riguzzi et al., 2010), which favor a complete rotation of the lithosphere rather than only a mean rotation (Figures 10, 11 and 12). Relevant evidence about the tidal role for the existence of a net rotation is that the latitude range of the estimated tectonic *mainstream* is about the same as the Moon maximum declination range ($\pm 28°$) during the nutation period (≈ 18.6 year). Further indications come from the fact that the induced geopotential variations and the solid Earth tide modeling (McCarthy & Petit, 2004) generate extreme amplitudes of the Earth bulges ($\approx \pm 30$ cm) that propagate progressively within the same latitude range (Biagi, Pierantonio, & Riguzzi, 2006). In particular, the track of the semidiurnal bulge crest is roughly directed from E to W, as small circles moving from latitudes 28°–18°, when the Moon moves from maximum to minimum declinations (the same happens at negative latitudes for the opposite bulge), thus corroborating the role, within plate tectonics, of rotational and tidal drag effects (Bostrom, 1971; 2000). The TE is the ideal line (great circle) along

which plates move over the Earth's surface with the fastest mean angular velocity toward the west relative to the mantle (Crespi et al., 2007). Consistently with the present-day Vs resolution, the TE-pert (which is not a great circle) describes the trajectory along which a global circuit, formed by a ubiquitous LVZ at least 1000 km wide and about 100 km thick, occurs in the asthenosphere, where the most mobile mantle LVZ is located. The existence of a continuous global flow within the Earth mantle LVZ, capable to drive plates, is thus granted by the existence of the perturbed equator (Panza et al., 2010). The westward drift of the lithosphere implies that plates have a general sense of motion and that they are not moving randomly. If we accept this postulate, plates move along this trend at different velocities, relative to the mantle, toward the west along the flow line of the TE. In this view, plates would be more or less dragged by the mantle, as a function of the decoupling at their base, the degree of decoupling being mainly controlled by the thickness and viscosity of the asthenosphere.

3. ASYMMETRIES ALONG OPPOSITE SUBDUCTION ZONES

When comparing W- versus E- (or NE-) directed subduction zones, there are several differences that arise in terms of morphology, structural elevation, kinematics of the subduction hinge, gravity anomalies, heat flow, metamorphic evolution, slab dip, subsidence and uplift rates, depth of the decollement planes, mantle wedge thickness, magmatism, seismicity, backarc development or not, etc. The W-class includes all the western Pacific subduction zones (apart few deviations such as northern Japan), plus the Barbados, Sandwich arc, Apennines—Maghrebides, Carpathians, and Banda arc. The E-class contains all the eastern Pacific slabs beneath north, central and south America, the Alps, Dinarides, Hellenides, Cyprus, Zagros, Makran, Himalayas, Indonesia, New Guinea, Taiwan, Eastern Molucche, New Hebrides, and Southern New Zealand. For example, the western Pacific margins have a much lower topography with respect to the eastern margins. This difference has generally been ascribed to the occurrence to the continental nature of the South America upper plate and the younger oceanic more buoyant Nazca lower plate. However, when moving along the TE, this is a global signal, occurring all along W- versus E- or NE-directed subduction zones, regardless the composition and thickness of the upper and lower plates and they are strictly constrained by their geographic polarity (Harabaglia & Doglioni, 1998). Both margins show asymmetric free air gravity signatures

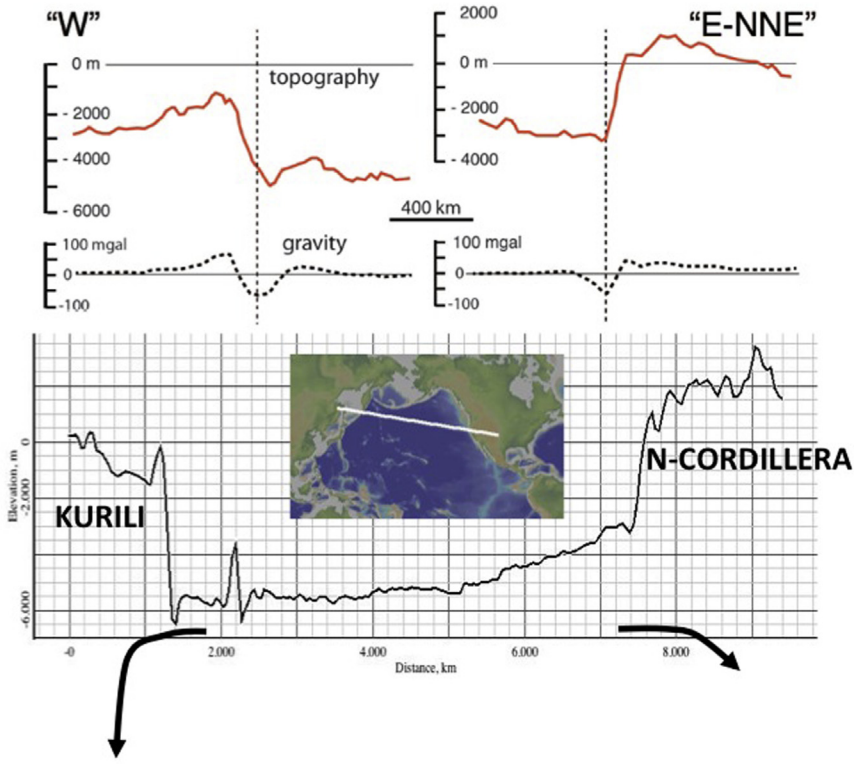

Figure 17 Average topography and free-air gravity profiles across subduction zones. Both data sets show distinct signatures that are function of the geographic polarity of the subductions. As an example the profile across the Pacific ocean shows low topography along the W-directed subduction zones of the western Pacific when compared to the eastern counterpart. Maxima and minima gravity anomalies are relatively more pronounced along the W-directed subduction zones and the negative gravity anomaly does not coincide with the lowest bathymetry along the trenches of the W-class. A similar asymmetry persists along all subduction zones of the world. *After Doglioni et al. (1999b). Pacific profile from the GeoMapApp software and database.*

(Figure 17). Moving along strike, an example is given by the high elevation of the southern island of New Zealand Alps associated to an NE-directed subduction zone, and the drastic lowering of topography—bathymetry when entering the W-directed Tonga—Kermadec subduction zone (Figure 18) in the northern island of New Zealand (e.g., Reyners, Eberhart-Phillips, Stuart, & Nishimura, 2006).

Subduction zones have been discovered and are usually marked by seismicity entering into the mantle. World seismicity disappears below 670 km of depth. Slabs generate earthquakes all along their dip, particularly in their

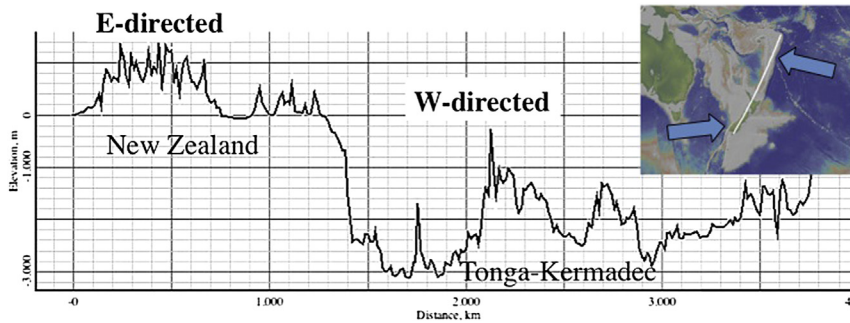

Figure 18 Moving from the New Zealand to the Tonga subduction zones, i.e., moving from an NE-directed subduction zone to a W-directed slab, the topography rapidly drops to much lower elevation. *Profile from the GeoMapApp software and database.*

elastic thickness where temperature remains lower with respect to the hosting mantle. In some slabs earthquakes are recorded from the shallow lithospheric layers down to the base of the upper mantle. This may occur along W-directed subduction zones, although not all of them show seismic events that deep (Figure 19). However, along the opposite E- or NE-directed slabs, the seismicity seems to disappear between 300 and 550 km of depth, and reappears between 550 and 670 km of depth. Therefore, along E- or NE-directed slabs, a peculiar seismic gap is visible, in particular beneath the Andes or the Indonesia Arc (Barazangi & Isacks, 1979; Chen, Bina, & Okal, 2001; Cahill & Isacks, 1992; Isacks & Barazangi, 1977; Milsom, 2005; Pardo, Comte, & Monfret, 2002; Pérez-Campos, Kim, Husker, Davis, Clayton, Iglesias, et al., 2008; Pilger, 1981; Rivera, Sieh, Helmberger, & Natawidjaja, 2002) before merging into the W-directed Banda arc subduction zone. Continental collisions are marked only by relatively shallow seismicity (hypocentral depth <300 km) and they occur only along E- or NE-directed subduction zones (Figure 19).

Another classical asymmetric signature of subduction zones is the steeper dip of W-directed slabs with respect to the opposite subduction zones (Figure 20), a difference that was known since the early stages of plate tectonics (e.g., Dickinson, 1978; Nelson & Temple, 1972; Uyeda & Kanamori, 1979). The slab dip was recently recomputed moving along the TE and confirming this angle variation (Riguzzi et al., 2010). Then the following questions arise quite logically about the origin of this asymmetric morphology of slabs: (1) Is there a relative easterly directed flow of the mantle that makes steep W-directed subduction zones and gentle the others (E- or NE-directed) as suggested by Nelson and Temple (1972) and Dickinson (1978)? (2) Is this

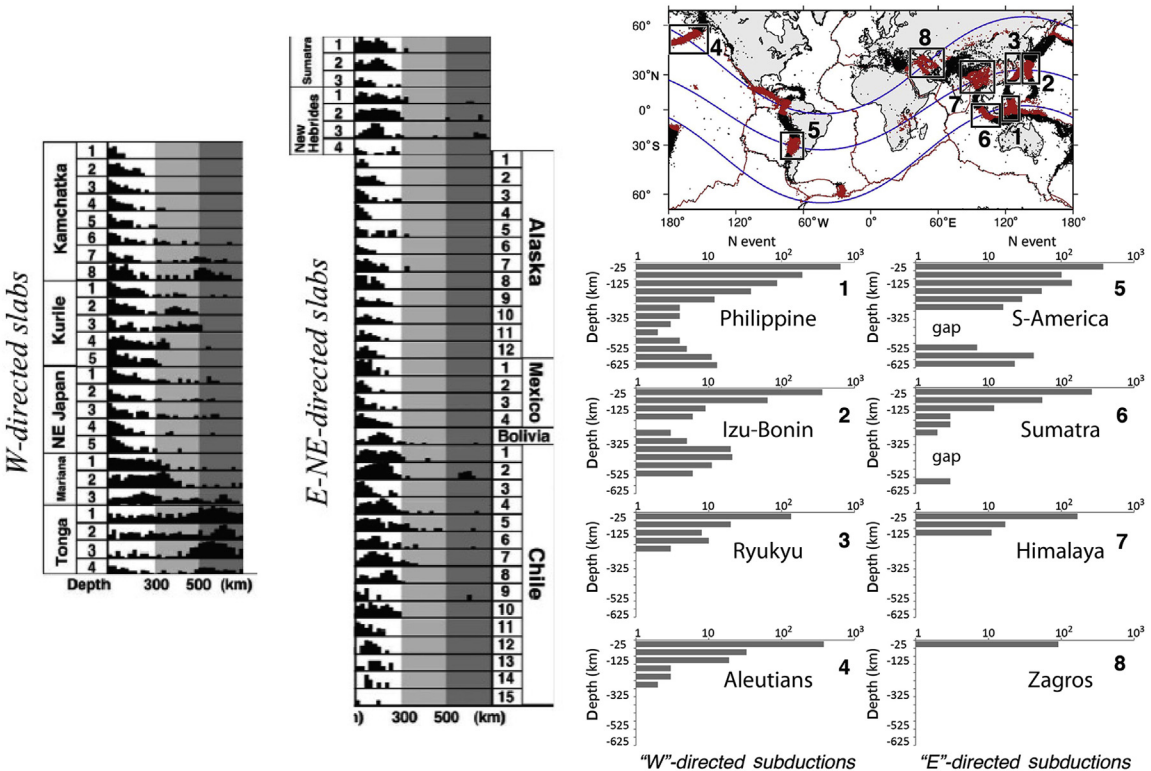

Figure 19 Left panels, the seismicity, reported by Omori, Komabayashi, and Maruyama (2004) along the main oceanic subduction zones, is plotted as a function of the geographic polarity, W- versus E- (or NE-) directed slabs. While in the slabs of the first group the earthquakes are distributed, rather continuously, from the surface down to their deep tip that may reach the bottom of the upper mantle, the opposite (E- or

asymmetry generated by the temperature contrast and negative buoyancy of slabs (e.g., Jarrard, 1986; Lallemand, Heuret, & Boutelier, 2005)? When comparing the slab age (which should correlate with their thermal state) and the dip of the slabs, no correlation is evident (Cruciani, Carminati, & Doglioni, 2005), therefore option (1) has more chances to be realistic.

A fundamental parameter that qualifies subduction zones is the slab hinge (e.g., Garfunkel et al., 1986; Waschbusch and Beaumont, 1996). Subduction zone kinematics predicts that, assuming a fixed lower plate, the velocity of the subduction (V_S) equals the velocity of the subduction hinge ($V_S = -V_H$). In all subduction zones the subduction hinge migrates toward the lower plate. However, if we rather refer to a fixed upper plate, the subduction hinge can instead either converge or diverge (Figure 21). Several interesting observations can be made assuming fixed the upper plate and converging the lower plate (Doglioni et al., 2006a; 2007). The velocity of subduction (V_S) is given by the rate of slab hinge (V_H) minus the convergence rate of the lower plate relative to the upper plate (V_L). When the slab hinge diverges, the subduction rate is higher than the convergence rate. If the slab hinge converges, the subduction rate decreases. The convergence is generally increased by the slab retreat, which is accompanied by backarc spreading along W-directed subduction zones (e.g., Tonga, Figure 21). The convergence is rather partitioned into subduction and contraction in the orogen associated to an E- or NE-directed subduction zone (e.g., Andes, Figure 21). The two end members, where the subduction hinge migrates away or toward the upper plate, largely match the two opposite cases of seismic decoupling or seismic coupling (e.g., Scholz & Campos, 1995) and mantle anelastic properties (Sacks & Okada, 1974).

NE-directed) subduction zones show a seismic gap from about 300 to 550 km depth. Right panels, global seismicity from ISC-GEM Global Instrumental Earthquake Catalogue (http://www.isc.ac.uk/iscgem), with lines corresponding to the tectonic equator and its related 30°N and 30°S small circles, *after Doglioni et al. (2014)*. These lines cross eight selected subduction zones (black rectangles), four W-directed (Philippine, Izu-Bonin, Ryukyu, Aleutians), and the other four E- (or NE-) directed (South America, Sumatra, Himalaya, Zagros). The depth distribution of the number of earthquakes, grouped in classes of 50 km depth, is shown. In panels 1, 2, the number of events is continuous, with a minimum in the range 200–350 km, while in panels 3 and 4 seismicity is shallower than about 300 km. Panels 5 and 6 show, on the contrary, the seismic gap typical of E- (or NE-) directed subduction zones; panels 7 and 8, represent continental subduction zones and the seismicity there is naturally shallow.

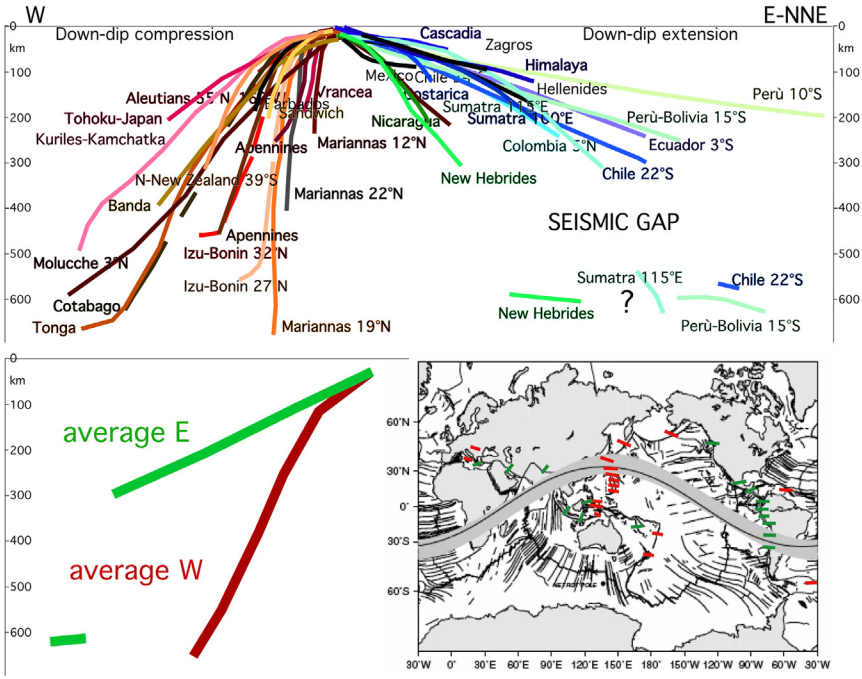

Figure 20 Compilation of the slab dip measured along cross sections perpendicular to the trench of most subduction zones. Each line represents the mean trace of the seismicity along every subduction. The asymmetry is marked by the steeper W-directed slabs and by the seismic gap, between around 300–550 km that occurs only along the E- (or NE-) directed subduction zones. Some E- (or NE-) subduction zones present a deeper scattered cluster of hypocenters between 550 and 670 km which may be interpreted either as a detached fragment of the slab, or as a portion of lower mantle sucked from below (by the tectonic syringe) in the wake left by the slab in its antisubduction (exhumation) motion. The W-directed slabs are, on average, dipping 65.6°, whereas the average dip of the E- (or NE-) directed slabs, to the right, is 27.1°. *After Riguzzi et al. (2010)*.

Combining the different possible movements, at least 14 kinematic settings can be distinguished along the subduction zones (Doglioni et al., 2007). Variable settings can coexist even along a single subduction zone. For example, along the Apennines subduction zone (e.g., Caputo, Panza, & Postpischl, 1970; 1972; Patacca & Scandone, 1989; Panza & Pontevivo, 2004; Pontevivo & Panza, 2006; Panza, 1978; Chiarabba et al., 2008) at least five different kinematic settings coexist. Along a single subduction zone there may be different kinematic settings, deviating from the standard model, and variable velocities, as a natural consequence of the combination V_H and V_L, can coexist (Devoti, Riguzzi, Cuffaro, & Doglioni, 2008). Relative to the

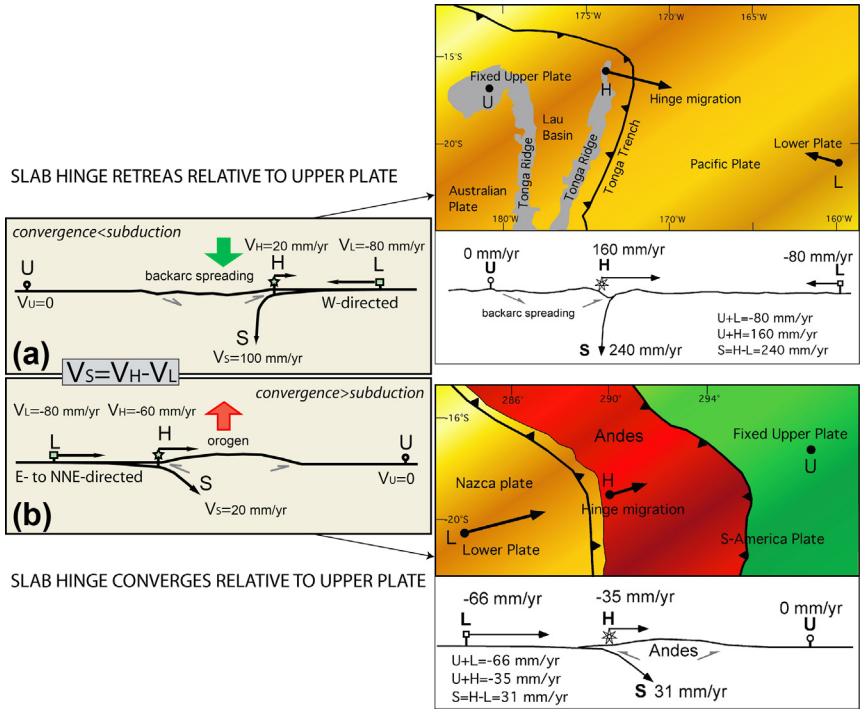

Figure 21 Left panel, basic kinematics of subduction zones, assuming fixed the upper plate U, a converging lower plate L, and a transient subduction hinge (H) that may either diverge or converge. The subduction rate S is given by $V_S = V_H - V_L$. Numerical values are given only as an example. S increases when H diverges relative to the upper plate (a), whereas S decreases if H converges (b). The movements diverging from the upper plate are positive, whereas they are negative when converging. The case (a) is accompanied by backarc spreading, a low prism, and it is typical of W-directed subduction zones. In case (b) that is more frequent along E-to NNE-directed subduction zones, double verging and elevated orogens form. In both W- and E- (or NE-) directed subduction zones, the hinge migrates eastward relative to the upper plate and suggests the action of a global tuning in subduction processes. Along the Tonga subduction zone, taken as fixed upper plate, the subduction rate is the sum of convergence between U and L, plus the motion of H. This is the fastest subduction in the world, where more than 700 km of lithosphere seem to sink in about 3 Ma. On the opposite side of the Pacific, along the E-directed Andean subduction zone, the convergence between Nazca and South America plates is faster than the shortening in the Andes. The upper plate shortening decreases the subduction rate. *After Doglioni et al. (2007).*

mantle, the W-directed slab hinges are almost fixed, whereas they move westward or south–westward along E- (or NE-) directed subduction zones. There are W- (or SW-) directed subduction zones that work also in absence of active convergence like the Carpathians or the Apennines. W-directed

subduction zones have shorter life (30–40 Ma) than E- or NE-directed subduction zones (even longer than 100 Ma). Therefore, the subduction process appears as a passive feature. Apart from few exceptions, the subduction hinge converges toward the upper plate along E- (or NE-) directed subduction zones, whereas it diverges from the upper plate along W-directed subduction zones accompanying backarc extension. W-directed subduction zones have usually shorter life and their backarc basin is eventually closed and its evolution inverted by an E-ward-directed subduction zone along the eastern margin of the backarc. In fact, at the present rates of hinge migration of the western Pacific subduction zones, if they were active since the Cretaceous, they would now be in the middle of the Pacific Ocean. An example of this cyclic evolution may be the northern Japan, where along a "W"-directed subduction zone (from north of the Tokyo triple junction), the slab hinge is converging relative to the upper plate, hence contracting since the Late Pliocene-Pleistocene(?) the previously extended Oligo–Pliocene backarc basin of the Japan Sea (Doglioni et al., 2007).

Consequently, backarc spreading forms in two settings: (1) along the W-directed subduction zones the "normal" backarc is determined by the hinge divergence relative to the upper plate, minus the volume of the accretionary prism, or, (2) in case of scarce or no accretion, minus the volume of the asthenospheric intrusion at the subduction hinge (Doglioni, 2008). Since the volume of the accretionary prism is proportional to the depth of the decollement plane, the backarc rifting is inversely proportional to the depth of the decollement. On the other hand, along E-directed subduction zones, few backarc basins form (e.g., Aegean, Andaman) and can be explained by the velocity gradient within the hanging wall lithosphere, separated into two plates. Before collision, orogen growth occurs mostly at the expenses of the upper plate shortening along E- (or NE-) directed subduction zones, whereas the accretionary prism of W-directed subduction zones increases at the expenses of the shallow layers of the lower plate. The convergence between the upper and lower plates and the shortening in the related accretionary prism or orogeny can be related into the convergence/shortening ratio. This value is <1 if the slab hinge diverges relative to the upper plate, whereas it is >1 if the hinge converges (Figure 22). For example, in the Andes this ratio is around 1.8 (Doglioni et al., 2006a). The convergence/shortening ratio in this type of orogens is inversely proportional to the strength of the upper plate and it is directly proportional to the coupling between upper and lower plates. The higher the strength and lower the coupling, the smaller the shortening and faster is the subduction rate.

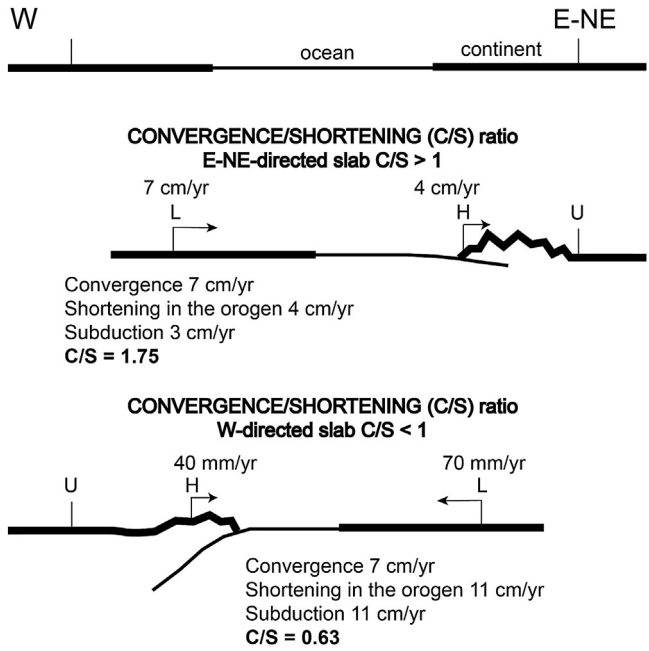

Figure 22 The convergence/shortening ratio (C/S) describes how the convergence between two plates is partitioned into subduction and shortening. The different behavior of the subduction hinge determines an increase or a decrease of the subduction rate. Along E- (or NE-) directed subduction zones, the C/S is larger than 1 and the convergence rate contributes to contraction and subduction. Along the opposite W-directed subduction zones the convergence rate adds to the hinge divergence rate and C/S < 1.

Typically, this opposite behavior occurs along W-directed subduction zones (C/S ratio <1) and along the E- or NE-directed slabs (C/S ratio >1). Deviations from this rule occur, for example, in northern Japan, where the subduction hinge after and Oligocene–Pliocene motion away relative to the Eurasia upper plate is now converging (Doglioni et al., 2007).

The steeper and faster slabs along W-directed subduction zones determine that the volume recycled into these subduction zones is about three times larger than that along the converse subductions. Moreover, the asthenospheric mantle wedge at the subduction hinge along the same W-directed slabs is thicker and likely warmer than in the converse E- or NE-directed subduction zones (Figure 23). This interpretation appears confirmed by the seismic velocity anomaly (fast) detected at 600 km depth along the western Pacific, suggesting a larger occurrence of colder slabs along W-directed subduction zones than in the converse subductions

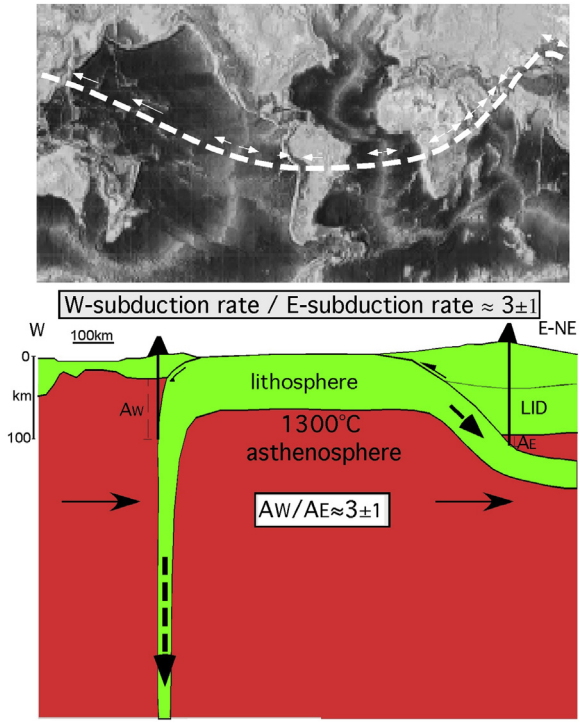

Figure 23 The main differences between subduction zones of opposite polarity along the tectonic equator, reported in the top map, can be naturally attributed to the relative "eastward" mantle counterflow. The volumes recycled along W-directed subduction zones are about 3 times larger than those recycled along the converse settings due to the aforementioned kinematic constraints. Moreover, the asthenospheric wedge above slabs along W-directed subduction zones (AW) is thicker than the asthenospheric wedge in E- (or NE-) directed subductions (AE). *After Doglioni et al. (2009).*

(Figure 24). The mantle wedge shows a systematic geophysical and magmatic signature that is a function of the composition and thickness of the involved plates and the polarity of the subduction (Figure 25). Besides the westward drift, there are at least two basic reasons why in the E- (or NE-) directed subduction zones (e.g., central America, Andes, Alps, Dinarides, Zagros, Himalayas, Indonesia) the mantle wedge is thinner when compared with that of the W-directed ones: (1) as a rule, the continental upper plate of the E- (or NE-) directed subductions is thick (e.g., Artemieva & Mooney, 2001; Chimera, Aoudia, Sarao, & Panza, 2003; Dal Piaz et al., 2003; Laubscher, 1988; Manea, Manea, Kostoglodov, Currie, & Sewell, 2004; Panza, 1980; Panza et al., 1982; Panza, Pontevivo, Chimera, Raykova, & Aoudia, 2003; Polino et al., 1990; Vinnik, Singh,

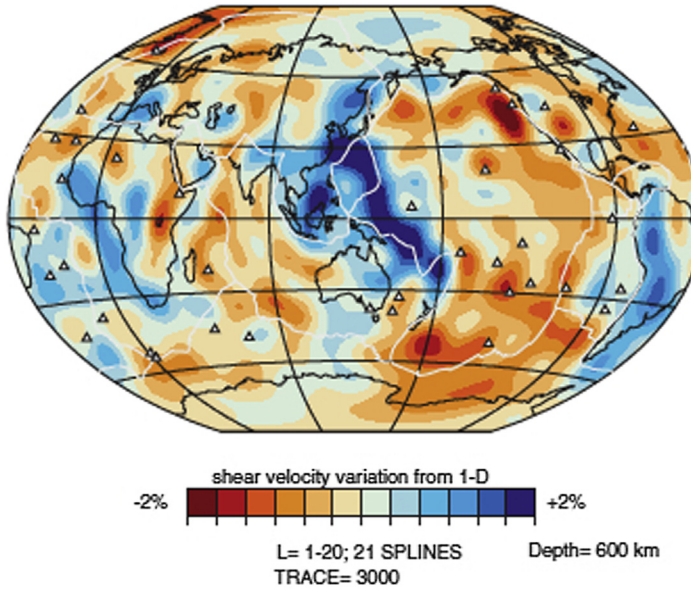

Figure 24 Shear-wave velocity anomalies at 600 km depth. *(After Ritsema (2005).)* The faster velocities, which are seen along the western side of the Pacific confirm the larger and deeper volumes of rigid lithosphere carried down in the mantle along the W-directed slabs, than elsewhere.

Kiselev, & Kumar, 2007) and (2) the slab is, on average, less steep than in W-directed subductions (Cruciani et al., 2005; Riguzzi et al. 2010). Moreover, W-directed subduction zones should generate a corner flow when entering the mantle. Relative to mantle and based on the kinematics derived from the hot spot reference frames, E- or NE-directed subduction zones are moving relatively "westward" with respect to the mantle, i.e, not moving in the direction of the subduction, but actually moving "out" of the mantle. This process, like the action of a tectonic syringe where the plate plays the role of the plunger and the ambient mantle that of the barrel, seems to be bound to generate an opposite mantle flow such a sucking upward of the underlying mantle (upduction). Subduction occurs because the upper plate moves "westerly" along the tectonic mainstream faster than the lower plate (Figure 26). Geochemical signatures support such different geometry and kinematics.

In principle, the volume accreted in a prism located along the trench of a subduction zone depends on (1) the amount of subduction occurred and (2) the depth of the basal decollement plane (Figure 27). Therefore, with a given subduction rate, the accretion depends upon the depth of the

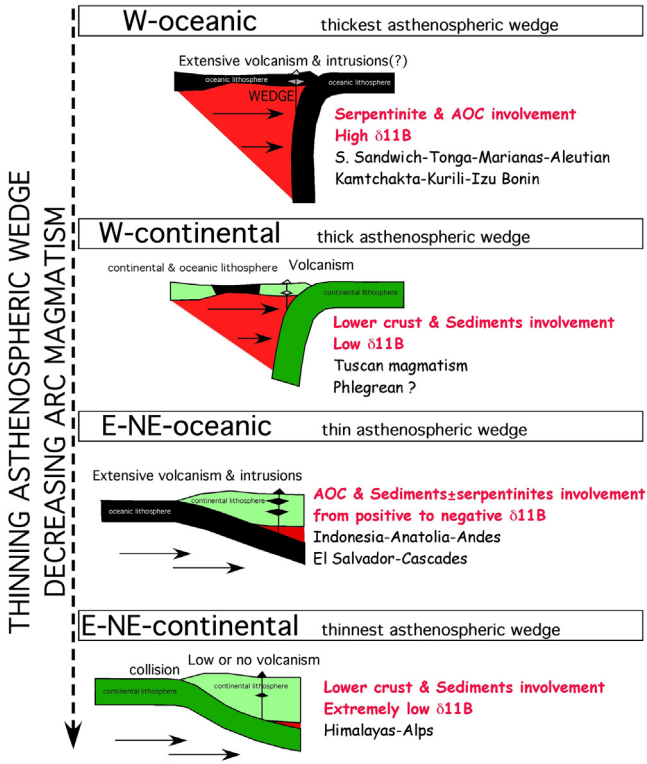

Figure 25 The four cases represent the possible settings of W-directed and E- (or NE-) directed subduction zones as a function of the composition of the lower plate (oceanic or continental). The volume of magmatism is very likely controlled by the slab dehydration, the asthenospheric wedge thickness, and the subduction rate. The thickness of the asthenospheric wedge increases with increasing slab dip while decreases with increasing thickness of the upper plate. The thickest mantle wedge of asthenosphere is seen along the W-oceanic case, where the slab is very steep and the upper plate is composed by young oceanic lithosphere. A slightly thinner asthenospheric wedge occurs in W-continental case, where it is expected a shallower melting of the lower plate. The steepness of the slab along the W-cases is controlled by the negative buoyancy (if any) and by the advancing mantle flow. Along the E-oceanic case, widespread volcanism forms; the upper plate can also be oceanic (usually older than the lower plate). The thinnest asthenospheric wedge likely occurs along the E- (or NE-) continental case, where in fact the lowest amount of volcanism is observed. The low negative (if any) or positive buoyancy and the sustaining mantle flow control the low dip of the slab in the E-cases. AOC, altered oceanic crust. *After Doglioni et al. (2009).*

decollement layer, which may vary along strike and move through lateral ramps into stratigraphic layers that have lower friction. The areas of the accretionary wedges in the hanging wall of W-directed subduction zones

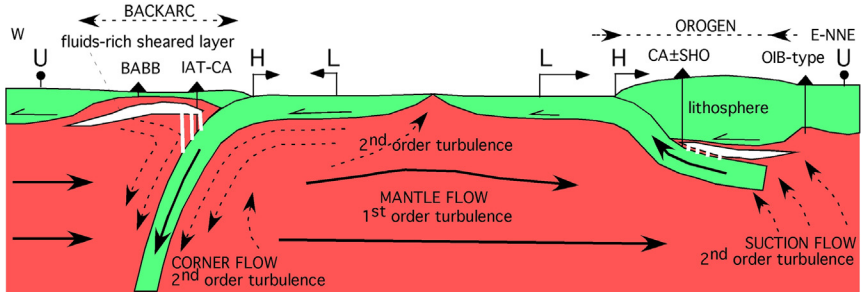

Figure 26 The subduction zones perturb or deviate the general "eastward" flow of the mantle relative to the lithosphere. W-directed slabs produce a corner flow, whereas the opposite slab could rather generate an upward suction flow from the underlying mantle (tectonic syringe). Such suction may cause the upraise of "fertile" mantle from below, and its decompression may generate locally OIB-type magmatism. The fluids released by both W- and E- (or NE-) directed slabs (e.g., the white lenses in the hanging wall of the subduction) decrease the viscosity at the top of the asthenosphere and speed up the upper plate. The fluids are sheared by the lithospheric decoupling, determine a migration away from the lower plate along W-directed subduction zones and generate backarc spreading. The suction triggers an opposite behavior along the E- (or NE-) directed subduction zones where the westward increase of the upper plate velocity rather facilitates the convergence between the upper and lower plate, i.e., it determines a double verging Andean Alpine-type orogen. BABB: backarc basin basalts; IAT: island-arc tholeiites; CA, SHO: calc-alkaline and shoshonitic series; OIB-type: basalts with ocean island or intraplate affinity. H, subduction hinge; L, lower plate; U, upper plate. The arrows indicate the velocity of L and H with respect to fixed U and not with respect to the mantle. *After Doglioni et al. (2009).*

are much smaller than the average area accreted in orogens associated to the opposite subduction zones. This implies that W- versus E-directed subduction zones have shallow and deep decollement planes, respectively. Therefore, having a deeper decollement, the orogens associated to the E-directed subduction zones may uplift deep-seated rocks and large volumes of the lower plate (Figure 27). This may explain why W-directed subduction zones mostly accrete shallow rocks of the lower plate, whereas E- or NE-directed subduction zones have uplifted ultradeep-seated rocks such as ultrahigh-pressure rocks of both the lower and the upper plate (e.g., diamond-bearing eclogites). The larger volumes involved in E- or NE-directed subduction zones determine higher critical taper with respect to the W-directed subduction zones (Figure 28).

All subduction zones show the flat foreland gradually merging into the trench or beneath the foredeep or foreland basin. This angle becomes steeper when approaching the belt and the inclined plane is called foreland

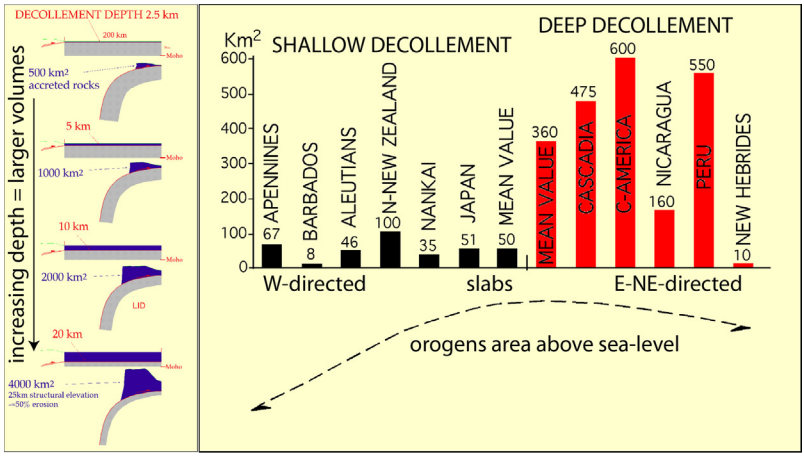

Figure 27 Left panel: with a given subduction amount, e.g., 200 km, the area/volume accreted in the accretionary prism depends on the depth of the decollement. The deeper the decollement, the bigger the orogen. Right panel: the average areas above sea level of the prisms of the main subduction zones, show that orogens above E- (or NE-) directed subduction zones are about 6–8 times larger than the accretionary prisms related to W-directed subduction zones *(after Lenci & Doglioni, 2007)*. This means that the decollements are deeper and exhume larger volumes along E- (or NE-) directed subduction zones than in the W-directed cases.

regional monocline. The angle is steeper beneath W-directed subduction zones with respect to the converse slabs (Figure 28). In fact, the foreland regional monocline is the shallow expression of the subduction hinge and reflects the attitude of W-directetd slabs for steep angles. Above the regional monocline develops the foredeep or foreland basin in all subduction zones. Therefore, the steeper the regional monocline, the deeper the foredeep basin is. W-directed subduction zones have the deepest and fastest subsiding foredeeps. The foredeep or trench may be filled (e.g., the 8 km of Plio–Pleistocene sediments of the Po Basin) or unfilled (e.g., the Mariana trench), and it subsides at the highest rates (>1 mm/yr). On the contrary, E- or NE-directed slabs have a foredeep in front of the forebelt and a conjugate foredeep in the foreland of the retrobelt. These two foredeeps have low subsidence rates (<0.3 mm/yr) and are generally quickly filled and bypassed by the large sediment supply of the higher associated orogens (Figure 29). The asymmetry of the foredeeps as a function of the subduction zone (Doglioni, 1992; 1993b; 1994) is also manifested by the ratio between the area of the orogen and the area of the foredeep which is <1 along W-directed subduction zones, whereas it is >1 along E- or NE-directed subduction zones

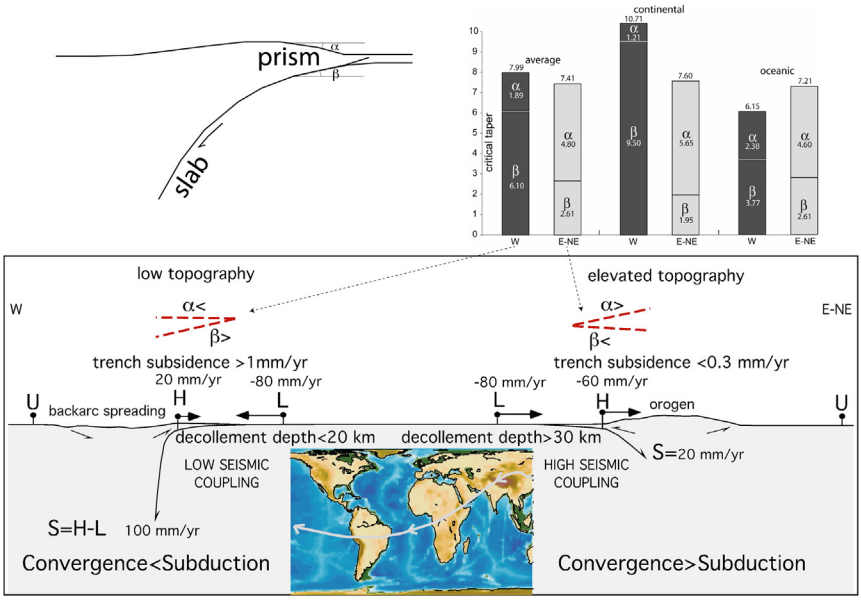

Figure 28 Average values of the topographic envelope (α), dip of the foreland monocline (β), and critical taper (= α + β) for the two classes of subduction zones, i.e., W-directed and E- (or NE-) directed. The "western" classes reach lower values of α and larger (steeper) values of β than "eastern" classes. Assuming fixed the upper plate U, along W-directed subduction zones the subduction hinge H frequently diverges relative to U, whereas it converges along the opposite subduction zones. L, lower plate. The subduction S is larger than the convergence along W-directed slabs, whereas S is smaller in the opposite case. The two end members of hinge behavior are respectively accompanied, on average, by low and high topography, steep and shallow foreland monocline, fast and slow subsidence rates in the trench or foreland basin, single vs double verging orogens, etc. All this highlights a worldwide subduction asymmetry along the flow lines of plate motions (tectonic equator) indicated in the insert. *Modified after Lenci and Doglioni (2007).*

(Figure 29). The shape of the foredeeps is regularly arcuate in case of W-directed subductions, while it is almost linear or it follows the shape of the inherited continental margin in case of E- (or NE-) directed subductions. Fold development in the two kinds of foredeeps is significantly different: in W- (or SW-) directed subductions the folds are carried down in subduction while they are forming and consequently they are poorly eroded. In the E- (or NE-) directed subduction folds and thrust sheets are instead uplifted and deeply eroded. The first-order arc of a W-directed subduction zone constrains the general geometry of the foredeep. However, variations in depth and forward propagation of the decollement generate

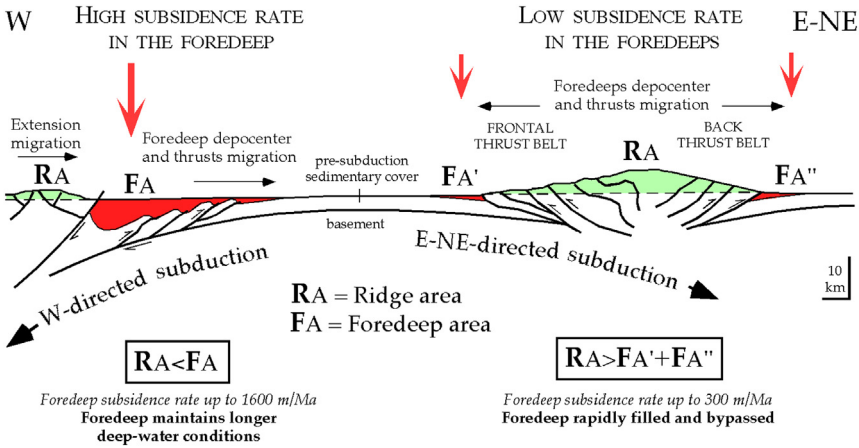

Figure 29 Foredeeps or foreland basins are asymmetric as a consequence of the polarity of the pertinent subduction zone. W-directed subduction zones are characterized by one foredeep with a basal steep monocline generated by slab retreat and have high (>1 mm/year) subsidence rates. The cross-section area of the foredeep is larger than that of the associate accretionary prism. Therefore, these basins provide huge accommodation space, which may be filled (e.g., Apennines, Carpathians) or unfilled (e.g., Marianas) by sediments. E- (or NE-) directed subduction zones rather have two foredeeps or foreland basins at the fronts of the forebelt and the retrobelt, respectively. They show a shallow foreland regional monocline dip and they are mostly generated by the lithostatic load of the orogen. The foredeeps have an area smaller than the area of the orogen and low (<0.3 mm/year) subsidence rates. These foredeep basins are quickly filled and bypassed. Collisional orogens related to plate subrotation (e.g., Pyrenees) show the characters of collisional orogens such as those pertaining to the E- (or NE-) directed class of subduction zones. *After Doglioni (1994).*

oscillations (arcs) of the thrust belt front, i.e., second-order salients and recesses (Doglioni, 1991).

In the past, W-directed subduction zones have been less investigated than the converse subduction zones because the former are mostly below sea level. Therefore, their different characters are less known. However, they have specific signatures, which are listed in Figure 30. They have an arcuate shape of the frontal part, whereas the backarc basin shows an opposite convexity. They are short lived (usually <50 Ma) and are associated to a backarc development; they may occur only if there is a thinned and heavier, possibly oceanic, lithosphere to the east of a lighter and thicker lithosphere; they present a new generated Moho in the hanging wall of the slab and they show the magmatic pair alkaline–calc-alkaline magmatism, etc. (Figure 30). E-verging arcs associated to W-directed slabs are a few thousand kilometers

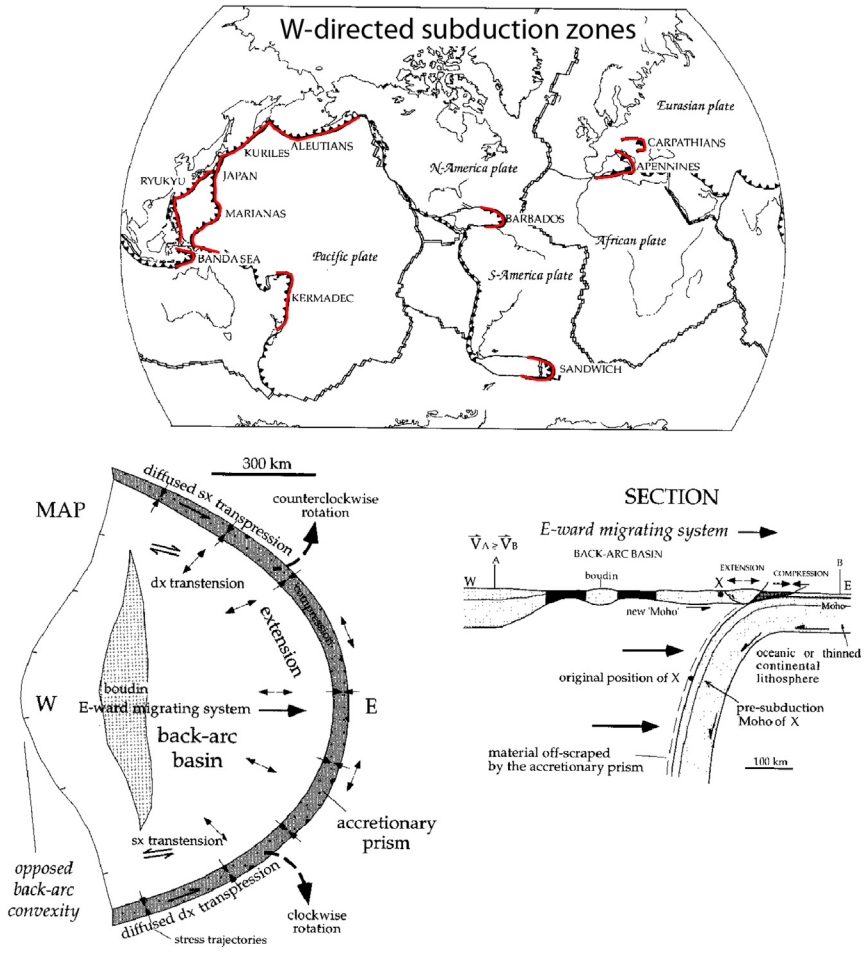

Figure 30 Main characters of W-directed subduction zones: (1) the arcuate shape toward the foreland; (2) the concave geometry of the western margin of the backarc basin opposed to the convexity of the external arc; (3) the presence of an accretionary wedge along the external arc and a backarc basin to the west; (4) the "E"-ward migration of the system; (5) the accretionary wedge dimension depends on the amount of subduction and depth of the decollement plane; (6) the relatively short-lived system (40–50 Ma) with respect to the opposite subduction which may last longer; (7) the lithospheric boudinage in the backarc setting; (8) the steep or vertical slab; (9) the fast retreat of the subduction hinge relative to the upper plate; (10) the deep trenches and fast subsidence rates in the external foredeep (>1 mm/year); (11) the lithosphere thinning in the backarc of the upper plate and fast subsidence rates (>0.5 mm/year); (12) the low elevation of the accretionary wedge (on average 1 km below sea level) and the entire upper plate setting; (13) the formation of a new Moho and new LID at the base of the upper plate; (14) the E-ward migrating magmatic pair of calc-alkaline–shoshonitic and alkaline–tholeiitic suites; (15) the thin-skinned tectonics in the accretionary wedge and thick-skinned in the backarc basin; (16) all the gravimetric, heat flow, seismological signatures that show extreme minima and maxima excursions of this geodynamic setting (e.g., high gravity and heat flow anomalies and low Q factor in the backarc basin and vice versa in the accretionary prism and trench).

long (1500–3000 km); they are characterized by a frontal accretionary wedge and backarc basin propagating together "eastward". The accretionary wedge scrapes off superficial layers of the downgoing plate (thin-skinned tectonics) whereas the backarc extension crosscuts the entire subduction hanging wall (thick-skinned tectonics). The slab of this type of subduction is steep to vertical and the hanging wall of the subduction has a mean depth of 1 km below sea level. Trenches and foredeeps are the deepest basins of the Earth and their mean depth is about 5 km below sea level. The foredeep in W-directed subduction zones can be explained by the slab retreat pushed by the relative eastward mantle flow (slab hinge diverging relative to the upper plate) while foredeep along the E- (or NE-) directed subduction zones can instead be generated by coexisting load of the orogen, the downward component due to the advancing upper plate plus the contrasting upward push of the mantle that flows in the direction of the subduction. W- (or SW-) directed subduction zones occur both in the case of the largest E–W convergence rates among plates (e.g., W-Pacific examples) and of no or very low convergence (e.g., Apennines, Carpathians). In the Mediterranean, the Adriatic continental lithosphere (e.g., Panza, Raykova, Carminati, & Doglioni et al., 2007; Venisti, Calcagnile, Pontevivo, & Panza, 2005) and the Ionian oceanic (?) lithosphere (e.g., Calcagnile, D'Ingeo, Farrugia, & Panza, 1982; Cernobori et al., 1996; Farrugia & Panza, 1981; Nicolich, Laigle, Hirn, Cernobori, & Gallart, 2000; Panza, Peccerillo, et al., 2007, Panza, Raykova, et al., 2007b; de Voogd et al., 1992) are subducting both under the Apennines (steep W-directed subduction) and under the Dinarides–Hellenides (shallow NE-directed subduction) (e.g., Brandmayr et al., 2010; Christova & Nikolova, 1993; El Gabry, Panza, Badawy, & Korrat, 2013; Selvaggi & Chiarabba, 1995) and with very scarce seismic activity (deformation) in the horizontal part of the plate.

The two-related thrust belts follow respectively the geological and geophysical characters of the east and west Pacific subduction zones discussed in this chapter, regardless age and thickness variations of the subducting lithosphere. In the Pacific, the W- (or SW-) directed subductions are the fastest in the world and the slab is steep, while the South America Cordillera (E- or NE-directed subduction related) is active since the Mesozoic and the slab inclination is less than about 25° (Riguzzi et al., 2010). This behavior cannot be explained in terms of age of the subducting lithosphere and of slab pull as well documented, for example, in the Mediterranean by Brandmayr, Marson, Romanelli, and Panza (2011) and El Gabry et al. (2013).

Subductions may initiate when two basic conditions are satisfied: (1) the two plates have at least an initial convergent component of relative plate motion and (2) one of the two plates is sufficiently denser, thinner, stronger, and wider to be overridden by the other. As a counterexample, when an oceanic rift opens to a width equal or smaller than the thickness of the adjacent continental lithosphere, a complete subduction cannot develop (Doglioni et al., 2007). In other words, small oceans (150–200 km wide) cannot generate normal, steady-state, subduction systems. This setting can rather evolve to obduction, where ophiolitic slices of the oceanic realm are buckled and squeezed on top of the continental lithosphere. One example could be the Oman ophiolite complex (Garzanti, Vezzoli, & Andò, 2002; Garzanti, Doglioni, Vezzoli, & Andò, 2007; Nicolas, Boudier, Ildefonse, & Ball, 2000), even if it is unclear whether this ocean was a narrow independent basin, or rather part of a wider Tethyan branch (Stampfli & Borel, 2002).

Following the Atlantic subduction zones (Barbados and Sandwich arcs), the W-directed subduction zones develop along the retrobelt of former E- (or NE-) directed subduction zones, where oceanic lithosphere occurs in the foreland to the east, where the northern and southern American continents narrow (Figure 31). This applies to the onset of the Apennines subduction

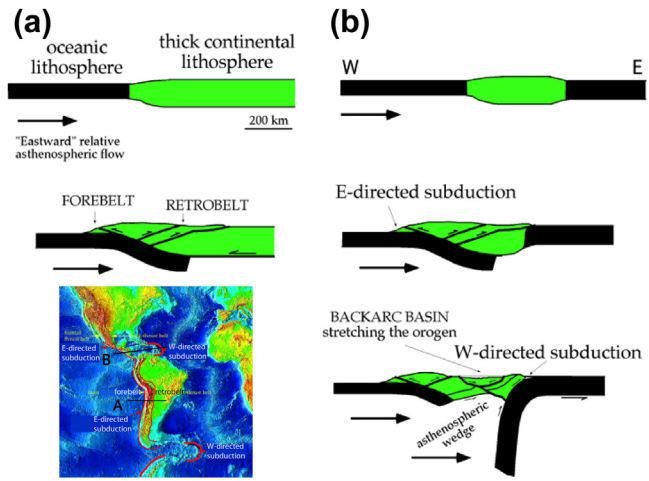

Figure 31 The Barbados and Sandwich arcs formed only where the American continents narrow. Their W-directed subduction zones evolved only where there was Atlantic oceanic lithosphere in the foreland of the retrobelts of the E-directed subduction zones of the northern and southern American Cordillera. Similarly the origin of W-directed subduction zones in the Mediterranean (Apennines and Carpathians) and elsewhere in the world can be explained. *After Doglioni et al. (1999a).*

along the retrobelt of the Alpine–Betic orogen where Tethys oceanic crust was present to the "east." The Alpine orogen was stretched and scattered in the Apennines backarc basin. The backarc extension is internally punctuated by necks (subbasins) and boudins, horsts of continental lithosphere. The asymmetric extension in the backarc basin appears controlled by differential drag between the eastward mantle flow and the overlying, passively transported, crustal remnants. Compression in the accretionary prism may be interpreted as the superficial expression of the shear occurring between the downgoing lithosphere and the horizontally moving mantle which compensates the slab rollback (see Chapter 5).

Opposite to the W-directed subduction zones, the E- or NE-directed subduction can nucleate only in case of an oceanic or thinned continental lithosphere located to the west of a thicker lithosphere to the east. For example, the future closure of the Atlantic Ocean should only start with a subduction along the African and European coasts, along the eastern margin of the basin, where oceanic lithosphere is located to the west of the continent. Therefore, the future subduction and closure should not form at the plate boundary, but within the African and European plates, at their continent–ocean transition. Unlike W-directed slabs, in the shallow hot spot reference frame, E- (or NE-) directed subduction zones should have the lower plate moving "out" of the mantle, i.e., the slab is not actively entering into the hosting mantle. If the kinematic reconstruction is correct, the subduction occurs because the upper plate moves westward or south–westward faster than the lower plate, overriding it. In Figure 32 is shown the Nicaragua example, where the Cocos plate moves westward relative to the mantle, slipping above the LVZ in which, by means of magnetotelluric data, melting can be inferred in a less resistive layer. In this model, the slab is entirely passive to plate tectonics, i.e., not actively driving neither its subduction nor the motion of the plate.

The orogens associated to conversely directed subduction zones exhibit the involvement of different crustal sections and different outcropping rocks. This is related to the peculiar PTt paths associated to the two typologies of subduction zones, as a function of their transit above or below the decoupling surfaces (Figure 33). The different decollements in the two end members of subduction should control different PTt paths and, therefore, generate variable metamorphic assemblages in the associated accretionary wedges and orogens (Figure 33). These asymmetries determine different topographic and structural evolutions that are marked by low topography and a fast "eastward" migrating structural wave along W-directed subduction zones,

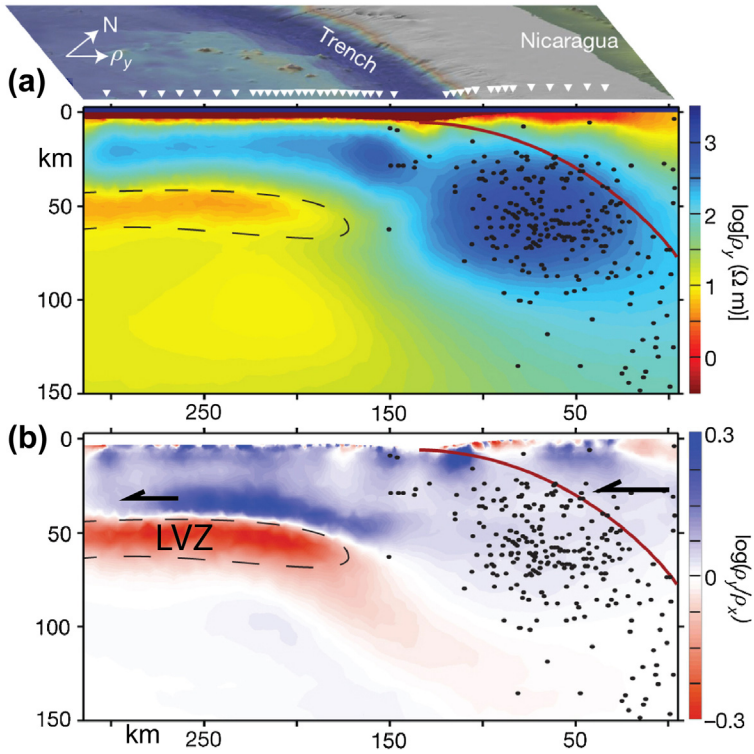

Figure 32 Resistivity model obtained from anisotropic inversion of the seafloor magnetotelluric data of the Cocos subduction beneath central America. *(Slightly modified after Naif et al. (2013).)* (a) The electrical resistivity in the direction parallel to plate motion (ρ_y). Blue (light gray in print versions) and red (gray in print versions) colors correspond to resistive and conductive (less resistive) features, respectively. The red (dark gray in print versions) line is a model of the top of the subducting slab. Earthquake hypocenters from up to 50 km off-axis are shown as black dots. The zone enclosed by the dashed black line is where the model is at least 1.5 times more conductive in the direction parallel to plate motion than in other directions. The relatively more conductive layer is interpreted as the LVZ containing melt and having low viscosity that allow for decoupling. According to the plate kinematics in the shallow hot spots reference frame, both lower and upper plates are moving "westerly" relative to the mantle and the subduction occurs because the upper plate is faster to the west. (b) Resistivity ratio for the plate-motion-parallel (ρ_y) and to trench-axis-parallel (ρ_x) model components. The color scale is for $\log(\rho_y/\rho_x)$ that shows the strong anisotropy of the conductive layer at 45–70 km depth (red (gray in print versions) regions >150 km offshore). The deeper mantle beneath the conductive layer is isotropic, and suggests that it is not being sheared, i.e. the slab is entirely passive to plate tectonics. *See Naif et al. (2013) for details.*

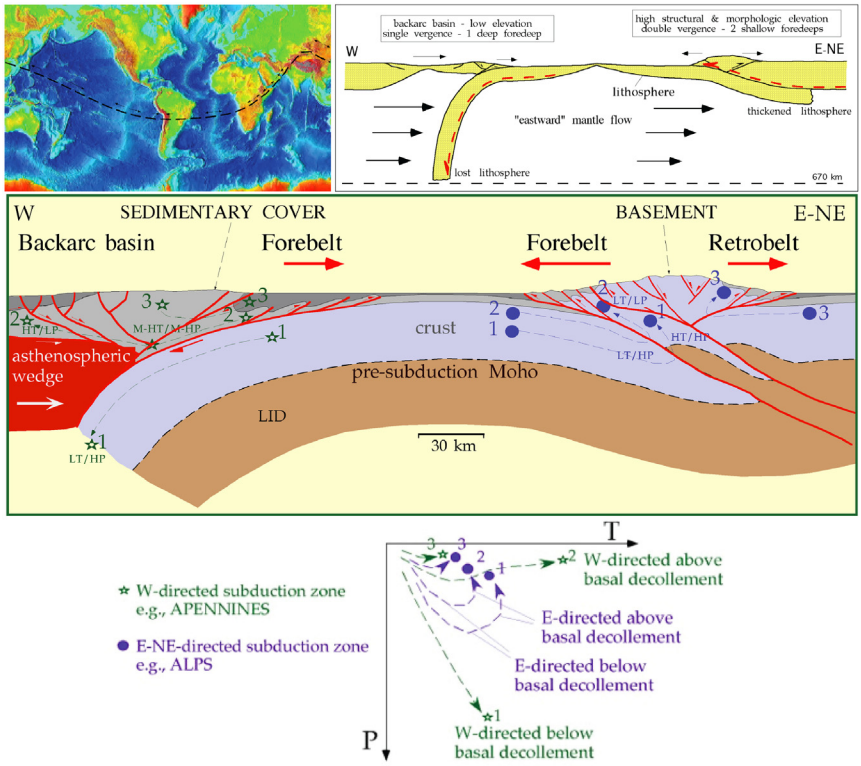

Figure 33 Main differences among subduction zones and related orogens as a function of their geographic polarity relative to the tectonic equator (upper panel). The two end members show distinct PTt evolution. The different paths of rocks in the two settings depend on the depth and migration of the decollement planes and on the original starting level of the PTt path of the sample (lower panel). The subductions opposing (W- or SW-directed) the mantle flow show low structural and morphological elevation with shallow rocks involved; the tangent to the anticlines of a predeformation marker is descending into the trench and the depocenter of the deep foredeep basin is within the accretionary wedge (e.g., Apennines). The subductions (E- or NE-directed) that follow the mantle flow rather show high structural and morphological elevation, deep rocks involved (i.e., America Cordillera) and the tangent to a predeformation marker is rising toward the hinterland. The shallow foredeep is mainly located in front of the belt. The basal decollement of the W-directed subduction accretionary prism travels in the upper layers of the downgoing slab, which is delaminated (i.e., most of it subducting). The basal decollement of the E- (or NE-) directed subduction is rather deeply rooted into the whole crust of the upper plate and eventually of the lower plate at the collisional stage. LT, low temperature; LP, low pressure; HT, high temperature; HP, high pressure, M, middle.

whereas the topography and the structure are rapidly growing upward and expanding laterally along the E- or NE-directed subduction zones.

The magmatic pair calc-alkaline and alkaline—tholeiitic volcanic products of the island arc and the backarc basin characterize the W-directed subduction zones. Magmatic rocks associated with E- (or NE-) directed subduction zones have higher abundances of incompatible elements, and mainly consist of calc-alkaline—shoshonitic suites, with large volumes of batholithic intrusions and porphyry copper ore deposits (Doglioni, Merlini, & Cantarella, 1999). Moreover, the thermal and gravity signatures depend on the variable average depth of the asthenosphere in the two settings (e.g., much shallower in the backarc of the W-directed subduction zones). The B and Nd isotopes confirm the asymmetry of subduction zones (Doglioni, Tonarini, & Innocenti, 2009). Hotter and thicker asthenosphere in the hanging wall of W- (or SW-) directed subduction zones is generally accompanied by positive and higher $\delta^{11}B$ and $^{143}Nd/^{144}Nd$, except where there is a significant crustal contribution (e.g., Apennines). The kinematics of W-directed subduction zones predicts a much thicker asthenospheric mantle wedge, larger volumes and faster rates of subduction with respect to the slabs E- (or NE-) directed. The larger volumes of lithospheric recycling, the thicker column of fluids-rich, hotter mantle wedge, all should favor greater volumes of magmatism per unit time in W-directed subduction zones. The E- (or NE-) directed subduction zones show a thinner, if any, asthenospheric mantle wedge due to a thicker upper plate and low-angle subducting slab. Along these settings, the mantle wedge, where the percolation of slab-delivered fluids generates melting, mostly involves the relatively cooler lithospheric mantle. Mantle wedge thickness, composition, and temperature are all affected by the asymmetries imposed by the westward drift of the lithosphere and the consequent differences among subduction zones.

The westward drift of the lithosphere (Bostrom, 1971; Doglioni, 1993a; Knopoff & Leeds, 1972; Moore, 1973) can explain the aforementioned asymmetries at subduction zones. W-directed subduction zones are steeper (average 65°) than those directed to E or NE (average 27°), and the associated orogens are respectively characterized by lower structural and topographic elevation, occurrence of backarc basins, whereas E- or NE-directed subductions show higher structural and morphological elevation and absence of backarc basin (Doglioni, 1993a; Riguzzi et al., 2010). This asymmetry is also marked by the opposite state of stress of the slabs (Ruff & Kanamori, 1980; Bevis, 1988; Billen & Hirth, 2007): down-dip

compression and down-dip extension for W- and E- or NE-directed slabs, respectively (Doglioni et al., 2007; Carminati & Petricca, 2010; Riguzzi et al., 2010). Such differences have been usually interpreted as related to the age of the downgoing oceanic lithosphere (usually older, cooler, and denser in the western side). However, these differences persist elsewhere, regardless of the age and composition of the downgoing lithosphere, e.g., in the Mediterranean Apennines and Carpathians versus Alps and Dinarides, or in the Banda and Sandwich arcs, where even continental or zero-age oceanic (mid-oceanic ridge) lithosphere is almost vertical along W-directed subduction zones (Cruciani et al., 2005; Doglioni et al., 2007). To summarize, W-directed subductions and E- or NE-directed ones have subduction hinges respectively diverging and converging relative to the upper plate, fast versus low subduction rates, low versus high topographic envelopes (α) and high versus low foreland monoclines (β). Finally, the lithospheric volume lost along subduction zones (Doglioni & Anderson, 2015) is about 300 km^3/year, but the subduction rate along W-directed slabs is three times larger (about 230 km^3/year) with respect to the converse E- or NE-directed subduction zones (about 70 km^3/year). W-directed subductions are zones where there is a negative volume balance of lithosphere, in other words, the lithosphere is almost entirely lost in subduction and replaced by the uprising asthenosphere in the backarc region. Along E- or NE-directed subduction zones, the volume balance of the lithosphere is positive because the hanging wall lithosphere is thickened from the footwall plate, which is sliding below and following the shape of the upper plate. This could provide an explanation for their higher structural and morphologic elevation.

The following tables indicate the several different relationships between extensional tectonic settings and subduction zones (Table 1), the main asymmetric parameters of opposite subduction zones (Table 2), and the dip of the main world's subduction zones (Table 3).

From the existing literature it is possible to identify nine main extensional types related to convergent geodynamic settings (Table 1). The uplift of deep crustal rocks at the surface is related to deep thrust planes that are associated with thrust belts that form with E- and NE-directed subduction zones; later extension of any of the former types may affect such orogens, in particular, type 1 (e.g., the Tyrrhenian Sea overprinting the Alpine orogen), or type 5 (e.g., Alps, Himalayas), or type 6 (e.g., Aegean rift), or type 7 (e.g., Atlantic and Tethys), or type 8 (e.g., Basin and Range) as shown in Figure 34. As a rule, interplay among the different types of extensional settings may be expected (Doglioni, 1995). Different types of extension

Table 1 Main extensional types related to convergent geodynamic settings. Other differences like shape, time evolution, and rheological parameters vary in each type of setting

Geodynamic setting planes	Subduction polarity	Syn- or Post-conv.	Generalized subsidence or uplift	Basal decollement	Extension migration	Number of plates	Opening rates
1 Backarc basin extension	Westward	syn	subsidence 700 m/Ma	Lithosphere–asthenosphere	E-ward	1 or 2	3–10 cm/yr
2 Asthenospheric wedging-related extension	Westward	syn	Uplift 500 m/Ma	Crust–asthenosphere	E-ward	1 or 2	
3 Subduction hinge extension	Westward	syn	subsidence or uplift	Upper lithosphere	E-ward	1 or 2	
4 Increasing arc length extension	Westward	syn	subsidence	Lithosphere–asthenosphere	E-ward	1 or 2	
5 Morphologic Gradient-related extension	Eastward or northeastward	syn	Uplift	Middle-upper crust		1 or 2	
6 Hanging wall gradient velocities	Eastward or northeastward	syn	subsidence	Lithosphere–asthenosphere	SW-eastward	3	0.1–5 cm/yr
7 Lithospheric roots-related extension	Eastward or northeastward	post	subsidence 100m/Ma	Lithosphere-asthenosphere		1 to 2	0.1–1 cm/yr
8 Inversion of velocity gradients	Eastward or northeastward	post	subsidence	Lithosphere–asthenosphere		3 to 2	1–10 cm/yr
9 Transfer zones-related extension	both west- and eastward	syn	subsidence or uplift	Basal thrust plane		1 or 2	

Table 2 Few main geometric, kinematic, and dynamic differences between orogens and subduction zones following or opposing the tectonic mainstream. Subduction zones parallel to the mainstream due to plate subrotation (e.g., Pyrenees) or oblique convergence have similar characters as the subduction zones that follow it

	Subductions opposing the tectonic mainstream (W- or SW-directed)	Subductions along the tectonic mainstream (E- or NE-directed)
Elevation average	−1250 m	+1200 m
Foreland monocline average dip	6.1°	2.6°
Trench or foredeep subsidence rate	>1 mm/yr	<0.3 mm/yr
Prism envelope average dip	1.9°	4.8°
Orogen-prism vergence	Single verging	Mostly double verging
Type of prism rocks	Mostly sedimentary cover and volcanics	Largely basement, sedimentary cover and volcanics
Prism decollement depth	0−10 km; (rarely up to 20 km) off scraping the top of the lower plate	>30 km; oceanic subduction, affecting mostly the whole section of the upper plate; continental subduction affecting also the lower plate
Seismic coupling	Mainly low	Mainly high
Moho	Shallow (<30 km) new upper plate Moho	Deep (>40 km) doubled old Mohos due to lithospheric doubling
Asthenosphere depth	Shallow (<20−50 km) beneath the arc	Deep (>70−100 km) beneath the arc
Seismicity	0−670 km; intraslab mostly down-dip compression and horizontal shear	0−250 km And scattered 630−670 km; intraslab mostly down-dip extension
Slab dip	25°−90°	15°−50°, steeper up to 70° along oblique subductions and thicker upper plate
Subduction hinge motion relative to upper plate	Mainly diverging eastward (except Japan where subduction started to flip)	Mainly converging E-ward or NE-ward

Subduction hinge motion relative to mantle	Fixed	W-ward or SW-ward
Subduction rate	S=H−L, faster than convergence rate; mainly slab retreating and entering the mantle	S=H−L, slower than convergence rate; slab "escaping" relative to the mantle overridden by the upper plate (upduction)
Backarc spreading rate	H (>0), prism accretion, hinge asthenospheric intrusion	Differential velocity between two hanging wall plates
Slab/mantle recycling	About three times higher than opposite	About three times lower than opposite
Subduction mechanism	Slab−mantle wind interaction + far-field plate velocities + slab density gradient relative to the country mantle	Far-field plate velocities + slab density gradient relative to the country mantle

Table 3 Dip of the slab of the W- (or SW-) and E- (or NE-) directed subduction zones, slightly modified after Riguzzi et al. (2010)

W- or SW-directed	Slab dip >100 km	E- or NE-directed	Slab dip >70 km	Deep cluster
Tohoku–Japan	35°	Nicaragua	50°	
Kuriles–Kamchatka	45°	Cascadia	18°	
Molucche 3°N	50°	Molucche 3°N	45°	
Aleutians 55°N/160°W	50°	New Hebrides	50°	Yes
N-New Zealand 39°S	65°	Zagros	18°	
Banda	55°	Himalaya	15°	
Tonga	58°	Peru 10°S	10°	
Cotabago	63°	Peru–Bolivia 15°S	18°	Yes
Mariannas 22°N	84°	Chile 22°S	21°	Yes
Izu–Bonin 32°N	72°	Chile 24°S	21°	
Izu–Bonin 27°N	83°	Ecuador 3°S	20°	
Apennines	72°	Costarica	50°	
Sandwich	69°	Colombia 5°N	25°	
Barbados	68°	Hellenides	23°	
Mariannas 12°N	85°	Mexico	10°	
Mariannas 19°N	84°	Sumatra 100°E	32°	
Vrancea	78°	Sumatra 115°E	35°	Yes
Average	**66°±15°**	**Average**	**27°±14°**	

can overprint the entire variety of preexisting tectonic fabrics. Orogens associated to subrotation of plates (e.g., the CCW rotation of Iberia, which generated the E–W trending Pyrenees, or the CW rotation of South America that constructed the Colombia–Venezuela E–W trending thrust belt) have characters of subduction zones where the subduction hinge converges relative to the upper plate, i.e., produces a contractional double verging orogen such as those generated by E- or NE-directed subduction zones.

4. ASYMMETRIES ALONG RIFT ZONES

The oceanic ridges are usually taken as the prototype of geological symmetric features. However, a number of deviations from this apparent regularity exist in the spreading rates, volcanic "plumes" interactions, and ridge jumps (Müller, Sdrolias, Gaina, & Roest, 2008 and references therein). For example, bathymetric analysis of ocean basins (Doglioni, Carminati, & Bonatti, 2003) shows that they are, on average, 100–300 m shallower in the eastern flank (Figures 35 and 36) than in the western one. This

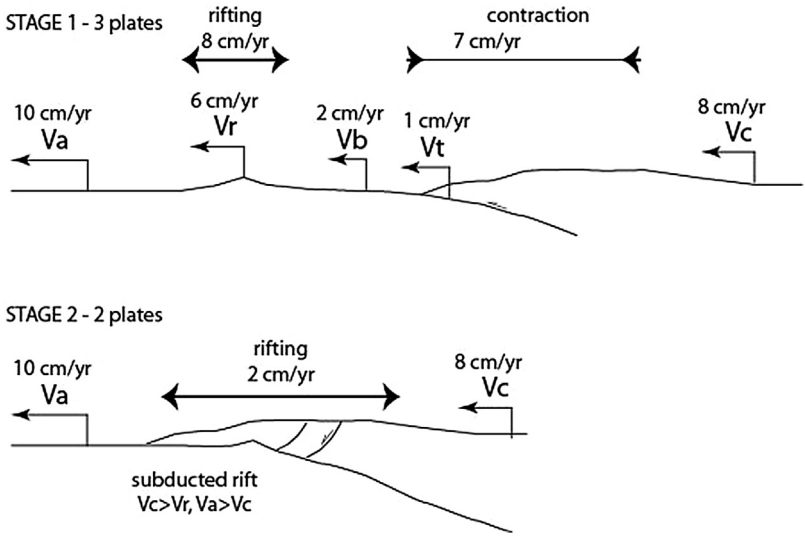

Figure 34 One of the several examples of relationship between extensional tectonics and subduction systems (type 8 of Table 1). Va, Vb, Vc, velocities of plates a, b, and c, respectively. Vr, velocity of the ridge; Vt, velocity of the trench. Since the plate c will eventually override the ridge, the system will be switched from subduction to rifting because plate a is faster than plate c, having lost the intervening slower plate. This evolution may explain the Basin and Range rifting.

asymmetry is confirmed also when plotted versus the square root of the age of the oceanic crust (Figure 37). A counterexample of this systematic asymmetry occurs at the Pacific superswell along the EPR. Ridges appear also to jump more frequently toward the west, leaving abandoned rift valleys to the east (e.g., the Aegir Ridge in the Norway Basin, northern Atlantic, Le Breton, Cobbold, Dauteuil, & Lewis, 2012). Moreover, shear waves velocities (VS) suggest a thicker western limb in the Middle Atlantic Ridge and the Indian Ridge with respect to a thinner eastern limb (Figure 38), whereas the LVZ is thinner under the western lithosphere with respect to the eastern one (Panza et al., 2010). These authors also emphasize the occurrence of the LVZ worldwide between the lithospheric mantle (LID) at 50–150 km and the upper asthenosphere at about 200–220 km depth. The global asymmetry is persistent regardless the age of the oceanic lithosphere. This finding is well visible along the TE or also along a perturbed path of it, suggesting a full decoupling between lithosphere and underlying mantle (Figure 39). Typical VS of the LID is about 4.7 km/s, whereas the LVZ may be around 4.3 km/s. Radial anisotropy becomes close to 1 at about 200 km depth and beneath oceanic ridges (Figure 39). Such a global signature can be interpreted in

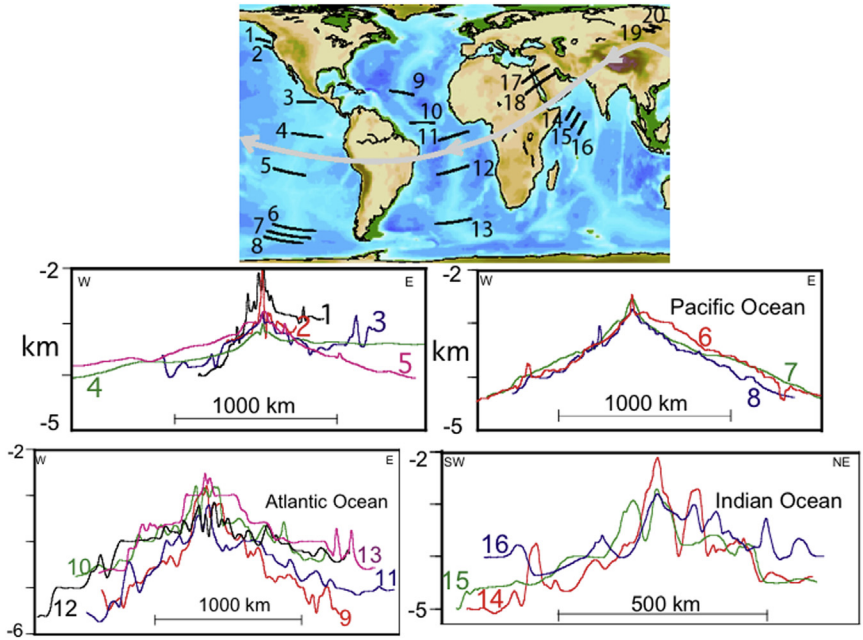

Figure 35 Topographic profiles across the major oceanic ridges and the Red Sea and Baikal rift. The locations are chosen to avoid, as much as possible, seamount tracks, triple points, and large deep-sea fans. Note how the eastern sides are generally more elevated. The gray sinusoidal line indicates the main direction of plate motion or tectonic equator. *After Doglioni et al. (2003).*

terms of a global discontinuity in the LVZ that allows for the relative motion between the westerly traveling lithosphere and the underlying mantle, that moves "eastward" relative to the lithosphere (Figure 40). This can be considered as the first-order flow, whereas second-order flows is represented by the local uplifts of the mantle beneath the oceanic spreading zones, being sort of Taylor instabilities (Figure 40). The morphologic and seismic asymmetries between the western and eastern limbs have been interpreted as related to the migration of the ridge over a relatively more fertile mantle (Doglioni et al., 2005). The uplift and decompression of the mantle generates partial melting in the LVZ and depletion of the mantle. After melting, the residual mantle is about 20–60 kg/m^3 lighter (Oxburgh & Parmentier, 1977). The lateral migration of the ridge allows permanent generation of MORB magmas from undepleted mantle sources (Figure 41). The ridge migration rate is given by the sum of the two plate velocities in the hot spot reference frame divided by 2 (Figure 41). Therefore, the decoupling between the lithosphere and the underlying mantle

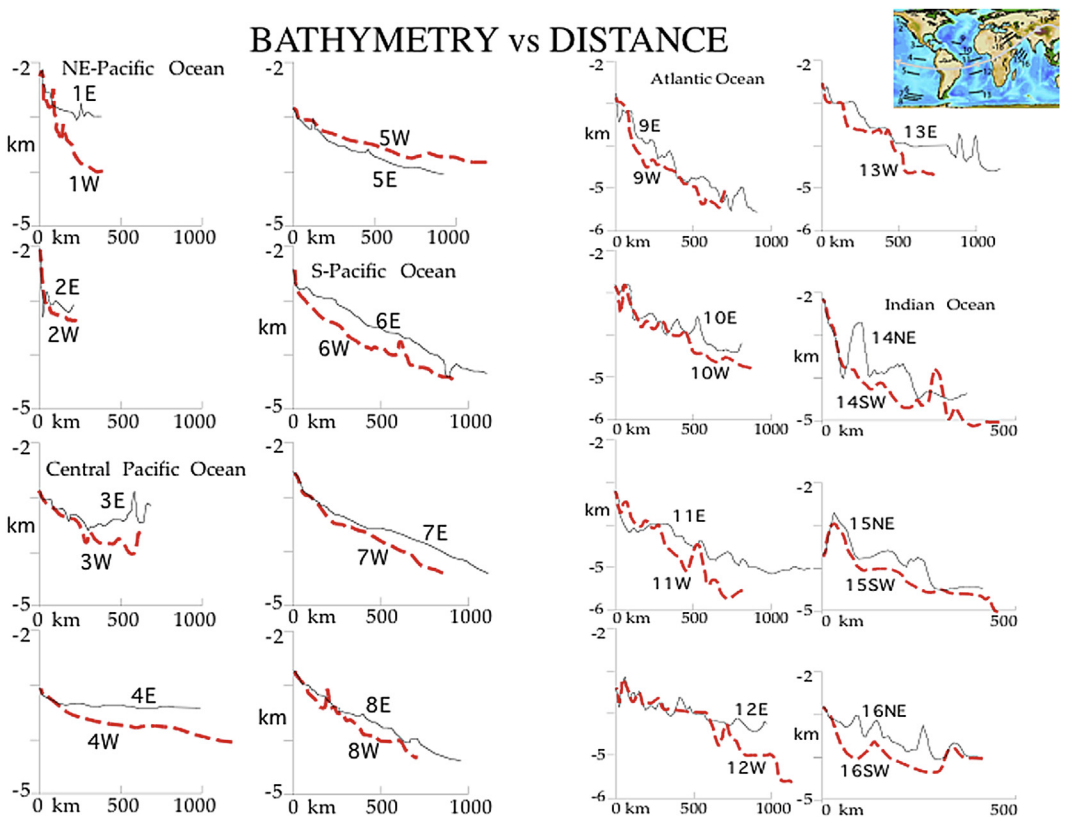

Figure 36 Topographic profiles across the Pacific, Atlantic, and Indian Oceans. The western (W) and eastern (E) sides are plotted together in order to better appreciate the altitude differences. Red dashed lines represent the western flanks, whereas the solid black lines are the eastern flanks. Eastern flanks are, on average, shallower. *After Doglioni et al. (2003)*.

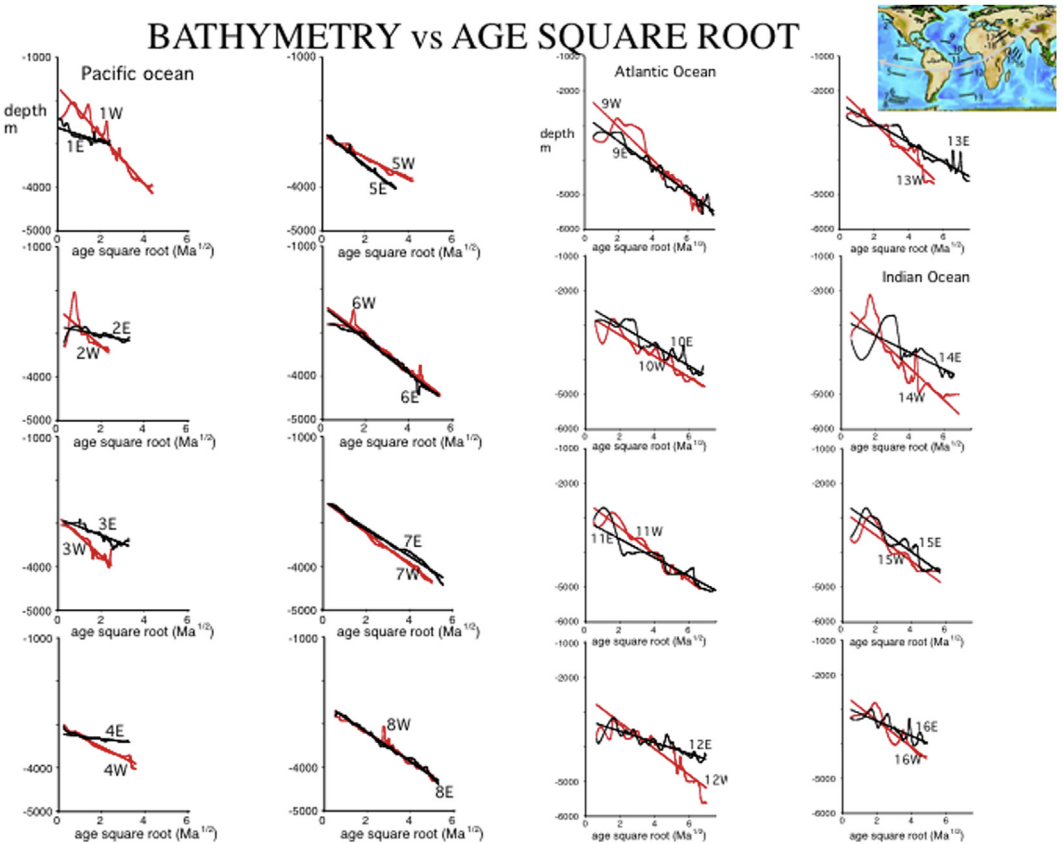

Figure 37 Elevation of the oceanic lithosphere versus the square root of age in the Pacific, Atlantic, and Indian sections. Red line dots represent the western flank. The asymmetry persists and shows an average less steep mean inclination (intercept of the regression line) of the eastern flanks; the steeper the slope the faster the subsidence as it is relatively more often seen in the western limb. *After Doglioni et al. (2003)*.

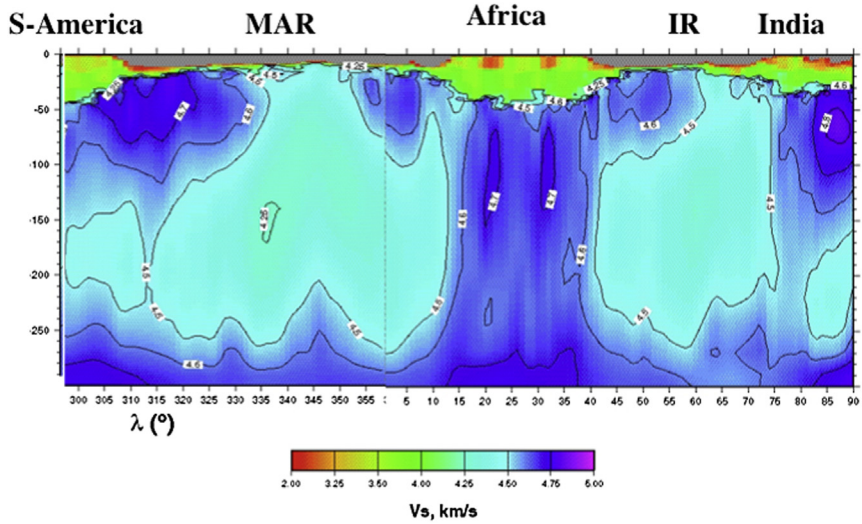

Figure 38 Vs cross section, 10° wide, along the tectonic equator, crossing the Atlantic and Indian oceans. The relatively faster western lithospheric flank of the Atlantic (MAR) and Indian (IR) oceanic ridges is clearly seen. *Data courtesy of Anatoli Levchin based on CUB2 Ritzwoller, Shapiro, Barmin, and Levshin (2002).*

continuously mixes the system and distributes a previously undepleted mantle into different layers and sides (Figure 42). In fact, part of the melt goes up to form new oceanic crust, which is split into the two plates spreading apart; some depleted LVZ, e.g., a lherzolite transformed into harzburgite beneath the ridge, gradually cools down to form the LID, whereas the lower eastern side of the rift continues to belong to the LVZ layer, but depleted (Figure 42). Each prerift mantle source in the LVZ to the west of the ridge may have a different evolution and final destination of its journey. Plate and mantle kinematics in the hot spots reference can explain the bathymetric, seismological, and geochemical different signatures between the two limbs of the ridge. Recently Cuffaro and Miglio (2012) reproduced the asymmetry of the thickness of the limbs at oceanic rift zones modeling mantle upwelling beneath a migrating Mid-Atlantic Ridge, using plate velocities relative to the hot spot reference frames as boundary conditions.

Some continents are uplifting without any apparent reason. For example, Africa, India, and Europe underwent a Cenozoic uplift (Carminati, Cuffaro, & Doglioni, 2009; Doglioni et al., 2003). Besides the Alpine orogen, the Mesozoic–Early Cenozoic Paris Basin was uplifted together with the whole European continental areas (Figure 43). In the framework of the westward

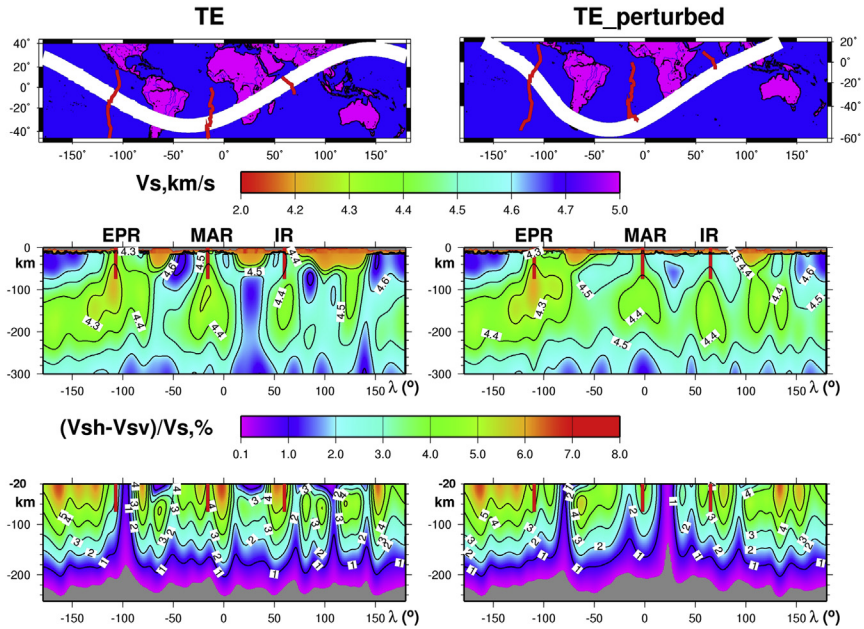

Figure 39 Vs cross section, 10° wide, along the tectonic equator (TE) to the left, and along a perturbed path (TE-pert). The generalized asymmetry across oceanic ridges is quite evident: the lithosphere (0–100 km thick) in the western side of the rift is faster than in eastern or northeastern side, whereas the upper asthenosphere (low-velocity layer, 100–200 km thick) is slower in the western side with respect to the conjugate counterpart. In the top panels red lines correspond to segments of Eastern Pacific, Mid-Atlantic, and Indian Ridges. Lower panels show the radial anisotropy along these sections. Vs radial cross sections have been obtained using bispline interpolation of velocities at fixed depths levels (on a 4 km grid) with subsequent Gaussian smoothing. Vs is taken here as average of Vsv and Vsh (see text) along a section 10° wide. Radial anisotropy sections are without crust, since crust is assumed to be isotropic. *After Panza et al. (2010)*.

drift of the lithosphere, the continental areas gradually shift over previously depleted mantle sections beneath the ridge to the west. Therefore, the depleted lighter mantle should eventually transit beneath the continent, generating an isostatic uplift of the continental lithosphere (Figure 44). This can naturally explain the slower thermal subsidence in the eastern flank of the ridges with respect to the western flank, the contemporaneous uplift of the continent to the east, and the tectonically active hinge between the two settings (Figure 45), which could potentially explain some enigmatic earthquakes such as the 1755 Lisbon event. Horizontal plate motions are generally one or two orders of magnitude faster than the vertical

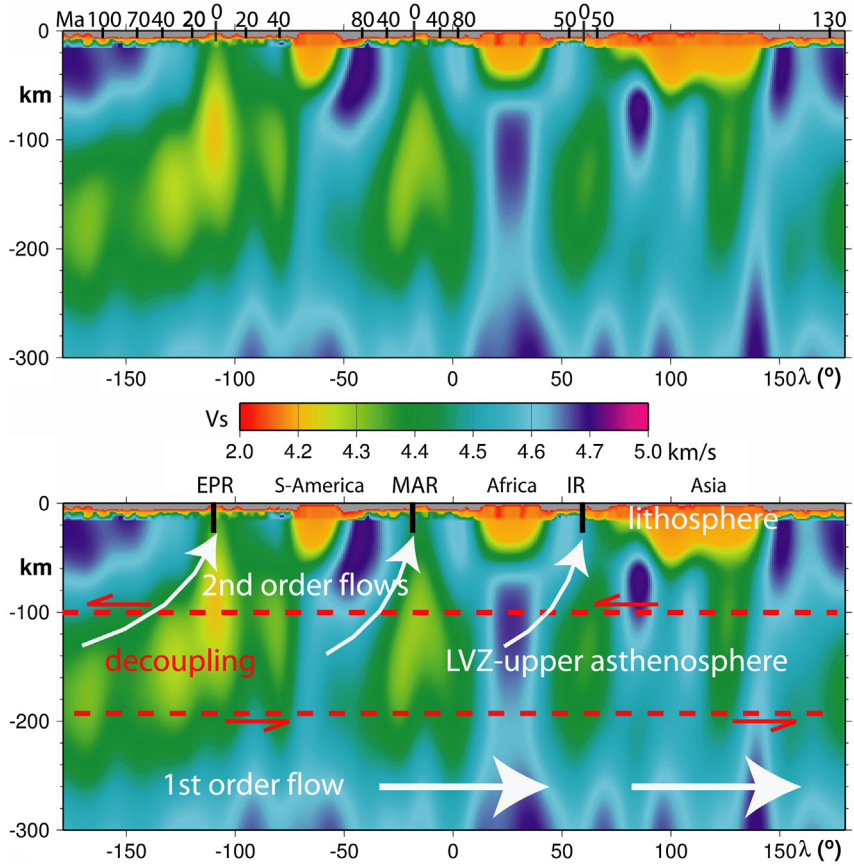

Figure 40 Uninterpreted (above) and interpreted (below) Vs section, of Earth's uppermost 300 km, along the tectonic equator. EPR—Eastern Pacific Ridge, MAR—Mid-Atlantic Ridge, IR—Indian Ridge. The upper asthenosphere contains the low-velocity layer (LVZ), that is supposed to allow both for the decoupling between lithosphere and underlying mantle and for the net rotation of lithosphere, i.e., first-order relative eastward mantle flow or westward drift of lithosphere. Secondary flow could be related to mantle obliquely upraised along oceanic ridges. Asymmetry between the two sides of ridges is independent from the age (shown at the top in million years, Ma) of the oceanic lithosphere. *After Panza et al. (2010).*

tectonic-related movements, e.g., 50 mm/year versus 0.5 mm/year (Doglioni et al., 2007). This supports the fact that in geodynamics tangential forces acting on an equipotential gravitational surface are stronger than the vertical ones. With the aforementioned geodynamic models of subduction and rift zones, we can define two different types of mechanisms capable

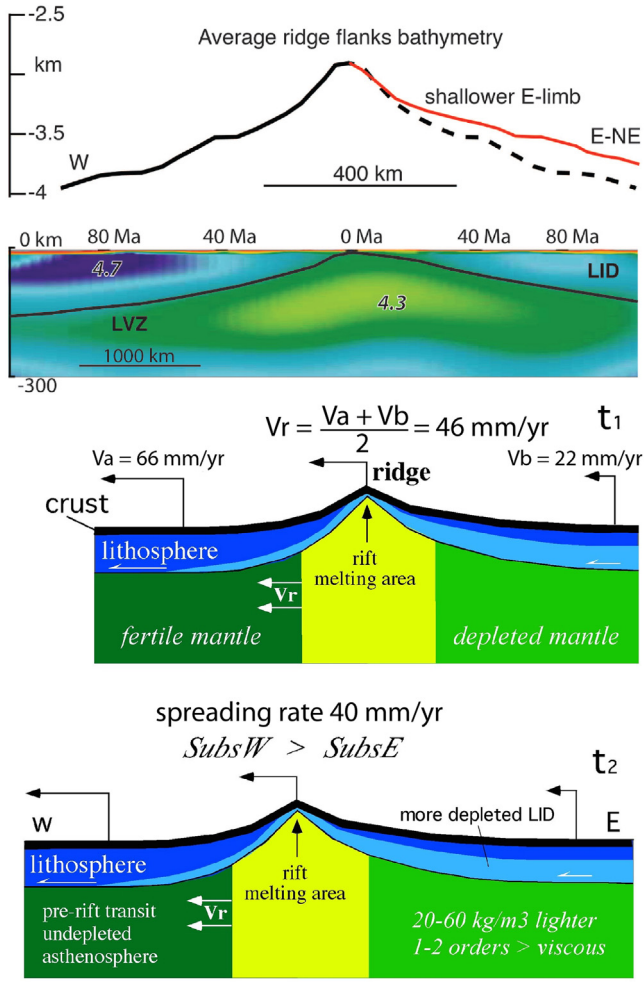

Figure 41 First panel from the top: average ridge flanks bathymetry after Doglioni et al. (2003). The average depth of western flanks compiled at mid-ocean ridges (black solid line) is larger with respect to that of the eastern one (red (light gray in print versions) solid line). For an easier comparison, the western flank is also reported on the eastern side (black dash line) to emphasize the difference (about 100 m shallower close to the ridge and 300 m more far away in the eastern limb with respect to the western one). Second panel: Vs beneath the Mid-Atlantic Ridge (MAR) along the tectonic equator, after Doglioni et al. (2014). Data show an asymmetry between the western limb of the MAR (thick lithosphere) and the eastern one (thin) and well delineate the low-velocity zone (LVZ) between the lithospheric mantle (LID) and the upper asthenosphere (between 100 and 200 km), LLAMA in Figure 1. Colors from light green (light gray in print versions) to dark blue (dark gray in print versions) represent Vs in the range from 4.3 to 4.7 km/s, respectively. Two lower panels: schematic oceanic rift with hypothetic velocities of plates (a) and (b), relative to fixed mantle. The ridge moves west with

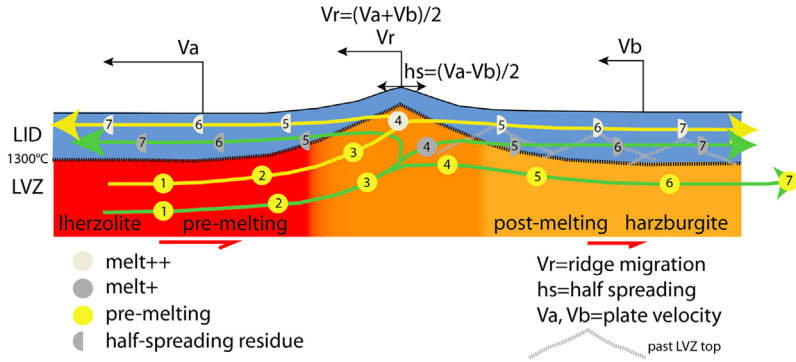

Figure 42 Inferred kinematics of different particles of rocks along a ridge. Numbers from 1—7 indicate progressive age evolution of the rock markers. Plates (a) and (b) move with velocity Va and Vb, respectively. Vr is the velocity of the ridge; hs is the half-spreading rate. Since the ridge is moving westward, new sections of undepleted lherzolitic mantle migrate "eastward". Due to isostasy, the mantle upraises at the ridge. Partial melting supplies magmas to generate oceanic crust of MORB composition. The depletion of the residual mantle generates harzburgite, which is lighter than the fertile mantle. The depleted mantle under the rift, while the ridge migrates laterally, is abandoned and spread into two volumes, one that moves back westward with plate a, and the other that is overridden by plate b. Since, moving away from the ridge, the depleted mantle cools down, it becomes LID, i.e., part of the LVZ becomes lithosphere. Depending upon the depth of the original pre-melting mantle, the LVZ is partitioned into material flowing to produce new oceanic crust and new LID or it remains, as depleted mantle or only partly depleted (4, 5, 6 yellow circles to the right), at the LVZ depth. Therefore, the LID is nothing but cooled asthenosphere. The harzburgite composition of the LID maintains the lower density of the lithosphere relative to the underlying mantle. It is quite obvious that the positive buoyancy of the lithosphere does not favor the initiation and progress of subduction, if driven by the slab pull alone. The lower red arrows indicates that the mantle is relatively shearing eastward and the LVZ represents the decoupling with the overlying lithosphere (after Chalot-Prat & Doglioni, (2015)).

velocity Vr. Lithospheric spreading at ridges triggers the uplift of undepleted mantle, previously located to the west. In the melting area, mantle loses Fe, Mg, and other minerals to form oceanic crust, while the residual mantle is depleted. Since the melting area moves west it gradually moves toward undepleted mantle and releases depleted mantle to the east. This can explain the slightly shallower bathymetry of the eastern limb and the observed asymmetry in seismic wave velocity. In this model, the differential velocity between plates is controlled by low-velocity layer viscosity variations that generate variable decoupling between lithosphere and mantle. t1 and t2 are two time stages. *Modified after Doglioni et al. (2005).*

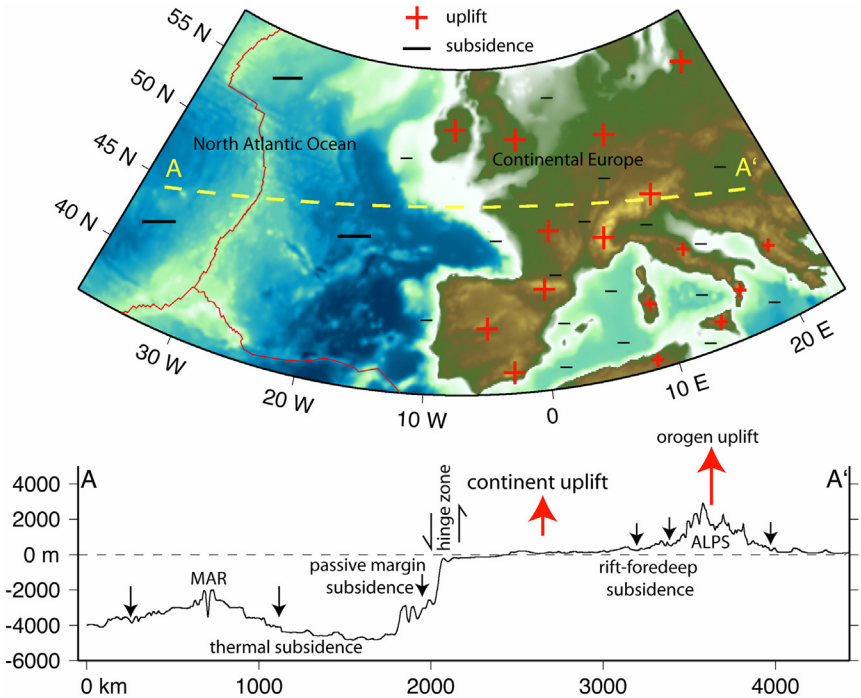

Figure 43 The European continental lithosphere underwent a generalized uplift since the Paleogene, except along rift and foredeep zones. Within the same plate, the thermal subsidence in the Atlantic Ocean has been contemporaneous with the uplift of continental Europe. A fault-hinge area separating the two realms is needed along the passive continental margin. Subsidence and uplift signs represent both present and past vertical qualitative trends. MAR, Mid-Atlantic Ridge. *After Carminati et al. (2009)*.

to generate uplift or subsidence: (1) shortening or stretching of the crust—lithosphere associated with faulting and folding, related erosion, or sedimentation, etc., and (2) uplift or subsidence due to compositional or thermal variations such as the underlying transit of a depleted or more fertile mantle, or the cooling of the oceanic lithosphere, i.e., density-related modifications (Figure 46). Each geodynamic environment has its different rates as a function of the polarity with respect to the westward drift of the lithosphere relative to the mantle.

5. MEDITERRANEAN GEODYNAMICS

The Mediterranean, where the preconception of N—S compression between Africa and Europe in the Tertiary has been at the base of the formulation of many unconvincing geodynamic models, represents a

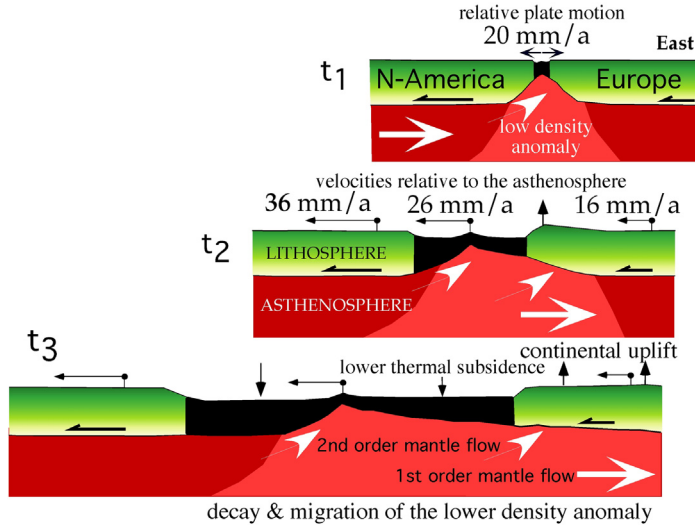

Figure 44 Cartoon describing the long-term 300–600 m uplift process of Europe. The phenomenon is generated by the eastward shift of the depleted lighter asthenosphere from the ridge beneath the continental lithosphere. *After Carminati et al. (2009).*

challenge for plate tectonics. The dominant motion along Atlantic transform faults that track Africa and Europe motion is E–W, therefore similar direction of motion must have been the one in the Mediterranean. A dominant N–S compression between the two continents is not compatible with the opening of the western Mediterranean and Tyrrhenian oceanic basins (e.g., Doglioni, 1991; Gueguen, Doglioni, & Fernandez, 1998; Malinverno and Ryan, 1986; Panza & Calcagnile, 1979; Rehault, Boillot, & Mauffret, 1985). Effects of an N–S (or NW–SE) compression are seen in the Pyrenees, in East–Central Alps, and in the Atlas and can be naturally explained as the result of local rotations or of local body forces, some of them originating from upper mantle heterogeneities, capable to modify the local stress

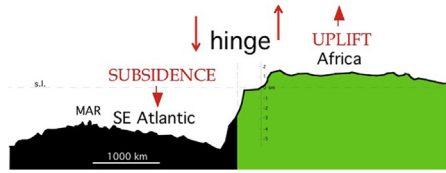

Figure 45 The passage of a depleted mantle under the ocean slightly decreases the thermal subsidence of the basin, but it determines an uplift of the continental area. Therefore, the ocean–continent boundary of the eastern Atlantic is a tectonically active (even though seismicity is very sporadic, but tragically represented by 1755 Lisbon earthquake) hinge zone that separates subsiding and uplifting regions.

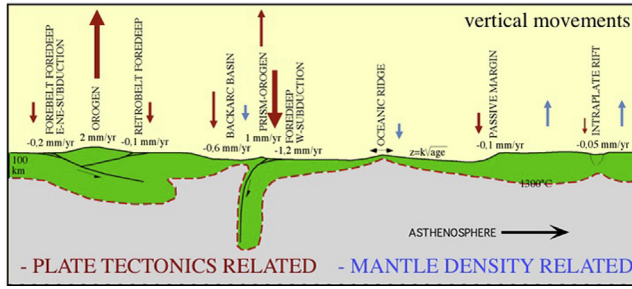

Figure 46 Summary of the main mechanisms and rates of vertical movements (both uplift and subsidence) as a function of the geodynamic setting. In red (black in print versions) are represented movement directly associated to deformation, such as stretching and shortening, whereas blue (light gray in print versions) arrows show motions associated with density variations due to either thermal cooling (oceanic subsidence) or mantle compositional depletion (intracontinental uplift).

field. Some of this NNW-SSE convergence may really be ascribed to the Africa Eurasia convergence, but it has been shown that this convergence is four to five times smaller than the west to east migration of the western Mediterranean (Gueguen et al., 1998). Therefore, since inertial forces in geodynamics are negligible (Turcotte & Schubert, 1982), the N–S convergence between Eurasia and Africa is an ancillary component of the Mediterranean geodynamics. Additional complications are given by subrotations of plates or microplates. In East–Central Alps the dextral transpression has been likely disturbed by the CCW rotation of the Ionian–Adria plate, which in the Neogene is responsible of N–S compression in the Eastern Alps and a simultaneous dextral transpression in the Dinarides. The geodynamics of the Mediterranean has been controlled by inherited lithospheric heterogeneities generated by the Mesozoic Tethyan rifting that controlled the location and polarities of the later Meso–Cenozoic subduction zones, the Alps–Betics, the Apennines-Maghrebides, and the Dinarides–Hellenides–Taurides. Closely related to the Mediterranean geodynamics are the Carpathian subduction (Vrancea zone) and the Pyrenees.

In Iberia, the Vs model of the lithosphere–asthenosphere system (LAS) shows the almost constant velocity in the uppermost mantle beneath the Iberian Massif, the well-developed LVZs in the Valencia trough and under northwest Africa, and specific features of the upper mantle layering in the zone of the Iberian range. The thickness of the crust varies between 25 and 35 km with exceptions in the zones of the Valencia trough (11–18 km) and Pyrenees (35–45 km). These models are well correlated with the geological structure along TRANSMED I geotraverse (Cavazza, Roure,

Spakman, Stampfli, & Ziegler, 2004) and evidence several features of the LAS in the Betic–Rif domain: quite distinct Iberian, Alboran, and Meseta crustal domains; relatively thin lithosphere under the Rif system; clearly defined boundary between the upper and lower asthenosphere (Raykova & Panza, 2010).

The Vrancea region is a further remarkable site of intracontinental intermediate-depth seismicity associated to the ongoing southeastern margin of the W-directed Carpathians subduction zone (Ismail-Zadeh et al., 2012; Oncescu & Trifu, 1987; Oncescu & Bonjer, 1997; Raykova & Panza, 2006). A large set of geological, geophysical, and geodetic observations has been accumulated in the last few decades and utilized to improve the knowledge of the shallow and deep structures beneath Vrancea, the crust and mantle dynamics, and the link between deep and surface processes in the region. According to Carminati and Doglioni (2005), the Carpathians (and Vrancea) had an evolution similar to that of the Apennines, where W-directed subduction initiated along the retrobelt of a preexisting orogen associated to E- (or NE-) directed subduction (the Alps for the Apennines and the Dinarides for the Carpathians). In this interpretation, the Vrancea seismicity might be the result of stress generation due to still active subduction (Ismail-Zadeh, Panza, & Naimark, 2000). This is coherent with the Pleistocene magmatism in the Pannonian and Transylvania backarc basins (Harangi & Lenkey, 2007; Seghedi et al., 2011). The subduction is hanging in an eastward mantle flow (Doglioni, Harabaglia, et al., 1999), which is triggering its rollback and is enhanced by the negative buoyancy (if any) of the subducted oceanic lithosphere, of the Outer Carpathians slab, during the closure of the Ceahlău–Severin Ocean. The seismic gap, in the depth range from about 40 km to about 60 km (Ismail-Zadeh et al., 2000) in the slab may well be interpreted as the boundary between the subducted oceanic lithosphere, and the inherited subducted passive continental margin, which intrinsically has a shallower termination of its brittle properties (Carminati, Giardina, & Doglioni, 2002).

The Ionian–Adria plate is an example of the same plate subducting with different styles, both W-directed and NE-directed. The subduction angle and the different geologic signatures of Ionian–Adria plate depend only on its orientation. The amount of relative N–S Africa–Europe relative motion seems to have been about five times slower with respect to the eastward migration of the Apennines arc which migrated eastward by about 600 km during the last 30 Ma, i.e., about 4 mm/year versus 20 mm/year (e.g., Gueguen, Doglioni, & Fernandez, 1997). Geodetic data confirm that the main directions of Africa and Europe motion are NE-directed in

the NNR reference frame (e.g., Nasa GPS time series Web page). The archetypes of the opposite subduction zones can be recognized when comparing the Apennines (W-directed) and the Alps (E–SE-directed slab) as shown in Figure 47. The Apennines have single vergence, low elevation, deep foredeep, and a steep foreland regional monocline; in the Apennines the accretionary prism is mostly composed by shallow rocks of the lower plate, the backarc basin, partly floored by oceanic crust, is fully developed and a new Moho is formed in the hanging wall of the subduction zone. The Alps, on the other side, are a double verging orogen, and they show high morphologic and structural elevation, two shallow foredeeps, shallow foreland regional monocline, and deep decollements involving the whole crust and lithospheric mantle (Carminati & Doglioni, 2012; Carminati, Lustrino, & Doglioni, 2012; Panza, Raykova, et al., 2007). In the Apennines the subduction hinge is diverging relative to the upper plate (apart

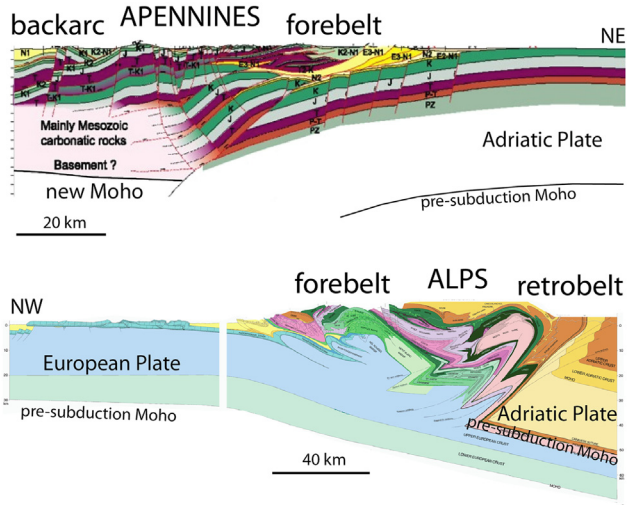

Figure 47 Synoptic comparison of two sections of the Southern Apennines (Scrocca, Carminati, & Doglioni, 2005) and the northwestern Alps (Escher & Beaumont, 1997). In the Apennines single vergence and backarc rifting in the hanging wall of the subduction zone are clearly visible. The accretionary prism is mainly composed of shallow upper crustal layers of the lower Adriatic plate. A new Moho formed in the hanging wall of the subduction zone. The Alps are instead a double verging orogen where two lithospheres with presubduction Mohos are doubled and thickened. The orogen deeply involved basement rocks and is no associated to backarc rifting. These differences mimic the same asymmetries that can be recognized worldwide when comparing accretionary prisms or orogens associated to W-directed versus E- (or NE-) directed subduction zones, respectively.

in Sicily), whereas in the Alps the hinge converges (Figure 48). In the Apennines, the accretionary wedge is even lower with respect to the foreland, whereas in the Alps it is always the opposite (Figure 48). The Apennines have low elevation, the amount of erosion is limited to few kilometers, and the most elevated area is affected by stretching. The opposite occurs in the Alps that are more than twice higher, but when repositioned the eroded material, their structural elevation is of few tens of kilometers; moreover the area of uplift corresponds to contraction at depth, even if some superficial stretching may occur (Figure 49). As a global signature, in the Apennines the foreland regional monocline is more than twice steeper than in the Alps, which paradoxically are more elevated (Mariotti & Doglioni, 2000). In fact the dip β of the foreland regional monocline in the Apennines beneath the accretionary wedge front may be between 6° and 22°; these are the lowest values occurring along recesses of the thrust belt front. In the Alps the dip is around 2°–8° (Figure 50). The opposite

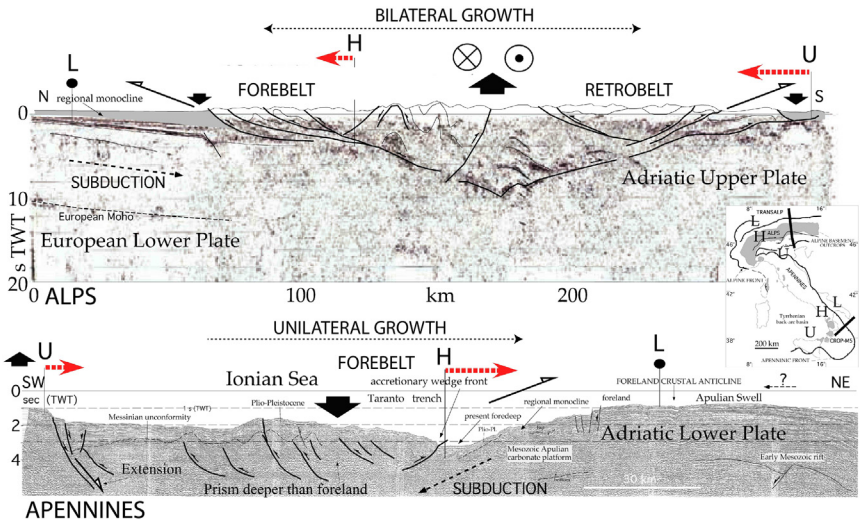

Figure 48 Seismic sections of the Alps (Transalp, 2002), top and of the Apennines, bottom (Doglioni et al., 2007). Note the Alpine double vergence vs the single Apennines vergence, where the prism is even deeper than the foreland and followed by extension to the left. L, lower plate, H, subduction hinge, U, upper plate. In the Alps, H migrates toward the upper plate, whereas, in the Apennines, it moves toward the lower plate faster than the upper plate. The Adriatic plate is the upper plate for the Alps, while it is the lower plate for the Apennines. The E–W segment of the Alps formed under right-lateral transpression. Thrusts and decollement planes in the Alps deeply affect the entire upper and lower plates; in the Apennines the prism involves the shallow layers of the lower plate and the prism subsides.

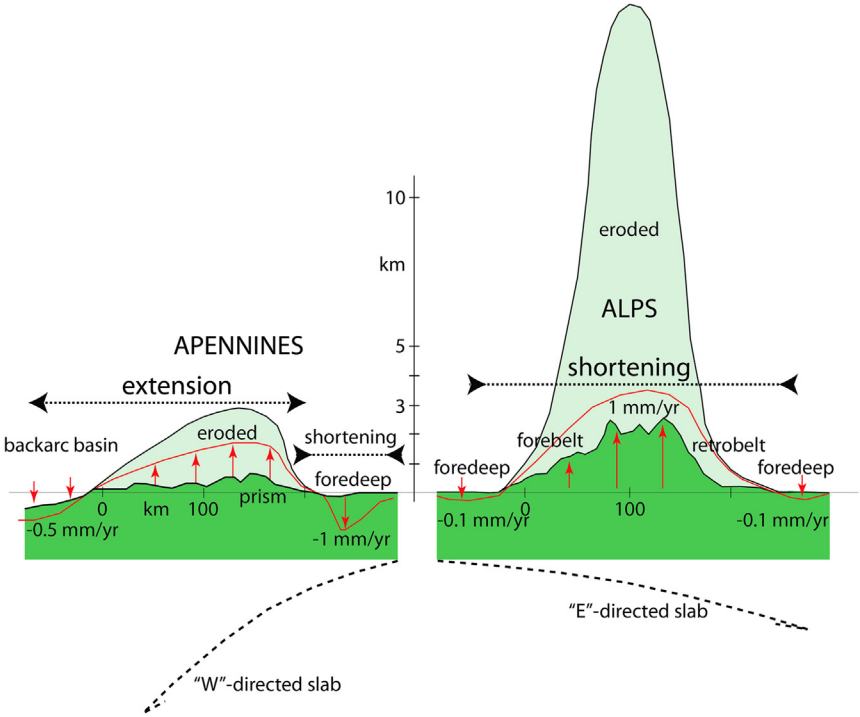

Figure 49 In the Alps the mean topography is more than twice that of the Apennines. The structural elevation of the Alps (i.e., the hypothetical elevation without erosion) is even more pronounced and exceeds by a factor of 5 that of the Apennines. Alps and Apennines represent good, even though complex examples, of the two end members of the subduction style, i.e., the elevation is similar to the structural elevation in the W-directed subduction zone of the Apennines, whereas the topography is much smaller than the structural elevation in the Alps. Moreover, in the internal part of the Apennines there may be the inherited relic of the preexisting Alps, with a pre-Apennines topographic and structural elevation characteristic of the alpine system, stretched and collapsed within the Tyrrhenian backarc basin. In the Apennines accretionary prism, shortening is paradoxically located in the area of largest subsidence, close or beneath the foredeep. The remaining portions of the belt (to the west) are rather uplifting while stretching. Along the western margin of the Apennines, uplift decreases and switches to subsidence in the Tyrrhenian backarc basin. The Alps are rather characterized by diffuse contraction (with only some extension parallel to the strike of the belt and possibly associated with local culminations of structural highs) and the belt is entirely uplifting, apart in the two adjacent foredeeps (in the forelands of the forebelt and of the retrobelt). *Modified after Carminati and Doglioni (2012).*

is for the structural envelope α to the prism, which is steeper and rising toward the hinterland in the Alps. The result is that the Apennines, in spite of being low elevated, have a very deep foredeep, whereas the Alps have

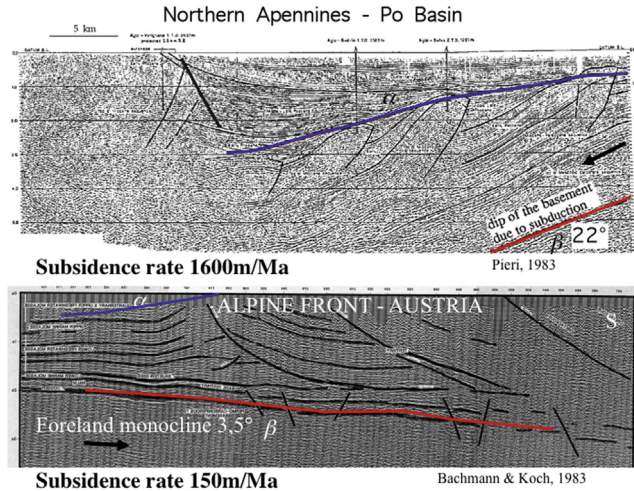

Figure 50 The foreland regional monocline in red (β) is steeper beneath the Apennines accretionary prism with respect to the Alps. Note the opposite behavior of the structural envelop in blue (light gray in print versions) (α) that is inclined toward the interior of the belt in the Apennines with respect to the Alps, where it is steeper and rises toward the hinterland. This asymmetry is a global feature where the steep foreland regional monocline and the shallow envelop pertain to W-directed subduction zones, whereas the opposite setting is typical of E- (or NE-) directed subduction zones.

two shallow foredeeps, even if they are much more elevated and have a much faster exhumation rate because the decollements planes are deeply rooted in the crust. This explains why the Alps have much wider outcrops of basements rocks with respect to the Apennines (Figure 51).

The Apennines and the Alps formed at the margins of the same plates: between the Ionian–Adria plate to the E or SE, and the European plate to the W or NW. The two orogens are diachronous and have very different rates of evolution. The Apennines subduction formed during the last 30–40 Ma. In contrast, the Alpine subduction began during Early Cretaceous (140–100 Ma). The Alps are more elevated with respect to the Apennines and have a much higher structural relief as also indicated by the outcrops of high-grade metamorphic rocks. Erosion eliminated a large part of the uplifted thrust sheets, which would have reached some tens of kilometers of altitude if they had remained in place. The Apennines, on the other hand, have extensive outcrops of sedimentary cover (Carminati and Doglioni, 2012), and only a few scattered outcrops of metamorphic rocks, mainly relics of the earlier Alpine phase. In contrast with the Alps, the Apennines did not have a thick pile of tens of kilometers of nappes that were

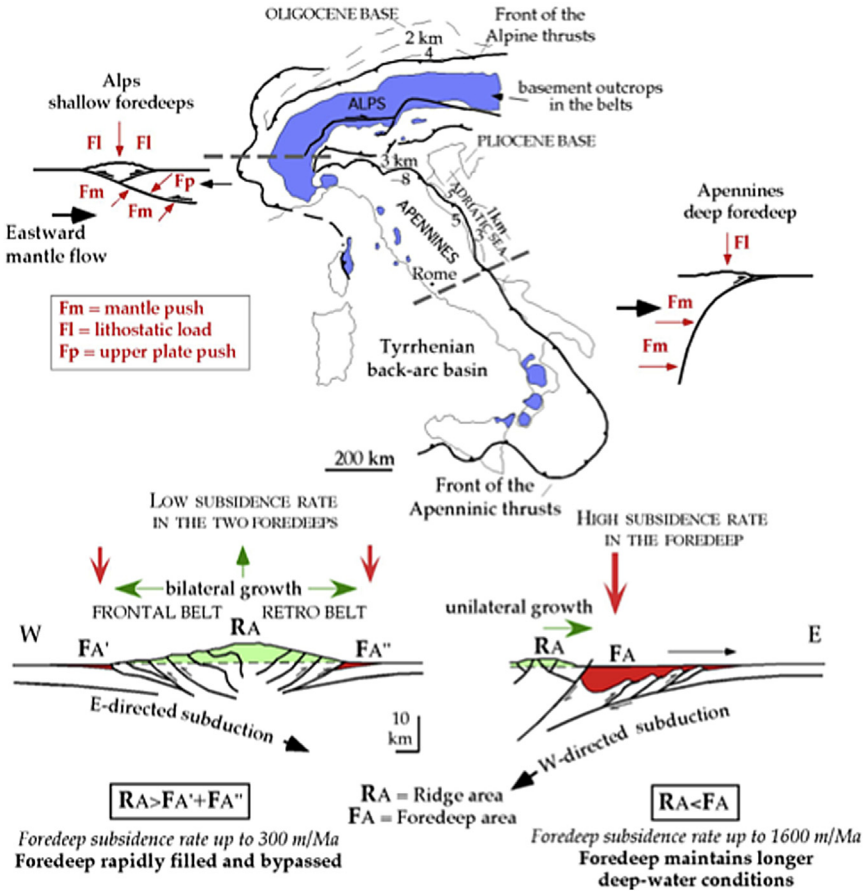

Figure 51 The asymmetry between Alps and Apennines is well marked by their respective foredeeps. In spite of the much higher elevation, the Alps have two shallow and low-subsiding foreland basins. The Apennines have one deep, fast subsiding, foreland basin. In cross section, the area of the Alps is larger than the area of the foreland basins. This explains why those basins have rapidly been filled and bypassed. In the Apennines the area of the belt is rather smaller than the foredeep, where deep water conditions have been maintained for longer period than in the Alps. Most of the filling of the Apennines foreland basin is supplied by the Alps. The Apennines have a steeper foreland regional monocline and a few scattered outcrops of basement rocks, which are interpreted as relics of the earlier alpine belt to the west. The Alps evolved growing both vertically and bilaterally. The Apennines rather developed mainly laterally and "eastward," with minor uplift related to the relatively shallower depth of the basal decollement of the accretionary prism. The interpretation of this asymmetry is ascribed to the "eastward" mantle flow, implicit in the net rotation of the lithosphere or "westward drift" phenomenon. The origin of the foredeeps in the Alps is favored by the load of the belt, but contrasted by the sustaining mantle flow. In the Apennines, where the load of the belt is insufficient to explain the subsidence, the mantle flow determines the retreat of the slab, and the consequent subsidence at its hinge. *After Carminati and Doglioni (2012).*

eroded. Moreover a backarc basin, i.e., the Tyrrhenian Sea, formed only to the west of the Apennines. Another unexpected difference between the Apennines and the Alps is that paradoxically the Alps have a shallow foredeep with low subsidence rates, in spite of the higher topographic relief and consequent higher lithostatic load compared to the Apennines. In the Alpine foredeep, the Oligocene base reaches a depth of 4000 m (Doglioni, 1994). Subsidence rates in the Alpine foreland range from 0 to 200 m/Ma. The Southern Alps are the retrobelt of the Alpine orogen. The Southalpine foredeep subsided at rates that rarely exceeded 300 m/Ma, as determined dividing the total thickness of the flysch and molasses deposits by the duration of the deposition (2–6 km of sediment deposited in 15–40 Ma or more).

Contrary to the Alps, the Apennines have a very pronounced foredeep; the Pliocene base reaches 8.5 km, indicating subsidence rates of 800–1600 m/Ma. Much of the Apenninic foredeep is located on top of the accretionary wedge, not to its front. Thus, the so-called piggyback basin is often the foredeep for the Apennines. Clastic material in the Apennines is provided not only by their ridge but also by the Alps and Dinarides surrounding the Ionian-Adria plate. Moreover, the average area of the elevated ridge of the Apennines above sea level, from the water divider eastward, is 40 km^2; the area of the foredeep is 180 km^2, so the ratio is 0.22:1. This ratio is always <1 in all W- (or SW-) directed subduction settings (Doglioni, 1994). The average area of the entire Alpine orogen above sea level is about 300 km^2, and the sum of the areas of the foredeeps of the frontal and back thrust belts is estimated as 150 km^2. Thus, the ratio of the area of the orogen to the area of the foredeeps is 2:1. As a rule this ratio is >1 in thrust belts related to E (or NE-) directed subduction.

It is from the studies of the Alps that the terms flysch and molasse were introduced and describe early and later stages of foredeep filling. Flysch and molasse are in general synonymous with deep and shallow clastic facies, respectively. The initial stages of subduction occurred when there was a deep-water environment collector for turbidites coming from the uplifting and eroding wedge. The foredeep was quickly filled, however, because the amount of sediment coming from the orogen was much larger than the accommodation space in the foredeep. As a consequence, the foredeep changed to molasse shallow-water conditions, and once the basin was filled, the foredeep was bypassed, and clastic sedimentation occurred in remote areas: for the Alps, in the Rhone and Po deltas, and in the North sea and the Black sea, by means of the Rhine and Danube rivers, respectively.

This bypassing occurred because the subsidence rate in the foreland basins around the Alps was insufficient to keep the sediments coming from the orogen. Therefore Alps and Apennines may be considered two different end members of thrust belts. However, the Apennines developed east of the southward continuation of the present-day Alps. In fact, in the hanging wall of the Apennines subduction there are boudinated remnants of the alpine belt, stretched by the extension of the Apennines backarc, well visible in the uppermost mantle as well (Brandmayr et al., 2011). Therefore, within the western internal parts of the Apennines there should be the record of the alpine evolution with alpine rocks of both the frontal thrust belt (e.g., Corsica) and the retrobelt (e.g., Cervarola Front? Doglioni et al., 1998). The origin of the two distinct foredeeps can be ascribed to the westward drift of the lithosphere; in fact the W-directed subductions may be anchored into the easterly moving mantle, thus resulting in slab retreat, hinge divergence relative to the upper plate and fast subsidence in the foredeep. E- or NE-directed subductions are rather dipping in the same direction of the mantle flow, which sustains the slab and contrasts the load of the upper plate, thus inhibiting its subsidence (Figure 51) and the subduction hinge converges relative to the upper plate. The steep foreland regional monocline in the Apennines is synonymous of fast subsidence rates (>1 mm/yr), which implies that along the salients of the accretionary prism front, the uplift of some anticlines may be slower than the subsidence, resulting in a negative fold total uplift (Doglioni & Prosser, 1997). In other words, while the fold forms, it subsides because the regional subsidence overwhelms its uplift (Figure 52). This setting is particularly promising for hydrocarbon exploration because the anticlines are not eroded and may be sealed by shaly formations to form traps and plays. In fact several oil or gas fields in the external Apennines occur in such setting. The Apennines are accompanied by the backarc spreading to the west, which started in the western Mediterranean in the Eocene—Oligocene, and migrated eastward, boudinating the preexisting lithosphere.

The Provencal, Algerian, and Tyrrhenian basins are floored or partially floored by oceanic crust with an age progressively younger, moving eastward (Carminati & Doglioni, 2005; Carminati et al., 2012; Gueguen et al., 1997, 1998). The backarc area is characterized by widespread uplift of the asthenosphere (Panza et al., 2007) and high heat flow values (Figure 53). The Adriatic plate subducts W-ward beneath the Apennines and NE-ward beneath the Dinarides (Figure 53), whereas it overrides the European plate in the Alpine subduction zone. The Apennines are about

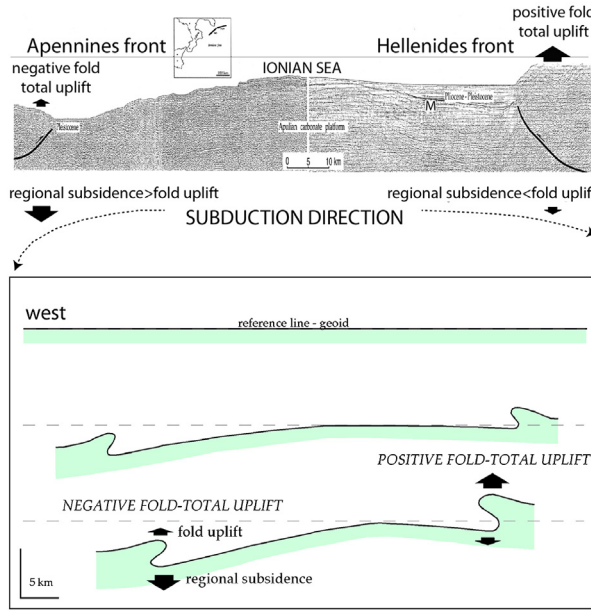

Figure 52 Comparison between the Apennines and Dinarides–Hellenides front in the northern Ionian Sea. The deepest foredeep is along the Apennines subduction and the highest structural elevation is in the Hellenides front. The Apennines front has negative fold-total uplift, whereas in the Hellenides it is positive. The fold-total uplift may be defined as the single fold uplift rate and the regional subsidence. This value can be either positive or negative. This last case may occur along the front of W-directed subduction zones where the subsidence rates may be faster than the fold uplift rate. M, Messinian. *After Doglioni et al. (1999b).*

30–40 Ma old, whereas the Alps possibly started more than 100 Ma ago. The Alps continued southwestward in Corsica and the Betics and were later stretched in the Apennines backarc basin. The basements rocks dragged in the Tyrrhenian basin and outcropping in Calabria and other smaller areas of the western Apennines represent remnants of the southern prolongation of the Alps eventually transposed and incorporated in the internal boudinated part of the Apennines.

The Atlantic subduction zones such as the Barbados and Sandwich arcs developed only where the northern and southern American continents narrow (Figure 31). They initiated along the retrobelt of the American Cordillera where there was oceanic lithosphere in the foreland to the east able to be subducted (Doglioni et al., 1999a). Similarly, the Apennines can be interpreted as a subduction zone initiated along the retrobelt of the Alps (Carminati & Doglioni, 2005; Carminati et al., 2012), where in their

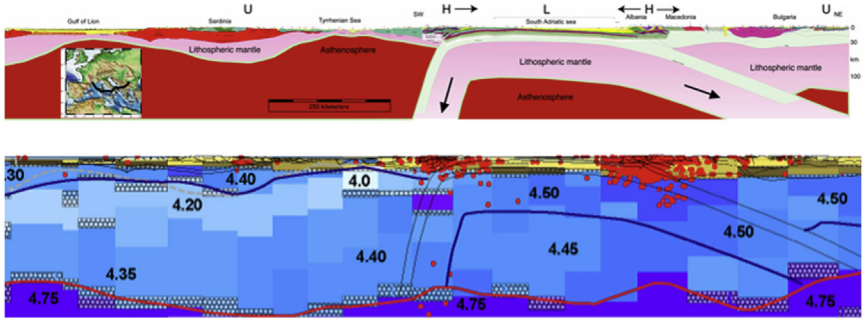

Figure 53 Geological and geophysical (absolute tomography) cross section across the central Mediterranean (Transmed III). *(After Carminati, Doglioni, and Scrocca (2004) (top) and Panza, Raykova, et al. (2007) (bottom).)* The subduction hinge diverges from the upper plate along the Apennines subduction while converges relative to the upper plate in the Dinarides. In the Apennines the slab retreat relative to the upper plate opened a backarc basin with the consequent uplift of the asthenospheric mantle, well delineated by absolute Vs tomography.

retrobelt there was a remnant of the ocean or thinned continental lithosphere inherited by the Mesozoic Tethyan rifting (Figure 54). During the subduction rollback, the backarc migrated eastward as testified by the magmatism and the progressive younging of the syntectonic sediments (Gueguen et al., 1998). The lithosphere was stretched and the boudins show a basal shear, being their roots displaced to the east with respect to the surface morphology (Figure 55). On account of the large averaging volumes involved in such kind of anisotropy measurements, this can be ascribed to the relative eastward mantle flow, also responsible for the dominant E–W trend of seismic anisotropy of the area described by Lucente, Margheriti, Piromallo, and Barruol (2006). In Figure 55 the seismic anisotropy becomes parallel to the strike of the Apennines slab, suggesting that the mantle flow is encroaching an obstacle and the olivine crystals are elongated parallel to it. The cross section of Figure 56 illustrates the present setting along the Crop-03 seismic reflection profile of the northern Apennines, with the frontal accretion in an area characterized by dominant subsidence, the uplift of the main backbone of the Apennines undergoing extension, and the subsidence in the remaining western side. Along the transect of Figure 56, uplift and subsidence have different origins which can locally interfere. Within the core of the Apennines there is the relict of the inherited preexisting Alpine double verging orogen that has been boudinated particularly by eastward dipping normal faults (Figure 56) generated during the slab retreat (Figures 57 and 58). The Apennines accretionary prism is located only to the east of the

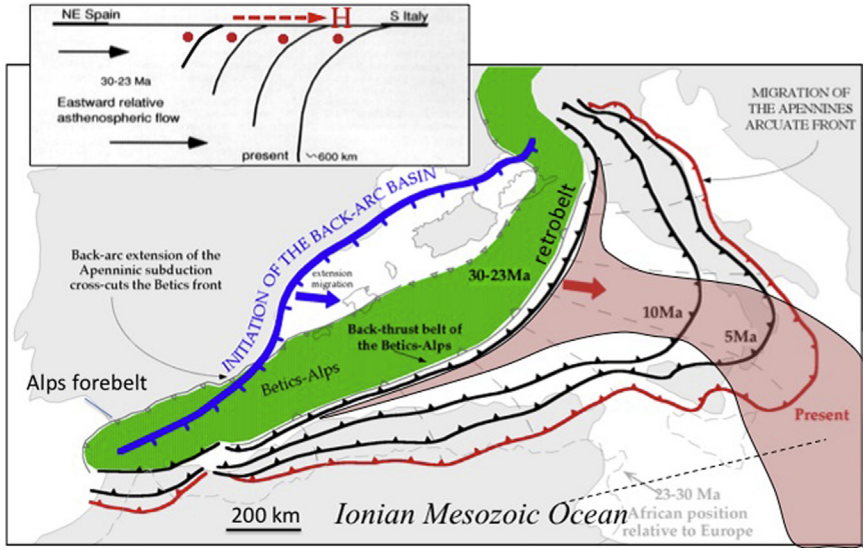

Figure 54 According to the Atlantic examples, the Apennines subduction zone might have initiated along the retrobelt of a preexisting opposite (NE-directed) subduction zone such as the Alps (marked in the green (dark gray in print versions) area). The subduction and its hinge H retreated "E"-ward since about 40 Ma to the present position. The larger salient of the Apennines–Maghrebides arc is located in the Ionian basin where relatively more subduction-prone lithosphere should be present. The amount of retreat is about five times larger than the N–S convergence of Africa. Such contraction represents an independent and secondary mechanism that acts on the Apennines subduction system. *After Doglioni et al. (1999a).*

Alpine-inherited body, supporting the notion that the Apennines subduction developed along the retrobelt of the Alps in its eastern foreland where there was oceanic or thinned continental lithosphere to be subducted as for the Atlantic subductions (Doglioni et al., 1999a). The slab retreat includes deepening of the slab and shearing at its margin. Therefore, the shear at the top of the subduction is transferred upward to the frontal accretionary wedge, determining the decoupling and accretion of the shallow layers of the downgoing plate (Figure 58, left panel). Note the displacement marked by the white arrows of the two markers in the slab and in the shearing mantle associated to the eastward migration of the hinge H (Figure 58, right panel). This explains the generation of tectonic accretion without contact and collision between the upper and lower plates. Based on these evidences and the aforementioned models, a kinematic reconstruction of the Mediterranean geodynamics indicates two "easterly directed" subduction zones (Alps–Betics and Dinarides–Hellenides) along whose retrobelts developed two "westerly

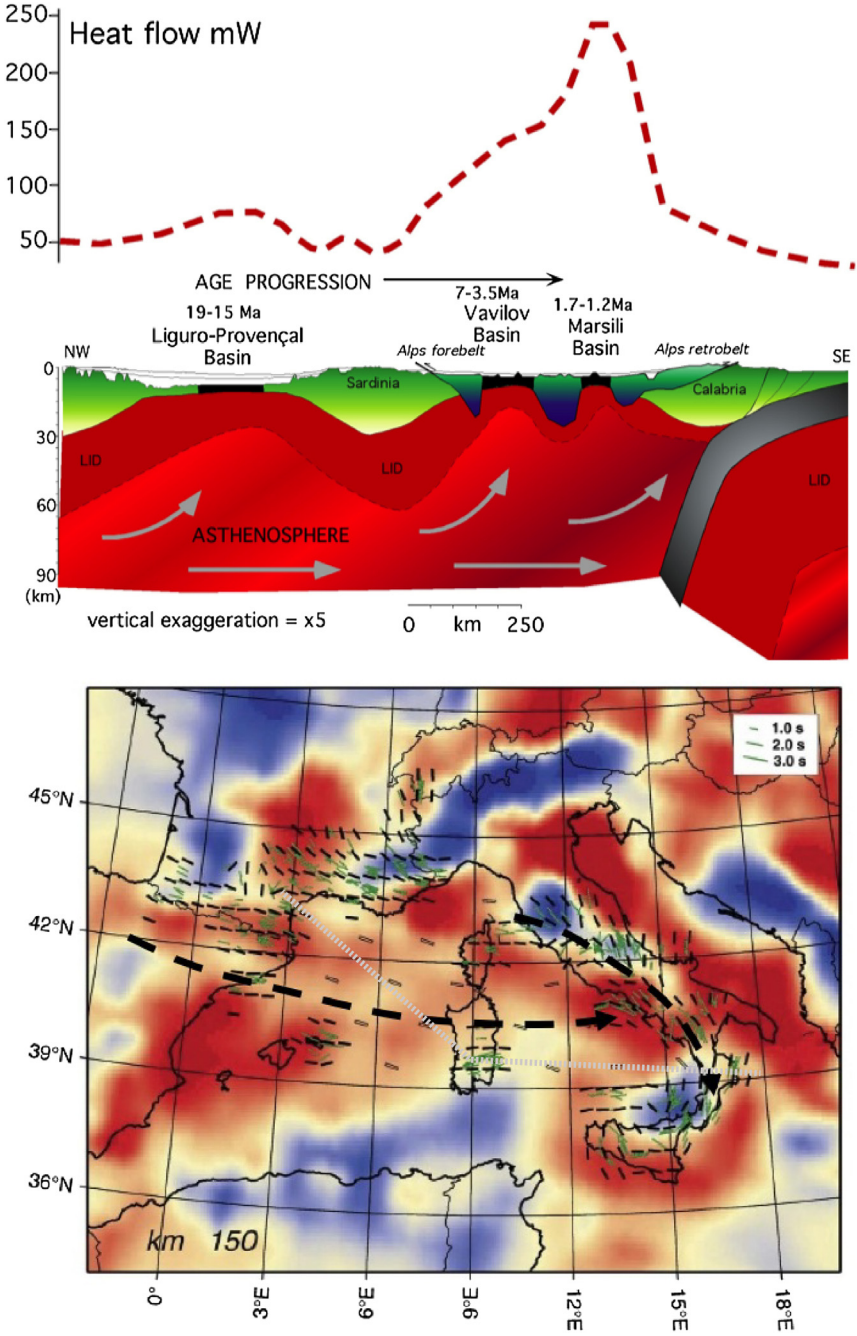

Figure 55 In the western Mediterranean section, large-scale boudinage of the lithosphere in the backarc extensional setting, which developed particularly in the last 30—40 Ma, and the E-ward migration of the extension and the related basins are clearly

directed" subduction zones (Apennines–Maghrebides) as schematically illustrated in Figure 59. The W-directed slabs are accompanied by two backarc basins (western Mediterranean and Pannonian Basin).

Disproving the observation that backarc basins form primarily in the hanging wall of W-directed slabs, the Aegean basin is usually considered a backarc basin as well. However, its origin is not related to the replacement of a retreating lithosphere by the asthenosphere. In fact the Hellenic slab is very shallow (Christova & Nikolova, 1993) and the overlying rifting is rather the result of the differential faster advancement of the Hellenic lithosphere over the Africa plate with respect to the Anatolian lithosphere. Therefore, extension is needed between Greece and Turkey, but the stretching had lower rates as demonstrated by the still thick continental crust–lithosphere in the Aegean Sea in spite of a subduction system active since the Cretaceous (Agostini, Doglioni, Innocenti, Manetti, & Tonarini, 2010). In the Tyrrhenian Sea, the backarc basin generated oceanic crust is about 10 Ma. Therefore, the rifting in the Aegean basin is not related to the loss of a retreated lithosphere relative to the upper plate as in the Tyrrhenian–Apennines or Pannonian–Carpathians systems, but it can rather be explained by the faster advancement of the Hellenic lithosphere over the Africa plate with respect to the slower Anatolia–Cyprus SW-ward motion over the same Africa plate (Agostini et al., 2010). In the eastern Mediterranean upduction is a preferable term to describe the main geodynamic process going on there. Below geotraverse TRANSMED VII (Cavazza et al., 2004) the convex asthenosphere interface (El Gabry et al., 2013) is consistent with the flow of a portion of lower mantle material, sucked from below in the wake left by the ongoing upduction (exhumation) of the Ionian–Adria portion of the African plate (Doglioni et al., 2009). This is consistent with

seen. The underlying mantle flow is required to compensate for the slab retreat. The heat flow maximizes in the most recent and wide Tyrrhenian–Marsili basin. *(After Gueguen et al., 1997; Zito, Mongelli, De Lorenzo, & Doglioni, 2003).* The cartoon is well consistent with the results described by Brandmayr et al. (2010, 2011) about the Vs and ρ in the Italic region. The trace of the section is marked in light gray in the underlying map view, *(modified after Lucente et al. (2006))*, where a comparison between P-wave velocity anomalies at 150 km depth (Piromallo & Morelli, 2003) and SKS splitting measurements in the western–central Mediterranean area is shown. The inferred flow pattern from west to east marked by the thick dashed black line, envelopes some SKS splitting measurements. The seismic anisotropy deviates when encroaching the Apennines slab where it becomes parallel to its strike, suggesting a flow perturbed by an obstacle.

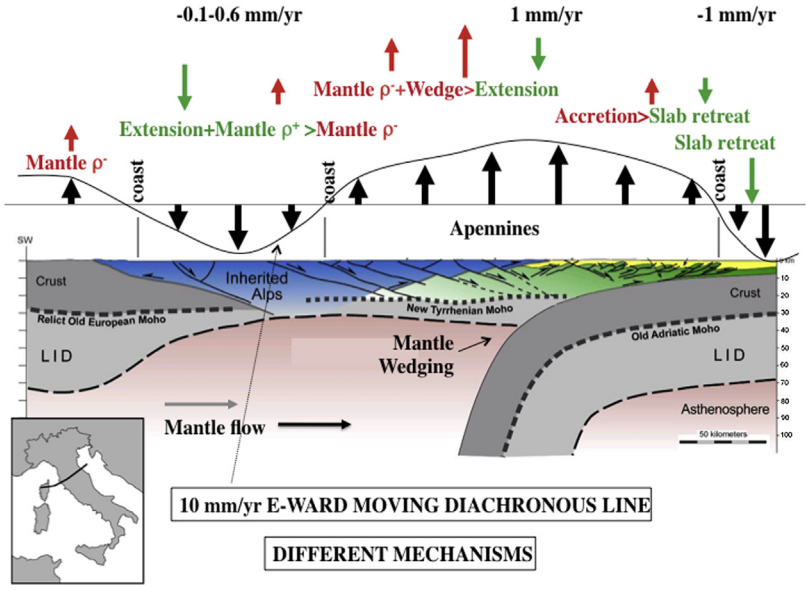

Figure 56 Schematic geological section through the Apennines–Tyrrhenian Sea system along the Crop-03 profile. The cartoon is well consistent with the results described by Brandmayr et al. (2010, 2011) about the Vs and ρ in the Italic region. It is noticeable the Moho doubling below the Val Tiberina with a shallower new Tyrrhenian Moho, at about 20 km, above a deeper presubduction in age Adriatic Moho, at about 52 km. According to these constraints, most of the Adriatic crust should be subducted below the northern Apennines accretionary wedge that, in turn, is mainly made up of stacked units of sedimentary cover off-scraped from the subducting plate. The double verging Alpine orogen (dotted) is stretched by the backarc extension related to the Apennine subduction. The metamorphic rocks outcropping in the Apennines may be interpreted as related to the Alpine type evolution, which implies deeper decollement planes, affecting both the upper and the lower plates. According to the model presented, in their western side the Apennines contain the boudinated relicts of the earlier Alpine orogen. The Apennines subduction should have developed along the retrobelt of the Alpine belt. *After Carminati et al. (2004).*

the down-dip tension of the seismicity. On the other side, in the Cyprian arc, the mantle structure (Vs and ρ) seems to indicate a less advanced ongoing process of upduction than in the Hellenic arc, well in agreement with the direction of motion of the Anatolian plate relative to the African and Hellenic plates, both in the deep and shallow reference frames. The stress pattern inferred from fault plane solutions (Papazachos, Karakostas, Papazachos, & Scordilis, 2000) is well consistent with down-dip extension within the upducting plate. The NE-directed Hellenic–Cyprus subduction (upduction) is a good example for the E- (or NE-) directed subduction

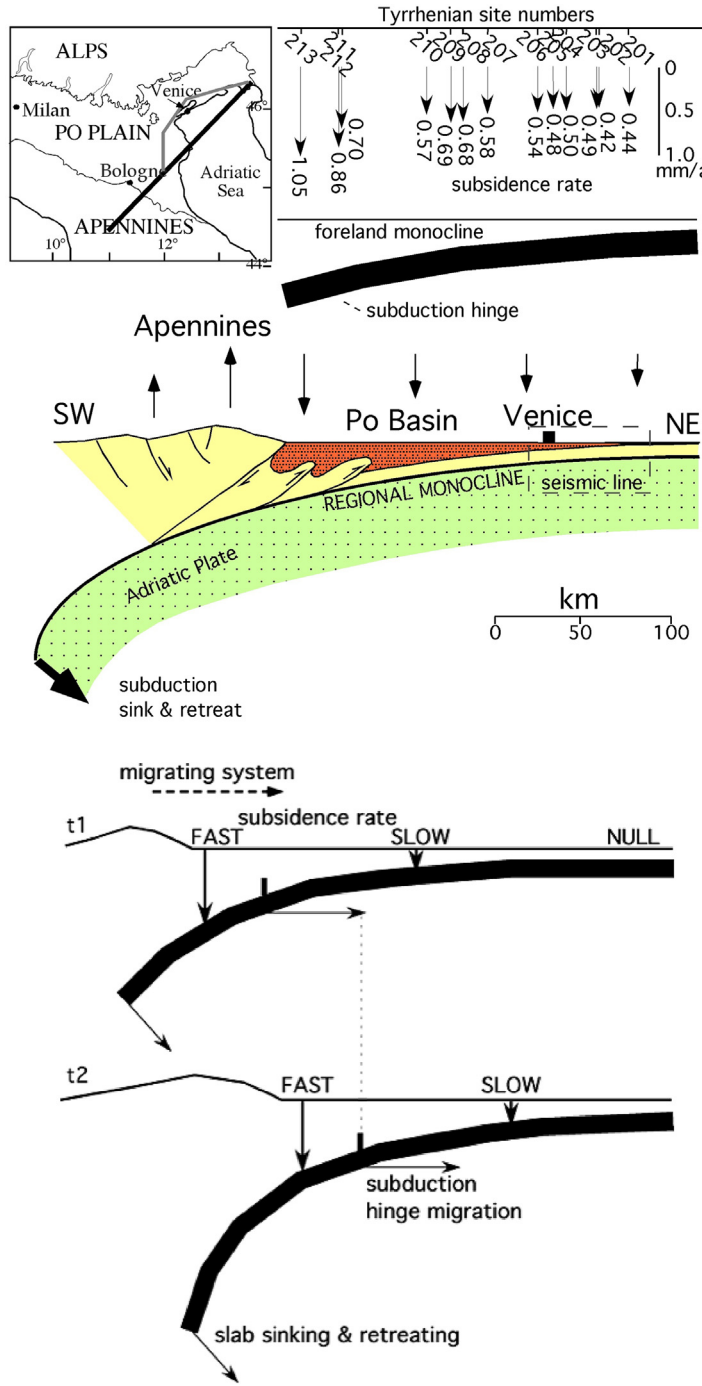

Figure 57 Subsidence rates in the northern Apennines foreland, determined by the depth of the Tyrrhenian (MIS 5.5) layer cored mostly along the gray line running on the coast, are displayed in the top panel. These rates indicate relatively faster subsidence in the southwestern part of the profile, i.e., an asymmetric active subsidence. The dip of the regional monocline in the northern Adriatic Sea recorded the relatively faster subsidence at the southwest end and it can be explained by the north–eastward slab retreat of the Adria, as shown in the lower panels. *After Cuffaro et al. (2010)*.

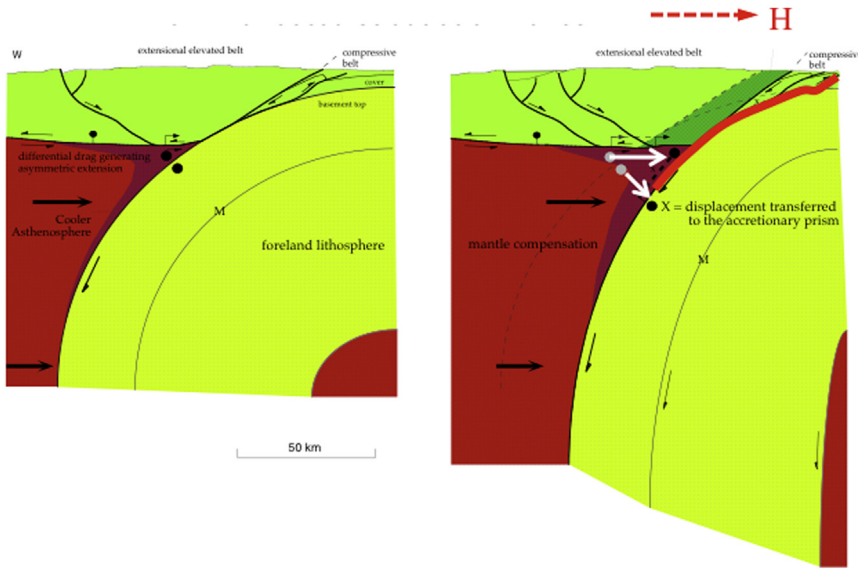

Figure 58 Kinematic model for the coexistence compression–extension of W-directed subduction zones as the Apennines. The extension in the hanging wall of a W-directed subduction may be attributed to the slab retreat relative to the upper plate. The shortening in the accretionary wedge can be explained as related to the shear between the downgoing and retreating lithosphere and the eastward compensating upper mantle. The displacement is transferred upward and peels-out the cover from the foreland lithosphere. Note the different trajectory of the two black spots in the asthenosphere and at the top of the slab. *(After Doglioni et al. 1999a)*. The coexistence compression–extension in the Apennines domain is well consistent with the viscoelastic models of LLAMA formulated by Aoudia et al. (2007) and Ismail-Zadeh, Aoudia, and Panza (2004; 2010).

zones. Directed opposite to the direction of motion of the African plate, the apparently subducted slab has a gentle angle of dipping and shallow depth of penetration ~220 km unlike to W-directed subduction zones that are steeper and can be seismically active till ~600 km of depth. Further studies taking into account both kinematic models and tomographic studies are undoubtedly necessary to refine the model supplied here about the nature of the subduction zones and the plate-driving forces, but what reported here casts well-rooted doubts on the role of slab break-off in the control of the geodynamic activity throughout the Aegean–Anatolian domain starting in latest Miocene to early Pliocene time evoked by Schildgen, Yıldırım, Cosentino, and Strecker (2014).

The gravity anomalies of the Apennines and Alps subduction zones have been inverted jointly with the seismic velocity and it appears that the slabs are lighter than the hosting mantle (Figure 60). This observation precludes

the negative buoyancy of the slab (slab pull) as the driving force both for subduction and plate motion (Brandmayr et al., 2011). Therefore, the asymmetry between the W and E classes of subduction zones that is visible worldwide is confirmed in the Mediterranean subduction zones and it may be attributed to the westward drift of the lithosphere relative to the mantle. In fact, the present seismogenic W-directed slabs such as the Tyrrhenian (under Calabria) and Carpathians (under Vrancea) are very steep (between 70° and 90°), whereas the NE-directed Hellenic slab is dipping only 15°–20°. This asymmetry is identical, in practical terms, to the one observed when comparing west and east Pacific subduction zones (Figure 61). However, while in the Pacific a different age of the subducting lithosphere was invoked to explain the different dip of the slabs, beneath the Apennines and Hellenides the same Ionian lithosphere is subducting. Therefore, regardless the Ionian lithosphere is oceanic (Catalano, Doglioni, & Merlini, 2001) or thinned continental (Calcagnile et al., 1982; Farrugia & Panza, 1981) it is a lithosphere with the same composition and thermal state that is subducting in both sides beneath the Apennines and Hellenides. Therefore, the different dip between Apennines and Hellenides slab must be rather related to the different relationship between slab and mantle dynamics (Agostini et al., 2010). In fact, like in the Pacific subduction zones (e.g., Castle & Creager, 1998; Vassiliou, Hager, & Raefsky, 1984), the intra-slab focal mechanisms of the W-directed slabs show dominant down-dip compression, whereas the opposite E- or NE-directed slabs generally show down-dip extension (Figure 62). This observation is coherent with the kinematics of the lithosphere relative to the mantle implicit with the notion of the westward drift of the lithosphere; W-directed slabs are somewhat pushed down, whereas E- or NE-directed slabs are rather shifting westward relative to the mantle, hence moving "out" of it (Figure 63). This relative motion of the Hellenic (or other E- or NE-directed subduction zones) with respect to the mantle should generate upraise of the underlying mantle. This process can naturally explain the high-velocity body that is often detected associated to such subduction zones. This high-velocity body is usually assumed as the slab continuation at depth beneath Greece and South America subductions, even if it is practically aseismic, three to four times thicker than a "standard" slab and has a quite large dip. While the very scarce seismicity illuminates with some confidence the "slab" position, the relative mantle tomography may be misleading and suggest the false presence of a slab (Figure 64). Let us consider, for example, the case schematized in section a of Figure 63. The plate motion of Africa, Greece, and

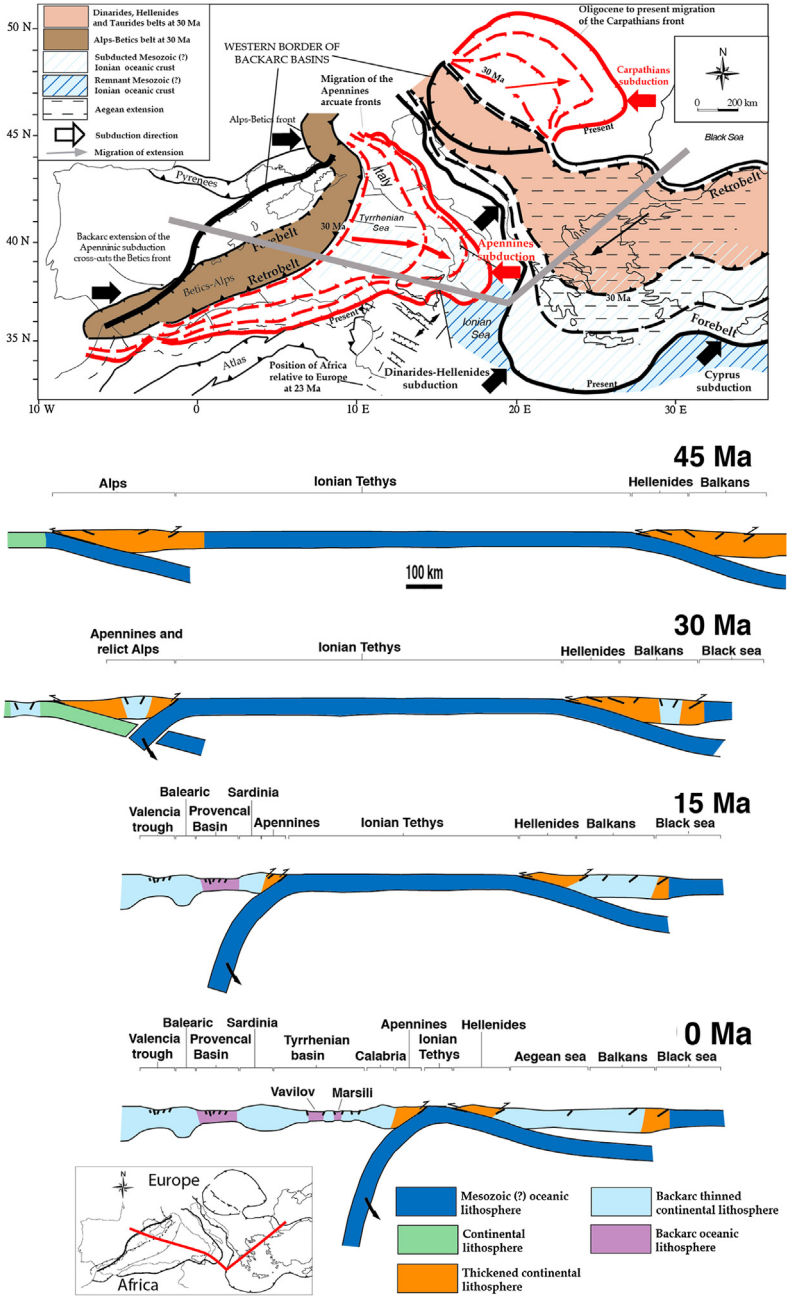

Figure 59 Kinematic reconstruction of the Mediterranean geodynamics during the last 45 Ma. *(After Carminati and Doglioni (2005).)* The W-directed Apennines and Carpathians subductions enucleated along the retrobelt of the preexisting Alpine and Dinarides

Anatolia relative to the deep hot spot reference frame (Figure 63(d)) shows that Africa moves westward faster than the underlying mantle and escapes from the subduction, i.e., it is upducting, as schematized in Figure 63(c). The westward or south–westward motion of Africa and its Hellenic slab would be even faster in the shallow hot spot reference frame (Doglioni et al., 2007). The short inclined arrows in Figure 63(a) indicate, on the other side, the possible flow of a portion of lower mantle, sucked from below (the tectonic syringe). Such a process is made possible by the wake left by the slab in its upduction (mantle exhumation) motion (Doglioni et al., 2009). Therefore, the upduction seems a much more natural process, consistent with the tomographic image, than the subduction of a slab, with rather complex shape. Similar conclusion can be reached considering the other sections given by Spakman, Wortel, and Vlaar (1988). In fact, when plate motion is considered relative to the hot spot reference frame, the Adria/Ionian plate moves out of the mantle (upduction). Such a possibility is well consistent with the tomographic images and gravity inversion in eastern Mediterranean (El Gabry et al., 2013). As shown in Figure 63(c), the white dot moves leftward relative to the underlying black dot in the mantle and subduction occurs because the dark gray dot, in the upper plate, moves leftward faster than the white dot in the slab. The subduction rate is the convergence minus the orogenic shortening. With different velocities, the upduction concept is applicable, in the shallow hot spot reference frame, to the AS as well.

This kinematic evidence of upducting slabs casts serious doubts on the slab pull as the dominant driving mechanism of plate motions. Moreover, the interpretation of relative mantle tomography (Foulger et al., 2013) that supports the slab detachment idea relies on the very stringent assumption that the chemical composition of the mantle is quite homogeneous and therefore the velocity variations are dictated by thermal anomalies. In

belts, respectively. Blue (dark gray in print versions) lithosphere is oceanic. In the map, the brown (gray in print versions) and orange (light gray in print versions) colors correspond to the alpine and dinaric belts, respectively. The evolution of the Mediterranean along the gray trace shown on the map is the result of three main subduction zones: (1) the early eastward-directed Alpine subduction; (2) the Apennines subduction later switch along the Alps retrobelt; (3) the Dinarides–Hellenides subduction. The last two slabs retreated at the expense of the inherited Tethyan Mesozoic oceanic or thinned continental lithosphere. In their hanging walls, a few rifts formed as backarc basins, which are progressively younger toward the subduction hinges. The slab is steeper underneath the Apennines, likely owing to the westward drift of the lithosphere relative to the mantle.

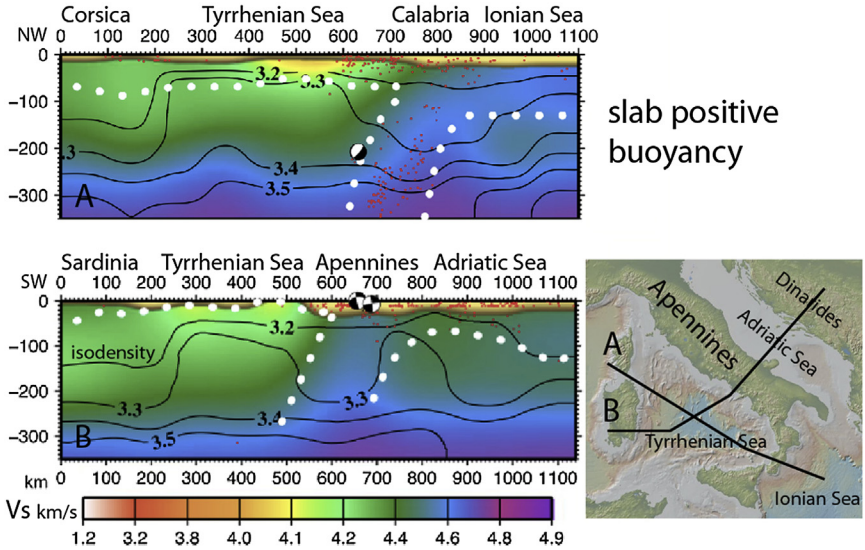

Figure 60 Two cross sections of the Tyrrhenian–Apennines backarc-subduction system (uppermost 350 km) that show the absolute Vs tomography and the inverted density model. Vs distribution is given by the color scale while continuous contour lines refer to ρ (g/cm^3). Both sections show that in the slabs (lid–LVZ margin marked by white dots) the velocity is higher than in surrounding (ambient) rocks. The isodensity lines (g/cm^3) are deflected downward, therefore the Apennines W-directed slab is lighter than the ambient mantle. As a consequence, the subduction is not driven by slab pull, being the slab positively buoyant. Seismicity (red (gray in print versions) dots) and focal mechanisms of major events of the past 20 years (beach balls are plotted in map view) are shown as well. In section A the mantle velocity is higher in the Ionian–Adria plate than in the Tyrrhenian basin. A prominent negative density anomaly characterizes the subducting slab and the Sardinia–Corsica block, whereas a positive anomaly characterizes both the active Tyrrhenian, with a 3.3 g/cm^3 density at about 60–70 km of depth, and the Ionian mantle, with a 3.3 g/cm^3 density reaching about 80 km of depth and a 3.4 g/cm^3 density at about 170 km of depth. Section B, Sardinia–Balkans section, partly covers also the NE-directed Dinarides subduction. The prominent positive density anomaly found below the Tyrrhenian Sea, where the asthenosphere is uplifted in the backarc basin, confirms that the asthenosphere is heavier than the lithosphere. *After Brandmayr et al. (2011).*

reality, it is evident from the geochemistry of magmas (Peccerillo, 2005) that the Mediterranean mantle is highly heterogeneous (Figure 65), once more suggesting extremely mixed and variable mantle sources. The tomoimages in which it is assumed homogenous mantle geochemistry are therefore not reliable if not false (Foulger et al., 2013). Therefore, the Mediterranean geodynamics follows the same rules of the rest of the planet, and the main asymmetries among W- versus E-directed slabs are maintained and can

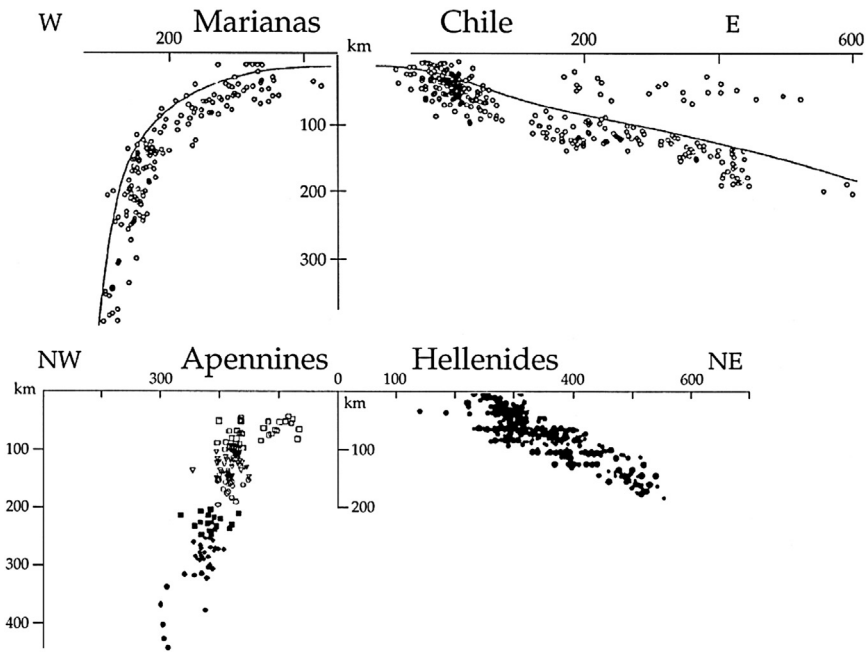

Figure 61 Paradigmatic cross sections of hypocenters of the Marianas and Chile converse subduction zones in the Pacific are compared with those of the hypocenters of the Apennines and converse Hellenic subduction zones in the central Mediterranean. The asymmetry in the dip of the Pacific slabs, which could be ascribed to the age difference of the subducting oceanic crust, is present also in the central Mediterranean subduction zones where the Ionian oceanic lithosphere (no age difference) is subducting contemporaneously both underneath the Apennines and the Hellenides. Therefore, the asymmetry is not linked to differences in age and temperature of the subducting lithosphere. *After Doglioni et al. (1999b)*.

be naturally explained by the westward drift of the lithosphere. In W-directed slabs (Apennines type) the subduction hinge diverges relative to the upper plate and generates backarc extension. The subduction is faster than the convergence and the accretionary prism is mostly composed by the off scraping of the shallow layers of the lower plate (Figure 66). E- or NE-directed slabs (Alpine type) are rather associated to the subduction hinge converging relative to the upper plate and the subduction is slower than the convergence. The orogen is double verging and is not associated to backarc basin. Moreover, during oceanic subduction it is composed by deep basement slices mostly of the upper plate while during collision also basement slices of the lower plate are involved (Figure 66).

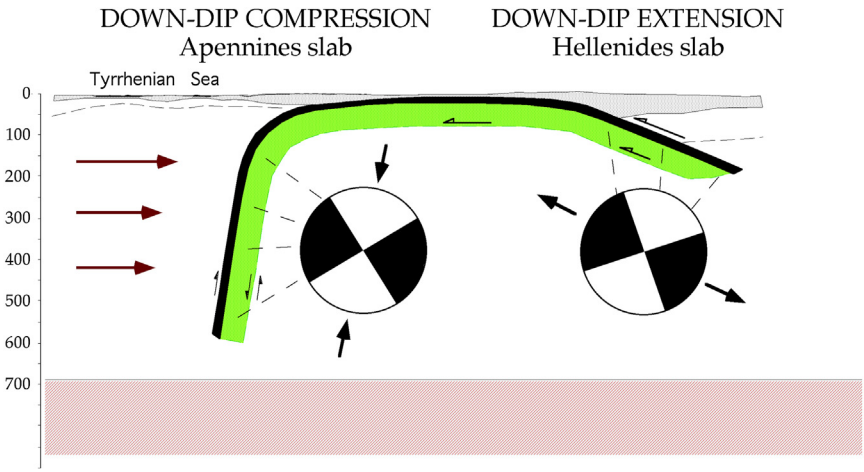

Figure 62 Comparing the intraslab state of stress of the Apennines and the Hellenic (converse) subduction zones, the W-directed slab appears characterized by down-dip compression, whereas the NE-directed slab is undergoing down-dip extension. The focal mechanisms are similar, but they are embedded in slabs with opposite dip. This asymmetric seismological signature is seen along the opposite Pacific subduction zones, as well. It is consistent with the fact that W-directed slabs are pushed down, whereas E- (or NE-) directed subductions are rather pulled out, as suggested by the global kinematics, and act as the plunger of the tectonic syringe. *After Doglioni et al. (2007).*

The eastward rejuvenation of lithospheric stretching of the western Mediterranean basin (Oligocene Ligurian–Provencal Seas, Late Miocene–Quaternary Tyrrhenian basin) is in agreement with an eastward relative migration of the underlying mantle, consistent with the eastward decrease in age of the magmatism. The Apenninic subduction acts as a nail responsible of the opening of the western Mediterranean basin. The present subduction of the Ionian–Adria plate in Calabria is the nail pushed eastward by the mantle (Gueguen et al., 1997). The Tyrrhenian backarc basin opens as a consequence of the Apennines slab retreat. There are striking differences between the magmatism associated with the Alpine orogen and that occurred during the formation of the Apennines. The Alpine orogenic magmatism is essentially represented by intrusive and hypabyssal rocks, with minor amounts of volcanic products. It was formed during two main stages of activity (Dal Piaz & Venturelli, 1983).

The first stage is basically Upper Cretaceous–Lower Eocene (100–40 Ma) and consists of andesitic volcanics, which were emplaced on the African continental margin. Evidence of this volcanism is only recorded by andesitic s.l. clasts occurring in some flysch and arenaceous sediments

(Taveyanne, Schliren flysch). The second stage is essentially Oligocene (34–23 Ma) and mainly consists of granitoid bodies, several dikes and a few, poorly preserved volcanites.

This magmatism, which is known as the "periadriatic igneous belt," marks a postcollisional extensional tectonic phase of the Alpine orogen. The plutonic rocks are mainly acid to intermediate in composition with a very few basic products. Intermediate compositions dominate among dikes. Petrochemical affinity is mainly calc-alkaline or high-K calc-alkaline with some shoshonites and few ultrapotassic lamproitic rocks (Beccaluva, Gatto, Gregnanin, & Piccirillo, 1979; Beccaluva et al., 1989; Bellieni, Peccerillo, & Poli, 1981; Bellieni, Cavazzini, Fioretti, Peccerillo, & Poli, 1991; Venturelli, Thorpe, Dal Piaz, Del Moro, & Potts, 1984). A few dikes of arc tholeiites are also present (Beccaluva et al., 1983). In its eastern sector, granodioritic–tonalitic plutons (Vedrette di Ries, Rensen, Monte Alto, etc., Bellieni et al., 1981, 1991) and several calc-alkaline to shoshonitic dikes represent the periadriatic belt. In the central sector, a few plutons (Bregaglia, Adamello) and a large number of dikes crop out. Compositions range from arc-tholeiitic to calc-alkaline and shoshonitic. Intermediate calc-alkaline and high-K calc-alkaline rocks represent the dominant lithologies (Beccaluva et al., 1983). Finally, the western sector contains few small intrusive bodies, some volcanites, and dikes with high-K calc-alkaline and shoshonitic intermediate composition. Ultrapotassic lamproitic dikes are also present in this zone (Venturelli et al., 1984).

Overall, dominant plutonic and hypoabissal rocks, with variable petrochemical affinity but with clear subduction-related geochemical and petrologic signatures, represent the magmatism associated with the Alpine orogen. Volcanic rocks are scarce or absent. Other effusive rocks with transitional to Na-alkaline affinity crop out south of the eastern Alps in the Euganei Hills magmatic zone, which is marked by a prominent LVZ below a depth of about 130 km and a positive density anomaly as shallow as 30 km opposite to the negative density anomaly characterizing the subducting LID (Brandmayr et al., 2011).

The magmatism associated with the Apennines orogen is much more abundant and petrologically complex. Magmatic rocks are spread over a very wide area, from southeastern France, Sardinia, and Corsica, to the Tyrrhenian basin and to central–southern Italy. These rocks are essentially extrusive, whereas only a few granite–granodiorite bodies (8.5–5 Ma), occurring in southern Tuscany and Tuscan Archipelago (Peccerillo, 2005), represent intrusive activity. Volcanic activity has given MORBs, island arc tholeiites, calc-alkaline, high-K calc-alkaline and shoshonitic

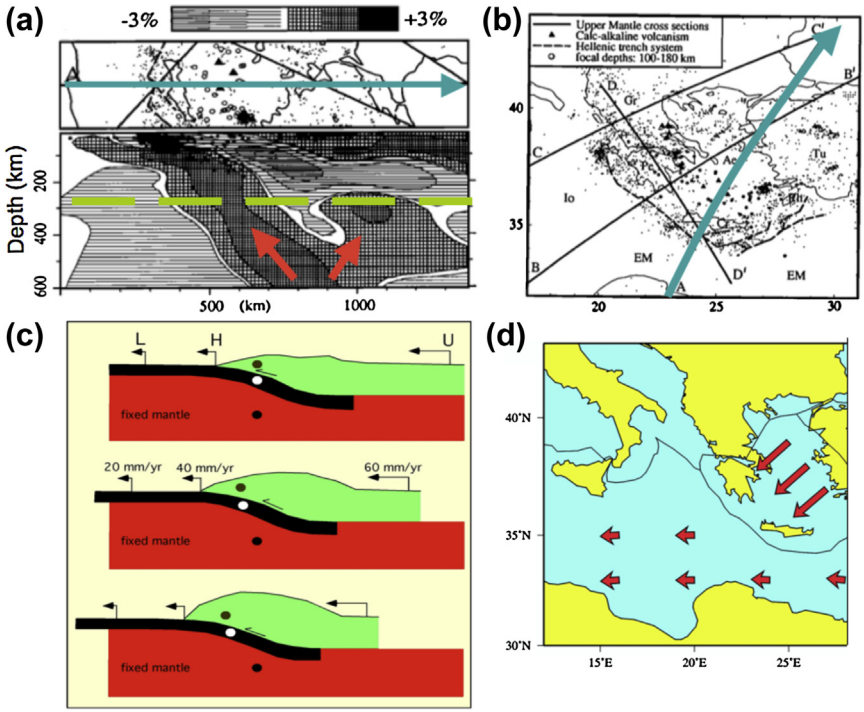

Figure 63 (a) Relative tomography image of the Aegean/Eastern Mediterranean upper mantle for the section shown in (b); the contouring is in percentages of the ambient Jeffreys–Bullen upper mantle velocity (see legend); cross (horizontal) hatching indicates positive (negative) anomalies; regions with poor spatial resolution are not contoured (large white areas); the interval −0.1%/+0.1% is also indicated in white; horizontal and depth axes are given without vertical exaggeration. Black symbols are the projection of hypocenters with $M > 4$, located within 100 km from the plane, that occurred from 1964 to 1984; the long dashed horizontal line delimits the maximum depth of hypocenters (<250 km) and the width of the location map is 3° (Spakman et al., 1988). The short inclined arrows indicate a possible flow of a portion of lower mantle sucked from below. Such a process is made possible by the wake left by the slab in its upduction (exhumation) motion (Doglioni et al., 2009); this interpretation seems more consistent with the tomoimage than the presence of a subducting slab, with rather complex shape. In the location map of the Eastern Mediterranean and Aegean area (b), the solid lines indicate the location of the upper mantle cross sections considered by Spakman et al. (1988) and the solid arrow indicates the cross section considered here; full dots indicate the epicenters of earthquakes with $M > 4$ and focal depths <100 km that occurred from 1964 to 1984, while open dots represent intermediate-depth events in the range 100–180 km, that occurred in the same period of time; Ae = Aegean basin, Cr = Crete, EM = Eastern Mediterranean, Gr = Greece, Io = Ionian basin, Pe = Peloponnesus, Rh = Rhodes, Tu = Turkey. (c) When plate motions are considered relative to the hot spot reference frame, i.e., assuming fixed the

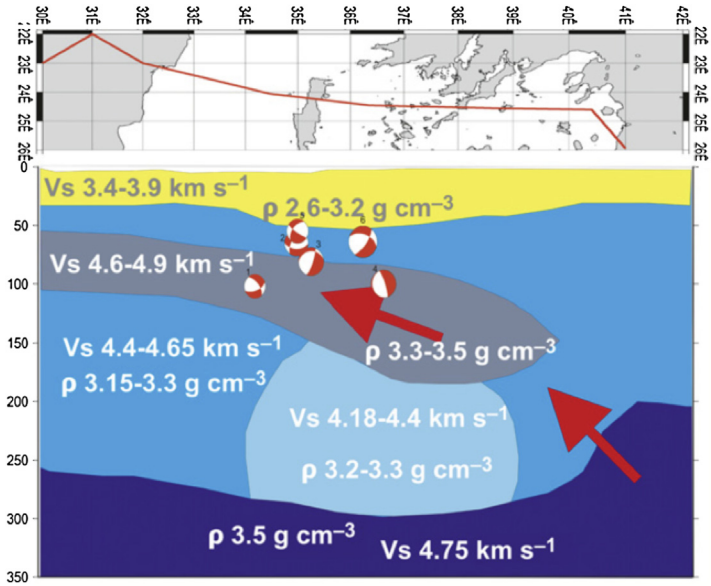

Figure 64 Ranges of Vs and ρ versus depth along Transmed VII, as given by El Gabry et al. (2013). The cartoon shows schematically the inferred upducted slab and the exhumation of the deeper mantle material (gray and dark blue (black in print versions) bodies, respectively). Focal mechanisms of the largest earthquakes in the period 1970–2009 are plotted in side view and well correlate with the upward motion (upduction and induced exhumation) indicated by arrows (tectonic syringe).

products, Na- and K-alkaline rocks. This large spectrum of rock composition makes the circum-Tyrrhenian area one of the most complex magmatic settings in the world. The petrologic and geochemical characteristics of this magmatism have been recently discussed in a number of papers (Conticelli & Peccerillo, 1992; Peccerillo & Manetti, 1985; Serri, 1990).

MORB-type rocks form part of the Tyrrhenian Seafloor and have been recovered by deep sea drilling (Serri, 1990 and references therein). Their genesis has been related to mantle melting during the opening of the

mantle, the slabs of E- (or NE) directed subduction zones, like the Adriatic/Ionian plate, may move out of the mantle (upduction); in the three stages sketch, the white dot moves leftward relative to the underlying black dot in the mantle and subduction occurs because the upper plate dark gray dot moves leftward faster than the white circle in the slab; the subduction rate is the convergence minus the orogenic shortening (in the model, the slab moves westward at a velocity of 20 mm/year relative to the mantle). (d) Plate motions of Africa and Greece relative to the mantle in the deep hot spot reference frame.

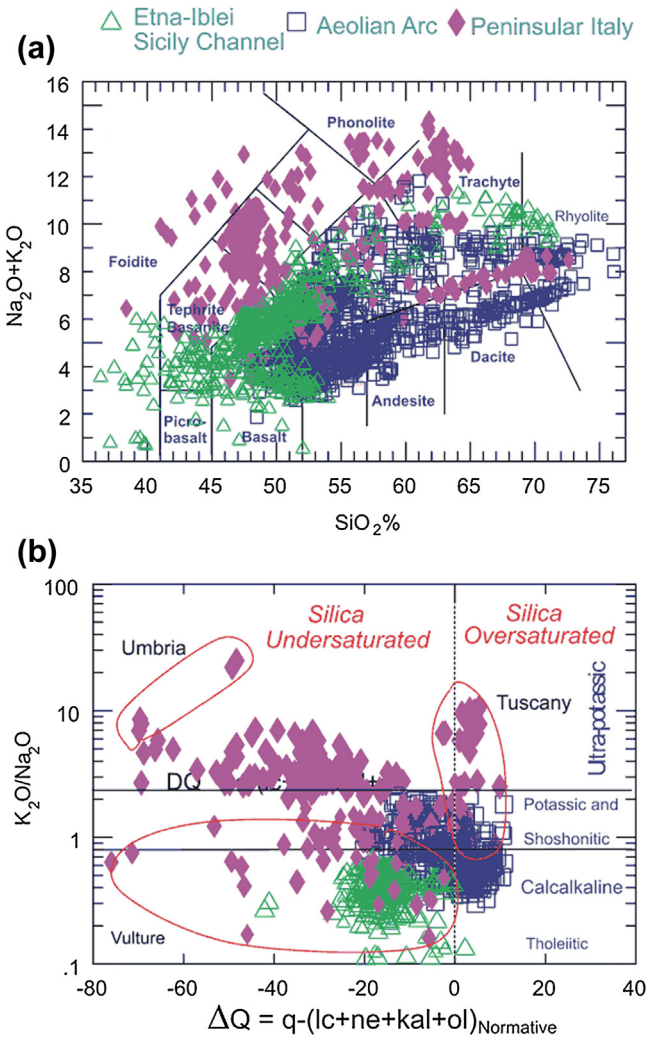

Figure 65 (a) Total alkali vs silica classification diagram for Italian Plio–Quaternary magmatic rocks (Peccerillo, 2002; 2005). (b) delta-Q versus K_2O/Na_2O classification diagram for Plio–Quaternary mafic volcanic rocks (MgO $>$ 4%) from Italy. Delta-Q is the algebraic sum of normative quartz (q), minus leucite (lc), nepheline (ne), kalsilite (kal), and olivine (ol). Silica oversaturated rocks have delta-Q $>$ 0, whereas silica undersaturated rocks have delta-Q $<$ 0. The extreme variability of the central Mediterranean magmatism geochemistry demonstrates the strong heterogeneity of the underlying mantle and it is strongly against the wrong assumption of a chemically homogeneous mantle often made in tomoimages interpretation.

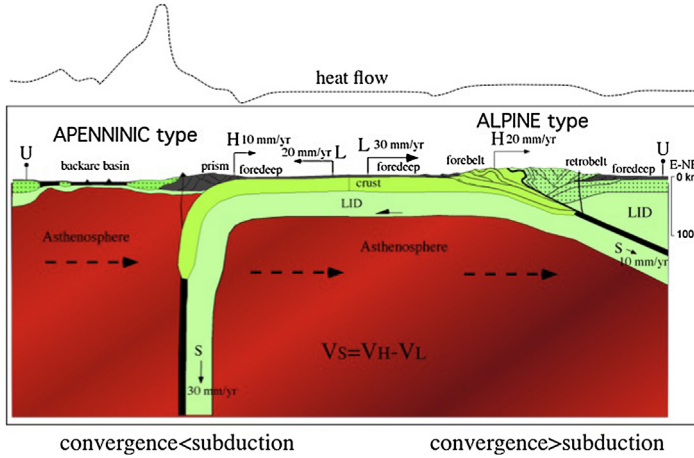

Figure 66 Schematic section showing that in the Alpine setting, the subduction rate is decreased by the migration of the hinge, H, toward the upper plate, U, and the orogen in the final collisional stage is composed both by the upper and lower plate, L, rocks. In the converse Apenninic setting, the subduction rate is rather increased by the migration of H away from U, and shallow rocks of L form the accretionary prism. The relatively shallower asthenosphere in the hanging wall is typical of W-directed subduction zones. This is coherent with the relatively higher heat flow in the hanging wall of the W-directed subduction zone along the backarc basin. *Modified after Doglioni et al. (2007).*

Tyrrhenian backarc basin. Other rocks with tholeiitic affinity are associated with prevailing Na-alkaline Plio–Quaternary volcanics in Sardinia and represent the lowest exposed products of Mt Etna. Plio–Quaternary Na-alkaline rocks occur in Sardinia, Ustica in the southern Tyrrhenian Sea, Mt Etna and in some seamounts, arising from the Tyrrhenian Seafloor, like Vavilov and Magnaghi (Locardi, 1991). Subduction-related volcanism is widespread in the area. The oldest activity follows the calc-alkaline volcanism of Provence, in southeastern France, which dates back to 50–35 Ma (Bellon, 1981) and it occurs in Sardinia (29–13 Ma) where orogenic rocks range from calc-alkaline basalts to rhyolites, with a dominance of intermediate and mafic rocks (Dostal, Coulon, & Dupuy, 1982 and references therein). Younger orogenic volcanism progressively shifted eastward up to its present position in the Aeolian arc. This consists of seven main islands and several seamounts, like Palinuro, Alcione, Lametini, Enarete, Eolo, Sisifo, and Glauco, which define an overall ring structure. Rocks are younger than about 1.2 Ma and mainly consist of intermediate and mafic calc-alkaline to shoshonitic volcanics, with minor leucite tephrites (at Vulcano and Stromboli) and arc tholeiites (at Lametini and Sisifo

seamounts). Acidic rocks are concentrated in the last 40 ka. Slightly older calc-alkaline to shoshonitic volcanics form an NE–SW-elongated Lower Pliocene volcanic belt (e.g., Anchise seamounts) east of the Aeolian arc (Locardi, 1991). High-K calc-alkaline and shoshonitic volcanics also form the Island of Capraia (6.7–3.5 Ma) in the Tuscan archipelago. The lamproites of Sisco (Corsica) have ages of about 14–15 Ma (Civetta, Orsi, Scandone, & Pece, 1978). Potassic and ultrapotassic magmatism of central and southern Italy (the so-called Roman Comagmatic Province) represents the most striking magmatological feature of the Tyrrhenian area. It spans a time interval between 4 Ma and the present time, with the bulk of potassic volcanics being younger than 0.6 Ma. Potassic and ultrapotassic rocks have variable petrochemical affinity, from Roman-type potassic series (KS), Roman-type high-potassium series (HKS), lamproites, and kamafugites (Peccerillo & Manetti, 1985). KS and HKS rocks represent by far the dominant volcanics, whereas lamproites are restricted to southern Tuscany and Corsica, and kamafugites form a few scattered centers east of the Roman province. KS are basically similar to shoshonites, whereas HKS are undersaturated in silica and show very strong enrichment in potassium and incompatible elements. However, both KS and HKS display low contents of high-field strength elements (HFSE) as typically observed in subduction-related rocks. Kamafugites show similar incompatible element patterns as HKS, but are more strongly undersaturated in silica and show higher CaO content and lower Na and Al content than HKS. Finally, lamproites are oversaturated in silica, contain negative anomalies of HFSE and have isotopic signatures that are closer to crust than to mantle values. However, their high values of Mg# (up to 80 ppm), Ni (up to 350 ppm), and Cr (up to 800 ppm) together with the presence of high-pressure ultramafic xenoliths strongly suggest a mantle origin. Carbonatitic rocks which have been recently suggested to occur east of the Roman province (Stoppa & Woolley, 1997) may actually represent silicate, kamafugitic, or HKS magmas that have undergone strong contamination by the thick carbonate sequences crossed by uprising magmas (Peccerillo, 1998).

Overall, the whole ultrapotassic magmatism of central–southern Italy appears to be subduction related and has been hypothesized to derive from an anomalous upper mantle whose composition has been strongly modified by addition of upper crustal material by subduction processes (e.g., Peccerillo, 1985), whereas low fractions of carbonate-rich melts have low density and viscosity that can migrate upward and form a carbonated partially molten CO_2-rich mantle, in the depth range from 130 to 60 km. Carbonate-rich

melts upwelling to depth <60–70 km induce massive outgassing of CO_2, that can migrate and be accumulated beneath the Moho and within the lower crust (Frezzotti, Peccerillo, & Panza, 2009, 2010).

In a nutshell, a large spectrum of magma types is associated with the Apennines orogen and the opening of the Tyrrhenian Sea. Most of these rocks (i.e., island arc tholeiites, calc-alkaline, shoshonitic, potassic and ultra-potassic rocks) are of obvious subduction-related origin. However, also some MORB and Na-alkaline rocks (including Ustica, Etna, and Vulture) show evidence for a role of subduction-related geochemical components in their genesis (e.g., Serri, 1990). Petrology and geochemistry reveal rocks ranging in composition from tholeiitic to calc-alkaline to sodium-and potassium-alkaline and ultra-alkaline. Several magmatic provinces can be recognized, which display distinct major and/or trace element and/or radiogenic isotope signatures. The data from mafic volcanic rocks define a number of distinct provinces that likely generated compositionally diverse mantle sources.

Most of these provinces can be identified in LAS structure, as well. The combined analysis of petrological, geochemical, and geophysical data reveals a surprisingly close match between geophysical characteristics of the LAS and the compositions of magmatic rocks erupted at the surface in the various regions (Frezzotti et al., 2009; Peccerillo, Panza, Aoudia, & Frezzotti, 2008). This suggests that variations of seismic waves velocity in the mantle could be related to compositional differences of mantle sources, and not only to pressure and temperature variations. The Vs of the Betics, where ultrapotassic lamproitic magmatism is observed, has features similar to those of other three areas in the western Mediterranean where ultrapotassic lamproitic magmatism of different age is observed: Western Alps, Tuscany, and Sardinia. The crust and upper mantle models in these four areas can be correlated with the age of the magmatism and the local heat flow and, at the same time, outline how, starting from a naturally quite undifferentiated mantle where magma genesis is currently in progress, the differentiation in lithosphere and asthenosphere can take place in time (Raykova & Panza, 2010). The recycling of crustal materials is likely to be the main contributor to the upper mantle heterogeneity of the observed Mediterranean magmatism.

Vertical slab windows related to differential slab retreat also provided preferential pathways for the upraise of mantle melts (e.g., Etna and Vulture, Doglioni, Innocenti, & Mariotti, 2001; D'Orazio, Innocenti, Tonarini, & Doglioni, 2007). Alkaline magmatism occurs in the Sicily Channel rift (Peccerillo, 2005). Africa is in fact moving south–westward, away relative to Europe, coherently with the geologic record of the Sicily

Channel, which is in extensional regime since at least the Pliocene. The data discussed so far put in the proper perspective the overstated assumption of the northern push of Africa relative to Europe. Moreover, in the Sicily Channel the rifting coexists with the accretionary prism of the Apennines–Maghrebides and indicates that more than one geodynamic setting can operate in a given area (Corti, Cuffaro, Doglioni, Innocenti, & Manetti, 2006). These observations support the passive role of plate boundaries.

The advantage of joining geophysical models with geological and petrological data in order to understand the complex evolution of the Mediterranean region has been described for the first time by Panza, Peccerillo, et al. (2007). The very shallow crust–mantle transition and the very low Vs in the mantle just below the Moho, in correspondence of the submarine volcanic bodies (Magnaghi and Vavilov in the southern Tyrrhenian Sea, central Mediterranean), indicate the presence of high amounts of magma. The joint use of geological and geophysical constraints along the TRANSMED III geotraverse (Cavazza et al., 2004) results in a new model of the mantle flow in a backarc setting and reveals an easterly rising LVZ in the active part of the Tyrrhenian basin. An upper mantle circulation in the western Mediterranean, mostly easterly directed, affects the boundary between upper and lower asthenosphere, which undulates between about 180 and 280 km (Panza, Raykova, et al., 2007).

In the geological interpretation of seismological models of the Earth interior it is often overlooked the fact that an increase with increasing depth of Vp or Vs means only that rigidity is increasing with increasing depth more than density, ρ. In spite of this fact, most empirical relations are based on the assumption that faster Vp or Vs mean denser material (e.g., Nafe–Drake relation, see Fowler, 1995; Ludwig, Nafe, & Drake, 1970). These relations, barely acceptable in stable areas, are obviously very weak, if not invalid, in tectonically very active regions like the Mediterranean (Aitken, Salmon, & Kennett, 2012; Brandmayr et al., 2011; El Gabry et al., 2013), where chemical mixing is very likely to occur (e.g., Panza, Raykova, et al., 2007). In spite of this obvious and severe shortcoming, Vp–ρ and Vs–ρ relations are widely used but improper constraints to interpret tomographic images in very complex areas as, for instance, the Mediterranean (e.g., Faccenna & Becker, 2010). In fact, as can be seen, for example, along an NW–SE profile from southern Corsica to Ionian Sea, Vs and ρ models contradict popular Vs–ρ relations and this is not surprising in a tectonically so complex area (Brandmayr et al., 2011). A similar situation has been recently evidenced in the Tibetan plateau domain and Iran (Deng et al., 2014; Motaghi

et al., 2014; Zhang et al., 2014). Prominent feature of the section, shown in Figure 7.4, is the high-velocity body that represents subducting LID beneath the Calabrian Arc, seismically active at all depths. To the west, a LID about 60–70 km thick marks the active part of the Tyrrhenian, with some very-low-velocity soft mantle LID beneath volcanic areas. LID is slightly thicker beneath Sardinia–Corsica block and reaches about 90 km of thickness. To the east of the Calabrian Arc, the Ionian LID is about 130 km thick, and the underlying mantle is relatively faster than the Tyrrhenian one. As a rule, the mantle velocity is higher in the Ionian plate than in the Tyrrhenian basin. A prominent negative density anomaly characterizes the subducting slab and the Sardinia–Corsica block, whereas a positive anomaly characterizes the mantle of both the Tyrrhenian ($\rho \sim 3.3$ g/cm^3 to about 60–70 km of depth) and the Ionian basins ($\rho \sim 3.3$ g/cm^3 to about 80 km of depth and $\rho \sim 3.4$ g/cm^3 at about 170 km of depth).

The asymmetry between W-directed (Apennines) and E- (or NE-) directed (Alps, Dinarides) subductions is thus a robust feature of the velocity model and the density model reveals that the subducting slab is not denser than the ambient mantle and supplies no evidence for slab pull process. The Tyrrhenian is a neogenic backarc basin very asymmetric. Extension maximizes in Southern Tyrrhenian and drastically reduces around 41°N (Pontine Islands). Similarly Apennines compression maximizes in Calabria and minimizes in Northern Apennines. There is therefore an evident relation between Tyrrhenian extension and compression in the Apennines. The asymmetry between the mountain chain and the basin, i.e., the boot shape of Italy, can be attributed to the kind of lithosphere that is subducting east of the Apennines: the lithosphere that was paving the Ionian Sea and now responsible of the intermediate-depth seismicity is very likely oceanic, cold, and well consistent with the subduction process (e.g., Tumanian, Frezzotti, Peccerillo, Brandmayr, & Panza, 2012). Going north from Gulf of Taranto to Basilicata the Ionian–Adria lithosphere is continental (Brandmayr et al., 2010).

6. MECHANISMS OF PLATE TECTONICS

In the previous chapters the main asymmetries of contractional and extensional plate boundaries have been listed (Figure 67). These data are particularly visible when moving along the TE and point to a worldwide polarized tectonics. When a slab enters the mantle it

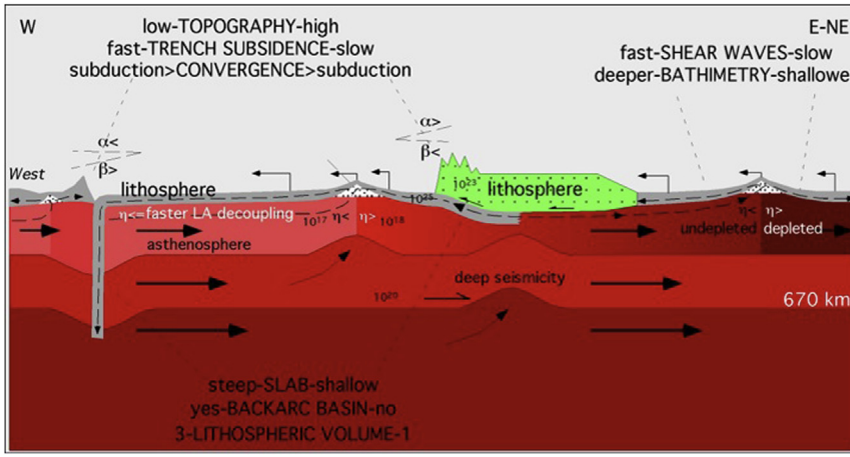

Figure 67 The "westward" drift of the lithosphere relative to the mantle produces a number of asymmetries at plate boundaries, both along subduction and rift zones. For example, slabs are steeper along W-directed subduction zones and are always associated to backarc spreading. E- (or NE-) directed subduction zones are rather shallower; the overlying double verging orogens show much higher topography and structural elevation shallower foredeeps and wider outcrops of metamorphic rocks, with respect to the opposite slabs. The subduction hinge generally diverges relative to the upper plates along the W-directed slabs, whereas it converges along the E- or (NE-) directed slabs. Gray layer, oceanic lithosphere; green (light gray in print versions), continental lithosphere. Legend: η viscosity in Pa s; α and β, dip of the orogens envelope and foreland regional monocline, respectively. *After Carminati & Doglioni (2012).*

contributes to mantle convection. The volume of lithosphere that is recycled at depth must be compensated by the same amount of material. Along oceanic ridges and backarc basins new oceanic crust and some LID form. However, the thickness of the downgoing slabs is thicker than that of the lithosphere at ridges. In terms of mass balance it means that part of the thickening occurs away from the ridges, within plates, where the isotherm is depressed and the LVZ is cooled to become LID. Therefore, the slab volume is requilibrated also by lithospheric generation taking place not necessarily at the ridges. Subduction zones provide cold lithosphere at depth, a process that cools down the hosting mantle, possibly determining its subadiabatic condition with a potential T lower than the shallow asthenospheric layers (Anderson, 2013). Moreover, the volume displaced by the slabs has to be moved away from them, involving larger and slowly flowing mantle volumes (Figure 68).

The remaining fundamental question is: what is the driving force of plate tectonics? The main known forces acting on the lithosphere are: (1) the

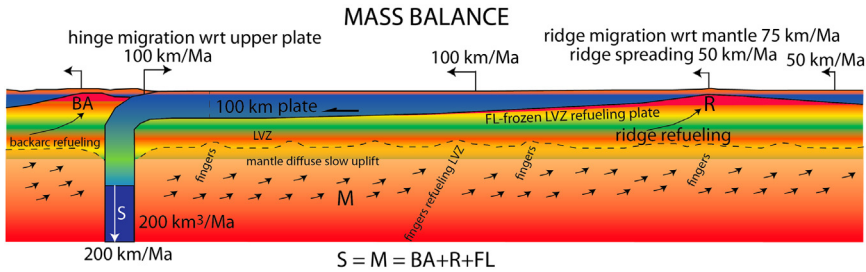

Figure 68 Slabs provide narrow range recycling into the mantle, which must be compensated by an equivalent volume of diffuse mantle uplift. Moreover, W-directed slabs contribute to lithospheric feeding of the mantle three times more than the E- (or NE-) directed slabs. Assuming a lithospheric thickness of 100 km (and 1 km along strike), the amount of slab volume entering the mantle every million years is given by the velocity of the subduction hinge relative to the upper plate, minus the convergence rate of the lower plate relative to the upper plate. In the example, 200 km^3 of slab (S) enter the mantle every Ma. The mass balance requires that a similar amount of mantle (M) should rise to compensate the slab flux. Mantle uplift is accommodated by ridge spreading (R), boundary layer cooling and freezing (FL), plus mantle uplift along backarc basins (BA) that accommodates slab rollback. LVZ, low-velocity zone. *After Doglioni and Anderson (2015).*

bottom-up-driven mantle convection, i.e., the way the Earth dissipates the internal heating, (2) the top-down-driven mantle convection, i.e., the slab pull process that is related to the superficial cooling of the lithosphere, which would favor its sinking due to its negative buoyancy, (3) the trench suction, i.e., the drag exerted by the downgoing lithosphere and adjacent mantle acting on the overlying upper plate, being a secondary effect of subduction zones, (4) the ridge push, i.e, the excess of mass formed at an oceanic ridge which tends to move away from the ridge, (5) the tidal drag and astronomical forces (Figure 69). Few of these mechanisms require sizeable coupling or

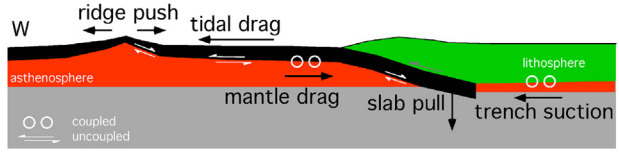

Figure 69 Main system of forces that may act on the lithosphere. Mantle drag and trench suction need high coupling (relatively higher viscosity) between lithosphere and asthenosphere to be effective. Ridge push, slab pull, and tidal drag rather need low coupling (relatively lower viscosity) to be efficient. Since the lithosphere is decoupled with respect to the asthenosphere, more than one force is acting on plate motions. Circles indicate coupled forces while white half arrows show the uncoupled forces. *After Doglioni et al. (2007).*

small coupling between the lithosphere and the underlying mantle. For example, bottom-up-driven convection and trench suction require coupling to be quite effective, whereas slab pull, ridge push, and tidal drag need some degree of decoupling between lithosphere and mantle.

6.1 Mantle Convection

Mantle convection may be driven from the heated bottom, from the cooled top and from the internal radiogenic heat (Figure 70). Computed Rayleigh numbers (Ra) are usually $>10^6$ and these values support the convection of the mantle (Montague & Kellogg, 2000; Schuberth et al., 2009 and reference therein) as subduction zones and generation of new oceanic crust testify. However, the mantle kinematics and its internal dynamics are far to be fully unraveled. Some questions can be summarized as follows. In how many layers of the Earth convection currents occur? What is the path of mantle particles? Is it chaotic or polarized? What is the relationship with plate motions? Many models have been produced so far, but no one is really able to satisfy the constraints posed by the plate kinematics, the TE, and the asymmetry of plate boundaries.

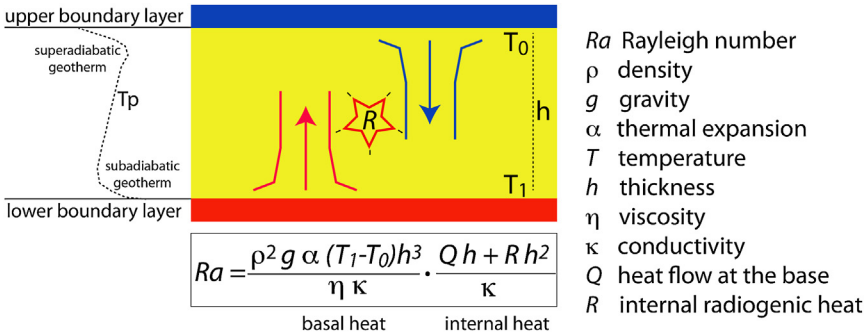

Figure 70 The dimensionless Rayleigh number (Ra), where parameters at the numerator favor convection, whereas parameters at the denominator favor conduction, synthetically describes the convection of a fluid heated from below and from internal radiogenic decay. However, all the parameters of Ra vary with depth (e.g., composition, thermal expansion, viscosity, density, etc.) and make the computation highly subjective in a vertically and laterally heterogeneous mantle. The Fe percent increase with depth very likely increases conductivity and, thus, decreases Ra. Moreover, phase changes can generate internal barriers in the mantle such as transition zones, which determine independent convecting layers. The thinner the convective layer, the lower the Ra number. The decrease of mantle potential temperature, Tp (Anderson, 2013), and the increase of viscosity and density with depth may also drastically decrease the Ra number and make mantle convection sluggish and passively dominated by the upper boundary layer, i.e., activated by subduction.

The mantle has been shown to be in nonadiabatic conditions (e.g., Anderson, 2013; Bunge, Ricard, & Matas, 2001). This can be related to the internal heating, the strong thermal buffer exerted by the upper thermal boundary layer (the lithosphere), the high T in the LVZ, due to the relatively higher conductivity of fluids, the cooling of the deeper mantle exerted by the slabs, etc. Subadiabaticity of the mantle may inhibit convection or decrease its Ra. Due to chemical variations and phase changes, the density and viscosity increase with increasing depth in the mantle. Therefore, convection models obviously contain a number of simplifications, which may prevent an accurate understanding of the convective pattern and its vigor. We still do not know the distribution in the mantle of Fe that is highly relevant element for conductivity and that decreases Ra. We do not know very accurately (about 1000 °C uncertainty) the temperature at the base of the mantle and the rate of heat transfer from the core. Moreover, the lower mantle should have a dense layer at its base (Montague & Kellogg, 2000), which is thickening and possibly irreversibly stratified (Anderson, 2002). The more numerous and thinner the mantle convecting layers, the lower the Ra. Mantle convection may be thermal or mechanical in the sense that material forced down needs that an equal volume is expelled. All models of mantle convection such as polygonal cells, mushrooms, cylinders, etc., do not fit the simple pattern of plate kinematics at the surface and the toroidal component of plate motion. Convection does not need a decoupling at the lithosphere base. It is rather more effective if the lithosphere is fully coupled to the mantle. However, from the Pacific "hot spots" we have kinematic evidence that the lithosphere is decoupled relative to the mantle in the LVZ. So, if it is not mantle convection, what is the force generating the decoupling in the LVZ? From these considerations, mantle convection appears driven from the top rather than from the deep mantle. This means that plate motion in a way is responsible for driving mantle convection (e.g., Anderson, 2001). Therefore, the shearing of the lithosphere and its penetration into the mantle should trigger internal motion. So the question is again what is determining the shearing? The usual answer is the negative buoyancy of slabs, which are pulling plates, i.e., the slab pull (e.g., Royden, 1993). It is obvious that convection occurs in the mantle, not only from modeling, but also from the kinematics of plate boundaries, where mantle upraises along ridges and lithosphere sinks along subduction zones. It is also evident that oceanic lithosphere circulates in the mantle much more easily than the continental lithosphere, since only relatively young (180−0 Ma) oceans cover the Earth's surface, compared to the much older cratons (>3000 Ma), since

the thick continental lithosphere is buoyant over the mantle. Convection is required to cool the Earth. But convection models are necessarily oversimplified and possibly overrated. Mantle Tp at ~200 km of depth is higher than between ~400 and 2800 km of depth. This is the most significant and far-reaching development in mantle petrology and geochemistry since Birch (1952) and Bullen (1947) established the nonadiabaticity (superadiabatic thermal gradient above 200 km, subadiabatic gradient below) of the mantle from seismology and physics. High Tp in the shallow mantle is consistent with petrology (Bullen & Bolt, 1985; Anderson, 2013). Temperatures in the upper 200 km of the mantle are ~200 °C higher than assumed in canonical geotherms. A recent clear evidence is supplied by Tumanian et al. (2012) in a backarc environment where it is shown that in the surface boundary layer Tp may exceed 1500 °C. In general, such a thermal situation may inhibit convection: thermal gradients stronger than adiabatic one lead to more vigorous convection while thermal gradients weaker than adiabatic one lead to inhibition of convection. As already mentioned, the mantle is considered compositionally quite homogeneous, but it is not, and it contains both vertical and lateral significant heterogeneities. The whole Earth is intensely stratified both in physical and chemical properties from the topmost atmosphere down to the core. The supposed convection cells should be made of an uprising relatively warmer buoyant mantle, laterally accompanied by downwelling relatively cooler currents. In the view of convection modelers, the surface expression of cells should be the plates. But the Atlantic, E-Africa, and Indian rifts have no intervening subductions; there are also several cases of paired subduction zones without rifts in between: this shows the inapplicability of the convection cells concept to the simple superficial plate tectonics kinematics. Insufficient attention has been paid to the general westward drift of the plates (Bostrom, 1971; Le Pichon, 1968) and the possible configuration of upper-mantle convection cells consistent with recent global absolute tomography images of the upper mantle represents a quite strong argument supporting the relevant role played by the westward drift, very likely of astronomical origin (Panza et al., 2010; Riguzzi et al., 2010).

Main controlling factors of plate tectonics are the lateral heterogeneities in the lithosphere and underlying upper mantle. If the decoupling, due to viscosity contrast, between the lithosphere and the asthenosphere is more or less the same everywhere within the Earth, the lithospheric shell would behave, in its westward drift, as a single coherent shell with no relative motion among different plates. That is not what is observed. Moreover,

different depths of the decollement would provide variations of the surface plate velocity due to the different radius: the longer the radius, (i.e., shallower decoupling), the faster the speed of the overlying plate. Similarly, in a lithosphere formed only by a layer of constant continental thickness (say 100–150 km) plate tectonics cannot occur. Such a homogenous layer would be in equilibrium and would not undergo compression or stretching. The absence of lateral heterogeneities and the light nature of the continental lithosphere would prevent subduction and plate tectonics. The density contrast between continental and oceanic lithosphere is at the base of the differential motion of the lithospheric plates. These inhomogeneities in the mantle are consistent with the presence of viscosity contrasts that favor the existence of nonzero differential velocities among plates. As a rule the subduction of lithosphere is oriented, along the TE, toward W if the thinner (more dense) plate lies to the E of the collision front, or vice versa toward E, if the thinner (more dense) plate lies to the W of the collision front. Plate tectonics comes true since the different plates move along the flow lines parallel to the TE, with relative velocities variable in the range 0–18 cm/year. In most of the convection models, uprising and downwelling mantle currents are stationary, but it is well known that all plate margins rather migrate. Convection styles frequently generate polygonal shapes for the cells, but plate margins can be very linear, e.g., the Atlantic Ridge, in contrast with the typical mushroom shape of mantle plumes (e.g., Tackley, 2000). The fastest W-ward moving plate relative to the mantle is the Pacific one, which is slipping over an LVZ (Doglioni et al., 2005) with low viscosity (Pollitz et al., 1998). Therefore, the Pacific is the most decoupled plate, while mantle convection requires that faster moving plates are more coupled (higher viscosity) with the mantle than slower ones. The Hawaii hot spot volcanic chain indicates that the underlying mantle is moving E–SE-ward. Doglioni et al. (2003) and Hammond and Toomey (2003) modeled, beneath the EPR, an eastward-migrating mantle. Motion of the underlying mantle has been suggested through shear-wave splitting analysis also beneath the Nazca plate by Russo and Silver (1994) and the South Victoria Land and the Ross Sea coast, Antarctica (Barklage et al., 2009). The hot spot reference frame is consistent with the existence of an eastward relative mantle flow beneath the South America plate (Van Hunen, van den Berg, & Vlaar, 2002). A relatively moving eastward mantle flow has been proposed also beneath North America (Silver & Holt, 2002) and beneath the Caribbean plate (Gonzalez, Alvarez, Moreno, & Panza, 2011; Negredo, Jiménez-Munt, & Villasenor, 2004). Beneath the Tyrrhenian Sea a similar west to east flow of the mantle is inferred from Vs

tomography (Panza, Raykova, et al., 2007) and from mantle anisotropy, averaged over large volumes (Margheriti, Lucente, & Pondrelli, 2003).

6.2 Slab Pull

A paradigm of plate tectonics is that the negative buoyancy of slabs (slab pull) drives plate motions (e.g., Conrad & Lithgow-Bertelloni, 2003). This is suggested by the relatively steeper dip of the slab bearing old oceanic crust (Forsyth & Uyeda, 1975) and the convergence rate at subduction zones, which is related to the age of the oceanic crust at the trench (e.g., Carlson, Hilde, & Uyeda, 1983; Jurdy & Stefanik, 1988). Slab pull process is conceived as the result of the cooling of the oceanic lithosphere that thus becomes denser than the underlying mantle. The cold slab should exert a pull down of the lithosphere, i.e, the older and the cooler the slab, the steeper, and the faster the subduction. Such an assertion is not proven at all; actually it is false. In fact, there is no correlation between convergence rates and age of the downgoing oceanic lithosphere at subduction zones as shown in Figure 71. Moreover, from the previous chapters, we have seen

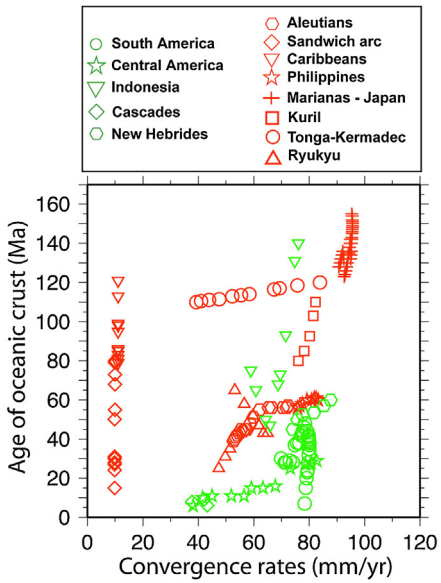

Figure 71 Age of oceanic lithosphere entering the trench (after Müller, Roest, Royer, Gahagan, & Sclater, 1997) versus velocity of convergence calculated using the NUVEL1A (DeMets, Gordon, Argus, & Stein, 1994) rotation poles. The diagram summarizes the results obtained for 13 subduction zones. The lack of correlation refutes any relation between plate motions speed and negative slab buoyancy. *Data taken from Cruciani et al. (2005).*

that the oceanic lithosphere is frozen LVZ which is the result of the chemical differentiation of the lighter elements of the mantle. Mantle models show that density tends to increase with depth (e.g., PREM). Based on xenoliths studies, also the continental lithospheric mantle has been shown to be lighter than the underlying mantle (Kelly, Kelemen, & Jull, 2003). The analysis of slab dip versus the age of the subducting oceanic lithosphere lack of correlation as well (Figures 72 and 73). There are several other issues that appear to mine the effectiveness of the slab pull. The negative buoyancy assumed in slab pull models often attributes an excess weight of the slab relative to the hosting mantle between 50 and 100 kg/m^3. Afonso, Ranalli, and Fernandez (2007) have shown that the maximum expected density contrast between the lithosphere and the asthenosphere is around 40 kg/m^3 and this extra weight is confined in a small percentage of the lithosphere, hence not affecting the whole plate (Figure 74). Moreover, the asthenosphere and the underlying transition zones have density increasing with increasing

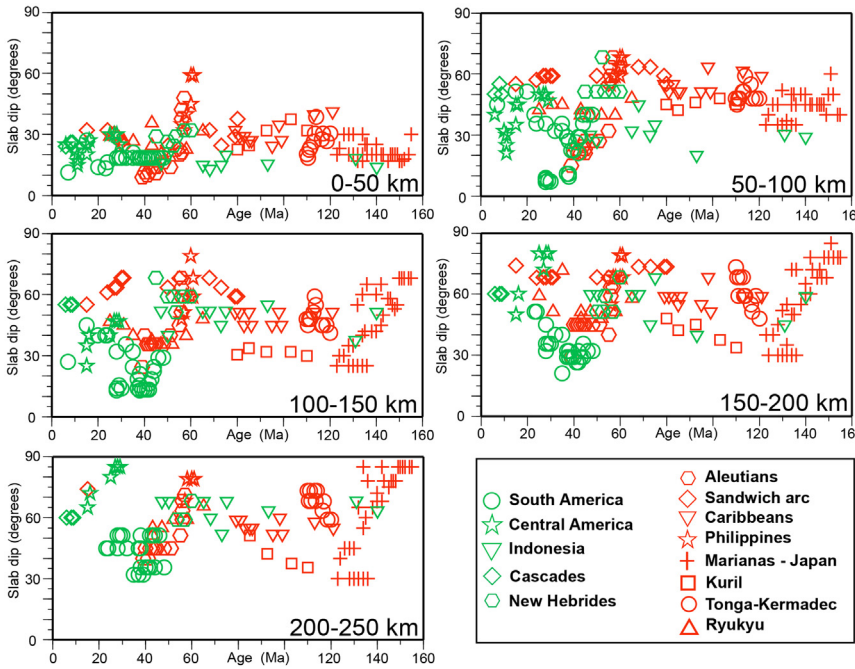

Figure 72 Age vs slab dip plots for five different depth ranges, with data measured along sections perpendicular to the trench of the main world subduction zones. No relation between age of the oceanic crust and slab dip can be observed; the dip of the slabs cannot be ascribed to their thermal state and refutes the supposed slab pull effect. *After Cruciani et al. (2005).*

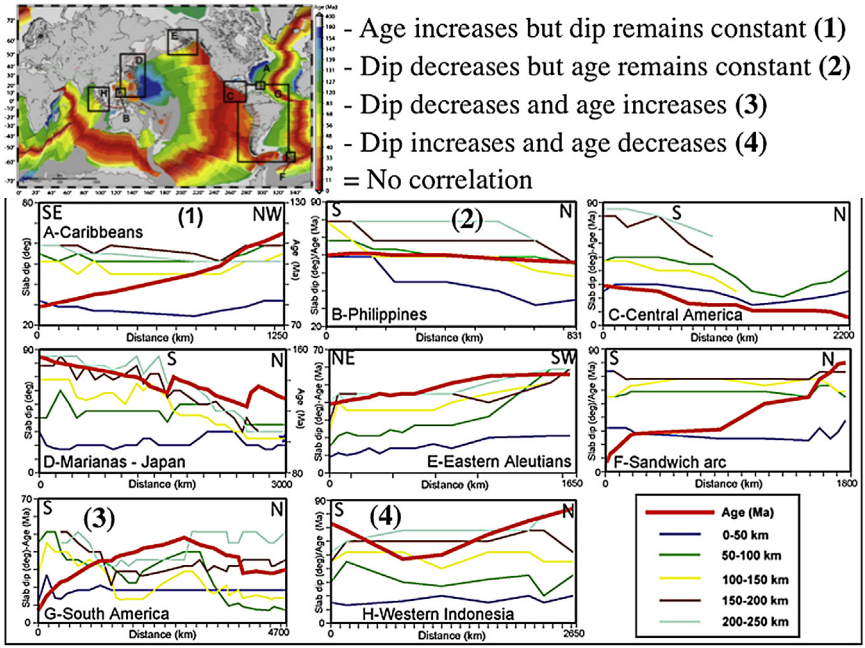

Figure 73 Variation of slab dip versus the age of the subducting lithosphere moving along the strike of the subducting lithosphere. The lack of correlation refutes the thermal state of the lithosphere as responsible of its dip and the concept of slab pull. *After Cruciani et al. (2005).*

depth that largely exceeds the assumed maximum lithospheric density. The depleted mantle forming the LID is usually harzburgitic, i.e., extremely light.

The negative buoyancy of slabs should determine the pull of plates, but the dip of the subduction zones is not correlated with the age and the thermal state of the downgoing plates (Cruciani et al., 2005). As an example, along the Sandwich subduction zone, the undergoing Atlantic and Antarctic oceanic lithospheres show age variations (from 5 to 120 Ma) but the subduction system maintains the steep dip and the overall characteristics of the W-class. In fact, Cruciani et al. (2005) measured the dip of the slabs down to depths of 250 km along 164 sections crossing 13 subduction zones and compared it with the age of the subducting oceanic lithosphere, both at the trench and at depth. They have shown that there is not correlation between the steepness of the slabs and the increasing age of the downgoing cooler lithospheres. Therefore, the negative buoyancy, if any, is not the controlling factor of the slab dip. In contrast with the prediction of the models

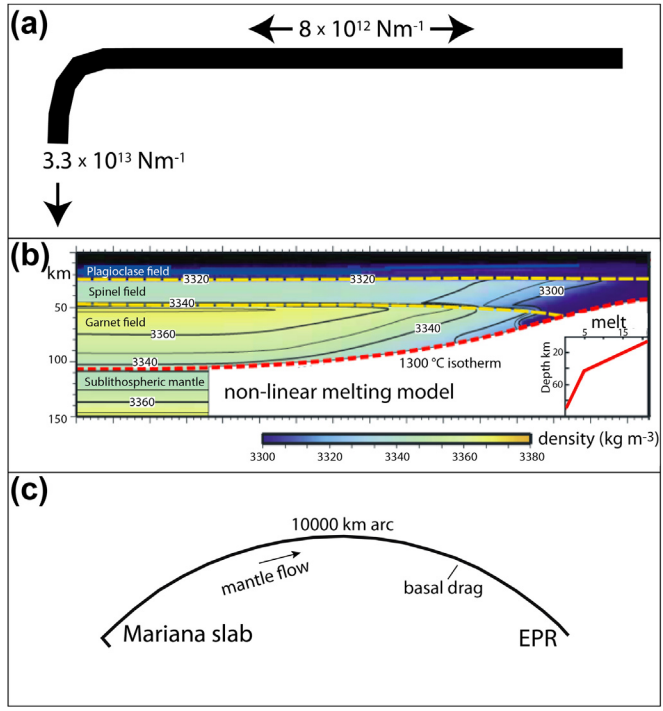

Figure 74 Few of the several pitfalls of the slab pull concept: (a) The slab pull maximum predicted force is larger than the strength of the lithospheric plate; therefore, it is difficult to transfer the energy of the pull without breaking the plate even before it becomes a slab. (b) Density structure of the oceanic lithosphere according to Afonso et al. (2007). The contour lines indicate density values in kilogram per cubic meter. The dashed yellow (light gray in print versions) lines indicate the approximate locations of the plagioclase–spinel and spinel–garnet phase transitions. According to this petrological model, the maximum negative buoyancy can be about 40 kg/m^3, i.e., twice lighter than several assumptions made in modeling the slab pull. Furthermore the volume of relatively denser lithosphere is possibly less than 10% with respect to the entire plate. Moreover, the harzburgite is lighter than the underlying asthenosphere and the lithosphere is only the frozen part of the upper depleted asthenosphere. Therefore, the lithosphere can hardly be heavier than the underlying upper mantle; it can get weight, and thus get denser, from the phase transition on the way down, but it is not a priori denser. (c) Sketch vertical section of the Pacific plate from the Mariana subduction zone to the East Pacific Rise (EPR). The ratio between the length of the slab portion assumed to be heavier than the hosting mantle (about 300 km) and the linear dimension of the plate (10000 km) is only about 3%, preventing the slab pull to be the driving force. The unrealistic negative buoyancy of the slab should be able to pull the 33 times longer plate, and to win the basal drag of a mantle that moves in the opposite direction according to the hot spots migration.

considering as driving force only (or mostly) slab pull, younger oceanic lithosphere may show steeper dip than older segments of oceanic slabs (e.g., Central America vs South America). The lack of a clear correlation between the observed dip angle of slabs and plate velocity and slab age in modern subduction zones has been explained with the hypothesis that subduction is a time-dependent phenomenon (King, 2001). A combination of slab age and subduction velocity correlates better with slab dip, but the correlation is still poor (correlation coefficient equal to 0.45). Therefore, supplemental forces to the negative buoyancy of the slab have to be considered such as (1) thickness and shape of the hanging wall plate, (2) absolute plate velocity, (3) presence of lateral density variations in the hosting upper mantle, (4) effects of accretion/erosion, (5) subduction of oceanic plateaus, and (6) slab deformation due to the motion of the mantle relative to the subducting plate. Plate kinematics, i.e., absolute motion of the upper plate (Luyendyk, 1970; Tovish & Schubert, 1978) could play a role, but other aspects have to be taken into account. The first one is the presence of lateral density variations in the hosting upper mantle, allowing different buoyancy contrasts with respect to the downgoing slab. However, apart from proven lateral heterogeneities in mantle tomography, there is no evidence yet for such large anisotropies in composition that can justify sufficient density anomalies in the upper mantle. Actually, along the Alps–Himalaya belt recent investigations give no evidence in support of slab pull mechanism as relevant plate-driving force (Brandmayr et al., 2011; Deng et al., 2014; Doglioni et al., 2006b; El Gabry et al., 2013; Motaghi et al., 2014; Zhang et al., 2014). The effect of latent heat released by phase transitions could, moreover, alter the thermal distribution and buoyancy of subducting slabs and control their dips (van Hunen, van den Berg, & Vlaar, 2001). The thickness and shape of the hanging wall plate may control the dip of the first 250 km, i.e., the thicker the hanging wall plate, the steeper is the slab. Still at shallow depths, the effects of accretion/erosion (Karig, Caldwell, & Parmentier, 1976; Lallemand, Schnurle, & Manoussis, 1992), the thickness of sediments in the trench and the subduction of oceanic plateaus (Cross & Pilger, 1982) could influence the geometry of the descending lithosphere. Another basic controlling action could be operated by resistance forces induced by the motion of the mantle relative to the subducting plate (Doglioni, Harabaglia, et al., 1999; Scholz & Campos, 1995). Moreover, relative convergence rates at subduction zones do not correlate with the age of oceanic lithosphere at the trench (Doglioni et al., 2007). One argument used to corroborate the slab pull is the trench length with respect to the plate velocity (Forsyth &

Uyeda, 1975). On the basis of a similar observation it could be argued that long-spreading ridges generate fast plate motions. However, these relations may be a circular reasoning, e.g., longer subduction and ridge zones form when plates move faster (Doglioni, Cuffaro, & Carminati, 2006). The relationship between trench length and plate velocity is also questionable for other reasons; for example, the absolute plate velocity can be recomputed either in the deep hot spot or in the shallow hot spot reference frame and the different results do not indicate a correlation between slab length percentage (length of the trench with respect to the length of the boundary surrounding the plate) and plate velocity (Doglioni et al., 2007).

The relationship between the area of plates (Schettino, 1999) and the angular velocity of plates in the deep hot spot reference frame (HS3-NUVEL1A, Gripp & Gordon, 2002) shows no correlation as already observed by Forsyth and Uyeda (1975). However, when plotting the area vs the absolute angular velocities of plates in the shallow hot spot reference frame, a correlation seems to be present, being bigger plates generally faster (Figure 75). Both analyses do not support a significant correlation casting additional doubts on the importance of the slab pull in plate tectonics, which has a number of further antagonizing arguments. For example, the assumption that the slab is heavier than the ambient mantle remains debatable, particularly because there are not constraints on the composition of both slab and mantle at variable depth (e.g., the amount of Fe in the lower asthenosphere and the lower upper mantle). Heavier ambient mantle than subducting slab is seen in the Apennines (Brandmayr et al., 2011) and Himalaya (Zhang et al., 2014) subductions.

More questions need to be addressed: (1) Is the slab pull a relevant source of energy for plate motions? (2) Is the amount of energy involved correctly calculated? and (3) Are the assumptions reliable? Most of the literature indicates that the slab pull is about 3.3×10^{13} N m^{-1} (e.g., Turcotte & Schubert, 2002). This is a force per unit length parallel to the trench. However, this value is very small when compared to other energy sources for the Earth, such the energy dissipated by tidal friction, heat flow emission, and Earth's rotation (e.g., Denis, Schreider, Varga, & Zavoti, 2002; Krasinsky, 1999; Riguzzi et al., 2010; Varga, 2006; Varga, Denis, & Varga, 1998; Zschau, 1986). Moreover, chemical and mineralogical stratification in the upper mantle makes the slab pull even weaker. Most of the Earth's volcanism is sourced from above 200 km: the subduction zones release magmatism at about 100–150 km of depth (Tatsumi & Eggins, 1995); mid-oceanic ridges are sourced by even shallower asthenosphere melting (100–30 km, e.g.,

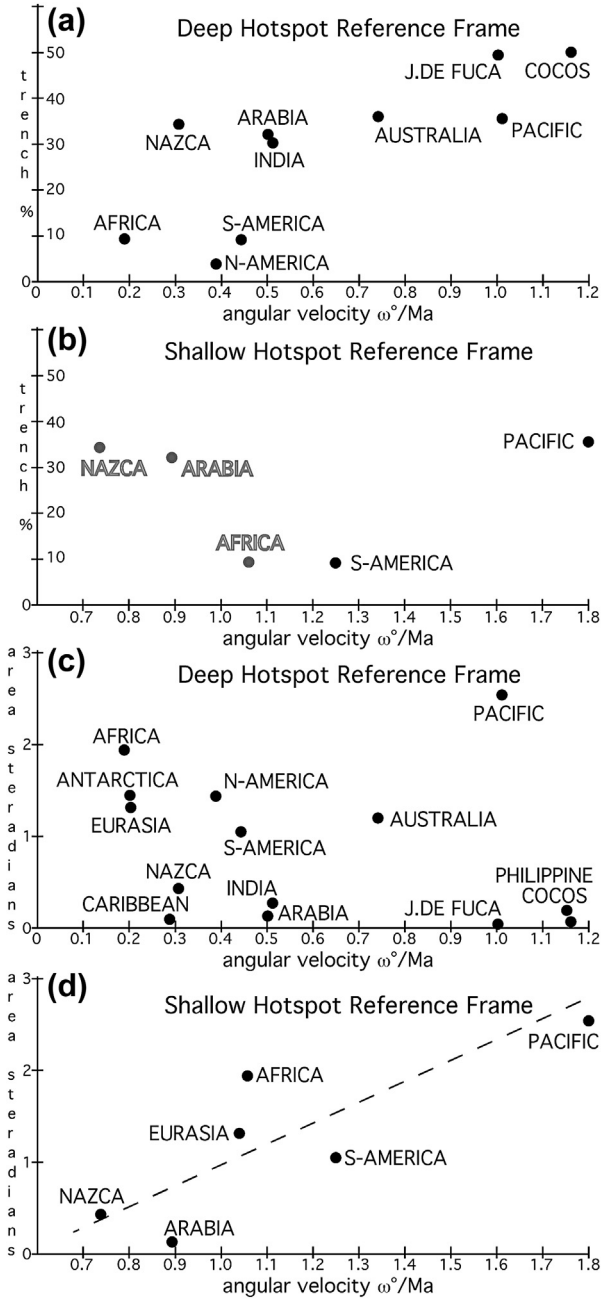

Figure 75 (a) Relationship between absolute plate angular velocity vs trench percent in the deep hot spot reference frame. There is not evident correlation between the two values. For example, the Nazca and Pacific plates have about the same percentage

Bonatti et al., 2003); hot spots are also debated as potentially very shallow, and sourced by the asthenosphere (Bonatti, 1990; Doglioni et al., 2005; Foulger et al., 2005; Smith & Lewis, 1999). Since even xenoliths in general and kimberlite chimneys originated at depth not deeper than the asthenosphere, there is no direct sampling of the composition of the standard lower part of the upper mantle. Therefore, it cannot be excluded, for example, a more Fe-rich fayalitic composition of the olivine, heavier and more compacted than the Mg-rich olivine (forsterite), which is presently assumed as the most abundant mineral of the upper mantle. In case more iron is present in the upper mantle olivine, the density of the ambient mantle would be slightly higher and reduce the slab pull smaller, if any exists. The slab pull concept is based on the hypothesis of a homogeneous composition of the upper mantle, with the lithosphere sinking only because it is cooler (e.g., Turcotte & Schubert, 2002). However, the oceanic lithosphere is nothing but frozen shallow asthenosphere, previously depleted beneath a mid-oceanic ridge. Depleted asthenosphere is lighter than the "normal" deeper undepleted asthenosphere (see Doglioni et al., 2003, 2005; Oxburgh & Parmentier, 1977; for a discussion). Therefore, the assumption that the lithosphere is heavier only because it is cooler might not be entirely true, and the slab pull could be overestimated if not negative (Brandmayr et al., 2011; Motaghi et al., 2014; Zhang et al., 2014).

Phase transitions within the subducting lithospheric mantle would enhance the slab pull in the transition zone (300–400 km of depth) (Poli & Schmidt, 2002; Stern, 2002), but again, the occurrence of relatively higher density ambient rocks due to chemical and not only phase transitions

of trench length with respect to the plate circumference, but the Pacific is much faster. Angular velocities after *Gripp and Gordon (2002)*. (b) Relationship between absolute plate angular velocity vs trench percent in the shallow hot spot reference frame. The absence of correlation between the two values is even more evident, but the gray points on the left (Nazca, Arabia, Africa) show a negative motion of the plates, i.e., away from the trench. Therefore, in this reference framework, plates cannot be moved by the slab pull. Angular velocities after *Crespi et al. (2007)*. (c) Plot of plate areas and absolute angular velocities in the deep hot spot reference frame. *Areas of plates after Schettino (1999)*. As already shown by *Forsyth and Uyeda (1975)*, no correlation is observable. (d) Plot of plate areas and absolute angular velocities in the shallow hot spot reference frame. Angular velocities after *Crespi et al. (2007)*. Contrary to panels A, B, and C, some correlation seems to exist in panel D, i.e., larger plates move faster, even if oceanic plates still move relatively faster than continental plates for comparable areas. *After Doglioni et al. (2007)*.

could make the effect of the slab pull smaller and smaller if not negative (positive buoyancy). Moreover, the occurrence of metastable olivine wedges in fast subducting oceanic lithosphere may create positive density anomalies that counteract the effects of slab pull (Bina, 1996). A further density anomaly that is suggested to drive slab pull is expected to come from the eclogitization of the subducting oceanic crust. This process involves only a thin layer (5–8 km thick) and not the entire downgoing lithosphere (70–90 km thick); therefore only 5–10% of the lithosphere could exhibit negative buoyancy, not enough to make the whole lithosphere denser than the mantle as remarked by Doglioni et al. (2007). Nevertheless, this type of metamorphic transition is often assumed to be able to determine the slab pull. The eclogites reach densities of about 3440–3460 $kg \cdot m^{-3}$ only at depths of about 100 km (Hacker, Abers, & Peacock, 2003; Pertermann & Hirschmann, 2003). The density of the ambient mantle at comparable depths according to the PREM model is 3370 $kg\ m^{-3}$ (Anderson, 2007), i.e., only slightly lighter than the eclogitized oceanic crust. At the 410 km deep transition zone, PREM model gives a mantle density of 3.7 $kg\ m^{-3}$, a value that inhibits the slab pull, if present. However, both eclogite and mantle densities are quite speculative. The small density contrast between subducting crust and ambient mantle casts doubts on the potential effect of the negative buoyancy of the oceanic crust. Therefore, there are not solid constraints on the depth at which the slab pull should turn on and at what depth it should turn off since the mineralogy of the slab and the ambient mantle is still largely unknown. Why then a slab should maintain its shape and coherence down to the 670 km discontinuity? The easiest explanation would be its higher stiffness governed by its cooler and poorly conductive nature. Since seismic wave velocity is inversely proportional to density, the high velocity of the slab detected by tomography could be related not to its higher density, but to its higher rigidity. Certainly the slab becomes heavier during sinking for phase transformations, but is it a priori denser, or does it become heavier on the way down? Is it continuously reaching density equilibrium while moving down (Doglioni, Cuffaro, et al., 2006)? Trampert et al. (2004) and Tumanian et al. (2012) have demonstrated that low-velocity volumes of the mantle detected by tomography can be due to lateral variations in composition rather than in temperature, i.e., they can be even higher density areas rather than hotter lighter buoyant material, as so far believed. In fact, considering the main low velocity in the mantle, such as the asthenosphere, or the liquid core, the decrease in speed of the P-waves propagating through them is related to their relatively lower

rigidity (e.g., Secco, 1995) either generated by CO_2 content in the asthenosphere, or relatively higher density–low viscosity iron alloys in the liquid core. As extreme examples, gold or lead has high density but low seismic velocity. Therefore, the interpretation of tomographic images of the mantle where the red (relatively lower velocity) areas are assumed as relatively lighter and hotter rocks can simply be wrong, i.e., these areas may even be, on the contrary, relatively cooler and denser (Foulger et al., 2013; Tumanian et al., 2012; Van der Hilst, 2004). With the same reasoning, blue (relatively higher velocity) areas, which are assumed as relatively denser and cooler rocks may be relatively warmer and lighter. Scalera, Calcagnile, and Panza (1981) and Trampert et al. (2004) suggest that, when present, the low velocity in the mantle, below about 400 km of depth, can be due, for example, to high concentration in iron. The conductivity of minerals increases with increasing iron concentration, thus, at lower mantle depths, the coefficient of thermal expansion must be very low. Both factors decrease the Rayleigh number and make the convection very sluggish (e.g., Anderson, 2002). The onion structure of the Earth with shells compositionally homogeneous (e.g., the PREM, see Anderson, 2007a) is, in this context, a misleading oversimplification, since the occurrence of lateral heterogeneities in the whole Earth layers has been widely demonstrated (e.g., Panza et al., 2010; Ritsema, 2005; Thybo, 2006; Zhang et al., 2014).

The main geometric, kinematic, and mechanical arguments against the slab pull as the primary mechanism for moving plates and for triggering subduction can be summarized as follows (mainly after Doglioni et al., 2007).

1. The dip of the slab is independent from the age of the oceanic lithosphere (Cruciani et al., 2005). Therefore, the supposed, increasing with age-negative buoyancy determined by the, progressive with time, cooling oceanic lithosphere does not control the slab dip.
2. There are no stringent constraints on the real composition of the upper mantle (Dalton & Wood, 1993): there could be more fayalite that increases the upper mantle density and decreases the slab negative buoyancy.
3. Subduction processes involve also continental lithosphere that descends to depths larger than 100–150 km (Ampferer, 1906; Dal Piaz, Hunziker, & Martinotti, 1972; van Hinsbergen, Hafkenscheid, Spakman, Meulenkamp, & Wortel, 2005; Panza & Mueller, 1978; Ranalli, Pellegrini, & D'Offizi, 2000; Trümpy, 1975), although the average continental crust subducted is most probably buoyant with respect to mantle rocks (Hermann, 2002).

4. The oceanic lithosphere is frozen shallow (30–100 km deep) asthenosphere, depleted below ridges before freezing. Therefore, the oceanic lithosphere is formed by the differentiated lighter uppermost part of the mantle (possibly harzburgite). Then why should it be a priori heavier than the undepleted deeper (100–300 km) asthenosphere? A pyrolite density of 3400 kg m^{-3} in the asthenosphere lying beneath the old oceanic lithosphere has been inferred (Jordan, 1988; Kelly et al., 2003), i.e., larger than that of the depleted LID. A small negative buoyancy of the lithosphere with respect to the mantle has been computed by Afonso et al. (2007).
5. Hydrothermal activity generates serpentinization of the mantle along the ridge that further decreases density.
6. If the oceanic lithosphere is heavier than the underlying mantle, why blobs of lithospheric mantle (LID), falling in the upper mantle below the western older side of the Pacific plate, have not been detected?
7. Within a slab, eclogitization is assumed to increase the lithosphere density. However, eclogitization is concentrated in the 6–8 km thick oceanic crust, whereas the remaining 60–80 km thick lithospheric mantle does not undergo this same transformation. Therefore, at the most, only in 1/10 of the slab density can increase and the main mass of the slab (90%) does not change significantly.
8. The density increase due to eclogitization is in contrast with the exhumation of the eclogitic prism that is usually detached with respect to the "lighter" lithospheric mantle.
9. Why the lithosphere should start to subduct? This crucial point arises particularly when considering an oceanic hydrated and serpentinized lithosphere (Ulmer & Trommsdorff, 1995) that has not yet been metamorphosed by the subduction process, and consequently it is still less dense than the surrounding rocks. In general the LID, once serpentinized, as it very often occurs along ridges and transform faults (e.g., Panza, Peccerillo, et al., 2007), is lighter than the asthenospheric mantle, thus how can plates be pulled?
10. Down-dip compression affects most of the slabs, all below 300 km (Isacks & Molnar, 1971), most of them even at shallower depth (e.g., Frepoli, Selvaggi, Chiarabba, & Amato, 1996) and point out for a slab forced to sink rather than actively sinking.
11. The 700 km long W-Pacific slab, where only the upper 300 km could be negatively buoyant should pull and carry the 10,000 km wide Pacific plate, 33 times bigger, winning the shear resistance at the

plate base and the opposing basal drag induced by the relative eastward mantle flow, inferred from the hot spots migration (Doglioni, Cuffaro, et al., 2006).

12. Kinematically, subduction rollback implies that the volumes left in the hanging wall of the slab have to be replaced by horizontal mantle flow, whether this is a consequence or the cause of the retreat (Doglioni, Cuffaro, et al., 1999). However, in order to allow for the slab to move back, the slab retreat needs that also the mantle in the footwall of the slab moves away in the direction of the slab retreat. This is true regardless this motion is generated by the slab pull or it is an independent mantle horizontal flow. But the energy required to push forward the mantle is much greater than that the slab pull can manage. Where there is no convergence or rather divergence occurs between upper and lower plates (Devoti et al., 2008), the slab pull has been postulated as the only possible driving mechanism. However, the energy generated by the slab pull is not sufficient to push back eastward the whole portion of mantle, that is located east of the slab, in order to allow for the slab rollback. A relative eastward motion of the mantle would be a process much more efficient, in terms of scale of the process and mass involved, to generate the eastward slab hinge retreat and determine active subduction without the need of plates convergence (e.g., Apennines, Barbados).
13. Are faster plates surrounded by long slabs and trenches? It might be a circular reasoning because long subduction zones might be a consequence of fast movements of plates and plates are fast in the NNR reference frame (Conrad & Lithgow-Bertelloni, 2003). For example, measuring plate motions in the hot spot reference frame, i.e., relative to the mantle, Nazca is very slow relative to the mantle, and the relation between plate velocity, slab age, and length of a subduction zone turns out to be not that simple or straightforward.
14. In both the shallow and deep hot spot reference frames some plates move even if there is no slab that pulls them, e.g., the westward movements of North America, Africa, and South America (Gripp & Gordon, 2002). Trench suction has been proposed to explain these movements, but beneath both North and South America the mantle is relatively moving eastward (Bokelmann, 2002; Russo & Silver, 1994), opposite to the kinematics required by the trench suction model.
15. Plate velocities in the hot spot reference frame seem to be inversely proportional to the viscosity of the LVZ rather than to the length of the

subduction zones and the age of the downgoing lithosphere. In fact in the asthenosphere of the Pacific, which is the fastest westerly moving plate (Gripp & Gordon, 2002), the viscosity is quite low (Pollitz et al., 1998).

16. The horizontal velocity of plates is 10–100 times faster than the vertical one (subduction-related uplift or subsidence along plate boundaries, Kreemer, Holt, & Haines, 2002) and this fact suggests that vertical motions are rather passive movements. Moreover, the kinematic analysis shows that subduction rates seem to be controlled by, rather than controlling horizontal plate motions. For example, along E- (or NE-) directed slabs, the subduction is slower than the convergence rate and therefore it cannot be the energetic source capable to speed up plate motion.
17. The energy necessary for shortening and building an orogen is probably larger than the one supposedly supplied by the slab pull (Doglioni at al., 2007).
18. When describing the plate motions relative to the mantle both in the shallow and deep hot spot reference frames, along E- (or NE-) directed subduction zones the slab might move out of the mantle, e.g., in the opposite direction of the subduction (upduction or tectonic syringe). It is sinking because the faster upper plate overrides it (e.g., El Gabry et al., 2013).
19. There are rift zones formed between plates not surrounded by oceanic subduction (e.g., the Red Sea); in such a case no pull force to move the lithosphere exists.
20. Although the knowledge of the rheological behavior of subducted lithosphere is very poor, it can be conjectured that the downgoing slab, being progressively heated, loses strength, and diminishes the possibility to mechanically transfer the pull (Mantovani et al., 2002).
21. The folding and unfolding of the lithosphere at the subduction hinge decreases the slab strength and the possibly correlated slab pull.
22. Slab pull has been calculated to be potentially efficient only at a certain depth (e.g., about 180 km, McKenzie, 1977) therefore the question: at shallower depth, how does subduction initiate?
23. At the Earth's surface, the oceanic lithosphere has low strength under extension (e.g., about 8×10^{12} N m^{-1}, Liu et al., 2004) and it is able to resist a force smaller than that requested by slab pull (about 3.3×10^{13} N m^{-1}, Turcotte & Schubert, 2002). If the slab pull is the main cause for the motion of the Pacific plate, this observation argues for a stretching of the Pacific lithosphere before slab pull is able to

move the plate. In other words, the plate cannot sustain the tensional stresses eventually due to slab pull. This problem connected with the low lithospheric strength could be, however, partly solved by the mantle flow and viscous tractions acting on the plates induced by slab sinking (e.g., Lithgow-Bertelloni and Richards, 1998). Due to low temperature and high pressure, the strength of the subducted oceanic lithosphere rises to some 2×10^{13}–6×10^{13}N m^{-1} (Wong A Ton & Wortel, 1997) and would make sustainable the eventual pull induced by density anomalies related to phase changes at depth. In summary the subducted slab is probably able to sustain the load induced by slab pull but probably this load cannot be transmitted to the not yet subducted portion of the plate without breaking it apart.

24. The slab pull force will hardly be able to generate the slab rollback, which is needed to push laterally the mantle.

25. Recent investigations of Vs and ρ distribution with depth by Brandmayr et al. (2011) and El Gabry et al. (2013) are suitable to outline the geodynamic context in the Mediterranean region. Asymmetry between W-directed (Apennines) and E-directed (Alps, Dinarides) subductions is a robust feature of the Vs model, while ρ model reveals that slabs are not denser than the ambient mantle and no evidence for slab pull is supplied.

This long list of geometric, kinematic, and mechanical arguments against the relevant role of slab pull in moving plates and triggering subduction casts serious doubts on the possibility that the slab pull can actually trigger subduction, slab rollback, and drive plate motions; at the most it can be a gregarious source of energy in some instances. Density anomalies due to phase changes occurring at depth within the slab could enhance the sinking of the slab. However, the slab pull alone, even if efficient at some depths, it is unable to explain the initiation of the subduction, and the mechanism perpetuating plate motions in general. The slab detachment model is conceived as a consequence of the negative buoyancy of the slab and it has been invoked many times to explain the supposed rupture of the slab in tomographic images (e.g., Wortel & Spakman, 2000) and to fit the geochemistry of magmatism (e.g., Lustrino, 2005). However, tomographic images, often biased by color scale saturation (Anderson, 2007b; Foulger et al., 2013), are based on reference velocity models that often overestimate the velocity of the asthenosphere where the detachment is usually modeled. Therefore, the (apparent) detachment disappears when using slower velocity for the asthenosphere in the reference velocity model or when considering regional

tomographic images (e.g., Piromallo & Morelli, 2003). Recently, Rychert et al. (2005) have shown how the base of the lithosphere—top of the asthenosphere (LVZ, e.g., Panza, 1980) is characterized by unexpected, few kilometers thick, extremely low velocities beneath northwestern North America, far from subduction zones. This implies a revision, particularly in areas characterized by strong lateral variations in composition of the subducting lithosphere (e.g., continental vs oceanic) where the use of 1D reference velocity model is meaningless, of the velocity models resulting from relative mantle tomography. The revision should also consider the limitations of the theoretical framework employed in tomography; ray theory does not handle diffraction and frequency dependence, whereas normal mode perturbation theory requires weak and smooth lateral variations of structure (Anderson, 2007a,b; Boschi et al., 2007; Boyadzhiev et al., 2008; Foulger et al., 2013; Panza, Raykova, et al., 2007; Romanowicz, 2003; Waldhauser et al., 2002).

Along W-directed subduction zones seismicity can reach the bottom of the upper mantle without discontinuity or gap. Along some E- or NE-directed subduction zones there is a seismic gap between the 300 and 550 km depth (Figure 76). The two small families of deep earthquakes (>550 km) seem to have quite distinct characters: the events in the W-directed slabs are characterized by faster ruptures of the fault (4 km/s) with respect to E-directed slabs slower rupture velocity (1.5 km/s) as noted by Zhan, Kanamori, Tsai, Helmberger, and Wei (2014). It is commonly accepted that intermediate and deep seismicity is confined within subducting plates. In fact earthquakes hypocenters delineate what is termed Wadati—Benioff zone and their mere presence is assumed as a sure proof of the existence of subducting lithosphere. However, their rupturing processes are still poorly understood. A number of possible explanations are given by Green and Burnley (1989), Meade and Jeanloz (1991), Kirby, Durham, and Stern (1991), Green and Houston (1995), all assuming that these deep earthquakes are due or triggered by various phase transitions. A comprehensive review is given by Frohlich (1989).

Along the W-directed slabs, the deep isolated seismicity between 550 and 670 km is usually interpreted as an abandoned fallen piece of slab (slab detachment). However, as we have previously discussed, this type of subduction zones has the lower plate moving westward relative to the mantle, i.e., not actively penetrating the mantle. Within the framework of a westward relative motion of the lithosphere with respect to the mantle, the mantle is relatively moving "eastward." Moreover, beneath a subduction zone, the section in which the mantle can flow is narrower than elsewhere and, according to

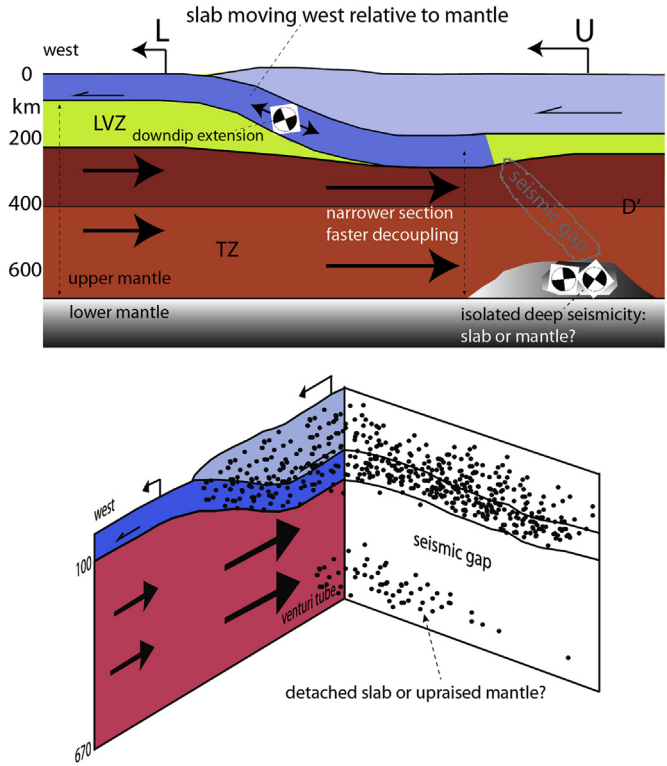

Figure 76 The E—NE-directed class of subduction zones often shows a shallow slab that reaches 200—300 km depth, sometimes flattening under the overriding plate. Below this seismically active volume, there is a seismic gap in the mantle (apart very few events of low magnitude). In some regions (see Figure 20) a deep cluster of earthquakes is present between 550 and 650 km depth. What is the origin of this deep seismicity often attributed to a detached slab? Here we propose that it may be related to the narrowing of the section where the upper mantle flows beneath the subduction zone that, accordingly with Venturi effect, generates an increment in the velocity of mantle flow. In addition, the upward motion of the slab relative to the mantle can generate exhumation of the underlying mantle. Therefore, the origin of deep seismicity can be alternatively attributed to the large shear generated by the increment in the horizontal mantle flow accompanied by a reduction in ambient pressure that acts on an upraised higher-rigidity lower mantle. The focal mechanisms-beach balls are plotted in side view.

the Venturi effect (or hydrodynamic paradox), the speed of the relative motion increases and the pressure decreases. This model, in our opinion, naturally explains the faster shear within the thinner upper mantle and the seismicity at its bottom generated by the upraise of the more rigid lower mantle due to (1)

the lower pressure and (2) the westward motion of the slab, which is sucking up the mantle (Figure 76). The presence of a high-velocity body at the bottom of the upper mantle could therefore not be related to a detached slab, but to an upraised part of the lower mantle. Its higher rigidity could explain the seismicity and the positive seismic velocity anomaly reported in relative tomography images (Figure 77). In fact pitfalls of relative tomography should be considered that may lead to misleading interpretations: a high-velocity body at some depth can be interpreted as a slab detachment, while, in reality, the slab is rather continuous, or alternatively the high-velocity body represents a portion of upraised lower mantle (Figure 77).

As an example, the great Bolivia earthquake of June 9, 1994 might originate within the upper mantle and not within a subducting slab. Since the lithospheric root in South America is not gravitationally in equilibrium (testified by a geoid height of about 20 m), a pressure gradient within the upper mantle must exist. Combining these two effects, the shear stress within the upper mantle concentrates at its base and is relevant enough (at least 10 MPa) to explain deep seismicity. This stress could in turn trigger a phase change from spinel to perovskite and magnesium oxide that would explain the volume reduction observed during the event. Kikuchi and Kanamori (1994) also notice that the Bolivia rupture, in the framework of the double-couple earthquake source model, takes place along a subhorizontal plane, which would be consistent with a horizontal shear generated by a relative mantle flow at the upper-lower mantle transition. The horizontal projections of P- and T-axis are almost parallel to the subduction trend instead of being perpendicular and their best-fit solution has a relevant implosive component. To this, we add that an event of this magnitude (Mw = 8.2) involves a volume far larger than the whole conceivable thickness the slab might have at that depth, unless a very high-stress drop, exceeding 100 MPa, is assumed, as Kikuchi and Kanamori (1994) do. Assuming that the Bolivia event took really place within the slab, its location requires that the slab, if continuous, deflected to assume a slope of at least 50° in the lower part. If the slab suddenly changes slope, and it is even interrupted, it means that it does not have much internal strength. It is hard, indeed, to find a mechanism that could explain how a weak slab can accumulate enough internal strength below 600 km, to accommodate a stress drop of the order of the one calculated by Kikuchi and Kanamori (1994). Most of the elastic energy radiated by deep events is concentrated in the depth interval between 580 and 640 km. Green (2007) proposed that deep earthquakes are related to shearing instabilities accompanying high-pressure phase

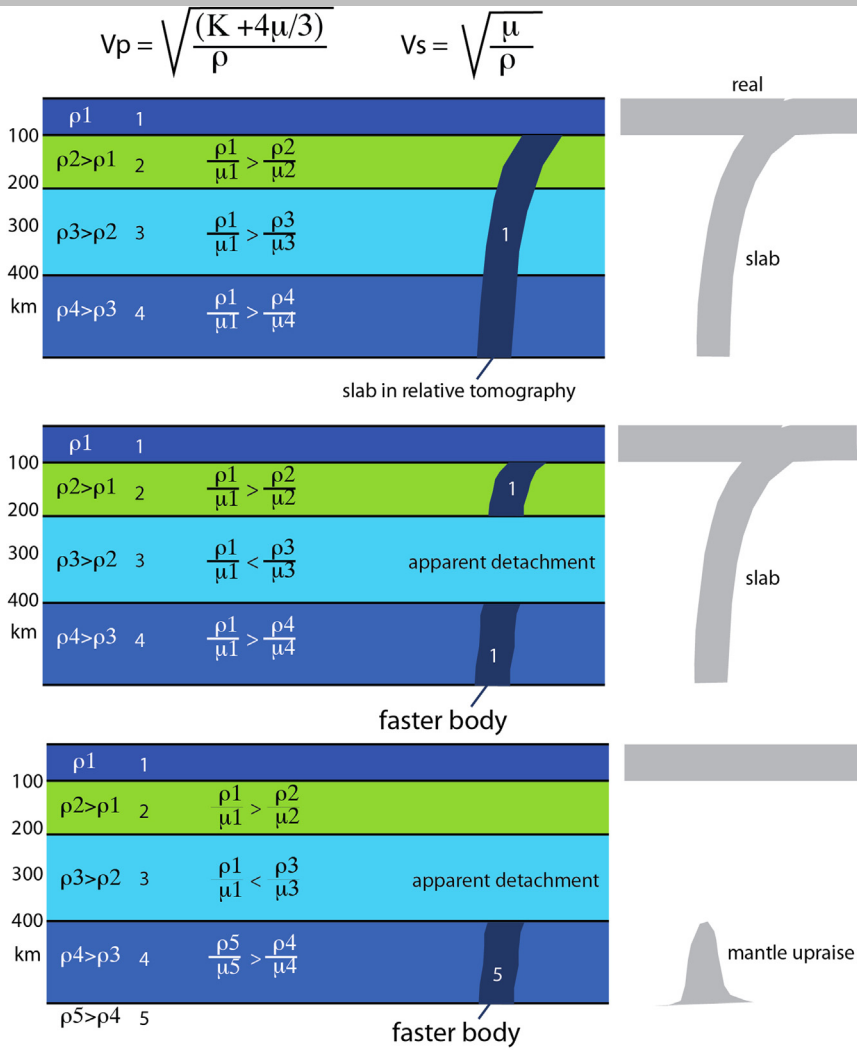

Figure 77 Relative mantle tomography evidences variations of velocity with respect to a reference model space. While the density, ρ, increases with increasing depth in a normally stratified mantle, the ratio of elastic parameters (e.g., rigidity) μ over ρ may increase or decrease with variations of the water content, composition, pressure, and thermal state (upper section). In the equations of seismic velocities (top), ρ appears at the denominator and therefore an increase of ρ without a properly larger increase of rigidity leads to a decrease of seismic velocity. Therefore, positive or negative variations of this ratio depend upon the initial mineralogical and physical state of the material involved. For example, the ratio decreases in the LVZ and/or in the subducted continental lithosphere μ/ρ can be lower with respect to some hosting mantle layer; if this is the case, in tomoimages, the lithosphere is not visible as a high-velocity body. Such a situation is at the base of the concept of slab detachment (middle cartoon) that in the case illustrated is only apparent. Therefore, this kind of pitfall may generate misleading interpretations on the importance of the negative buoyancy of slabs in triggering not existing slab detachment. Similarly, a volume of upraised mesosphere can determine a relatively higher velocity due to its higher μ/ρ ratio. Along E- (or NE-) directed subduction zones, such relatively faster body can be neither a slab nor a detached slab ghost. The faster velocity of an upraised more rigid mantle (mesosphere) supplies a quite natural alternative interpretation for the relative tomography image (lower section).

transformations. Most of the 35 focal mechanisms given in the Harvard CMT Catalogue for the deep (h > 500 km) events with $M_W \geq 7.0$ occurred in the time interval 1979–2013 have a major extensional component, well consistent with an accelerated mantle flow through narrow structures (e.g., Van der Hilst, 1995) across the lower boundary of the upper mantle. This phenomenon leads to the reduction in pressure (Venturi effect) that is reflected in the extensional character of the focal mechanism of the deep earthquakes with $M_W \geq 7$ which occurred close to the bottom of the transition zone, below the E- (or NE-) directed subduction zones. Therefore, the deep seismicity of E- or NE-directed slabs can be a phenomenon naturally attributed to the narrowing of the section in the upper mantle beneath the slab, that causes a speed up of the relative motion of the mantle and decrease the vertical pressure (Figure 76); the positive velocity anomaly in relative tomography images can be explained by some upraise of the lower mantle (Figure 77).

The Venturi's effect is the well-known paradox of fluid dynamics according to which an incompressible fluid in laminar flow through a narrowing tube increases its velocity at the expenses of its internal pressure, the total energy to be conserved. It can be derived from Bernoulli principle of conservation of energy:

$$\frac{v^2}{2} + gz + \frac{p}{\rho} = const$$

where v is the velocity of the fluid, z is the depth, g is gravitational acceleration, p is the fluid pressure, and ρ is its density. It is possible to write:

$$\frac{v_1^2}{2} + gz_1 + \frac{p_1}{\rho} = \frac{v_2^2}{2} + gz_2 + \frac{p_2}{\rho}$$

where the subscripts 1, 2 refer respectively to the wider and to the narrower section. Rearranging the terms:

$$\rho\frac{v_2^2 - v_1^2}{2} + \rho g\left(z_2 - z_1\right) = p_1 - p_2$$

That is the formulation of Venturi's effect, provided that the second term at LHS is negligible; this condition is satisfied if the value of vertical dimension of the section is negligible with respect to that of the variation of the potential energy.

In order to prove whether or not such an effect can occur in a mantle flow narrowed by a subducting slab and thus evaluate at least the order of magnitude of different terms, some simplifying assumptions are necessary. At first we take for v_1 and v_2 the reference velocities of the overlying plates (i.e., the hanging and the footing plate involved in the subduction). This is not a heavy assumption, at least in the Stokes flow approximation validity range, in which the motion is transferred instantaneously between the plate and the underlying mantle. Then we impose the mantle flow to take place, under normal conditions, between 120 and 670 km of depth, therefore z_1 is fixed. The order of magnitude of the kinetic term

$$\rho \frac{v_2^2 - v_1^2}{2}.$$

as estimated from the assumed values of the parameters is $\sim 10^{-14}$ Pa (ρ has a mean value of 3750 kg/m^3, $v_1 = 1.58 \times 10^{-9}$ m/s, i.e., 5 cm/year, and $v_2 = 3.17 \times 10^{-9}$ m/s, i.e., 10 cm/year). It follows that the kinetic term is negligible with respect to the potential term

$$\rho g(z_2 - z_1)$$

that for $z_2 = 300$ km (i.e., a slab reaching 300 km of depth), $g \sim 10$ m/s^2, and $z_2 - z_1 = -180$ km, is $\sim 10^{10}$ Pa. Therefore, due to the vertical dimension involved, Venturi's effect is negligible. However, the parametric test reported by Brandmayr (2012) where, in order to find the effect on pressure (i.e. on stress), ΔP, of different depths of the subducting slab, different values of z_2 are considered, shows that the values of ΔP vary from 1 to 9 GPa, that is a significant fraction of ambient mantle pressure at any given depth (Table 4).

On the other hand, if we apply the conservation of the flow rate through an upper mantle section, which narrows from A_1 to A_2, it is possible to estimate v_2, holding v_1 fixed:

$$v_2 = v_1 \cdot \frac{A_1}{A_2}$$

As can be seen from Table 5, which shows different Z_{sub} depths, the value of 3.5×10^{-9} m/s (about 10 cm/year) corresponds to a slab reaching 300 km of depth and it is well compatible with the velocity of

Table 4 Parametric test on the pressure variation (ΔP) with slab reaching different depth (Z_{sub})

Z_{sub} (10^5 m)	z_2 (10^5 m)	z_2-z_1 (10^5 m)	ΔP (10^9 Pa)
1.5	5.2	−0.3	−1.2
1.8	4.9	−0.6	−2.4
2.1	4.6	−0.9	−3.6
2.4	4.3	−1.2	−4.8
2.7	4.0	−1.5	−6.1
3.0	3.7	−1.8	−7.3
3.6	3.1	−2.4	−9.7
3.9	2.8	−2.7	−11.0
4.2	2.5	−3.0	−12.0
4.5	2.2	−3.3	−13.0

the Hellenic plate in the shallow hot spot reference frame (Doglioni et al. 2007).

6.3 Astronomical Tuning

Earth's seismicity (e.g., Engdahl & Villaseñor, 2002) decreases toward the polar areas (Figure 78) and points to an astronomical tuning of plate tectonics (Varga, Gambis, Bus, & Bizouard, 2005; Varga et al., 2012). Both the number of earthquakes and their energy release increase toward low latitudes, although their maximum does not coincide with the geographic equator, but rather shows two peaks. This is coherent with the geographic distribution of the TE and its interceptions with plate boundaries that have

Table 5 Parametric test on the upper plate velocity variation (v_2) with slab reaching different depths Z_{sub}

Z_{sub} (10^5 m)	z_2 (10^5 m)	z_2-z_1 (10^5 m)	v_2 (10^{-9} m/s)	$\Delta v/v_1$
1.5	5.2	−0.3	1.8	0.1
1.8	4.9	−0.6	2.0	0.3
2.1	4.6	−0.9	2.3	0.4
2.4	4.3	−1.2	2.6	0.6
2.7	4.0	−1.5	3.0	0.9
3.0	3.7	−1.8	3.5	1.2
3.3	3.4	−2.1	4.1	1.6
3.6	3.1	−2.4	5.0	2.2
3.9	2.8	−2.7	6.1	2.9
4.2	2.5	−3.0	7.7	3.8
4.5	2.2	−3.3	9.9	5.3

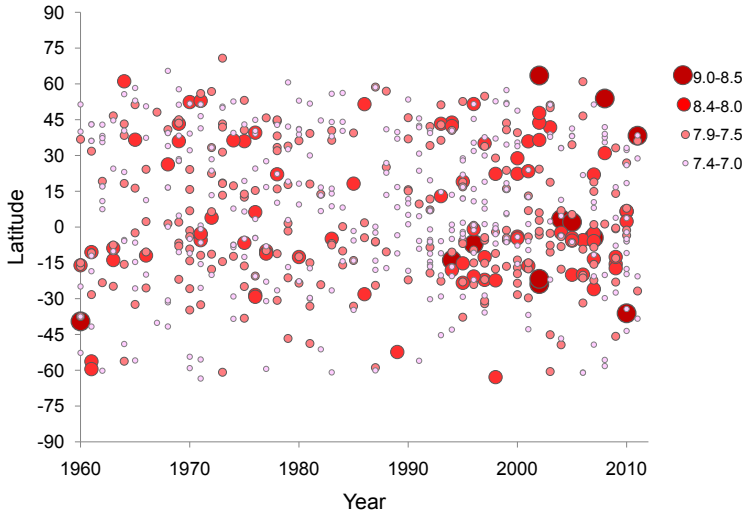

Figure 78 Space–time distributions of the main shocks listed in the global earthquakes catalog in the time interval 1960–2011. The size of circles is proportional to the four M classes considered. The decrease of seismicity toward the polar areas is a strong indication, if not an evidence, of the influence of the astronomical forces on plate tectonics. *After Varga et al. (2012).*

variable latitudes (Figure 79). Moreover, the number of earthquakes and their energy release is mostly (>90%) concentrated within the uppermost 50 km of the Earth. The segments of slabs deeper than 50 km deliver only about 10% of the elastic energy (Figure 80). This observation suggests a concentration of the momentum primarily acting on the lithosphere (Riguzzi et al., 2010; Varga et al., 2012). The Gutenberg–Richter or frequency/magnitude relation of seismicity indicates that there is a given amount of energy budget available each year that is dissipated globally. In fact, the Gutenberg–Richter relation is rectilinear at a global scale and suggests that the energy distribution acts on the lithosphere at the scale of the planet (Figure 81). Earthquakes with $M > 6.9$ deliver >90% of the seismic energy. Seismicity is the "instantaneous" result of plate tectonics, and the understanding of the forces governing geodynamics may provide fundamental clues for unraveling earthquakes occurrence. Therefore, the mechanisms that move plates are of paramount importance for tackling, in a reliable way, the issue of seismic hazard. In fact global seismic hazard assessment has been shown totally inadequate even when estimated by recent international program like GSHAP (Kossobokov & Nekrasova, 2012; Wyss, Nekrasova, & Kossobokov et al., 2012).

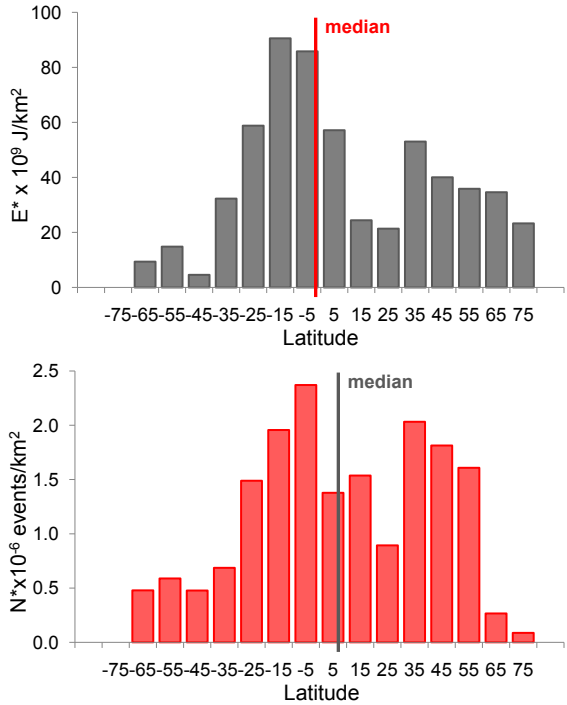

Figure 79 Distributions (per km^2) of N* (number of events) and E* (energy) of the earthquakes with M $\geq$ 7.0 along Earth's latitude (10° discretization step) for the time interval 1960–2011. The seismicity decreases toward the polar areas and has a maximum in the latitude range from −10° to 0°. The increase toward low latitudes of N* and E* supports the existence of a contribution of the Earth's rotation to plate tectonics. *After Varga et al. (2012).*

The most energetic earthquakes form along subduction zones because they are cold zones, and to break rocks that are under contraction needs more energy than to break those under extension. The Gutenberg–Richter law implies that large magnitude earthquakes are very rare events (Stein & Wysession, 2003), thus the energy released by one big earthquake seems to deplete temporally the energy budget of plate tectonics, i.e., a slab interacting with the surrounding mantle is not an isolated system, but it participates to a global expenditure of the stored energy. Plate tectonics is an Earth's scale phenomenology, and the energy necessary for its existence is not concentrated in limited zones (e.g., subduction zones), but it is contemporaneously distributed all over the whole Earth's lithosphere, like the Earth's rotation. Romashkova (2009) has recently shown how the planet seismicity indicates that the Earth's lithosphere can be considered as a single whole. Only the global seismicity

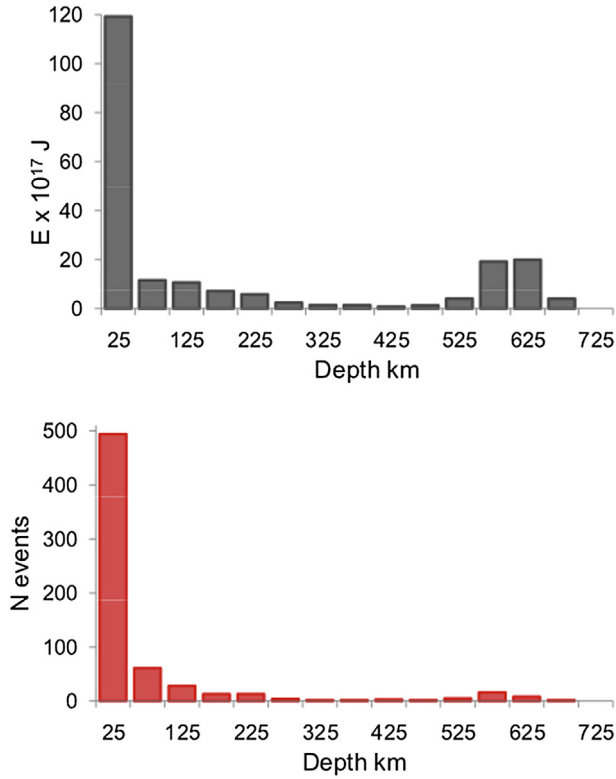

Figure 80 Depth distribution of seismicity with M $\geq$ 6.9 based on not declustered seismic catalogs (i.e., including aftershocks). Most of the earthquakes and energy are delivered in the first 50 km, and show that the main force acting on the system is likely concentrated on the lithosphere. *Courtesy of Federica Riguzzi and Peter Varga.*

follows the Gutenberg—Richter law, while this simple relation does not hold when considering smaller portions of the Earth (Molchan, Kronrod, & Panza, 1997; Nekrasova & Kossobokov, 2006).

All these evidence and models are in favor, even if not conclusive, of a significant energy contribution to plate tectonics by the Earth's rotation. Therefore, when there is a great earthquake in Japan, the lithosphere in Indonesia "knows" that some energy has been delivered elsewhere. This favors the concept of the lithosphere as a self-organized system in a critical state—SOC system (Keilis-Borok & Soloviev, 2003; Stern, 2002) that can be extended to the whole geodynamic setting (Riguzzi et al., 2010). The slab pull concept is a local process that takes place between the slab and the ambient mantle. The only mechanism that acts globally on the lithosphere and mantle is the Earth's rotation. Tidal

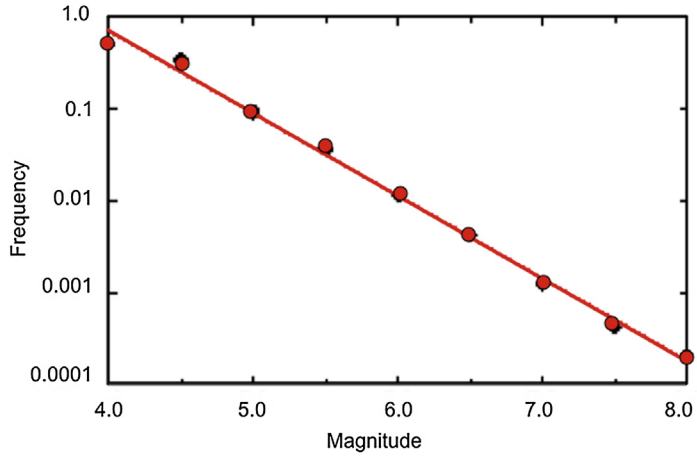

Figure 81 The Gutenberg–Richter law supports that the whole lithosphere is a self-organized system in critical state, i.e., a force is acting contemporaneously on all the plates and distributes the energy over the whole lithospheric shell, a condition that can be satisfied by a force acting at the astronomical scale.

drag and rotational effects can trigger the westerly displacement of the lithosphere and polarize the convection system as well as the dissipation of the elastic energy in the shallow Earth's layers (Figure 82). The larger (possibly three to one) volumes of lithosphere recycled along W-directed subduction

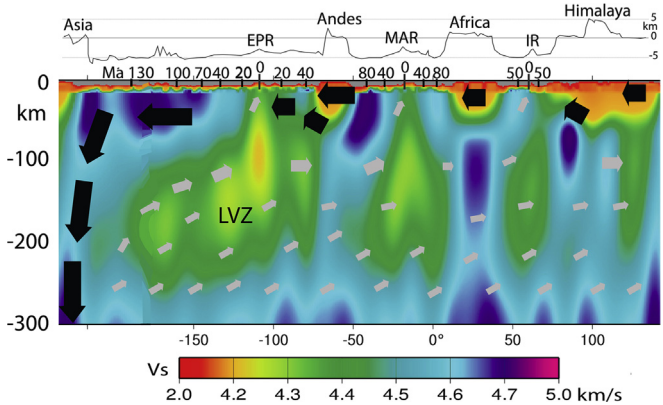

Figure 82 Vs absolute tomography after Panza et al. (2010) along the tectonic equator in which are schematized the inferred westerly polarized velocity vectors of the lithosphere (black arrows) and of the mantle "eastward" relative motion (gray arrows). Concentrated large volumes of lithosphere are recycled along the western Pacific slabs. The mantle compensates for the lithospheric loss with a diffuse relatively easterly directed upwelling, up to the sheared LVZ, where the lithosphere is decoupled and shifts to the west. Numbers above the tomographic section indicate the age of the oceanic crust. *After Doglioni and Anderson (2015).*

zones with respect to the E- or NE-directed ones suggest the existence of a polarized mantle convection consistent with the asymmetric pattern of contractional or diverging plate boundaries previously discussed (Figure 83). Larger W-directed volumes along narrow subduction zones imply a mass balance of a large-scale return slow flow of the mantle toward the "east" (Figures 82 and 83). The Earth's rotation and the misalignment of the tidal bulge exert on the Earth a permanent westerly directed torque that is likely responsible for the polarized westward drift of the lithosphere along the TE (Figure 84). This torque slows down Earth's rotation speed and explains the receding of the Moon relative to the Earth for the conservation of the angular momentum. The tidal oscillations determine variations of g, which modify the lithostatic load. The increase or decrease of the acceleration of gravity enlarges or reduces the differential stress, hence favoring or contrasting the rupture of rocks. In fact, the extensional earthquakes tend to occur more frequently during low tides (high g and dominant $\sigma 1$, enlarging the Mohr circle to the right), whereas contractional earthquakes develop more often during high tides (low g and dominant $\sigma 3$, enlarging the Mohr circle to the left) as suggested by Riguzzi et al. (2010) and illustrated in Figure 85. In fact, it has been observed some correlation between seismicity and ocean tides (i.e., at continent–ocean margins) (Cochran, Vidale, & Tanaka, 2004; Métivier et al., 2009; Wilcock, 2001). For example, along the Cascadia subduction zone in the western North America, it has been noted that tremors are correlated during the high tide. Conversely, normal

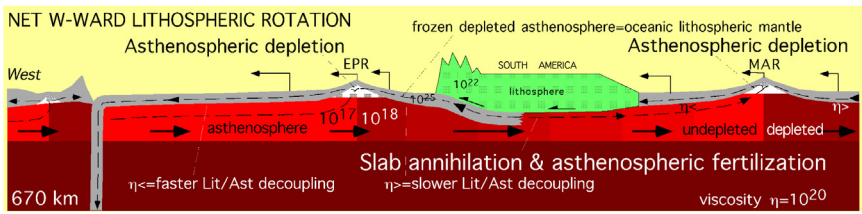

Figure 83 Model for the upper mantle circulation. The lower the asthenospheric viscosity, the faster the W-ward displacement of the overlying plate. The asthenospheric depletion at oceanic ridges increases the local viscosity while decreases the lithosphere–asthenosphere decoupling. As a consequence the plate to the east is perpetuating to be the slowest. The oceanic lithosphere subducting E-ward enters the asthenosphere where again it undergoes melting thus refertilizing the asthenosphere. W-directed subductions provide deeper circulation than E- (or NE-) ones. The E-directed slab (the Andes) moves out of the mantle (upduction), but it is overridden by the upper plate. *After Doglioni et al. (2007).*

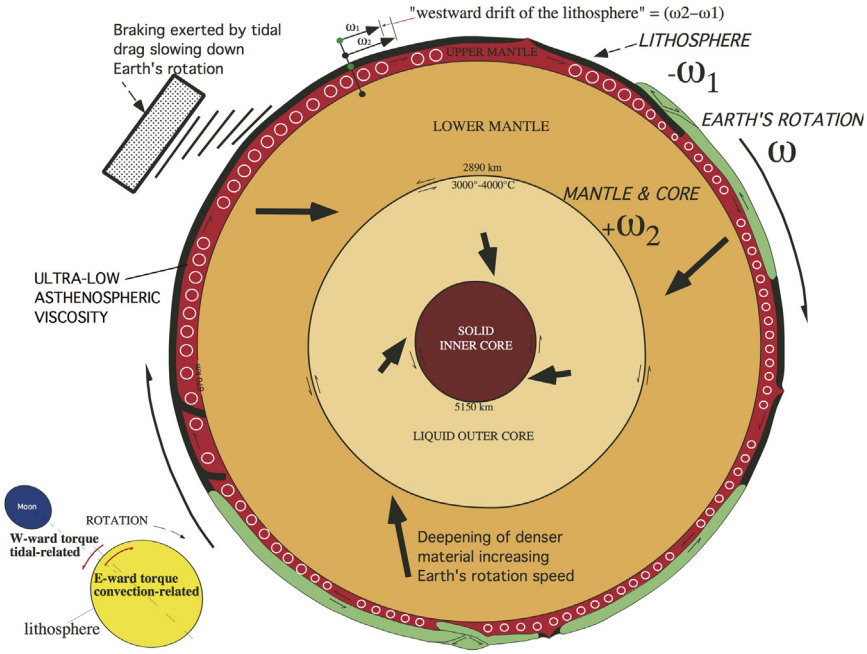

Figure 84 Cartoon showing how Earth, viewed from the southern pole, is undergoing two opposite torques. The tidal torque is opposing Earth's rotation, whereas convection is speeding up the spinning due to the accumulation of heavier material toward the inner parts of the planet. Such accumulation process increases the dimension of the inner core and increases the density of the lower mantle. Very-low viscosity, hydrated layers are inferred in the nonlinear rheology asthenosphere where the tides cause mechanical fatigue. The combination of these different processes can lead to decoupling between the lithosphere and the underlying upper mantle, where vigorous convection takes place. *After Scoppola et al. (2006).*

fault-related earthquakes seem more frequent during the low tide (Figure 85). The tidal forces are too small to generate earthquakes within continental areas, and for this reason they have been disregarded for long time. However, the tide can be decomposed into a horizontal and a vertical component. In our model, under the effect of the "westerly" oriented tidal friction, the horizontal component of the solid Earth (body) tide has a hysteresis, resulting in a westerly directed shift of plates. This motion inputs energy to a given locked fault. When the critical state is reached, even a small change in the lithostatic load can trigger the earthquake. During the high tide (regardless if oceanic or solid Earth), the gravity is at a minimum, whereas during the low tide, it is at a maximum. Since the lithostatic load ρgz (being ρ, the density of rocks, g, the acceleration of gravity, and z,

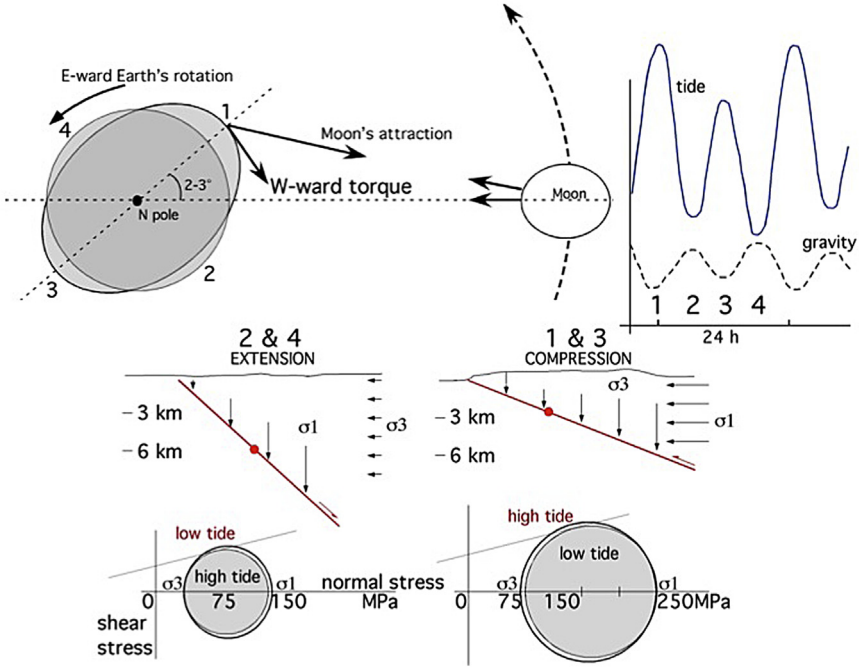

Figure 85 The misalignment (delay) of the Earth's tidal bulge with respect to the (gravitational) Earth—Moon alignment. The 2°—3° shift is due to the viscoelastic nature of the Earth. This distribution of the mass tends to pull the planet along the gravitational alignment that acts on the Moon's revolution plane, permanently toward the "west." Since this action is opposed to the E-ward rotation of the planet, this torque is considered responsible for the slow Earth's despinning. The torque can push the lithosphere horizontally, westward relative to the underlying mantle: body tides generate waves that swing the lithosphere horizontally and vertically, and are accompanied by gravity variations of opposite sign. Therefore, the lithosphere undergoes a permanent and isoriented oscillation. During their passage, tidal waves determine very small variations of gravity. These slight variations of the lithostatic load act on a lithosphere, which is slowly but persistently pushed westward, and determine the increase or decrease of the maximum stress tensor ($\sigma 1$) in extensional environments, or the minimum stress tensor ($\sigma 3$) in compressional tectonic settings. Therefore, the same variation of the lithostatic load acts in an opposite way in the two different tectonic settings. In this model, the horizontal component of the solid Earth tide slowly accumulates the stress, whereas the vertical component allows for the downloading of the stress as a function of the tectonic setting and the orientation of the faults relative to the tidal waves. Normal faults may activate more easily during a low tide (relatively higher gravity and stronger lithostatic load increase the differential stress and facilitate rock failure), whereas reverse faults may move more easily during a high tide (relatively lower gravity and smaller lithostatic load increase the differential stress and facilitate rock failure). *Modified after Riguzzi et al. (2010).*

the thickness of the rocks column) acts as the minimum stress tensor ($\sigma 3$) in compressional tectonic settings and the maximum stress tensor ($\sigma 1$) in extensional tectonic settings, their variation determines opposite effects on the activation of faults. The differential stress increases during the high tide in compressional regimes (i.e., the lithostatic load decreases with decreasing g), thus favoring earthquake nucleation. Alternatively, the differential stress increases during the low tide in extensional regimes (i.e., the lithostatic load increases with increasing g). Therefore, high tide favors fault slip in compressional environment, whereas the low tide may rather trigger normal faulting, which is exactly what observed due to the change of the lithostatic load which has an opposite effect as a function of the tectonic setting (Figure 85). For these reasons, the two tidal components could be considered as potentially relevant for earthquake occurrence, since the horizontal one under the effect of the tidal friction contributes to the accumulation of energy during the centuries, and the vertical one acts as the final drop that generates the instability of the fault at the coseismic stage. Moreover, besides astronomical variations, even loading or unloading of snow may be an effective seismic trigger in varying the vertical load (Heki, 2003; Panza, Peresan, & Zuccolo, 2011).

Based on the previous discussions, the observed phenomenology of plate tectonics confirms mantle convection, but it appears to be governed from the top, i.e., an astronomically sheared lithosphere travels westward along the TE, facilitated by the decoupling allowed by the presence, at the top of the asthenosphere, of a continuous global flow within the Earth low-viscosity LVZ that is in superadiabatic conditions (Figure 86).

The westerly directed torque of the tidal drag can drive the shear if the LVZ has a sufficiently low viscosity (Figure 87). Therefore, a sort of polarized CCW flow of lithosphere and mantle can be envisaged, e.g., the "bicycle" circuit proposed by Doglioni and Anderson (2015) shown in Figure 88. To summarize, the lithospheric movement can be compared to the motion of a worm that is contracted and uplifted, then elongated and lowered while advancing (Figure 89). This model explains why, unlike Earth, satellites where stronger gravitational tides operate (e.g., the Moon, the four largest of Jupiter's satellites, Io, Europa, Ganymede, Callisto) and internal convection is low or absent have reached the orbital resonance condition (Boccaletti & Pucacco, 2002), or tidal locking, where the time of rotation equals the time of revolution around the main planet, and plate tectonics do not occur. On the other hand, moonless and single plate with

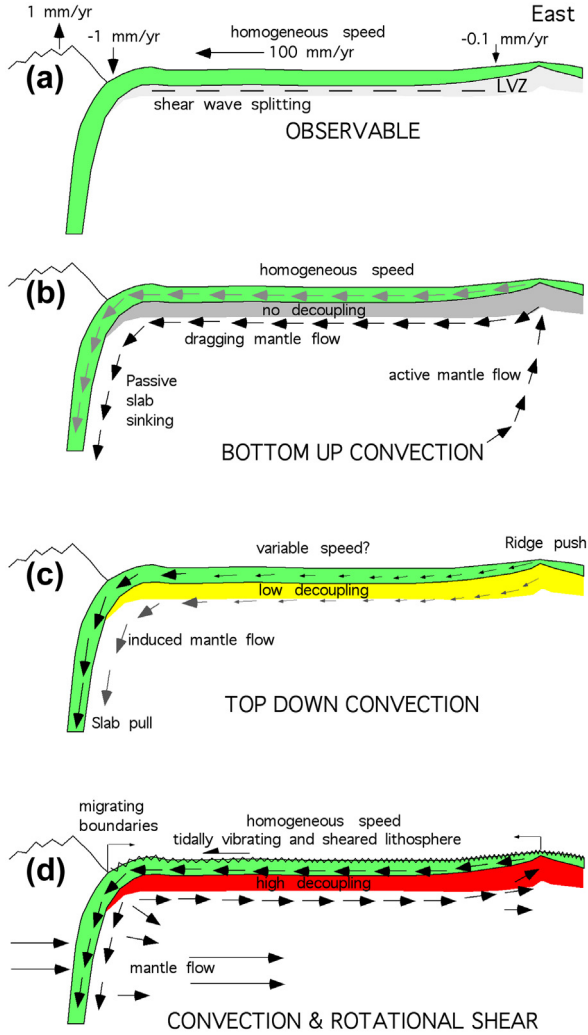

Figure 86 The surface observables (a) are compared with three models of plate dynamics, where plate motion is induced by classic mantle convection (b), boundary forces (c), or the combination of the aforementioned mechanism plus the rotational drag (d). *After Doglioni et al. (2007).*

stagnant crust-LID planets do not show plate tectonics similar to that of the Earth (Breuer & Spohn, 2003), while recently Kobayashi and Sprenke (2010) have shown that the crustal magnetic anomalies on Mars may represent hot spot tracks resulting from lithospheric drift on ancient Mars. The "pole-fleeing" mechanism of Eötvös (1913) has also been invoked as a potential mechanism (Varga et al., 2014).

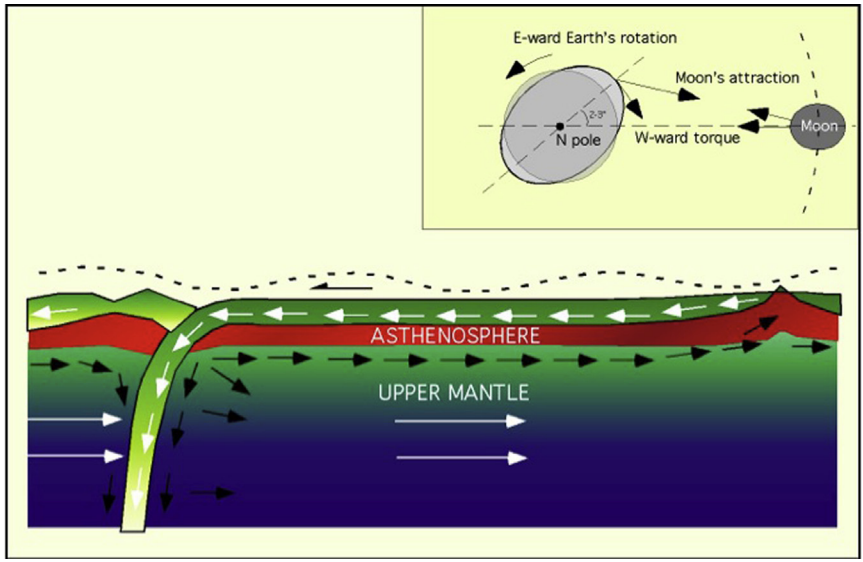

Figure 87 The westward drift of the lithosphere relative to the mantle can be generated by the torque exerted by the misalignment of the excess of mass of the Earth's bulge with respect to the Earth–Moon gravitational alignment. This motion is consistent with the presence of a hot, low-viscosity layer at the base of the lithosphere, within the low-velocity zone (LVZ) in the uppermost asthenosphere. The tidal oscillation of the lithosphere facilitates the decoupling. Mantle convection appears polarized due to the oscillating westerly directed tidal drag. The horizontal component of the body tide can slowly but steadily shift the lithosphere relative to the underlying mantle. Therefore, plate tectonics can be a combination of mass transfer within the planet, but polarized by the astronomical tuning.

7. DISCUSSION

As it is well known, Plate tectonics is the theory explaining the evolution of the outermost and brittle shell of the Earth, fragmented in several different pieces that move relative to each other and relative to the underlying mantle. This motion controls not only the present structure of the Earth lithosphere and the seismic phenomena in it but also the structure of the deeper layers of the upper mantle. Although this theory is today widely accepted and several geological, geophysical, and geodetic evidence corroborate it, there is not general consensus on the driving mechanisms that cause the plate's motion. As a matter of fact, the plate motion is the result of different conspiring force fields.

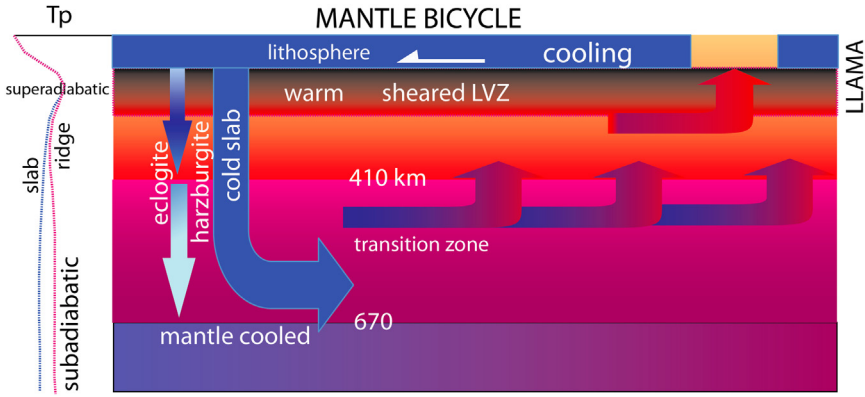

Figure 88 The counterclockwise convection results in lateral variations of mantle potential temperature (Tp). The Tp of a parcel of fluid at pressure P is the temperature that the parcel would acquire if adiabatically brought to a standard reference pressure Po, usually 1 bar (e.g., the Earth's surface). Along subduction zones the ambient mantle is inferred to be cooler than elsewhere. The thermal buffer exerted by the cold lithosphere, the radiogenic decay, and the shear heating in the LVZ, they all concur to the existence of an upper asthenosphere in superadiabatic conditions and a lower upper mantle in subadiabatic conditions. The westward drift of the lithosphere polarizes the "bicycle" and the relative easterly directed compensating mantle flow that balances the slab loss along W-directed subduction zones. The intrinsically buoyant harzburgite component of slabs contributes to the upward return flow. *After Doglioni and Anderson (2015)*.

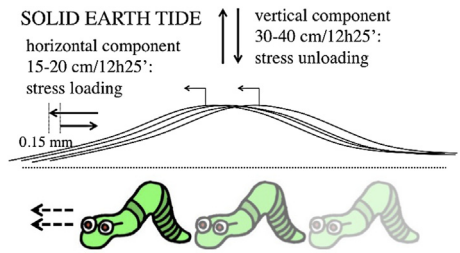

Figure 89 The solid Earth's tide generates a wave, which uplifts and shifts horizontally the lithosphere. A hysteresis of about 0.15 mm (variable with latitude) should accumulate after every solid Earth's passage, due to the westerly directed torque acting on the lithosphere. At the end of the year, this sums up to the few centimeters motion of the lithosphere relative to the mantle. The horizontal component of tides may be the energy pumping system at plate boundaries where faults are gradually loaded of energy over the centuries. The vertical oscillation modifies the acceleration of gravity (g), and is interpreted as the triggering mechanism of earthquakes on faults that have reached the critical state. The model proposes that the westward drift deforms the lithosphere as a worm, which is crawling.

Two different reference frames are generally used to represent absolute plate motion: (1) the hot spots reference, which is based on the assumption that hot spots are fixed with respect to the mesosphere (the mantle underlying the asthenosphere) and to one another; (2) the mean-lithosphere reference, which is based on the NNR condition (Solomon & Sleep, 1974) and it assumes a uniform coupling between lithosphere and asthenosphere. This hypothesis is contradicted, as we have seen, by an increasing number of seismological proofs and laboratory experiments. In the deep hot spot reference frame the plates show an average westward motion with respect to the underlying mantle which turns out into a complete westward polarization in the shallow hot spot reference frame (Cuffaro & Doglioni, 2007), that is usually referred to as "westward drift" of the lithosphere. The westward motion persists even if the plate's motion is calculated with respect to Antarctica plate (Knopoff & Leeds, 1972; Le Pichon, 1968).

In the interpretation of the shallow hot spot reference all plates on Earth move westward relative to the subasthenospheric mantle (the mesosphere), although with different velocities, and with a trend parallel to the TE (Doglioni, 1993a). For example, in the shallow hot spot reference frame the mantle is relatively moving eastward with respect to the Nazca plate, as suggested from the shear-wave splitting analysis (Russo & Silver, 1994). Such a reference frame would provide a mechanism that makes continuously available new fertile asthenosphere that melts beneath the westward-migrating EPR (Panza et al., 2010). In contrast with these data, the deep hot spot reference would rather predict a subasthenospheric mantle that shifts westward beneath the Nazca plate, which is at odd with all the aforementioned discussion.

There are two competing hypotheses about the kinematics and the mechanism driving the W-ward rotation of the lithosphere relative to the mantle. Hypothesis A states that lateral viscosity and density variations in the mantle can be the primary sources of the net rotation, and the net rotation is only a mean rotation mainly generated by the relatively stronger pull of slabs surrounding the western Pacific. Consequently the relatively faster W-ward velocity of the Pacific plate dominates the global kinematics of plates and gives a W-ward residual to the whole lithosphere (e.g., O'Connell, Gable, & Hager, 1991; Ricard et al., 1991). The alternative hypothesis B interprets the net rotation as the result of the rotational drag on the lithosphere due to the tides that affect both the fluid and solid Earth (e.g., Bostrom, 1971; Knopoff & Leeds, 1972; Moore, 1973; Nelson & Temple, 1972). According to hypothesis B, the motion of the lithosphere

to the W is driven by the concurrent action of Earth's rotation, tidal despinning, and mantle convection (e.g., Crespi et al., 2007; Cuffaro & Doglioni, 2007; Doglioni et al., 2005; Riguzzi et al., 2010).

The amount of the net rotation of the lithosphere with respect to the mantle is controlled by the viscosity contrast in the upper asthenosphere, whose lateral variations control the plate interactions (Doglioni et al., 2011). Crespi et al. (2007) introduced the concept of tectonic mainstream based on geological evidence and consistently with geodetic data under three different hypotheses regarding the source depths of Pacific hot spot. This lead to the definition TE, which is the great circle depicting the flow line that approximates the path of the westward mainstream of the lithosphere with respect to the mantle, i.e., the line along which plates move over the Earth's surface with the fastest mean angular velocity toward the W, relative to the mantle. Its latitude range is about the same of the Moon maximum declination range of its revolution plane (about 28°), indirectly supporting the relevance of Moon's tidal drag for plate's motion. A global reconstruction of the seismic shear-wave anisotropy in the asthenosphere (Debayle et al., 2005; Montagner & Guillot, 2003) fits quite well the flow of plate's motion, apart along subduction zones where the shear-wave splitting anisotropy shows orthogonal trend compatible with the reorientation of a flow encroaching an obstacle (Figure 55).

When considering a migrating subduction hinge, the kinematics of convergent geodynamic settings shows that subduction zone rates can be faster or slower than convergent rates as a function of whether the subduction hinge migrates away or toward the upper plate. This (opposite) behavior occurs in particular along W-directed and E- (or NE-) directed subduction zones, respectively. Along W-directed slabs, the subduction rate is the convergence rate plus the slab retreat rate, which tends to equal the backarc extension rate minus the accretion rate. Along E- (or NE-) directed slabs, the subduction rate is decreased by the shortening in the upper plate. Relative to the mantle, the W-directed slab hinges are fixed, whereas they move west or southwest along E- (or NE-) directed subduction zones. Therefore, subduction zones appear as passive features controlled by the far-field plate velocities and their motion relative to the underlying "eastward" mantle flow, rather than by the negative buoyancy alone of the downgoing plate (Brandmayr et al., 2011; Doglioni, Cuffaro et al., 2006; El Gabry et al., 2013). The convergence/shortening ratio is regularly >1 along E- (or NE-) directed subduction zones, whereas it is < 1 along the converse W-directed slabs. This value is sensitive to the viscosity of the

upper continental lithosphere. High ratio means high viscosity of the lithosphere, i.e., the lithosphere is stiffer and it sustains the convergence, while most of it is absorbed by subduction. The observation that the convergence is faster than the shortening supports the notion that the plate boundary (subduction and related orogen) is a passive feature, and does not provide relevant driving energy for plate motions. Kinematically, when plate motions are analyzed relative to the shallow hot spot reference frame the slab is moving out of the mantle along E- (or NE-) directed subduction zones, i.e., moving in the direction opposite to the one predicted by the slab pull (Doglioni et al., 2007; El Gabry et al., 2013). This kinematic reconstruction is coherent with the frequent intraslab down-dip earthquakes with extension focal mechanism that characterizes E- (or NE-) directed subduction zones (e.g., Isacks & Molnar, 1971). Accordingly with Doglioni et al. (2009) the corner flow induced in the ambient mantle by the subduction zones (e.g., Turcotte & Schubert, 2002) is not a general mechanism but it occurs dominantly along W- (or SW-) directed subduction systems. Along the E- (or NE-) directed subduction zones, where plates move W-ward or SW-ward relative to the mantle, in a direction opposite to that of the subduction (Cuffaro & Doglioni, 2007), where the dominant process is upduction, i.e., the motion of the slab generates an upward flow of the mantle beneath the subduction zone, sucking up the mantle and depressurizing it (the tectonic syringe).

The upduction of the mantle inferred at depth along E- (or NE-) directed subduction zones provides a mechanism for syn-subduction alkaline magmatism in the upper plate, with or without contemporaneous rifting in the backarc. In fact, relative to the mantle, the lower plate is moving westward out of the mantle, in the direction opposed to the dip of the slab (upduction). The subduction occurs because the upper plate is moving westward faster than the lower plate. A number of subduction zones are characterized by alkaline magmatism in the foreland of the retrobelt or within the orogen itself (e.g., Mineralnie Vodi in the northern Caucasus; Euganei Hills in the Southern Alps; Patagonia in the Andes; the Kula Na-rich magmatism in the northern Taurides). This magmatism may be related to upduction of the mantle due to the opposite slab motion. The deeper, more viscous, and rigid is the mantle the crystallographic structure is more compact and seismic velocities are larger. The fluids released from the slab into the overlying mantle should cause a decrease of viscosity in the hanging wall of the subduction, at the bottom of the upper plate. The top of the asthenosphere is the main decollement surface of the lithosphere, and the decrease of the

viscosity can increase the decoupling. Therefore, the upper plate increases its velocity and moves away from the lower plate along the W- (or SW-) directed subduction zones. This facilitates the formation of the backarc spreading. Along the E- (or NE-) directed subduction zones, the upper plate is converging faster with respect to the lower plate and this facilitates the generation of double verging orogens such as the Andes and Himalayas. This mechanism upraises the mantle from deeper levels, where seismic velocities are faster with respect to the shallower mantle. This could explain the ghost of a slab of tomographic origin, beneath E- (or NE-) directed subduction zones, where the presence of a real slab is questioned by the absence of space continuity in hypocenter's distribution.

The rise of denser material from below is in quite good agreement with the geoid undulations. Therefore, W- (or SW-) directed subduction zones bring larger volumes of lithosphere back into the mantle than the converse E- (or NE-) directed subduction zones. The rate of sinking of W- (or SW-) directed subduction zones is controlled by the interaction of the slab with the "easterly" relative mantle wind, the main responsible of the retreat of the subduction hinge, and by the far-field velocities of the plates and the size of the negative slab buoyancy. On the other side, E- (or NE-) directed subduction zones have rates chiefly determined by the far-field velocity of plates, since the subduction hinge generally advances toward the upper plate and decreases the subduction rate. A quite remarkable feature of E- (or NE-) directed subductions is the fact that the deep seismicity (focal depth >580 km) occurs only where the intermediate one, which delineates the subducting slab, reaches about 300 km of depth while it is absent elsewhere, as can be seen in Figure 4 of Riguzzi et al. (2010). This may indicate that some critical value in the pressure variation due to Venturi effect is necessary to allow for the shear stress, built at the lower–middle mantle discontinuity and primarily due to phase changes in its pyroxene–garnet part (Anderson, 1976), to give rise to earthquakes. This is the main difference between the two examples considered: Hellenides and Andes.

Regardless the hot spot reference frame considered, the Africa plate moves westward, i.e, opposite to a hypothetic Atlantic ridge push (Crespi et al., 2007; Gripp & Gordon, 2002) even if it does not have any subducting slab in its western side. The only slabs attached to Africa are at its northern margin, i.e., the Hellenic–Cyprus and Apennines subduction zones. Although problematic, another small, finger-like, E-directed slab has been supposed beneath the Gibraltar arc (Gutscher et al., 2002). The Hellenic–Cyprus slab is also NE-ward directed, i.e., opposite to the direction of

motion of the Africa plate to which is attached. However, since it is WSW-ward moving together with Africa relative to the mantle, it provides kinematic evidence of no dynamic relationship between the motion of Africa, which is moving away from the trench, and the slab. Moreover, since the slab is not actively entering into the mantle, its existence cannot be ascribed to the negative buoyancy of the downgoing lithosphere. The Apennines slab is retreating and W-directed. These northern Africa subduction zones are a small percentage of the plate boundaries surrounding Africa, and they dip in opposite directions with respect to the absolute motion of the plate. Therefore, they cannot be the cause of its motion. The analyzed kinematics frames suggest that subduction zones have rates of sinking controlled by far-field plate velocities, hinge migration direction, and subduction polarity and claim for a passive behavior of the slabs. This is even truer if the net "westward" rotation of the lithosphere is a global phenomenon rather than the simple average of plate motions (Scoppola et al., 2006).

Rift zones are also asymmetric, with the eastern side more elevated with respect to the western one by ~100–300 m worldwide (Doglioni et al., 2003) and this asymmetry extends to mantle depths (Panza et al., 2010). Based on a surface wave tomographic three-dimensional model of the Earth's uppermost 300 km, a global cross section parallel to the equator of the net rotation of the lithosphere, the TE, shows that Vs are different at the western when compared to those of the eastern flanks of the three major oceanic rift basins (Pacific, Atlantic, and Indian ridges). In general, the western limbs have a faster velocity and thicker lithosphere relative to the eastern or northeastern one, whereas the uppermost asthenosphere is faster in the eastern limb than in the western limb. The difference between the two flanks can be the result of the combination of mantle depletion along the oceanic rifts and of the westward migration of the ridges and of the lithosphere relative to the mantle. The low-velocity layer in the upper asthenosphere in the depth range 120–200 km represents the decoupling zone between the lithosphere and the underlying mantle, as it is well defined by the distribution of radial anisotropy that reaches minimum values close to the rifts, but with an eastward offset (Panza, et al. 2010). The fertile asthenosphere coming from the west melts and depletes along the ridge. Continuing its journey to the east, the depleted asthenosphere is more viscous and lighter and slows down the motion of the plate to the east (Doglioni et al., 2005; Panza et al., 2010). Subduction zones directed to the E (or NE), along the mantle counterflow, might refertilize the upper mantle, whereas W- (or SW-) directed subduction zones would penetrate deeper into the mantle.

Mantle convection is also inadequate to explain the Earth's surface kinematics. It is generally assumed that "purely" oceanic plates travel faster than plates that encompass large fractions of continental lithosphere. However, Gripp and Gordon (2002), even in the deep hot spot reference frame, have shown that the South American plate is moving faster than the purely oceanic Nazca plate. Another common assumption is that plates move away from ridges, but again, in the deep reference frame, Africa is moving toward the mid-Atlantic ridge, although slower than South America. Moreover, Africa is moving away from the Hellenic subduction zone.

The subduction rate of about 300 km^3/yr along over 76,000 km of subduction zones would take about only 170 Ma to consume the whole lithosphere. This is very much interesting because this value is close to the oldest oceanic crust of the world, which confirms its robustness. Moreover it would take about 857 Ma for recycling the upper mantle down to the 670 km discontinuity. Therefore the upper mantle should have been re-homogeneized at least 4–5 times since the Earth's accretion, supporting a more vigorous convection in the upper mantle with respect to the lower mantle. Moreover, another intriguing result is that the W-directed subduction zones (31,700 km) provide a volume recycling more than three times larger than along the E- or NE-directed subduction zones (44,700 km), confirming an asymmetric pattern of plate tectonics.

So what is moving the lithosphere relative to the mantle? The only reasonable mechanisms are the slab pull and/or rotational forces and the tidal friction. However, the slab pull model is hampered by a number of inconsistencies previously discussed. Slab pull alone does not seem to be able to determine plate motions in general, although it could facilitate subduction once started. An alternative and/or complementary source of energy for plate's motion is the tidal drag exerted by the Moon and the Sun on the Earth rotation. Plate motions driven by the Earth's rotation seem to be the simplest and natural explanation for the observed asymmetry along the subduction and rift zones (Panza et al., 2010; Riguzzi et al., 2010).

In plate tectonics it is assumed that the inertia and acceleration of the individual plates are nonexistent or negligible, and thus the plates are in dynamic equilibrium (Forsyth & Uyeda, 1975). At present, the solid Earth can be considered in energetic equilibrium: there is no statistically meaningful difference between the total of income and expenditure energy rates (Riguzzi et al. 2010). This circumstance allows for relatively small energy sources to influence global tectonic processes and therefore the tidal despinning can contribute to plate tectonics through the westward lithospheric

drift (Bostrom, 1971; Knopoff & Leeds, 1972). Small perturbations in the velocity of rotation trigger the release of a large amount of energy and seismicity (Press & Briggs, 1975).

The asymmetries between "W"-directed (e.g., Tonga, Barbados) and "E"- or NE-directed (e.g., Andes, Zagros, Himalaya) subduction zones are robust features of a polarized geodynamics. The Mediterranean orogens show two distinct signatures as well, which are similar to those occurring on opposite sides of the Pacific Ocean. High morphological and structural elevations, double vergence, thick crust, involvement of deep crustal rocks, and shallow foredeeps characterize E- (or NE-) directed subduction zones (Alps—Betics and Dinarides—Hellenides—Taurides). Conversely, low morphological and structural elevations, single vergence, thin crust, involvement of shallow rocks, deep foredeeps, and a widely developed backarc basin characterize the W-directed subduction zones of the Apennines and Carpathians. This asymmetry can be ascribed to the generalized westward drift of the lithosphere relative to the underlying mantle (Carminati & Doglioni, 2005).

The slabs whose density reveals to be possibly lighter than that of the ambient mantle (Brandmayr et al., 2011), supply no evidence for slab pull as the driving mechanism of plate motion. In the eastern Mediterranean the LAS exhibits features, which suggest the presence of upducted asthenosphere exhumed to the north of the Hellenic arc, where the slab extension is limited to depths of about 220 km (El Gabry et al., 2013). The evidence presented by Cruciani et al. (2005) casts further doubts on the effectiveness of the slab pull, as indicated also by the down-dip compression occurring in several slabs (Frepoli et al., 1996; Isacks & Molnar, 1971) and the subduction of continental lithosphere is now a quite widely accepted process by the Earth Sciences community (e.g., Frezzotti et al., 2009; Panza, Raykova, et al., 2007). On the other hand, in the Red Sea and in the Gulf of Suez, it has been demonstrated that the uprising of the mantle postdates the stretching in the lithosphere (Bohannon, Naeser, Schmidt, & Zimmermann, 1989; Moretti & Chènet, 1987) and consequently the mantle rise seems to be more a passive isostatic phenomenon than the primary driving mechanism (ridge push).

All the data and interpretations listed so far point to an asymmetric Earth, whose origin is here tentatively related to the Earths rotation and its tidal despinning (Riguzzi et al., 2010). Tidal drag maintains the lithosphere under a permanent high-frequency vibration, polarized and sheared toward the west (Doglioni et al., 2011). Earth's rotation and the resisting force exerted by the lag of the tidal bulge (Bostrom, 1971; Knopoff & Leeds, 1972; Le

Pichon, 1968; Moore, 1973; Scoppola et al., 2006) have been proved to be efficient only if very-low-viscosity material occurs at the lithosphere–asthenosphere transition. Jordan (1974), Ricard et al. (1991), and Ranalli (2000) have suggested that this hypothesis is incompatible with current estimates of upper mantle viscosities. It is clear that a main and crucial key point is to determine realistic values for the viscosity of the asthenosphere. Postglacial rebound analysis provided important constraints on mantle viscosity structure, but the use of this method cannot reveal the presence of a relatively thin low-viscosity layer hosted in the asthenospheric LVZ (Doglioni et al., 2011; Scoppola et al., 2006, and reference therein). Moreover, the viscosity in the asthenospheric low-velocity zone can be even three orders of magnitude lower when measured under horizontal shear with respect to the viscosity computed by vertical unloading, due to postglacial rebound (Doglioni et al., 2011; Riguzzi et al., 2010; Scoppola et al., 2006). This is confirmed by Jin et al. (1994) who showed how intracrystalline melt in the asthenospheric peridotites under shear could generate a viscosity as low 10^{12} Pa s, compatible with the efficiency of tidal drag. These very low values require the presence of high melt fractions, which is compatible with a hotter than expected asthenosphere (Anderson, 2011) and the low values of radial anisotropy in the LVZ (Panza et al., 2010). Anderson (2013) inferred that temperatures at 200 km of depth can be as high as 1600 °C, which explains the low strength/viscosity as well as temperatures of some midplate magmas (Hawaii).

As discussed, gravitational body forces produced at subduction zones (slab pull) and at oceanic ridges (ridge push) have been considered potential driving forces of the plate-tectonic process. However, in Chapter 6.2, we have shown an endless number of reasons why the slab pull alone cannot be the driving force for plate tectonics, and the ridge push is even one order of magnitude lower than the slab pull (e.g., Ranalli, 1995). Moreover, the ridge push, related to the topographic excess, should be higher along elevated orogens, where on the contrary, plates converge rather than diverge. Boundary forces such as slab pull and ridge push should in principle decrease moving away from the energy source, but plates rather show internal homogeneous velocity.

Mantle convection could satisfy a steady-state speed of the overlying lithosphere, assuming low or no decoupling at the asthenosphere interface. However, mantle convection, which can be inhibited by thermal gradients weaker than the adiabatic one (Anderson, 2007b; 2013; Birch, 1952; Bullen, 1947) is kinematically problematic in explaining the migration of plate

boundaries and the occurrence of a decoupling surface at the base of the lithosphere. Although a combination of all forces acting on the lithosphere is likely, the decoupling between lithosphere and mantle suggests that a torque acts on the lithosphere independently of the mantle drag. Slab pull and ridge push are candidates for contributing to this torque, but they have a number of aforementioned counterarguments. Unlike these boundary forces, the Earth's rotation and related tidal drag are volume forces that act simultaneously and tangentially on the whole plates, with obvious energetic advantages. Tidal drag maintains the lithosphere under a permanent short period (hours) vibration, polarized and sheared toward the "west." Earth's rotation and the break exerted by the lag of the tidal bulge (Bostrom, 1971) can be efficient only if very-low viscosity occur at the lithosphere–asthenosphere transition (Jordan, 1974) and growing evidence are emerging about the presence of a very-low-viscosity layer at the very top of the asthenosphere (e.g., Rychert et al., 2005), possibly related to very high fluids concentration in the mantle, and superadiabaticity of the LVZ that may allow plate decoupling (Doglioni et al., 2011).

During the last years it has been proposed that the misalignment of the tidal bulge relative to the gravitational Earth–Moon alignment, due to the anelastic reaction of the Earth with respect to the Moon gravity field (Figures 85 and 87), could be responsible for the westerly directed torque acting on the lithosphere (Riguzzi et al., 2010; Scoppola et al., 2006). A permanent oscillation acting on two layers with a difference in viscosity of about 8–10 orders of magnitude allow for the decoupling between the lithosphere and the asthenosphere (Doglioni et al., 2011). Within the decoupling layer, the mantle is undergoing shearing and crystals may roll due to the intracrystalline melt and lower the viscosity along the horizontal shear (Figure 2). If a segment of lithosphere is moving westward faster relative to another segment to the east, a lower viscosity, which generates a rifting in the overlying lithosphere, can be inferred within the LVZ beneath that plate (Figure 13). The spreading is transferred up toward the surface into the brittle regime layer where most of the faults and related earthquake develop. In case of faster plate to the east relative to a plate to the west, a subduction and related orogeny will occur in between.

All these asymmetries are compatible with the westward drift of the lithosphere with a speed $>1°$Ma and can be envisaged moving along the flow lines of plate motions described by the TE. Therefore, we need a dynamic model to explain this polarized system. Solid Erath's tides (or body tides)

generate significant and often disregarded oscillations in the lithosphere. They uplift the ground of 20–40 cm, swinging back and forth horizontally of 10–20 cm at every passage of the Moon and Sun (0.46 of the Moon tide) gravitational waves. Therefore, the lithosphere is constantly subject to a vibration, which is westerly oriented due to the misalignment of the tide-induced Earth's bulge. We infer that, after the passage of the body tide, a residual permanent shear remains like a floating bottle subject to the wind at sea. The lithosphere appears to behave like a worm, i.e., it is uplifted and sheared horizontally under the effects of the solid Earth's tide (Figure 88). For example, a hysteresis of about 0.15 mm every Moon passage (12 h and 25′) explains a lithospheric drift >1°/Ma relative to the mantle.

Lateral variations in the viscosity of the LVZ can control the different velocity of plates. The Earth's rotation contribution to the lithosphere motion can account for: (1) the homogeneous internal velocity of each plate, (2) the decoupling occurring at the lithosphere base, and (3) the westerly polarized migration of the lithosphere and of the plate boundaries, consistent with the geological asymmetries of subduction and rift zones as a function of the geographic polarity. In this view, plate dynamics could be the result of the combination of mantle convection with the shear induced by the tidal drag.

The energy necessary to move the Earth's Precambrian shields, i.e., to move the thickest lithosphere relative to the underlying poorly developed low-velocity channel (as in the Baltic area), has been estimated at about 4×10^{18} J/year (Knopoff, 1972). Similar value is found by considering the energy for the formation of tectonic dislocations that can be estimated as the consumption of energy rate, $\dot{E}$, necessary for lateral displacement of the lithosphere plates relative to the viscous mantle. For a mantle viscosity of 10^{21} Pa s one gets $\dot{E} = 6.5 \times 10^{19}$ J/year (Riguzzi et al., 2010). Recent papers suggest viscosity values of 10^{17} Pa s (Aoudia, Ismail-Zadeh, & Romanelli, 2007; Melini, Cannelli, Piersanti, & Spada, 2008), consequently, the power needed to move the lithosphere could be significantly less, possibly $\dot{E} = 6.5 \times 10^{15}$ J/year. The tidal friction in the Earth–Moon system can be estimated as $\dot{E} = 1 \times 10^{20}$ J/year (Riguzzi et al., 2010), a value not too far from the energy dissipated by the tectonic moment rate (1×10^{21} J/year). However, the real amount of energy dissipated by the solid Earth's tide (or body tide) is far to be entirely measured (Ray, 2001), especially if most of it is dissipated into ductile shear in the LVZ. The energy budget of the Earth is summarized in Table 6.

Table 6 The energy budget of the Earth

Energy income (J/year) $\times 10^{21}$		Energy expenditure (J/year) $\times 10^{21}$	
Accretion $\dot{E}_A$	1.9–5.5	Heat flow $\dot{E}_{HF}$	1.4–1.5
Core formation $\dot{E}_C$	3.2–3.6		
Radioactive decay $\dot{E}_R$	0.2–2.1	Tectonic moment rate $\dot{E}_{TM}$	5.7–7.6
Tidal friction $\dot{E}_T$	0.04–0.1		
Total energy income	5–11	Total energy expenditure	7–9

After Riguzzi et al. (2010).

8. CONCLUSIONS

Further studies on the composition, water content and viscosity of the asthenosphere and LVZ might significantly contribute to answer the following basic questions: (1) are plates dragged horizontally by mantle convection (e.g., Bercovici, 1998)? (2) Are they dragged and sheared at the base by a faster moving mantle (Bokelmann, 2002)? (3) Are they rather pulled by slab pull forces (Anderson, 2001; Forsyth & Uyeda, 1975)? (4) Could they be driven by Earth's rotation and tidal drag (Riguzzi et al., 2010; Scoppola et al., 2006)? (5) If ridges and subduction zones trigger convection, but are nevertheless still passive features, what does move plates?

Both "active plates and passive asthenosphere" and "an active asthenospheric flow dragging passive plates" may be consistent with the observed relatively westerly polarized horizontal plate motions. The mantle convection alone cannot explain the lithosphere kinematics. Therefore, the uncoupled forces appear to dominate, but we cannot exclude that more than one force, both coupled and uncoupled, is responsible of plate motions. Earth's rotation cannot work alone because mantle convection is required to maintain the mantle fertile and the low viscosity in the asthenosphere. Moreover density contrasts (e.g., slab pull) allow for differential sinking of plates at convergent margins. A very-low-velocity layer (LVZ), with a sizable fraction of melting that allows for very-low viscosity in the uppermost asthenosphere (100–150 km), has been recently revealed in the Mediterranean (Panza, Peccerillo, et al., 2007; Panza, Raykova, et al., 2007; Tumanian et al., 2012). Consistently with the present-day Vs resolution, Panza et al. (2010) have identified along the TE-pert a ubiquitous LVZ circuit, at least 1000 km wide and about 100 km thick, in the asthenosphere,

that allows for the persistence of a continuous global flow within the Earth without any relevant obstacle. Relatively small forces can easily move a floating plate horizontally, because no work has to be done against gravity, whereas nonisostatic vertical motions require work to be done against gravity. Such condition can occur when at the base of the lithosphere there is a very-low viscosity in the decoupling layer, i.e., the weak low-velocity zone in the upper asthenosphere, like the TE-pert defined by Panza et al. (2010).

The rates of subduction do not determine plate velocities, but are rather a consequence of them. Therefore, plates are passive features of the convective system. The Earth's models are generally performed assuming internal dynamics controlled by lateral density variations due to thermal gradients, which should generate both vertical and horizontal movements in the mantle and in the overlying lithospheric plates. The analysis of the geometry at plate boundaries and the kinematic constraints point to a "westerly" polarized flow of plates, which implies a relative opposed motion of the underlying Earth's mantle. This flow determines an asymmetric pattern along subduction zones and two end members of orogens associated to the downgoing slabs, such as the differences between the low topography, in the hanging wall of the western Pacific subduction zones, versus the high topography and deep rocks exhumation, along the eastern Pacific subduction zones. Rift zones are also asymmetric: on average the western flank is few hundreds meters deeper than the eastern one and the lithosphere in the western flank is thicker and faster with respect to that of the eastern flank. All plate boundaries move "west." The decoupling of the lithosphere in the LVZ at about 100–200 km depth allows for the "westerly" directed rotation of the lithosphere with respect to the underlying mantle (Figure 82). As a consequence of this asymmetric movement, larger volumes of lithosphere return to the mantle along the W-directed subduction zones than in the converse E- (or NE-) directed subduction zones and constrain the kinematic reconstruction of the convection pattern in the upper mantle (Figure 83).

In general, thermal gradients weaker than the adiabatic one lead to inhibition of convection (Anderson, 2013). Therefore, the motion of the lithosphere is very likely the combination of an astronomically driven "westerly" directed horizontal shear that acts on plates, combined with the heat dissipation of the planet that maintains the temperature high enough in the LVZ to keep the viscosity as low as required for the lithospheric decoupling (Figure 87). The variations in viscosity within the LVZ control variations in velocity among plates, and eventually seismicity at plate boundaries.

Therefore, the global scale asymmetry of tectonic features and the westward drift of the lithosphere support the need of a rotational component for the origin of plate tectonics (Scoppola et al., 2006). The westward drift could be the combined effect of three processes: (1) tidal torques acting on the lithosphere and generating a westerly directed torque that decelerates Earth's spin; (2) downwelling of relatively denser material toward the bottom of the mantle and in the core, slightly decreasing the moment of inertia and speeding up Earth's rotation and only partly counterbalancing tidal drag; and (3) thin (3–30 km) layers of very-low-viscosity hydrate channels in the asthenosphere. These layers are beyond the reach of tomography due to the limitations of the theoretical framework employed (Anderson, 2007a,b; Boschi et al., 2007; Boyadzhiev et al., 2008; Panza, Peccerillo, et al., 2007; Romanowicz, 2003; Waldhauser et al., 2002), nevertheless a contrast up to 10–15 orders of magnitude between the viscosity of the lithosphere and that of the asthenosphere can be expected from experiments reported in literature (Jin et al., 1994; O'Driscoll et al., 2009; Pollitz et al. 1998). Such a contrast is well consistent with the decoupling, within the asthenosphere, between the lithosphere and the underlying mantle (Doglioni et al., 2011). Shear heating and the mechanical fatigue may self-perpetuate one or more channels of this kind, within the TE and the TE-pert (Panza et al. 2010), which provide the necessary decoupling zone of the lithosphere. Consistently with the present-day Vs resolution, the TE-pert (which is not a great circle) describes the trajectory along which a ubiquitous LVZ at least 1000 km wide and about 100 km thick occurs in the asthenosphere, where the most mobile mantle LVZ is located. The existence of TE-pert is a necessary condition for the existence of a continuous global flow within the Earth (Panza et al., 2010).

To consider the role of the solid Earth's tide is crucial to understand geodynamics and earthquakes. The horizontal component, which is westerly polarized due to the misalignment of the Earth's bulge, may provide the source for shearing the lithosphere and loading the faults. The vertical component generates oscillations of the lithostatic load, which may locally trigger earthquakes along fault planes at critical state (Figure 85). The effect of tides on faults is a function of the tectonic style. In fact low solid tide (relatively larger gravity) favors extensional tectonics, whereas high solid tide (relatively lower gravity) triggers compressional tectonics. Tidal force on the early lithosphere of Mars exerted by former satellites in retrograde orbits may have pulled the lithosphere in an east–west direction over hot mantle (Kobayashi & Sprenke, 2010).

The Earth's rotation contributes to plate tectonics, and if a very-low-viscosity layer is present in the upper asthenosphere, this layer enables the horizontal component of the tidal oscillation to generate a torque able to slowly shift the lithosphere relative to the mantle. This is true even in the case the dimensions of the very-low-viscosity layer are so small to be beyond the reach of tomography. For example, in a car engine, shear friction between piston and sleeve is minimized by an extremely thin film of lubricating fluid that is practically incompressible in the direction normal to the piston motion. If the extremely thin film is absent the engine cannot work.

Therefore, we may state (1) that plates move along a westerly polarized flow that forms an angle relative to the equator close to the revolution plane of the Moon, (2) that plate boundaries are asymmetric, being their geographic polarity the first-order tuning factor in controlling all the geological and geophysical parameters described in the Chapters 3, 4 and 5, (3) that the global seismicity depends on latitude and correlates with the decadal oscillations of the length of day, (4) that the Earth's deceleration supplies energy to plate tectonics comparable to the computed budget dissipated by the deformation processes, and (5) that the Gutenberg–Richter law indicates that the whole lithosphere is a self-organized system in critical state, that is subject to a torque acting contemporaneously on all the plates and distributing the energy over the whole lithospheric shell. Only by a force that acts at the astronomical scale can naturally satisfy such a condition. Thus plate tectonics is fueled both by the tidal drag and by the concomitant global Earth's cooling. Therefore, mantle convection, widely assumed as the only cause of plate tectonics, even if it can be inhibited by thermal gradients weaker than the adiabatic one (Anderson, 2007b; 2013; Birch, 1952; Bullen, 1947), plays an ancillary role and it is possibly top driven and westerly polarized by the steady-state torque provided by the tidal bulge misalignment.

ACKNOWLEDGMENTS

This article summarizes past and ongoing researches performed with a number of colleagues who are deeply thanked: Don Anderson, Samuele Agostini, Salvatore Barba, Michael Bevis, Enrico Bonatti, Enrico Brandmayr, Eugenio Carminati, Françoise Chalot-Prat, Mattia Crespi, Marco Cuffaro, Adriana Garroni, Paolo Harabaglia, Fabrizio Innocenti, Eduardo Garzanti, Alik Ismail-Zadeh, Anatoli Levshin, Corrado Mascia, Franco Mongelli, Enzo Nesi, Angelo Peccerillo, Federica Riguzzi, Fabio Romanelli, Davide Scrocca, and Peter Varga. Anatoli Levshin provided invaluable shear waves data. Partial financial support from MIUR/PRIN2011 project "La subduzione e l'esumazione di litosfera continentale: i suoi effetti sulla struttura degli orogeni, sull'ambiente e sul clima" is acknowledged.

REFERENCES

Abers, G. A. (2005). Seismic low-velocity layer at the top of subducting slabs beneath volcanic arcs: observations, predictions, and systematics. *Physics of the Earth and Planetary Interiors, 149*, 7–29. http://dx.doi.org/10.1016/j.pepi.2004.10.002.

Abers, G. A., van Keken, P. E., Kneller, E. A., Ferris, A., & Stachnik, J. C. (2006). The thermal structure of subduction zones constrained by seismic imaging: implications for slab dehydration and wedge flow. *Earth and Planetary Science Letters, 241*, 387–397.

Afonso, J. C., Ranalli, G., & Fernandez, M. (2007). Density structure and buoyancy of the oceanic lithosphere revisited. *Geophysical Research Letters, 34*, L10302. http://dx.doi.org/10.1029/2007GL029515.

Agostini, S., Doglioni, C., Innocenti, F., Manetti, P., & Tonarini, S. (2010). On the geodynamics of the Aegean rift. *Tectonophysics, 488*, 7–21.

Aitken, A. R. A., Salmon, M. L., & Kennett, B. L. N. (2012). Australia's Moho: a test of the usefulness of gravity modelling for the determination of Moho depth. *Tectonophysics, 609*, 468–479. http://dx.doi.org/10.1016/j.tecto.2012.06.049.

Altamimi, Z., Collilieux, X., Legrand, J., Garayt, B., & Boucher, C. (2007). ITRF2005. A new release of the international terrestrial reference frame based on time series of station positions and Earth orientation parameters. *Journal of Geophysical Research, 112*, B09401. http://dx.doi.org/10.1029/2007JB004949.

Ampferer, O. (1906). Uber das Bewegungbild von Faltengebirge, Austria. *Jahrbuch der Geologischen Bundesanstalt, 56*, 539–622.

Anderson, D. L. (1976). The 650 km mantle discontinuity. *Geophysical Research Letters, 3*, 347–349. http://dx.doi.org/10.1029/GL003i006p00347.

Anderson, D. L. (1989). *Theory of the Earth*. Blackwell. pp. 1–366.

Anderson, D. L. (1999). A theory of the Earth: hutton and Humpty-Dumpty and Holmes. In G. Y. Craig, & J. H. Hull (Eds.), *Geol. Soc. Spec. Publ.: Vol. 150. James Hutton: present and future* (pp. 13–35).

Anderson, D. L. (2001). Topside tectonics. *Science, 293*, 2016–2018.

Anderson, D. L. (2002). The case for irreversible chemical stratification of the mantle. *International Geology Review, 44*, 97–116.

Anderson, D. L. (2006). Speculations on the nature and cause of mantle heterogeneity. *Tectonophysics, 416*, 7–22.

Anderson, D. L. (2007a). *The new theory of the earth*. Cambridge University Press, 384 pp. ISBN:978-0-521-84959-3, 0-521-84959-4.

Anderson, D. L. (2007b). *Slabs on command—Is there convincing tomographic evidence for whole mantle convection?* www.mantleplumes.org/TomographyProblems.html.

Anderson, D. L. (2011). Hawaii, boundary layers and ambient mantle geophysical constraints. *Journal of Petrology, 52*, 1547–1577.

Anderson, D. L. (2013). The persistent mantle plume myth. *Australian Journal of Earth Sciences, 60*(6-7), 657–673. http://dx.doi.org/10.1080/08120099.2013.835283.

Aoudia, A., Ismail-Zadeh, A. T., & Romanelli, F. (2007). Buoyancy-driven deformation and contemporary tectonic stress in the lithosphere beneath Central Italy. *Terra Nova, 19*, 490–495.

Argus, D. F., Gordon, R. G., & DeMets, C. (2011). Geologically current motion of 56 plates relative to the no-net-rotation reference frame. *Geochemistry, Geophysics, Geosystems, 12*, 11. http://dx.doi.org/10.1029/2011GC003751.

Artemieva, I. M., & Mooney, W. D. (2001). Thermal structure and evolution of precambrian lithosphere: a global study. *Journal of Geophysical Research, 106*, 16,387–16,414.

Asimow, P. D., & Langmuir, C. H. (2003). The importance of water to oceanic mantle melting regimes. *Nature, 421*, 815–820. http://dx.doi.org/10.1038/nature01429.

Bachmann, G. H., & Koch, K. (1983). Alpine front and molasse Basin, Bavaria. In A. W. Bally (Ed.), *Vol. 15. Seismic expression of structural styles; a picture and work atlas; Volume 3* (pp. 3.4.1-27–3.4.1-32). American Association of Petroleum Geologists, Studies in Geology.

Barazangi, M., & Isacks, B. L. (1979). Subduction of the Nazca plate beneath Peru: evidence from spatial distribution of earthquakes. *Geophysical Journal of Royal Astronomical Society, 57*, 537–555.

Barklage, M., Wiens, D. A., Nyblad, A., & Anandakrishnan, S. (2009). Upper mantle seismic anisotropy of South Victoria land and the Ross Sea coast, Antarctica from SKS and SKKS splitting analysis. *Geophysical Journal International, 178*, 729–741. http://dx.doi.org/10.1111/j.1365-246X.2009.04158.x.

Beccaluva, L., Bigioggero, B., Chiesa, S., Colombo, A., Fanti, G., Gatto, G. O., et al. (1983). Post collisional orogenic dyke magmatism in the Alps. *Memorie della Societa Geologica Italiana, 26*, 341–359.

Beccaluva, L., Brotzu, P., Macciotta, G., Morbidelli, L., Serri, G., & Traversa, G. (1989). Cainozoic tectono-magmatic evolution and inferred mantle sources in the Sardo-Tyrrhenian area. In Boriani, et al. (Eds.), *The lithosphere in Italy* (pp. 229–248). Accad. Naz. Lincei.

Beccaluva, L., Gatto, G. O., Gregnanin, A., & Piccirillo, E. M. (1979). Geochemistry and petrology of dyke magmatism in the Alto Adige (eastern Alps) and its geodynamic significance. *Neues Jahrbuch für Geologie und Paläontologie, Monatshefte, 1979*, 321–339.

Bellieni, G., Cavazzini, G., Fioretti, A., Peccerillo, A., & Poli, G. (1991). Geochemical and isotopic evidence for a role of crystal fractionation, AFC and crustal anatexis in the genesis of the Rensen plutonic complex (Eastern Alps, Italy). *Chemical Geology, 92*, 21–43.

Bellieni, G., Peccerillo, A., & Poli, G. (1981). The Vedrette di Ries plutonic complex: petrological and geochemical data bearing on its genesis. *Contributions to Mineralogy and Petrology, 78*, 145–156.

Bellon, H. (1981). Chronologie radiometrique ^{Z}KrAr· des manifestations magmatiques autour de la Mediterranee occidentale entre 33 et 1 Ma. In F. C. Wezel (Ed.), *Sedimentary basins of mediterranean margins* (pp. 342–360). Bologna: Tecnoprint.

Bercovici, D. (1998). Generation of plate tectonics from lithosphere mantle flow and void-volatile self-lubrication. *Earth and Planetary Science Letters, 154*, 139–151.

Bevis, M. (1988). Seismic slip and down-dip strain rates inWadati–Benioff zones. *Science, 240*, 1317–1319.

Biagi, L., Pierantonio, G., & Riguzzi, F. (2006). Tidal errors and deformations in regional GPS networks. In F. Sansò, & A. J. Gil (Eds.), *IAG symp: 131. Geodetic deformation monitoring: From geophysical to engineering roles* (pp. 73–82). Berlin: Springer. ISBN/ISSN: 0939-9585.

Billen, M. I., & Hirth, G. (2007). Rheologic controls on slab dynamics. *Geochemistry, Geophysics, Geosystems, 8*, Q08012. http://dx.doi.org/10.1029/2007GC001597.

Bina, C. R. (1996). Phase transition buoyancy contributions to stresses in subducting lithosphere. *Geophysical Research Letters, 23*, 3563–3566.

Birch, F. (1952). Elasticity and constitution of the Earth's interior. *Journal of Geophysical Research, 57*, 227–286.

Boccaletti, D., & Pucacco, G. (2002). *Theory of orbits: Perturbative and geometrical methods* (Vol. 2, pp. 278–286). Berlin: Springer Verlag.

Bohannon, R. G., Naeser, C. W., Schmidt, D. L., & Zimmermann, R. A. (1989). The timing of uplift, volcanism and rifting peripheral to the Red sea: a case for passive rifting? *Journal of Geophysical Research, 94*(B2), 1683–1701, 10.

Bokelmann, G. H. R. (2002). Which forces drive North America? *Geology, 30*, 1027–1030. http://dx.doi.org/10.1130/0091-7613.

Bonatti, E. (1990). Not so hot "hot spots" in the oceanic mantle. *Science, 250*, 107–111.

Bonatti, E., Ligi, M., Brunelli, D., Cipriani, A., Fabretti, P., Ferrante, V., et al. (2003). Mantle thermal pulses below the mid Atlantic Ridge and temporal variations in the oceanic lithosphere. *Nature, 423*, 499–505.

Boschi, L., Ampueroa, J.-P., Peter, D., Maia, P. M., Soldati, G., & Giardini, D. (2007). Petascale computing and resolution in global seismic tomography. *Physics of the Earth and Planetary Interiors, 163*, 245–250.

Bostrom, R. C. (1971). Westward displacement of the lithosphere. *Nature, 234*, 536–538.

Bostrom, R. C. (2000). *Tectonic consequences of the Earth's rotation*. Oxford University Press. pp. 1–266.

Boyadzhiev, G., Brandmayr, E., Pinat, T., & Panza, G. F. (2008). Optimization for non-linear inverse problems. *Rendiconti Lincei, 19*, 17–43.

Brandmayr, E. (2012). *The geodynamics of the mediterranean in the framework of the global asymmetric earth: Evidences from seismological and geophysical methods*. Tesi di dottorato in Geofisica della Litosfera e Geodinamica. Università di Trieste.

Brandmayr, E., Marson, I., Romanelli, F., & Panza, G. F. (2011). Lithosphere density model in Italy: no hint for slab pull. *Terra Nova, 23*, 292–299. http://dx.doi.org/10.1111/j.1365-3121.2011.01012.x.

Brandmayr, E., Raykova, R., Zuri, M., Romanelli, F., Doglioni, C., & Panza, G. (2010). The lithosphere in Italy: structure and seismicity. In M. Beltrando, A. Peccerillo, M. Mattei, S. Conticelli, & C. Doglioni (Eds.), *Journal of the Virtual Explorer, volume 36, paper 1*. http://dx.doi.org/10.3809/jvirtex.2009.00224.

Breuer, D., & Spohn, T. (2003). Early plate tectonics versus single-plate tectonics on Mars: evidence from magnetic field history and crust evolution. *Journal of Geophysical Research, 108*(E7), 5072. http://dx.doi.org/10.1029/2002JE001999.

Bullen, K. (1947). *An introduction to the theory of seismology*. Cambridge: Cambridge University Press, 276 pp.

Bullen, K., & Bolt, B. (1985). *An introduction to the theory of seismology*. Cambridge: Cambridge University Press, 499 pp.

Bunge, H. P., Ricard, Y., & Matas, J. (2001). Non-adiabaticity in mantle convection. *Geophysical Research Letters, 28*(5), 879–882.

Cahill, T., & Isacks, B. L. (1992). Seismicity and shape of the subducted Nazca plate. *Journal of Geophysical Research, 97*, 17503–17529. http://dx.doi.org/10.1029/92JB00493.

Calcagnile, G., D'Ingeo, F., Farrugia, P., & Panza, G. F. (1982). The lithosphere in the central-eastern Mediterranean area. *Pageoph, 120*, 389–406.

Caputo, M., Panza, G. F., & Postpischl, D. (1970). Deep structure of the Mediterranean basin. *Journal of Geophysical Research, 75*, 4919–4923.

Caputo, M., Panza, G. F., & Postpischl, D. (1972). New evidences about the deep structure of the Lipari Arc. *Tectonophysics, 15*, 219–231.

Carlson, R. L., Hilde, T. W. C., & Uyeda, S. (1983). The driving mechanism of plate tectonics: relation to age of the lithosphere at trenches. *Geophysical Research Letters, 10*, 297–300.

Carminati, E., Cuffaro, M., & Doglioni, C. (2009). Cenozoic uplift of Europe. *Tectonics, 28*, TC4016. http://dx.doi.org/10.1029/2009TC002472.

Carminati, E., & Doglioni, C. (2005). Europe–Mediterranean tectonics. In R. Selley, R. Cocks, & I. Plimer (Eds.), *Encyclopedia of geology* (pp. 135–146). Elsevier.

Carminati, E., & Doglioni, C. (2012). Alps vs Apennines: the paradigm of a tectonically asymmetric Earth. *Earth Science Reviews, 112*, 67–96. http://dx.doi.org/10.1016/j.earscirev.2012.02.004.

Carminati, E., Doglioni, C., & Scrocca, D. (2004). Alps vs apennines. In *Special volume of the Italian geological society for IGC 32 florence*.

Carminati, E., Giardina, F., & Doglioni, C. (2002). Rheological control of subcrustal seismicity in the Apennines subduction (Italy). *Geophysical Research Letters, 29*(18). http://dx.doi.org/10.1029/2001GL014084.

Carminati, E., Lustrino, M., & Doglioni, C. (2012). Geodynamic evolution of the central and western Mediterranean: tectonics vs. igneous petrology constraints. *Tectonophysics, 579*, 173–192. http://dx.doi.org/10.1016/j.tecto.2012.01.026.

Carminati, E., & Petricca, P. (2010). State of stress in slabs as a function of large scale plate kinematics. *Geochemistry, Geophysics, Geosystems, 11*. http://dx.doi.org/10.1029/2009GC003003.

Castle, J. C., & Creager, K. C. (1998). NW Pacific slab rheology, the seismicity cutoff, and the olivine to spinel phase change. *Earth Planets Space, 50*, 977–985.

Catalano, R., Doglioni, C., & Merlini, S. (2001). On the mesozoic ionian basin. *Geophysical Journal International, 144*, 49–64.

Cathles, L. M. (1975). *The viscosity of the Earth's mantle*. Princeton University Press, 386 pp.

Cavazza, W., Roure, F., Spakman, W., Stampfli, G., & Ziegler, P. (2004). In *The TRANSMED atlas-the Mediterranean region from crust to mantle* (p. 141). Heidelberg: Springer-Verlag. CD-ROM.

Cernobori, L., Hirn, A., McBride, J. H., Nicolich, R., Petronio, L., Romanelli, M., &, STREAMERS/PROFILES Working Groups. (1996). Crustal image of the ionian basin and its Calabrian margin. *Tectonophysics, 264*, 175–189.

Chalot-Prat, F., & Doglioni, C. (2015). Lateral heterogeneity and no evidence for negative buoyancy of the oceanic lithosphere. In prep.

Chen, P.-F., Bina, C. R., & Okal, E. A. (2001). Variations in slab dip along the subducting Nazca plate, as related to stress patterns and moment release of intermediate-depth seismicity and to surface volcanism. *Geochemistry, Geophysics, Geosystems, 2*. http://dx.doi.org/10.1029/2001GC000153.

Chen, Q., Freymueller, J., Wang, Q., Yang, Z., Xu, C., & Liu, J. (2004). A deforming block model for the present day tectonics of Tibet. *Journal of Geophysical Research, 109*. http://dx.doi.org/10.1029/2002JB002151.

Chiarabba, C., De Gori, P., & Speranza, F. (2008). The southern Tyrrhenian subduction zone: deep geometry, magmatism and Plio-Pleistocene evolution. *Earth and Planetary Science Letters, 268*, 408–423.

Chimera, G., Aoudia, A., Saraò, A., & Panza, G. F. (2003). Active tectonics in central Italy: constraint from surface wave tomography and source moment tensor inversion. *Physics of the Earth and Planetary Interiors, 138*, 241–262.

Christova, C., & Nikolova, S. B. (1993). The Aegean region: deep structures and seismological properties. *Geophysical Journal International, 115*, 635–653.

Civetta, L., Orsi, G., Scandone, P., & Pece, R. (1978). Eastwards migration of the Tuscan anatectic magmatism due to anticlockwise rotation of the Apennines. *Nature, 276*(5866), 604–606.

Cochran, E. S., Vidale, J. E., & Tanaka, S. (2004). Earth tides can trigger shallow thrust fault earthquakes. *Science, 306*(1164), 1166.

Conder, J. A., & Wiens, D. A. (2006). Seismic structure beneath the Tonga arc and Lau back-arc basin determined from joint Vp, Vp/Vs tomography. *Geochemistry, Geophysics, Geosystems, 7*, Q03018.

Conrad, C. P., & Behn, M. (2010). Constraints on lithosphere net rotation and asthenospheric viscosity from global mantle flow models and seismic anisotropy. *Geochemistry, Geophysics, Geosystems, 11*. http://dx.doi.org/10.1029/2009GC002970.

Conrad, C. P., & Lithgow-Bertelloni, C. (2003). How mantle slabs drive plate tectonics. *Science, 298*, 207–209.

Conticelli, S., & Peccerillo, A. (1992). Petrology and geochemistry of potassic and ultrapotassic volcanism in central Italy; petrogenesis and inferences on the evolution of the mantle sources. *Lithos, 28*(3–6), 221–240.

Corti, G., Cuffaro, M., Doglioni, C., Innocenti, F., & Manetti, P. (2006). Coexisting geodynamic processes in the sicily Channel. In Y. Dilek, & S. Pavlides (Eds.), *Geological society of America special paper: 409. Postcollisional tectonics and magmatism in the Mediterranean region and Asia* (pp. 83–96).

Craig, C. H., & McKenzie, D. (1986). The existence of a thin low-viscosity layer beneath the lithosphere. *Earth and Planetary Science Letters, 78*, 420–426. http://dx.doi.org/10.1016/0012-821X(86)90008-7.

Crépisson, C., Morard, G., Bureau, H., Prouteau, G., Morizet, Y., Petitgirard, S., et al. (2014). Magmas trapped at the continental lithosphere–asthenosphere boundary. *Earth and Planetary Science Letters, 393*, 105–112. http://dx.doi.org/10.1016/j.epsl.2014.02.048.

Crespi, M., Cuffaro, M., Doglioni, C., Giannone, F., & Riguzzi, F. (2007). Space geodesy validation of the global lithospheric flow. *Geophysical Journal International, 168*, 491–506. http://dx.doi.org/10.1111/j.1365-246X.2006.03226.x.

Cross, T. A., & Pilger, R. H. (1982). Controls of subduction geometry, location of magmatic arcs, and tectonics of arc and back-arc regions. *Geological Society of America Bulletin, 93*, 545–562.

Cruciani, C., Carminati, E., & Doglioni, C. (2005). Slab dip vs. lithosphere age: no direct function. *Earth and Planetary Science Letters, 238*, 298–310.

Cuffaro, M., Caputo, M., & Doglioni, C. (2008). Plate sub-rotations. *Tectonics, 27*, TC4007. http://dx.doi.org/10.1029/2007TC002182, 200827, TC4007.

Cuffaro, M., Carminati, E., & Doglioni, C. (2006). Horizontal versus vertical plate motions. *Earth Discussion, 1*, 1–18.

Cuffaro, M., & Doglioni, C. (2007). Global kinematics in deep versus shallow hotspot reference frames. In G. R. Foulger, & D. M. Jurdy (Eds.), *Geological society of America special paper: Vol. 430. Plates, plumes, and planetary processes* (pp. 359–374). http://dx.doi.org/10.1130/2007.2430(18).

Cuffaro, M., & Miglio, E. (2012). Asymmetry of thermal structure at slow-spreading ridges: geodynamics and numerical modeling. *Computers & Fluids, 68*, 29–37.

Cuffaro, M., Riguzzi, F., Scrocca, D., Antonioli, F., Carminati, E., Livani, M., & Doglioni, C. (2010). On the geodynamics of the northern Adriatic plate. *Rendiconti Lincei, 21*(Suppl 1), S253–S279. http://dx.doi.org/10.1007/s12210-010-0098-9.

Dal Piaz, G. V., Bistacchi, A., & Massironi, M. (2003). Geological outline of the Alps. *Episodes, 26*(3), 175–180.

Dal Piaz, G. V., Hunziker, J. C., & Martinotti, G. (1972). La Zona Sesia- Lanzo e l'evoluzione tettonico-metamorfica delle Alpi nordoccidentali interne. *Memorie della Società Geologica Italiana, 11*, 433–466.

Dal Piaz, G. V., & Venturelli, G. (1983). Brevi riflessioni sul magmatismo post-ofiolitico nel quadro dell'evoluzione spazio-temporale delle Alpi. *Memorie della Società Geologica Italiana, 26*, 5–19.

Dalton, J. A., & Wood, B. J. (1993). The partitioning of Fe and Mg between olivine and carbonate and the stability of carbonate under mantle conditions. *Contributions to Mineralogy and Petrology, 114*, 501–509.

Debayle, E., Kennett, B., & Priestley, K. (2005). Global azimuthal seismic anisotropy and the unique plate-motion deformation of Australia. *Nature, 433*, 509–512. http://dx.doi.org/10.1038/nature03247.

DeMets, C., Gordon, R. G., & Argus, D. F. (2010). Geologically current plate motions. *Geophysical Journal International, 181*, 1–80.

DeMets, C., Gordon, R. G., Argus, D. F., & Stein, S. (1994). Effect of recent revisions to the geomagnetic reversal time scale on estimates of current plate motions. *Geophysical Research Letters, 21*, 2191–2194. http://dx.doi.org/10.1029/94GL02118.

Deng, Y., Zhang, Z., Romanelli, F., Ma, T., Doglioni, C., Wang, P., et al. (2014). Transition from continental collision to tectonic escape: a geophysical perspective on lateral expansion of the northern Tibetan Plateau. *Earth, Planets and Space*, 1–12. http://dx.doi.org/10.1186/1880-5981-66-10. ISSN:1880-5981.

Denis, C., Schreider, A. A., Varga, P., & Zavoti, J. (2002). Despinning of the Earth rotation in the geological past and geomagnetic paleointensities. *Journal of Geodynamics, 34*, 667–685. http://dx.doi.org/10.1016/S0264-3707(02)00049-2.

Devoti, C., Riguzzi, F., Cuffaro, M., & Doglioni, C. (2008). New GPS constraints on the kinematics of the Apennines subduction. *Earth and Planetary Science Letters, 273*, 163–174.

Dickinson, W. R. (1978). Plate tectonic evolution of North Pacific rim. *Journal of Physical Earth, 26*(Suppl.), 51–519.

Dilek, Y., & Furnes, H. (2011). Ophiolite genesis and global tectonics: geochemical and tectonic fingerprinting of ancient oceanic lithosphere. *Geological Society of America Bulletin, 123*(3/4), 387–411. http://dx.doi.org/10.1130/B30446.1.

Dingwell, D. B., Courtial, P., Giordano, D., & Nichols, A. R. L. (2004). Viscosity of peridotite liquid. *Earth and Planetary Science Letters, 226*, 127–138.

Doglioni, C. (1990). The global tectonic pattern. *Journal of Geodynamics, 12*, 21–38.

Doglioni, C. (1991). A proposal of kinematic modelling for W-dipping subductions—possible applications to the Tyrrhenian–Apennines system. *Terra Nova, 3*, 423–434.

Doglioni, C. (1992). Main differences between thrust belts. *Terra Nova, 4*, 152–164.

Doglioni, C. (1993a). Geological evidence for a global tectonic Polarity. *Journal of the Geological Society of London, 150*, 991–1002.

Doglioni, C. (1993b). Some remarks on the origin of foredeeps. *Tectonophysics, 228*, 1–20.

Doglioni, C. (1994). Foredeeps versus subduction zones. *Geology, 22*, 271–274.

Doglioni, C. (1995). Geological remarks on the relationships between extension and convergent geodynamic settings. *Tectonophysics, 252*, 253–268.

Doglioni, C. (2008). Comment on "The potential influence of subduction zone polarity on overriding plate deformation, trench migration and slab dip angle" by W.P. Schellart. *Tectonophysics, 463*, 208–213.

Doglioni, C. (2014). Asymmetric Earth: mechanisms of plate tectonics and earthquakes. Rendiconti Accademia Nazionale delle Scienze detta dei XL, Memorie di Scienze Fisiche e Naturali, 9–27, ISBN 987-88-548-7171-7, http://dx.doi.org/10.4399/97888548717171.

Doglioni, C., & Anderson, D. L. (2015). Top driven asymmetric mantle convection. In Plates, P., and Physics: Papers written in honor of the life and work of Don L. Anderson. AGU-GSA.

Doglioni, C., Carminati, E., & Bonatti, E. (2003). Rift asymmetry and continental uplift. *Tectonics, 22*, 1024–1037. http://dx.doi.org/10.1029/2002TC001459.

Doglioni, C., Carminati, E., Crespi, M., Cuffaro, M., Penati, M., & Riguzzi, F. (2014). Tectonically asymmetric Earth: from net rotation to polarized westward drift of the lithosphere. *Geoscience Frontiers*. http://dx.doi.org/10.1016/j.gsf.2014.02.001.

Doglioni, C., Carminati, E., & Cuffaro, M. (2006a). Simple kinematics of subduction zones. *International Geological Review, 48*, 479–493.

Doglioni, C., Carminati, E., Cuffaro, M., & Scrocca, D. (2007). Subduction kinematics and dynamic constraints. *Earth Science Reviews, 83*, 125–175. http://dx.doi.org/10.1016/j.earscirev.2007.04.001.

Doglioni, C., Cuffaro, M., & Carminati, E. (2006b). What moves slabs? *Bollettino Geofisica Teorica e Applicata, 47*, 224–247.

Doglioni, C., Green, D. H., & Mongelli, F. (2005). On the shallow origin of hotspots and the westward drift of the lithosphere. In G. R. Foulger, J. H. Natland, D. C. Presnall, & D. L. Anderson (Eds.), *Geological society of America special paper: Vol. 388. Plates, plumes, and paradigms* (pp. 735–749). http://dx.doi.org/10.1130/2005.2388(42).

Doglioni, C., Gueguen, E., Harabaglia, P., & Mongelli, F. (1999a). On the origin of W-directed subduction zones and applications to the western Mediterranean. In B. Durand, et al. (Eds.), *Geol. soc. spec. publ.: Vol. 156. The mediterranean Basins: Tertiary extensions within the Alpine orogen* (pp. 541–561).

Doglioni, C., Harabaglia, P., Merlini, S., Mongelli, F., Peccerillo, A., & Piromallo, C. (1999b). Orogens and slabs vs their direction of subduction. *Earth-Science Reviews, 45*, 167–208.

Doglioni, C., Innocenti, F., & Mariotti, G. (2001). Why Mt. Etna? *Terra Nova, 13*(1), 25–31.

Doglioni, C., Ismail-Zadeh, A., Panza, G., & Riguzzi, F. (2011). Lithosphere-asthenosphere viscosity contrast and decoupling. *Physics of the Earth and Planetary Interiors, 189*, 1–8.

Doglioni, C., Merlini, S., & Cantarella, G. (1999). Foredeep geometries at the front of the Apennines in the Ionian sea (central Mediterranean). *Earth & Planetary Science Letters, 168*(3–4), 243–254.

Doglioni, C., Mongelli, F., & Pialli, G. P. (1998). Boudinage of the Alpine belt in the Apenninic back-arc. *Memorie Società Geologica Italiana, 52*, 457–468.

Doglioni, C., & Prosser, G. (1997). Fold uplift versus regional subsidence and sedimentation rate. *Marine and Petroleum Geology, 14*(2), 179–190.

Doglioni, C., Tonarini, S., & Innocenti, F. (2009). Mantle wedge asymmetries along opposite subduction zones. *Lithos, 113*, 179–189. http://dx.doi.org/10.1016/j.lithos.2009.01.012.

Dostal, J., Coulon, C., & Dupuy, C. (1982). Cainozoic andesitic rocks of Sardinia. In R. S. Thorpe (Ed.), *Andesites: Orogenic andesites and related rocks* (pp. 353–370). Chichester: Wiley.

Drewes, H., & Meisel, B. (2003). An actual plate motion and deformation model as a kinematic terrestrial reference system. *Geotechnologien Science Report, 3*, 40–43.

Dziewonski, A. M., & Anderson, D. L. (1981). Preliminary reference earth model. *Physics of the Earth and Planetary Interiors, 25*, 297–356.

D'Orazio, M., Innocenti, F., Tonarini, S., & Doglioni, C. (2007). Carbonatites in a subduction system: the Pleistocene alvikites from Mt. Vulture (southern Italy). *Lithos, 98*, 313–334. http://dx.doi.org/10.1016/j.lithos.2007.05.004.

El Gabry, M. N., Panza, G. F., Badawy, A. A., & Korrat, I. M. (2013). Imaging a relic of complex tectonics: the lithosphere-asthenosphere structure in the Eastern Mediterranean. *Terra Nova, 25*(2), 102–109. http://dx.doi.org/10.1111/ter.12011.

Engdahl, E. R., & Villaseñor, A. (2002). Global seismicity: 1900–1999. In W. H. K. Lee, H. Kanamori, P. C. Jennings, & C. Kisslinger (Eds.), *International handbook of earthquake and engineering seismology* (Vol. 41, pp. 665–690). Academic Press.

Eotvos, L. (1913). *Verhandlungen der 17. Allgemeinen Konferenz der Internationalen Erdmessung, Part 1* (p. 111 pp).

Escher, A., & Beaumont, C. (1997). Formation, burial and exhumation of basement nappes at crustal scale: a geometric model based on the Western Swiss–Italian Alps. *Journal of Structural Geology, 19*(7), 955–974.

Faccenna, C., & Becker, T. W. (2010). Shaping mobile belts by small-scale convection. *Nature, 465*, 602–605. http://dx.doi.org/10.1038/nature09064.

Farrugia, P., & Panza, G. F. (1981). Continental character of the lithosphere beneath the Ionian sea. In R. Cassinis (Ed.), *The solution of the inverse problem in geophysical interpretation* (pp. 327–334). New York: Plenum.

Fischer, K. M., Fouch, M. J., Wiens, D. A., & Boettcher, M. S. (1998). Anisotropy and flow in Pacific subduction zone back-arcs. *Pure and Applied Geophysics, 151*, 463–475.

Forsyth, D., & Uyeda, S. (1975). On the relative importance of driving forces of plate motion. *Geophysical Journal of the Royal Astronomical Society, 43*, 163–200.

Forte, A. A., & Peltier, W. R. (1987). Plate tectonics and aspherical Earth structure: the importance of poloidal-Toroidal coupling. *Journal of Geophysical Research, 92*(B5), 3654–3679.

Foulger, G. R., & Jurdy, D. M. (2007). Plates, plumes, and planetary processes. *Geological Society of American Special Papers, 430*, 1–998. http://dx.doi.org/10.1130/2007.2430(18).

Foulger, G. R., Natland, J. H., Presnall, D. C., & Anderson, D. L. (2005). Plates, plumes, and paradigms. In *GSA sp. paper* (Vol. 388).

Foulger, G. R., Panza, G. F., Artemieva, I. M., Bastow, I. D., Cammarano, F., Evans, J. R., et al. (2013). Caveats on tomographic images. *Terra Nova, 25*, 259–281. http://dx.doi.org/10.1111/ter.12041.

Fowler, C. M. R. (1995). *The Solid Earth. An introduction to global geophysics*. Cambridge Univ. Press, 700 pp.

Frepoli, A., Selvaggi, G., Chiarabba, C., & Amato, A. (1996). State of stress in the Southern Tyrrhenian subduction zone from fault-plane solutions. *Geophysical Journal International, 125*, 879–891.

Frezzotti, M. L., Peccerillo, A., & Panza, G. F. (2009). Carbonate metasomatism and CO_2 lithosphere-asthenosphere degassing beneath the Western Mediterranean: an integrated model arising from petrological and geophysical data. *Chemical Geology, 262*, 108–120.

Frezzotti, M. L., Peccerillo, A., & Panza, G. F. (2010). Earth's CO_2 degassing in Italy. In M. Beltrando, A. Peccerillo, M. Mattei, S. Conticelli, & C. Doglioni (Eds.) (Electronic edition)*Journal of the virtual explorer: Vol. 36. The geology of Italy: Tectonics and life along plate margins*. http://dx.doi.org/10.3809/jvirtex.2010.00227. ISSN:1441–8142, paper 21.

Frohlich, C. (1989). The nature of deep-focus earthquakes. *Annual Reviews of Earth and Planetary Sciences, 17*, 227–254.

Garfunkel, Z., Anderson, C. A., & Schubert, G. (1986). Mantle circulation and the lateral migration of subducted slabs. *Journal of Geophysical Research, 91*(B7), 7205–7223.

Garzanti, E., Doglioni, C., Vezzoli, G., & Andò, S. (2007). Orogenic Belts and Orogenic Sediment Provenances. *Journal of Geology, 115*, 315–334.

Garzanti, E., Vezzoli, G., & Andò, S. (2002). Modern sand from obducted ophiolite belts (Sultanate of Oman and United Arab Emirates). *Journal of Geology, 110*, 371–391.

Gonzalez, O. F., Alvarez, J. L., Moreno, B., & Panza, G. F. (2011). S-waves's velocities of the lithopshere-asthenosphere system in the Caribbean region. *Pure and Applied Geophysics, 169*(1–2), 101–122. http://dx.doi.org/10.1007/s00024-011-0321-3.

Green, D. H. (2003). *"Hot-spots" and other intraplate settings: Constraints on mantle potential temperatures*. http://www.mantleplumes.org/.

Green, D. H., Hibberson, W. O., Kovacs, I., & Rosenthal, A. (2010). Water and its influence on the lithosphere–asthenosphere boundary. *Nature, 467*, 448–451. http://dx.doi.org/10.1038/nature09369.

Green, H. W. (2007). Shearing instabilities accompanying high-pressure phase transformations and the mechanics of deep earthquakes. *Proceedings of the National Academy of Sciences, 104*(22), 9133–9138. http://dx.doi.org/10.1073/pnas.0608045104.

Green, H. W., II, & Burnley, P. C. (1989). A new self-organizing mechanism for deep focus earthquakes. *Nature, 341*, 733–734.

Green, H. W., II, & Houston, H. (1995). The mechanics of deep earthquakes. *Annual Reviews of Earth and Planetary Science, 23*, 169–213.

Gripp, A. E., & Gordon, R. G. (2002). Young tracks of hotspots and current plate velocities. *Geophysical Journal International, 150*, 321–361.

Grove, T. L., Chatterjee, N., Parman, S. W., & Médard, E. (2006). The influence of H_2O on mantle wedge melting. *Earth and Planetary Science Letters, 249*, 74–89. http://dx.doi.org/10.1016/j.epsl.2006.06.043.

Gueguen, E., Doglioni, C., & Fernandez, M. (1997). Lithospheric boudinage in the Western Mediterranean back-arc basin. *Terra Nova, 9*, 184–187.

Gueguen, E., Doglioni, C., & Fernandez, M. (1998). On the post 25 Ma geodynamic evolution of the western Mediterranean. *Tectonophysics, 298*, 259–269.

Gutenberg, B. (1959). Wave velocities below the Mohorovicic discontinuity. *Geophysical Journal of the Royal Astronomical Society, 2*, 348–352.

Gutscher, M.-A., Malod, J., Rehault, J.-P., Contrucci, I., Klinghoefer, F., Mendes-Victor, L., et al. (2002). Evidence for active subduction beneath Gibraltar. *Geology, 30*, 1071–1074.

Hacker, B. R., Abers, G. A., & Peacock, S. M. (2003). Subduction factory 1: theoretical mineralogy, densities, seismic wave speeds and H_2O contents. *Journal of Geophysical Research, 108*(B1), 2029. http://dx.doi.org/10.1029/2001JB001127.

Hammond, W. C., & Toomey, D. R. (2003). Seismic velocity anisotropy and heterogeneity beneath the mantle electromagnetic and tomography experiment (MELT) region of the East Pacific Rise from analysis of P and S body waves. *Journal of Geophysical Research, 108*, 2176. http://dx.doi.org/10.1029/2002JB001789.

Hansen, L. N., Zimmerman, M. E., & Kohlstedt, D. L. (2012). Laboratory measurements of the viscous anisotropy of olivine aggregates. *Nature, 492*(7429), 415–418. http://dx.doi.org/10.1038/nature11671.

Harabaglia, P., & Doglioni, C. (1998). Topography and gravity across subduction zones. *Geophysical Research Letters, 25*, 703–706.

Harangi, S., & Lenkey, L. (2007). Genesis of the Neogene to Quaternary volcanism in the Carpathian–Pannonian region: role of subduction, extension, and mantle plume. In *Geological society of America special papers* (Vol. 418, pp. 67–92).

Harpp, K. S., Wirth, K. R., & Korich, D. J. (2002). Northern Galapagos province: hotspot-induced, near ridge volcanism at Genovesa island. *Geology, 30*, 399–402.

Heflin, M., et al. (2007). *GPS time series, global velocities*. http://sideshow.jpl.nasa.gov/mbh/series.html.

Heki, K. (2003). Snow load and seasonal variation of earthquake occurrence in Japan. *Earth and Planetary Science Letters, 207*, 159–164. http://dx.doi.org/10.1016/S0012-821X(02)01148-2.

Hermann, J. (2002). Experimental constraints on phase relations in subducted continental crust. *Contributions to Mineralogy and Petrology, 143*, 219–235.

van Hinsbergen, D. J., Hafkenscheid, E., Spakman, W., Meulenkamp, J. E., & Wortel, R. (2005). Nappe stacking resulting from subduction of oceanic and continental lithosphere below Greece. *Geology, 33*, 325–328.

Hirschmann, M. M. (2010). Partial melt in the oceanic low velocity zone. *Physics of the Earth and Planetary Interiors, 179*, 60–71.

Hirth, G., & Kohlstedt, D. L. (1995). Experimental constraints on the dynamics of the partially molten upper mantle, 2, deformation in the dislocation creep regime. *Journal of Geophysical Research, 100*, 15441–15449.

Hirth, G., & Kohlstedt, D. L. (1996). Water in the oceanic upper mantle: implications for rheology, melt extraction and the evolution of the lithosphere. *Earth and Planetary Science Letters, 144*, 93–108.

Hirth, G., & Kohlstedt, D. (2003). Rheology of the upper mantle and the mantle wedge: a view from the experimentalists. In J. Eiler (Ed.), *Geophys. monogr. ser.: Vol. 138. Inside the subduction factory* (pp. 83–105). Washington, D. C: AGU.

Hofmeister, A. M., & Criss, R. E. (2005). Earth's heat flux revised and linked to chemistry. *Tectonophysics, 395*, 159–177.

Holtzman, B. K., Groebner, N. J., Zimmerman, M. E., Ginsberg, S. B., & Kohlstedt, D. L. (2003). Stress-driven melt segregation in partially molten rocks. Geochemistry, Geophysics. *Geosystems, 4*, 8607. http://dx.doi.org/10.1029/2001GC000258.

van Hunen, J., van den Berg, A. P., & Vlaar, N. J. (2001). Latent heat effects of the major mantle phase transitions on low-angle subduction. *Earth and Planetary Science Letters, 190*, 125–135.

Isacks, B. L., & Barazangi, M. (1977). Geometry of Benioff zones: lateral segmentation and downward bending of the subducted lithosphere. In M. Talwani, & W. M. Pitman, III (Eds.), *Maurice ewing series: Vol. 1. Island arcs, deep sea trenches and back-arc basins* (pp. 99–114). Washington, D. C: AGU.

Isacks, B., & Molnar, P. (1971). Distribution of stresses in the descending lithosphere from a global survey of focal-mechanism solutions of mantle earthquakes. *Reviews of Geophysics, 9*, 103–174.

Ismail-Zadeh, A. T., Aoudia, A., & Panza, G. F. (2004). Tectonic stress in the Central Apennines due to lithospheric buoyancy. Trans. (Dokl.). *USSR Academy of Sciences, Earth Science Sections, 395*, 369–372.

Ismail-Zadeh, A., Aoudia, A., & Panza, G. F. (2010). Three-dimensional numerical modeling of contemporary mantle flow and tectonic stress beneath the Central Mediterranean. *Tectonophysics, 482*, 226–236.

Ismail-Zadeh, A., Matenco, L., Radulian, M., Cloetingh, S., & Panza, G. (2012). Geodynamics and intermediate-depth seismicity in Vrancea (the south-eastern Carpathians): Current state-of-the art. *Tectonophysics*, 530–531. http://dx.doi.org/10.1016/j.tecto.2012.01.016, 50–79.

Ismail-Zadeh, A. T., Panza, G. F., & Naimark, B. M. (2000). Stress in the descending relic slab beneath the vrancea region, Romania. *Pure and Applied Geophysics, 157*, 111–130.

Ismail-Zadeh, A., & Tackley, P. (2010). *Computational methods for geodynamics*. Cambridge: Cambridge University Press, 336 pp.

Jarrard, R. D. (1986). Relations among subduction parameters. *Reviews of Geophysics, 24*, 217–284.

Jin, Z.-M., Green, H. G., & Zhou, Y. (1994). Melt topology in partially molten mantle peridotite during ductile deformation. *Nature, 372*, 164–167.

Jordan, T. H. (1974). Some comments on tidal drag as a mechanism for driving plate motions. *Journal of Geophysical Research, 79*(14), 2141–2142.

Jordan, T. H. (1988). Structure and formation of the continental tectosphere. *Journal of Petrology*, 11–37. Special Lithosphere Issue.

Jurdy, D. M. (1990). Reference frames for plate tectonics and uncertainties. *Tectonophysics, 182*, 373–382. http://dx.doi.org/10.1016/0040-1951(90)90173-6.

Jurdy, D. M., & Stefanik, M. (1988). Plate-driving forces over the cenozoic Era. *Journal of Geophysical Research, 93*(B10), 11,833–11,844.

Karato, S., Jung, H., Katayama, I., & Skemer, P. (2008). Geodynamic significance of seismic anisotropy of the upper mantle: new insights from laboratory studies. *Annual Reviews of Earth and Planetary Sciences, 36*, 59–95.

Karig, D. E., Caldwell, J. G., & Parmentier, E. M. (1976). Effects of accretion on the geometry of the descending lithosphere. *Journal of Geophysical Research, 81*, 6281–6291.

Keilis-Borok, V., & Soloviev, A. (Eds.). (2003), *Springer series in synergetics: Vol. XIII. Nonlinear dynamics of the lithosphere and earthquake prediction* (p. 338). ISBN:978-3-662-05298-3.

Kelly, R. K., Kelemen, P. B., & Jull, M. (2003). Buoyancy of the continental upper mantle. *Geochemistry, Geophysics, Geosystems, 4*, 1017. http://dx.doi.org/10.1029/2002GC000399.

Kikuchi, M., & Kanamori, H. (1994). The mechanism of the deep Bolivia earthquake of June 9, 1994. *Geophysical Research Letters, 21*, 2341–2344.

King, S. C. (2001). Subduction zones: observations and geodynamic models. *Physics of the Earth and Planetary Interiors, 127*, 9–24.

Kirby, S. H., Durham, W. B., & Stern, L. A. (1991). Mantle phase changes and deep-earthquake faulting in subducting lithosphere. *Science, 252*, 216–225.

Knopoff, L. (1972). Observations and inversion of surface-wave dispersion. *Tectonophysics, 13*, 497–519.

Knopoff, L., & Leeds, A. (1972). Lithospheric momenta and the deceleration of the Earth. *Nature, 237*, 93–95.

Kobayashi, D., & Sprenke, K. F. (2010). Lithospheric drift on early Mars: evidence in the magnetic field. *Icarus, 210*, 37–42. http://dx.doi.org/10.1016/j.icarus.2010.06.015.

Koper, K. D., Wiens, D. A., Dorman, L., Hildebrand, J., & Webb, S. (1999). Constraints on the origin of slab and mantle wedge anomalies in Tonga from the ratio of S to P velocities. *Journal of Geophysical Research, 104*, 15,089–15,104.

Korenaga, J., & Karato, S. (2008). A new analysis of experimental data on olivine rheology. *Journal of Geophysical Research, 113*, B02403. http://dx.doi.org/10.1029/2007JB005100.

Kornig, H., & Muller, G. (1989). Rheological model and interpretation of postglacial uplift. *Geophysical Journal International, 98*, 243–253.

Kossobokov, V. G., & Nekrasova, A. K. (2012). Global seismic hazard assessment program maps are erroneous. *Seismic Instruments, 48*(2). http://dx.doi.org/10.3103/S0747923912020065. Allerton Press, Inc., 2012, 162–170.

Krasinsky, G. A. (1999). Tidal effects in the Earth-Moon system and the Earth's rotation. *Celestial Mechanics and Dynamical Astronomy, 75*, 39–66. http://dx.doi.org/10.1023/A:1008381000993.

Kreemer, C., Holt, W. E., & Haines, A. J. (2002). The global moment rate distribution within plate boundary zones. *American Geophysical Union Geodynamics Series, 30*, 173–189.

Lallemand, S., Heuret, A., & Boutelier, D. (2005). On the relationships between slab dip, back-arc stress, upper plate absolute motion and crustal nature in subduction zones. *Geochemistry, Geophysics, Geosystems, 6*, Q09006. http://dx.doi.org/10.1029/2005GC000917.

Lallemand, S. E., Schnurle, P., & Manoussis, S. (1992). Reconstruction of subduction zone paleogeometries and quantification of upper plate material losses caused by tectonic erosion. *Journal of Geophysical Research, 97*, 217–239.

Laubscher, H. P. (1988). The arcs of the Western Alps and the Northern Apennines: an updated view. *Tectonophysics, 146*, 67–78.

Lay, T., Hernlund, J., & Buffet, B. A. (2008). Core-mantle boundary heat flow. *Nature Geoscience, 1*, 25–32.

Le Breton, E., Cobbold, P. R., Dauteuil, O., & Lewis, G. (2012). Variations in amount and direction of seafloor spreading along the northeast Atlantic Ocean and resulting deformation of the continental margin of northwest Europe. *Tectonics, 31*, TC5006. http://dx.doi.org/10.1029/2011TC003087.

Le Pichon, X. (1968). Sea-floor spreading and continental drift. *Journal of Geophysical Research, 73*(12), 3661–3697.

Lenci, F., & Doglioni, C. (2007). On some geometric prism asymmetries. In O. Lacombe, J. Lavé, F. Roure, & J. Verges (Eds.), *Frontiers in earth sciences: Vol. 24. Thrust belts and foreland Basins: From fold kinematics to hydrocarbon systems* (pp. 41–60). Springer.

Lithgow-Bertelloni, C., & Richards, M. A. (1998). The dynamics of cenozoic and mesozoic plate motions. *Reviews of Geophysics, 36*, 27–78.

Liu, S., Wang, L., Li, C., Li, H., Han, Y., Jia, C., et al. (2004). Thermal-rheological structure of lithosphere beneath the northern flank of Tarim Basin, western China: implications for geodynamics. *Science China, Series. D: Earth Sciences, 47*(7), 659–672.

Liu, M., Yang, Y., Stein, S., Zhu, Y., & Engeln, J. (2000). Crustal shortening in the Andes: why do GPS rates differ from geological rates? *Geophysical Research Letters, 27*, 3005–3008.

Locardi, E. (1991). Geodinamica delle strutture profonde dell'Appennino centro-meridionale. *Memorie della Società Geological Italiana, 47*, 325–332.

Lucente, F. P., Margheriti, L., Piromallo, C., & Barruol, G. (2006). Seismic anisotropy reveals the long route of the slab through the western-central Mediterranean mantle. *Earth and Planetary Science Letters, 241*(3–4), 517–529.

Ludwig, W. J., Nafe, J. E., & Drake, C. L. (1970). Seismic refraction. In *The sea* (Vol. 4, pp. 53–84). New York: Wiley-Intersci. Part 1.

Lustrino, M. (2005). How the delamination and detachment of lower crust can influence basaltic magmatism. *Earth-Science Reviews, 72*, 21–38.

Luyendyk, B. P. (1970). Dips of downgoing lithospheric plates beneath island arcs. *Geological Society of America Bulletin, 81*, 3411–3416.

Malinverno, A., & Ryan, W. B. F. (1986). Extension in the Tyrrhenian sea and shortening in the Apennines as a result of arc migration driven by sinking of the lithosphere. *Tectonics, 5*, 227–245.

Manea, V. C., Manea, M., Kostoglodov, V., Currie, C. A., & Sewell, G. (2004). Thermal structure, coupling and metamorphism in the Mexican subduction zone beneath Guerrero. *Geophysical Journal International, 158*, 775–784.

Mantovani, E., Viti, M., Albarello, D., Babbucci, D., Tamburelli, C., & Cenni, N. (2002). Generation of backarc basins in the Mediterranean region: driving mechanisms and quantitative modelling. *Bollettino della Società Geologica Italiana, 1*, 99–111.

Margheriti, L., Lucente, F. P., & Pondrelli, S. (2003). SKS splitting measurements in the Apenninic–Tyrrhenian domain (Italy) and their relation with lithospheric subduction and mantle convection. *Journal of Geophysical Research, 108*, 2218. http://dx.doi.org/10.1029/2002JB001793.

Mariotti, G., & Doglioni, C. (2000). The dip of the foreland monocline in the Alps and Apennines. *Earth and Planetary Science Letters, 181*, 191–202.

Marone, F., & Romanowicz, B. (2007). The depth distribution of azimuthal anisotropy in the continental upper mantle. *Nature, 447*, 198–202. http://dx.doi.org/10.1038/nature05742.

McCarthy, D. D., & Petit, G. (2004). *IERS Conventions (2003).* IERS Technical Note No.32. Frankfurt am Main: Verlag des Bundesamts für Kartographie uns Geodäsie.

McKenzie, D. P. (1977). The initiation of trenches: a finite amplitude instability. In M. Talwani, & Pitman, III (Eds.), *Maurice ewing ser: Vol. 1. Island arcs, deep sea trenches and back-arc basins* (pp. 57–61). Washington, D.C: Am. Geophys. Un.

McKenzie, D., & Bickle, M. J. (1988). The volume and composition of melt generated by extension of the lithosphere. *Journal of Petrology, 29*, 625–679.

Meade, C., & Jeanloz, R. (1991). Deep-focus earthquakes and recycling of water into the Earth's mantle. *Science, 252*, 68–72.

Mei, S., Bai, W., Hiraga, T., & Kohlstedt, D. L. (2002). Influence of melt on the creep behavior of olivine basalt aggregates under hydrous conditions. *Earth and Planetary Science Letters, 201*, 491–507. http://dx.doi.org/10.1016/S0012-821X(02)00745-8.

Melini, D., Cannelli, V., Piersanti, A., & Spada, G. (2008). Post-seismic rebound of a spherical Earth: new insights from the application of the Post-Widder inversion formula. *Geophysical Journal International, 174*(4), 672–695.

Métivier, L., de Viron, O., Conrad, C. P., Renault, S., Diament, M., & Patau, G. (2009). Evidence of earthquake triggering by the solid earth tides. *Earth and Planetary Science Letters, 278*, 370–375.

Milsom, J. (2005). The Vrancea seismic zone and its analogue in the Banda Arc, eastern Indonesia. *Tectonophysics, 410*, 325–336.

Molchan, G., Kronrod, T., & Panza, G. F. (1997). Multi-scale seismicity model for seismic risk. *Bulletin of the Seismological Society of America, 87*, 1220–1229.

Montagner, J.-P. (2002). Upper mantle low anisotropy channels below the Pacific plate. *Earth and Planetary Science Letters, 202*, 263–274.

Montagner, J. P., & Guillot, L. (2003). Seismic anisotropy and global geodynamics. *Mineralogical Society of America, 51*, 353–385.

Montague, N., & Kellogg, L. H. (2000). Numerical models of a dense layer at the base of the mantle and implications for the geodynamics of D. *Journal of Geophysical Research, 105*, 11101–11114.

Moore, G. W. (1973). Westward tidal lag as the driving force of plate tectonics. *Geology, 1*, 99–100.

Moretti, I., & Chènet, P. Y. (1987). The evolution of the suez rift: a combination of stretching and secondary convection. *Tectonophysics, 133*, 229–234.

Motaghi, K., Tatar, M., Priestley, K., Romanelli, F., Doglioni, C., & Panza, G. F. (2014). The deep structure of the Iranian plateau. *Gondwana Research*. http://dx.doi.org/10.1016/j.gr.2014.04.009.

Mueller, S., & Panza, G. F. (1986). Evidence of a deep-reaching lithospheric root under the Alpine Arc. In F. C. Wezel (Ed.), *The origin of arcs* (Vol. 21, pp. 93–113). Elsevier.

Müller, R. D., Roest, W. R., Royer, J. Y., Gahagan, L. M., & Sclater, J. G. (1997). Digital isochrons of the world's ocean floor. *Journal of Geophysical Research, 102*, 3211–3214.

Müller, R. D., Sdrolias, M., Gaina, C., & Roest, W. R. (2008). Age, spreading rates, and spreading asymmetry of the world's ocean crust. *Geochemistry, Geophysics, Geosystems, 9*, Q04006. http://dx.doi.org/10.1029/2007GC001743.

Naif, S., Key, K., Constable, S., & Evans, R. L. (2013). Melt-rich channel observed at the lithosphere–asthenosphere boundary. *Nature, 495*, 356–359. http://dx.doi.org/10.1038/nature11939.

Negredo, A. M., Jiménez-Munt, I., & Villasenor, A. (2004). Evidence for eastward mantle flow beneath the Caribbean plate from neotectonic modeling. *Geophysical Research Letters, 31*, L06615. http://dx.doi.org/10.1029/2003GL019315.

Nekrasova, A. K., & Kossobokov, V. G. (2006). General law of similarity for earthquakes: evidence from the Baikal region. *Doklady Earth Sciences, 407A*, 484–485. http://dx.doi.org/10.1134/S1028334X06030305.

Nelson, T. H., & Temple, P. G. (1972). Mainstream mantle convection; a geologic analysis of plate motion. *American Association of Petroluem Geologists Bulletin, 56*(2), 226–246.

Nicolas, A., Boudier, B., Ildefonse, B., & Ball, E. (2000). Accretion of Oman and United Arab Emirates ophiolite: discussion of a new structural map, with three structural maps, scale 1:500,000. In F. Boudier, & T. Juteau (Eds.), *Marine geophysical research: Vol. 21. The ophiolite of Oman and United Arab Emirates* (pp. 147–179).

Nicolich, R., Laigle, M., Hirn, A., Cernobori, L., & Gallart, J. (2000). Crustal structure of the Ionian margin of Sicily: Etna volcano in the frame of regional evolution. *Tectonophysics, 329*, 121–139.

Omori, S., Komabayashi, T., & Maruyama, S. (2004). Dehydration and earthquakes in the subducting slab: empirical link in intermediate and deep seismic zones. *Physics of the Earth and Planetary Interiors, 146*, 297–311. http://dx.doi.org/10.1016/j.pepi.2003.08.014.

Oncescu, M. C., & Bonjer, K.-P. (1997). A note on the depth recurrence and strain release of large Vrancea earthquakes. *Tectonophysics, 272*, 291–302.

Oncescu, M. C., & Trifu, C.-I. (1987). Depth variation of moment tensor principal axes in Vrancea (Romania) seismic region. *Annals of Geophysics, 5B*, 149–154.

Oxburgh, E. R., & Parmentier, E. M. (1977). Compositional and density stratification in oceanic lithosphere; causes and consequences. *Journal of the Geological Society of London, 133*, 343–355.

O'Connell, R., Gable, C. G., & Hager, B. (1991). Toroidal–poloidal partitioning of lithospheric plate motions. In R. Sabadini, et al. (Eds.), *Sea-level and mantle rheology: Vol. 334. Glacial isostasy* (pp. 535–551). Kluwer Academic Publisher.

O'Driscoll, L. J., Humphreys, E. D., & Saucier, F. (2009). Subduction adjacent to deep continental roots: enhanced negative pressure in the mantle wedge, mountain building and continental motion. *Earth and Planetary Science Letters, 280*, 61–70.

Panza, G. F. (1978). The crust and upper mantle in southern Italy from geophysical data. *Rivista Italiana Geofisica Scienze Affini V*, 17–22.

Panza, G. (1980). Evolution of the Earth's lithosphere. In P. A. Davies, & S. K. Runcorn (Eds.), *Mechanisms of continental drift and plate tectonics* (pp. 75–87). Academic Press.

Panza, G. F., & Calcagnile, G. (1979). The upper mantle structure in Balearic and Tyrrhenian bathyal plains and the Messinian salinity crisis. *Palaeogeography, Palaeoclimatology, Palaeoecology, 29*, 3–14.

Panza, G. F., Calcagnile, G., Scandone, P., & Mueller, S. (1982). Die Geologische Tiefenstruktur des Mittelmeerraumes. *Spektrum der Wissenschaft, 1*, 18–28.

Panza, G. F., Doglioni, C., & Levshin, A. (2010). Asymmetric ocean basins. *Geology, 38*(1), 59–62. http://dx.doi.org/10.1130/G30570.1.

Panza, G. F., & Mueller, S. (1978). The plate boundary between Eurasia and Africa in the Alpine Area. *Memorie della Società Geologica Italiana, 33*, 43–50.

Panza, G. F., Peccerillo, A., Aoudia, A., & Farina, B. (2007). Geophysical and petrological modeling of the structure and composition of the crust and upper mantle in complex geodynamic settings: the Tyrrhenian Sea and surroundings. *Earth-Science Reviews, 80*, 1–46.

Panza, G. F., Peresan, A., & Zuccolo, E. (2011). Climatic modulation of seismicity in the Alpine–Himalayan mountain ranges. *Terra Nova, 23*, 19–25. http://dx.doi.org/10.1111/j.1365-3121.2010.00976.x.

Panza, G. F., & Pontevivo, A. (2004). The Calabrian arc: a detailed structural model of the lithosphere–asthenosphere system. *Rendiconti dell'Accademia Nazionale dei, XL*(XXXVIII), 51–88.

Panza, G. F., Pontevivo, A., Chimera, G., Raykova, R., & Aoudia, A. (2003). The Lithosphere–Asthenosphere: Italy and surroundings. *Episodes, 26*, 169–174.

Panza, G. F., Raykova, R. B., Carminati, E., & Doglioni, C. (2007). Upper mantle flow in the western Mediterranean. *Earth and Planetary Science Letters, 257*, 200–214.

Panza, G. F., & Romanelli, F. (2014). Seismic waves in 3D: from mantle asymmetries to reliable seismic hazard assessment. *Earthquake Science, 27*(5), 567–576. http://dx.doi.org/10.1007/s11589-014-0091-y.

Panza, G. F., & Suhadolc, P. (1990). The Mediterranean area: a challenge for plate tectonics. In V. Beloussov, et al. (Eds.), *Critical aspects of the plate tectonics theory* (Vol. 1, pp. 339–363). S.A., Athens: Theophrastus Publications.

Papazachos, B. C., Karakostas, V. G., Papazachos, C. B., & Scordilis, E. M. (2000). The geometry of the Wadati–Benioff zone and lithospheric kinematics in the Hellenic arc. *Tectonophysics, 319*, 275–300.

Pardo, M., Comte, D., & Monfret, T. (2002). Seismotectonic and stress distribution in the central Chile subduction zone. *Journal of South America Earth Sciences, 15*, 11–22. http://dx.doi.org/10.1016/S08959811(02)00003-2.

Patacca, E., & Scandone, P. (1989). Post-tortonian mountain building in the Apennines. The role of the passive sinking of a relic lithospheric slab. In A. Boriani, et al. (Eds.), *The lithosphere in Italy* (Vol. 80, pp. 157–176). Accademia Nazionale dei Lincei.

Peccerillo, A. (1985). Roman comagmatic province ^{Z}central Italy: evidence for subduction-related magma genesis. *Geology, 13*, 103–106.

Peccerillo, A. (1998). Relationships between ultrapotassic and carbonate-rich volcanic rocks in central Italy: petrogenetic implications and geodynamic significance. *Lithos, 43*, 267–279.

Peccerillo, A. (2002). Quaternary magmatism in Central-Southern Italy: a new classification scheme for volcanic provinces and its geodynamic implications. *Bollettino della Società Geologica Italiana, 1*, 113–127.

Peccerillo, A. (2005). *Plio-quaternary volcanism in Italy*. Petrology, geochemistry, geodynamics. Heidelberg: Springer, 365 pp.

Peccerillo, A., & Manetti, P. (1985). The potassium alkaline volcanism of central—southern Italy: a review of the data relevant to petrogenesis and tectonic significance. In J. W. Bristow (Ed.), *Transactions of the geological society of South Africa* (Vol. 88, pp. 379—394).

Peccerillo, A., Panza, G. F., Aoudia, A., & Frezzotti, M. L. (2008). Relationships between magmatism and lithosphere—asthenosphere structure in the western Mediterranean and implication for geodynamics. *Rendiconti Lincei, 19*, 291—309. http://dx.doi.org/10.1007/s12210-008-0020-x.

Pérez-Campos, X., Kim, Y., Husker, A., Davis, P. M., Clayton, R. W., Iglesias, A., et al. (2008). Horizontal subduction and truncation of the Cocos plate beneath central Mexico. *Geophysical Research Letters, 35*, L18303. http://dx.doi.org/10.1029/2008GL035127.

Pertermann, M., & Hirschmann, M. M. (2003). Anhydrous partial melting experiments on MORB-like eclogite: phase relations, phase compositions and mineral-melt partitioning of major elements at 2—3 Gpa. *Journal of Petrology, 44*, 2173—2201.

Pfiffner, O. A., Lehner, P., Heitzmann, P., Müller, St, & Steck, A. (1997). *Deep structure of the Swiss alps*. Results of NRP 20. Basel: Birkhauser Verlag, 380 pp.

Pieri, M. (1983). Three seismic profiles through the Po Plain. In A. W. Bally (Ed.), *American association of petroleum geologists studies in geology: Vol. 15. Seismic expression of structural styles. A picture and work atlas* (pp. 3.4.1/8—3.4.1/26).

Pilger, R. H. (1981). Plate reconstructions, aseismic ridges, and low-angle subduction beneath the Andes. *Geological Society of America Bulletin, 92*, 448—456. http://dx.doi.org/10.1130/0016-7606.

Piromallo, C., & Morelli, A. (2003). P wave tomography of the mantle under the Alpine-Mediterranean area. *Journal of Geophysical Research, 108*. http://dx.doi.org/10.1029/2002JB001757.

Polino, R., Dal Piaz, G. V., & Gosso, G. (1990). Tectonic erosion at the Adria margin and accretionary processes for the Cretaceous orogeny of the Alps. *Mémoire Societè Géologique de France, 156*, 345—367.

Poli, S., & Schmidt, M. W. (2002). Petrology of subducted slabs. *Annual Reviews of Earth and Planetary Sciences, 20*, 207—235.

Pollitz, F. F., Bürgmann, R., & Romanowicz, B. (1998). Viscosity of oceanic asthenosphere inferred from remote triggering of earthquakes. *Science, 280*, 1245—1249. http://dx.doi.org/10.1126/science.280.5367.1245.

Pontevivo, A., & Panza, G. F. (2006). The lithosphere-asthenosphere system in the calabrian arc and surrounding seas—southern Italy. *Pure and Applied Geophysics, 163*, 1617—1659.

Presnall, D. C., & Gudfinnsson, G. H. (2011). Oceanic volcanism from the low-velocity zone—without mantle plumes. *Journal of Petrology, 32*, 1533—1546.

Press, F., & Briggs, P. (1975). Chandler wobble, earthquakes, rotation and geomagnetic changes. *Nature, 256*, 270—273.

Ranalli, G. (1995). *Rheology of the Earth*. Chapman and Hall, 413 pp.

Ranalli, G. (2000). Westward drift of the lithosphere: not a result of rotational drag. *Geophysical Journal International, 141*, 535—537.

Ranalli, G., Pellegrini, R., & D'Offizi, S. (2000). Time dependence of negative buoyancy and the subduction of continental lithosphere. *Journal of Geodynamics, 30*, 539—555.

Ray, R. (2001). Tidal friction in the Earth and Ocean. *Journées Luxembourgeoises de Géodynamique*. JLG 89th, Nov. 12—14 http://www.ecgs.lu/.

Ray, R. D., Eanes, R. J., & Lemoine, F. G. (2001). Constraints on energy dissipation in the earth's body tide from satellite tracking and altimetry. *Geophysical Journal International, 144*, 471—480.

Raykova, R. B., & Panza, G. F. (2006). Surface waves tomography and non-linear inversion in the southeast Carpathians. *Physics of the Earth and Planetary Interiors, 157*, 164–180.

Raykova, R. B., & Panza, G. F. (2010). The shear-wave velocity structure of the lithosphere-asthenosphere system in the Iberian area and surroundings. Springer *Rendiconti Fisiche Accademia Lincei, 21*, 183–231.

Rehault, J. P., Boillot, G., & Mauffret, A. (1985). The western Mediterranean basin. In D. J. Stanley, & F. C. Wezel (Eds.), *Geological evolution of the Mediterranean basin* (pp. 101–130). New York: Springer-Verlag.

Reyners, M., Eberhart-Phillips, D., Stuart, G., & Nishimura, Y. (2006). Imaging subduction from the trench to 300 km depth beneath the central North Island, New Zealand, with Vp and Vp/Vs. *Geophysical Journal International, 165*, 565–583. http://dx.doi.org/10.1111/j.1365-246X.2006.02897.x.

Ricard, Y., Doglioni, C., & Sabadini, R. (1991). Differential rotation between lithosphere and mantle: a consequence of lateral viscosity variations. *Journal of Geophysical Research, 96*, 8407–8415.

Riguzzi, F., Panza, G., Varga, P., & Doglioni, C. (2010). Can Earth's rotation and tidal despinning drive plate tectonics? *Tectonophysics, 484*, 60–73. http://dx.doi.org/10.1016/j.tecto.2009.06.012.

Ritsema, J. (2005). Global seismic structure maps. In G. R. Foulger, J. H. Natland, D. C. Presnall, & D. L. Anderson (Eds.), *Geological society of America special paper: Vol. 388. Plates, plumes, and paradigms* (pp. 11–18).

Rittmann, A. (1942). Zur Thermodynamik der Orogenese. *Geologische Rundschau, 33*, 485–498.

Ritzwoller, M. H., Shapiro, N. M., Barmin, M. P., & Levshin, A. L. (2002). Global surface wave diffraction tomography. *Journal of Geophysical Research, 107*(B12), 2335.

Rivera, L., Sieh, K., Helmberger, D., & Natawidjaja, D. (2002). A comparative study of the Sumatran subduction-zone earthquakes of 1935 and 1984. *Bulletin of the Seismological Society of America, 92*, 1721–1736.

Romanowicz, B. (2003). Global mantle tomography: progress status in the past 10 Years. *Annual Review of Earth and Planetary Science, 31*, 303–328. http://dx.doi.org/10.1146/annurev.earth.31.091602.113555.

Romashkova, L. L. (2009). Global-scale analysis of seismic activity prior to 2004 Sumatra-Andaman mega-earthquake. *Tectonophysics, 470*, 329–344. http://dx.doi.org/10.1016/j.tecto.2009.02.011.

Royden, L. H. (1993). The tectonic expression slab pull at continental convergent boundaries. *Tectonics, 12*, 303–325.

Ruff, L., & Kanamori, H. (1980). Seismicity and the subduction process. *Physics of the Earth and Planetary Interiors, 23*, 240–252.

Russo, R. M., & Silver, P. G. (1994). Trench-parallel flow beneath the Nazca plate from seismic anisotropy. *Science, 263*, 1105–1111.

Rybach, L. (1976). Radioactive heat production in rocks and its relation to other petrophysical parameters. *Pure and Applied Geophysics, 114*, 309–317.

Rychert, C. A., Fischer, C. M., & Rondenay, S. (2005). A sharp lithosphere–asthenosphere boundary imaged beneath eastern North America. *Nature, 436*, 542–545.

Rychert, C. A., Laske, G., Harmon, N., & Shearer, P. M. (2013). Seismic imaging of melt in a displaced Hawaiian plume. *Nature Geoscience, 6*, 657–660. http://dx.doi.org/10.1038/ngeo1878.

Rychert, C. A., & Shearer, P. M. (2009). A global view of the lithosphere-asthenosphere boundary. *Science, 324*(5926), 495–498. http://dx.doi.org/10.1126/science.1169754.

Sacks, I. S., & Okada, H. (1974). A comparison of the anelasticity structure beneath western South America and Japan. *Physics of the Earth and Planetary Interiors, 9*, 211–219. http://dx.doi.org/10.1016/0031-9201(74)90139-3.

Savage, M. K. (1999). Seismic anisotropy and mantle deformation: what have we learned from shear wave splitting? *Reviews of Geophysics, 37*, 65–106.

Scalera, G., Calcagnile, G., & Panza, G. F. (1981). On the "400-kilometers" discontinuity in the Mediterranean area. In R. Cassinis (Ed.), *The solution of the inverse problem in geophysical interpretation* (pp. 335–339). Plenum Pub. Corp.

Schettino, A. (1999). Computational methods for calculating geometrical parameters of tectonic plates. *Computers & Geosciences, 25*, 897–9907.

Schildgen, T. F., Yıldırım, C., Cosentino, D., & Strecker, M. R. (2014). Linking slab break-off, Hellenic trench retreat, and uplift of the Central and Eastern Anatolian plateaus. *Earth-Science Reviews, 128*, 147–168. http://dx.doi.org/10.1016/j.earscirev.2013.11.006.

Schmerr, N. (2012). The Gutenberg discontinuity: melt at the lithosphere-asthenosphere boundary. *Science, 335*, 14801483.

Scholz, C. H., & Campos, J. (1995). On the mechanism of seismic decoupling and back arc spreading at subduction zones. *Journal of Geophysical Research, 100*(B11), 22,103–22,115.

Schuberth, B. S. A., Bunge, H. P., Steinle-Neumann, G., Moder, C., & Oeser, J. (2009). Thermal versus elastic heterogeneity in high-resolution mantle circulation models with pyrolite composition: high plume excess temperatures in the lowermost mantle. *Geochemistry, Geophysics, Geosystems, 10*(1), Q01W01. http://dx.doi.org/10.1029/2008GC002235.

Schubert, G., Turcotte, D. L., & Olson, P. (2001). *Mantle convection in the Earth and planets*. Cambridge, UK: Cambridge University Press, 940 pp.

Scoppola, B., Boccaletti, D., Bevis, M., Carminati, E., & Doglioni, C. (2006). The westward drift of the lithosphere: a rotational drag? *Geological Society of America Bulletin, 118*, 199–209. http://dx.doi.org/10.1029/2004TC001634.

Scrocca, D., Carminati, E., & Doglioni, C. (2005). Deep structure of the Southern Apennines (Italy): thin-skinned or thick-skinned? *Tectonics, 24*, TC3005. http://dx.doi.org/10.1029/2004TC001634.

Secco, R. A. (1995). Viscosity of the outer core. Mineral physics and crystallography. In *A handbook of physical constants* (Vol. 2, pp. 218–226). AGU Reference Shelf.

Seghedi, I., Matenco, L., Downes, H., Mason, P. R. D., Szakács, A., & Pécskay, Z. (2011). Tectonic significance of changes in post-subduction Pliocene-Quaternary magmatism in the south east part of the Carpathian-Pannonian Region. *Tectonophysics, 502*, 146–157.

Sella, G. F., Dixon, T. H., & Mao, A. (2002). REVEL: a model for recent plate velocity from space geodesy. *Journal of Geophysical Research, 107*, 2081. http://dx.doi.org/10.1029/2000JB000033.

Selvaggi, G., & Chiarabba, C. (1995). Seismicity and P-wave velocity image of the southern Tyrrhenian subduction zone. *Geophysical Journal International, 121*, 818–826.

Serri, G. (1990). Neogene–Quaternary magmatism of the Tyrrhenian region: characterization of the magma sources and geodynamic implications. *Memorie della Società Geologica Italiana, 41*, 219–242.

Shaw, H. R., & Jackson, E. D. (1973). Linear island chains in the Pacific, result of thermal plumes or gravitational anchors? *Journal of Geophysical Research, 78*, 8634–8652.

Silver, P. G., & Holt, W. E. (2002). The mantle flow field beneath western North America. *Science, 295*, 1054–1057.

Smith, A. D., & Lewis, C. (1999). The planet beyond the plume hypothesis. *Earth-Science Reviews, 48*, 135–182.

Solomon, S., & Sleep, N. H. (1974). Some simple physical models for absolute plate motions. *Journal of Geophysical Research, 79*, 2557–2567.

Spakman, W., Wortel, M. J. R., & Vlaar, N. J. (1988). The Hellenic Subduction zone: a tomographic image and its geodynamic implications. *Geophysical Research Letters, 15*, 60–63.

Stampfli, G. M., & Borel, G. D. (2002). A plate tectonic model for the paleozoic and mesozoic constrained by dynamic plate boundaries and restored synthetic oceanic isochrons. *Earth and Planetary Science Letters, 196*, 17–33.

Stein, S., & Wysession, M. (2003). *An introduction to seismology, earthquakes, and Earth structure*. Oxford: Blackwell Science, 498 pp.

Stern, R. J. (2002). Subduction zones. *Reviews of Geophysics, 40*, 1012.

Stevenson, D. J. (1994). Weakening under stress. *Nature, 372*, 129–130.

Stoppa, F., & Woolley, A. R. (1997). The Italian carbonatites: field occurrence, petrology and regional significance. *Mineralogy and Petrology, 59*, 43–67.

Suhadolc, P., Panza, G. F., & Mueller, S. (1988). Lateral variations of the lithosphere-asthenosphere system and plate boundaries in Europe. In P. Baldi, & S. Zerbini (Eds.), *Proc. third int. conf. WEGENER/MEDLAS project* (pp. 53–60). Bologna: Esculapio.

Syracuse, E. M., & Abers, G. A. (2006). Global compilation of variations in slab depth beneath arc volcanoes and implications. *Geochemistry, Geophysics, Geosystems, 7*, Q05017. http://dx.doi.org/10.1029/2005GC001045.

Tackley, P. J. (2000). Mantle convection and plate tectonics: toward an integrated physical and chemical theory. *Science, 288*, 2002–2007.

Tackley, P. (2008). Modelling compressible mantle convection with large viscosity contrasts in a three-dimensional spherical shell using the yin-yang grid. *Physics of the Earth and Planetary Interiors, 171*, 7–18.

Tatsumi, Y., & Eggins, S. (1995). *Subduction zone magmatism. Frontiers in earth sciences*. Blackwell Science, 211 pp.

Thybo, H. (2006). The heterogeneous upper mantle low velocity zone. *Tectonophysics, 416*, 53–79.

Torsvik, T. H., Steinberger, B., Gurnis, M., & Gaina, C. (2010). Plate tectonics and net lithosphere rotation over the past 150 my. *Earth and Planetary Science Letters, 291*, 106112.

Tovish, A., & Schubert, G. (1978). Island arc curvature, velocity of convergence and angle of subduction. *Geophysical Research Letters, 5*, 329–332.

Trampert, J., Deschamps, F., Resovsky, J., & Yuen, D. (2004). Probabilistic tomography maps chemical heterogeneities throughout the lower mantle. *Science, 306*, 853–856.

TRANSALP Working Group. (2002). First deep seismic reflection images of the Eastern Alps reveal giant crustal wedges and transcrustal ramps. *Geophysical Research Letters, 29*, 10. http://dx.doi.org/10.1029/2002GL014911.

Trümpy, R. (1975). On crustal subduction in the Alps. In M. Mahel (Ed.), *Tectonic problems in the Alpine system* (pp. 121–130). Bratislava: Slovak Academy of Sciences.

Tumanian, M., Frezzotti, M. L., Peccerillo, A., Brandmayr, E., & Panza, G. F. (2012). Thermal structure of the shallow upper mantle beneath Italy and neighbouring areas: correlation with magmatic activity and geodynamic significance. *Earth-Science Reviews, 114*, 369–385. http://dx.doi.org/10.1016/j.earscirev.2012.07.002.

Turcotte, D. L., & Schubert, G. (1982). *Geodynamics*. New York: Wiley, 450 pp.

Turcotte, D. L., & Schubert, G. (2002). *Geodynamics*. Cambridge University Press, 456 pp.

Ulmer, P., & Trommsdorff, V. (1995). Serpentine stability to mantle depths and subduction related magmatism. *Science, 268*, 858–861.

Uyeda, S., & Kanamori, H. (1979). Back-arc opening and the mode of subduction. *Journal of Geophysical Research, 84*(B3), 1049–1061.

Van Hunen, J., van den Berg, A. P., & Vlaar, N. J. (2002). The impact of the South-American plate motion and the Nazca Ridge subduction on the flat subduction below South Peru. *Geophysical Research Letters, 29*, 14. http://dx.doi.org/10.1029/2001GL014004.

Van Keken, P. E. (2003). The structure and dynamics of the mantle wedge. *Earth and Planetary Science Letters, 215*, 323–338.

Van der Hilst, R. (1995). Complex morphology of subducted lithosphere in the mantle beneath the Tonga trench. *Nature, 374*(6518), 154–157.

Van der Hilst, R. (2004). Changing views on Earth's deep mantle. *Science, 306*, 817–818.

Varga, P. (2006). Temporal variation of geodynamical properties due to tidal friction. *Journal of Geodynamics, 41*, 140–146.

Varga, P., Denis, C., & Varga, T. (1998). Tidal friction and its consequences in paleogeodesy, in the gravity field variations and in tectonics. *Journal of Geodynamics, 25*, 61–84. http://dx.doi.org/10.1016/S0264-3707(97)00007-0.

Varga, P., Gambis, D., Bus, Z., & Bizouard, C. (2005). *The relation between the global seismicity and the rotation of the Earth*. Observatoire de Paris, Systémes de reference temps-espace UMR8630/CNRS, pp. 115–121.

Varga, P., Krumm, F. W., Grafarend, E. W., Sneeuw, N., Schreider, A. A., & Horvath, F. (2014). Evolution of the oceanic and continental crust during neo-proterozoic and phanerozoic. *Rendiconti Lincei, 25*, 255–263. http://dx.doi.org/10.1007/s12210-014-0298-9.

Varga, P., Krumm, F., Riguzzi, F., Doglioni, C., Süle, B., Wang, K., et al. (2012). Global pattern of earthquakes and seismic energy distributions: Insights for the mechanisms of plate tectonics. *Tectonophysics, 530*, 80–86.

Vasco, D. W., Johnson, L. R., & Marques, O. (2003). Resolution, uncertainty, and whole Earth tomography. *Journal of Geophysical Research, 108*. http://dx.doi.org/10.1029/2001JB000412.

Vassiliou, M. S., Hager, B. H., & Raefsky, A. (1984). The distribution of earthquakes with depth and stress in subducting slabs. *Journal of Geodynamics, 1*, 11–28.

Venisti, N., Calcagnile, G., Pontevivo, A., & Panza, G. F. (2005). Tomographic study of the adriatic plate. *Pure and Applied Geophysics, 162*, 311–329.

Venturelli, G., Thorpe, R. S., Dal Piaz, G. V., Del Moro, A., & Potts, P. J. (1984). Petrogenesis of calc-alkaline, shoshonitic and associated ultrapotassic oligocene volcanic rocks from the Northern Alps. *Contributions to Mineralogy and Petrology, 86*, 209–220.

Vinnik, L., Singh, A., Kiselev, S., & Ravi Kumar, M. (2007). Upper mantle beneath foothills of the western Himalaya: subducted lithospheric slab or a keel of the Indian shield? *Geophysical Journal International, 171*, 1162–1171. http://dx.doi.org/10.1111/j.1365-246X.2007.03577.x.

de Voogd, B., Truffert, C., Chamot-Rooke, N., Huchon, P., Lallemant, S., & Le Pichon, X. (1992). Two-ship deep seismic soundings in the basins of the eastern Mediterranean sea (Pasiphae cruise). *Geophysical Journal International, 109*, 536–552.

Waldhauser, F., Lippitsch, R., Kissling, E., & Ansorge, J. (2002). High-resolution teleseismic tomography of upper-mantle structure using an a priori three-dimensional crustal model. *Geophysical Journal International, 150*, 403–414.

Walter, M. J., & Trønes, R. G. (2004). Early earth differentiation. *Earth and Planetary Science Letters, 225*, 253–269.

Waschbusch, P., & Beaumont, C. (1996). Effect of slab retreat on crustal deformation in simple regions of plate convergence. *Journal of Geophysical Research, 101*(B12), 28133–28148.

Wegener, A. (1915). *Die Entstehung der Kontinente und der Ozeae: Samml. 23* pp. 1–94). Braunschweig: Vieweg.

Wilcock, W. S. D. (2001). Tidal triggering of microearthquakes on the Juan de Fuca Ridge. *Geophysical Research Letters, 28*(20), 3999–4002.

Wong A Ton, S. Y. M., & Wortel, M. J. R. (1997). Slab detachment in continental zones: an analysis of controlling parameters. *Geophysical Research Letters, 24*, 2095–2098.

Wortel, M. J. R., & Spakman, W. (2000). Subduction and slab detachment in the Mediterranean–Carpathian region. *Science, 290*, 1910–1917.

Wyss, M., Nekrasova, A., & Kossobokov, V. (2012). Errors in expected human losses due to incorrect seismic hazard estimates. *Nature Hazards, 62*, 927–935.

Ying, J. F., Zhang, H. F., Kita, N., Morishita, X. H., & Shimoda, G. (2006). Nature and evolution of Late Cretaceous lithospheric mantle beneath the eastern North China Craton: constraints from petrology and geochemistry of peridotitic xenoliths from Jünan, Shandong province, China. *Earth and Planetary Science Letters, 244*, 622–638.

Yuan, K., & Beghei, C. (2013). Seismic anisotropy changes across upper mantle phase transitions. *Earth and Planetary Science Letters, 374*, 132–144. http://dx.doi.org/10.1016/j.epsl.2013.05.031.

Zhang, H. F., & Sun, M. (2002). Geochemistry of Mesozoic basalts and mafic dikes in southeastern North China craton, and tectonic implication. *International Geology Reviews, 44*, 370–382.

Zhang, Z., Teng, J., Romanelli, F., Braitenberg, C., Ding, Z., Zhang, X., et al. (2014). Geophysical constraints to the link between cratonization and orogeny: evidence from Tibetan plateau and North China craton. *Earth-Science Reviews, 130*, 1–48. http://dx.doi.org/10.1016/j.earscirev.2013.12.005.

Zhan, Z., Kanamori, H., Tsai, V. C., Helmberger, D. V., & Wei, S. (2014). Rupture complexity of the 1994 Bolivia and 2013 Sea of Okhotsk deep earthquakes. *Earth and Planetary Science Letters, 385*, 89–96. http://dx.doi.org/10.1016/j.epsl.2013.10.028.

Zito, G., Mongelli, F., De Lorenzo, S., & Doglioni, C. (2003). Heat flow and geodynamics in the Tyrrhenian Sea. *Terra Nova, 15*(6), 425–432. http://dx.doi.org/10.1046/j.1365-3121.2003.00507.x.

Zschau, J. (1986). Tidal friction in the solid Earth: constraints from the Chandler wobble period. In A. J. Anderson, et al. (Eds.), *Space geodesy and geodynamics* (pp. 315–344).